Isolation and Structure Elucidation of Bioactive Secondary Metabolites from Marine Sponges

Isolierung und Strukturaufklärung von bioaktiven Sekundärmetaboliten aus marinen Schwämmen

Inaugural-Dissertation
zur
Erlangung des Doktorgrades
der Mathematisch-Naturwissenschaftlichen Fakultät
der Heinrich-Heine-Universität Düsseldorf

vorgelegt von
Georgios Daletos
aus Nafpaktos, Griechenland

Düsseldorf, 2015

Aus dem Institut für Pharmazeutische Biologie und Biotechnologie
der Heinrich-Heine Universität Düsseldorf

Referent: Prof. Dr. Peter Proksch
Koreferent: Prof. Dr. Matthias U. Kassack

Tag der mündlichen Prüfung: 20.05.2015

Erklärung

Hiermit erkläre ich ehrenwörtlich, dass ich die vorliegende Dissertation mit dem Titel „Neue Naturstoffe aus Marinen Schwämmen -Strukturaufklärung und Biologisches Screening" selbst angefertigt habe. Außer den angegebenen Quellen und Hilfsmitteln wurden keine weiteren verwendet. Diese Dissertation wurde weder in gleicher noch in abgewandelter Form in einem anderen Prüfungsverfahren vorgelegt. Weiterhin erkläre ich, dass ich früher weder akademische Grade erworben habe, noch dies versucht habe.

Düsseldorf, den 31.03.2015

Georgios Daletos

Acknowledgments

Zusammenfassung

Meeresschwämme gehören mit ihrer Vielfalt an einzigartigen und faszinierenden Strukturen zu den wichtigsten Quellen an Sekundärstoffen. Diese weisen zu einem großen Teil biologische Aktivität in pharmazeutisch relevanten Biotest-Systemen auf und stellen somit potenzielle Leitsubstanzen dar, die zur Entwicklung effektiver therapeutischer und bioaktiver Arzneistoffe beitragen können.

Die vorliegende Studie umfasste die Isolierung, Strukturaufklärung und biologische Analyse der aktiven Bestandteile von sechs Meeresschwamm-Proben, die aus verschiedenen Sammelgebieten in Indonesien und der Türkei stammen.

Die Strukturaufklärung der Sekundärstoffe wurde durch moderne analytische Verfahren durchgeführt, beispielsweise mit Hilfe von 1D (^{1}H, ^{13}C)- und 2D (COSY, TOCSY, ROESY, HSQC, HMBC)-Kernresonanzspektroskopie (NMR) und mit Hilfe von Massenspektrometrie (EI, ESI, MALDI-TOF). Zusätzlich wurden für einige optisch aktive Naturstoffe chirale Derivatisierungsreaktionen angewendet, um deren absolute Konfiguration zu ermitteln. Schließlich wurden die ermittelten Substanzen verschiedenen Biotests unterzogen, um ihre zytotoxischen und antimykobakteriellen Eigenschaften sowie ihre Wirkung als Inhibitoren verschiedener Proteinkinasen zu ermitteln.

1. *Dactylospongia metachromia*

Die chemische Untersuchung des Schwamms *Dactylospongia metachromia* (Indonesien) ergab fünf neue Sesquiterpen-Aminochinone und zwei neue Benzoxazol-Sesquiterpene. Weiterhin wurden drei bekannte Stoffe isoliert: ein Sesquiterpen-Hydrochinon, ein Indol-Derivat und ein Glycerolipid. Die Derivate des Sesquiterpen-Hydrochinons zeigten hohe zytotoxische Aktivität im Test gegen Maus-Lymphom (L5178Y)-Zellen sowie eine ausgeprägte inhibitorische Aktivität gegenüber Proteinkinasen.

2. *Callyspongia aerizusa*

Eine genaue chemische Untersuchung von vier separaten Proben von *Callyspongia aerizusa* (Indonesien) ergab 12 strukturell ähnliche zyklische Peptide (Callyaerine), einschließlich fünf neuer Analoga. Alle Stoffe wurden *in vitro* gegen *M. tuberculosis* getestet sowie gegen THP-1 (akute monozytische Leukämie beim

Menschen) und MRC-5 (fetale humane Lungenfibroblasten)-Zellen, um ihre allgemeinen zytotoxischen Eigenschaften zu ermitteln. Callyaerin A und Callyaerin B wirken demnach in geringen mikromolaren Mengen als Inhibitoren gegen *M. tuberculosis*, wodurch diese Stoffe interessante Kandidaten für weiterführende Studien sind.

3. *Acanthostrongylophora ingens*

Die chemische Untersuchung des Schwamms *Acanthostrongylophora ingens* (Indonesien) ergab die zwei bekannten β-Carbolin Alkaloide Annomontin und 1-Hydroxy-3,4-dihydronorharman. Die isolierten Stoffe wurden auf ihre antibakterielle Aktivität gegenüber *S. aureus*, *E. coli*, und *P. Aeruginosa* getestet. Weiterhin wurden die isolierten Stoffe Biotests unterzogen, um ihre zytotoxischen Eigenschaften und ihre inhibitorischen Profile gegenüber Proteinkinase zu ermitteln. Annomontin zeigte eine schwache inhibitorische Aktivität gegen *S. aureus*. Desweiteren zeigte es moderate inhibitorische Aktivität gegen PIM1-Kinase, wohingegen 1-Hydroxy-3,4-dihydronorharman keinerlei Aktivität zeigte.

4. *Sarcotragus spinosulus*

Die biotest-geführte Fraktionierung von *Sarcotragus spinosulus* (Türkei) führte zu der Isolierung einer 3:1-Mischung der zwei bekannten linearen Sesterterpene Ircinin 1 und Ircinin 2. Ircinin-1,2 (3:1) wurde Biotests unterzogen, um die zytotoxischen Eigenschaften und das inhibitorische Profil gegenüber Proteinkinasen dieser Stoffe zu ermitteln. Interessanterweise stellte sich heraus, dass Ircinin-1,2 (3:1) äußerst aktiv gegenüber einer Reihe von Proteinkinasen ist, wohingegen es gegenüber Maus-Lymphom (L5178Y)-Zellen nur schwache Aktivität zeigte.

5. *Dysidea avara*

Zwei bekannte Sesquiterpene Chinone/Chinole wurden gereinigt und aus dem methanolischen Extrakt des Meeresschwammes *Dysidea avara* (Türkei) isoliert: Avarol und Avaron. Avarol zeigte in verschiedenen Biotests interessante bioaktive Ergebnisse, beispielsweise zytotoxische (MTT), antibakterielle und *in vitro* inhibitorische Eigenschaften gegenüber Proteinkinasen.

6. *Agelas oroides*

Die chemische Untersuchung des Schwammes *Agelas oroides* (Türkei) resultierte in der Isolierung eines bekannten Bromopyrrol-Alkaloid. 4,5-Dibromopyrrole-2-carboxyl-Säure wurde auf zytotoxische Eigenschaften und antibakterielle Aktivitäten getestet, zeigte jedoch keinerlei Aktivität.

Table of contents

1. Introduction

Marine sponges are among the oldest invertebrate animals (phylum Porifera) exhibiting a wide range of shapes and colors (Proksch *et al.*, 2010). These sessile invertebrate animals are mostly attached to a substratum in marine or freshwater habitats (Koopmans *et al.*, 2009). Sponges have various types of cells with different functions, which together carry out distinct body functions (Koopmans *et al.*, 2009). Moreover, a large amount of water is filtered through their bodies in order to provide them with nutrients and oxygen, as well as to excrete waste products and carbon dioxide (Koopmans *et al.*, 2009).

Currently, there are around 8.600 species of sponges inhabiting different marine and freshwater ecosystems (Sagar *et al.*, 2010; Van Soest *et al.*, 2015). Marine sponges continue to draw the attention of natural product chemists, due to their broad array of bioactive metabolites, which are considered to be produced as a defense against pathogenic fungi, bacteria, algae, and predators; a system that has successfully evolved throughout millions of years (Sagar *et al.*, 2010). Notably, more than 15,000 sponge-derived metabolites have been discovered, and every year numerous novel metabolites are being isolated and identified (Yasuhara-Bell & Lu, 2010).

Marine sponges are viewed not only as a prolific source of compounds with novel chemical structures, but also as a source of bioactive metabolites with pharmaceutical potential. These compounds are interesting candidates in drug discovery, primarily in the area of cancer, anti-inflammatory and analgesy (Proksch *et al.*, 2002).

1.1. Significance of the study

Marine organisms represent a largely unexploited source of potential pharmaceuticals with a great variety of fascinating structures (Blunt *et al.*, 2013). Such bioactive compounds are believed to play an important role in the protection, adaptation and survival of marine organisms in the unique environmental conditions of the sea (Pawlik, 2011, Daletos *et al.*, 2014). Many marine invertebrates, including sponges, are sessile and soft-bodied animals lacking a hard outer shell, which makes them vulnerable to potential predators (Leal *et al.*, 2010). It is assumed that sponges like other marine invertebrates rely mainly on chemical defense, producing a wide range of bioactive metabolites to deter predators or compete with neighbors for resources or space (Proksch *et al.*, 2010, Daletos *et al.*, 2014).

Indonesia, as the central part of the larger Indo West Pacific region, has been reported to possess high marine biodiversity including sponges (Van Soest *et al.*, 2015). The highest frequency of deterrent or toxic metabolites arises in high competing environments as a result of competition for space or environmental stress factors, including overgrowth of fouling organisms (Proksch *et al.*, 1994). Notably, sponges that are susceptible to predators are commonly more toxic than those growing in less exposed areas (Koopmans *et al.*, 2009). For instance, chemical deterrence of predators was found considerably greater for tropical marine sponge extracts than that found from extracts of temperate sponges, where less predation takes place (Proksch *et al*., 2002) Therefore, study on the Indonesian sponges is of great importance, due to them being a prospective source of numerous bioactive metabolites that serve as lead structures in drug development (Proksch *et al.*, 2003).

The main function of these bioactive metabolites is to modulate cellular defense or communication (Sagar et al. 2009). Several of them have entered the market as anti-cancer or antiviral agents or are currently in different stages of clinical trials as remarkably fascinating constituents for applications in drug discovery. (Sagar *et al.*, 2010; Martins *et al*., 2014).

Undoubtedly, marine sponges are among the most prolific sources of bioactive metaboiltes from marine organisms (Laport *et al*., 2009). Taking into account, the eminent development and advancement of more sponge-derived bioactive compounds into the current marine drug pipeline, the prospective of sponge-derived metabolites as sources of new drugs seems to be high (Liu, 2012).

1.2.The biological importance of marine natural products

1.2.1. Anti-inflammatory marine natural products

Inflammation is an elaborate defence process, in which leukocytes migrate into damaged tissues to eradicate potential agents that may cause tissue injury (Gabay, 2006). The body reacts by increasing the blood flow and the permeability of the blood vessels, facilitating the escape of cells from the blood into the tissues (Tan *et al.*, 1999). Chronic inflammation of the skin or joints may lead to psoriasis or rheumatic arthritis and severely damage the body (Pope *et al.*, 1999). Sponges have proved to be a remarkable source of anti-inflammatory compounds (Fig. 1).

Manoalide, is an unusual sesquiterpenoid, which was originally obtained from the sponge *Luffariella variabilis* (De Silva and Scheuer, 1980). Its anti-inflammatory action is based on the irreversible inhibition of the release of arachidonic acid from membrane phospholipids by inhibiting the binding of the the enzyme phospholipase A2 to the membranes (Glaser *et al.*, 1989).

Scalaradial is a tetracyclic sesterterpene possessing a scalarane carbon skeleton, which was originally isolated from the sponge *Cacospongia mollior* (Cimino *et al.*, 1974). Scalaradial is an inhibitor of PMA-induced arachidonic acid release *in vivo* in the mouse peritoneal macrophage, as well as a potent bee venom PLA2 inhibitor (Carvalho and Jacobs, 1991).

Contignasterol is a highly oxygenated sterol, which was originally isolated from the sponge *Petrosia contignata* (Burgoyne *et al.*, 1992). Contignasterol was shown to inhibit the histamine release induced by anti-immunoglobulin E (anti-Ige) from sensitized rat mast cells in a dose dependent manner, indicating that this is a potential anti-inflammatory compound (Takei *et al.*, 1994).

Topsentin is a bis-indole alkaloid isolated from the Mediterranean sponge *Topsentia genitrix* (Bartik *et al.,* 1987). It was found to inactivate PLA2 and to inhibit PMA-induced mouse ear oedema, comparable to the anti-inflammatory effects of standards such as hydrocortisone and indomethacin B. (Wylie *et al.,* 1995).
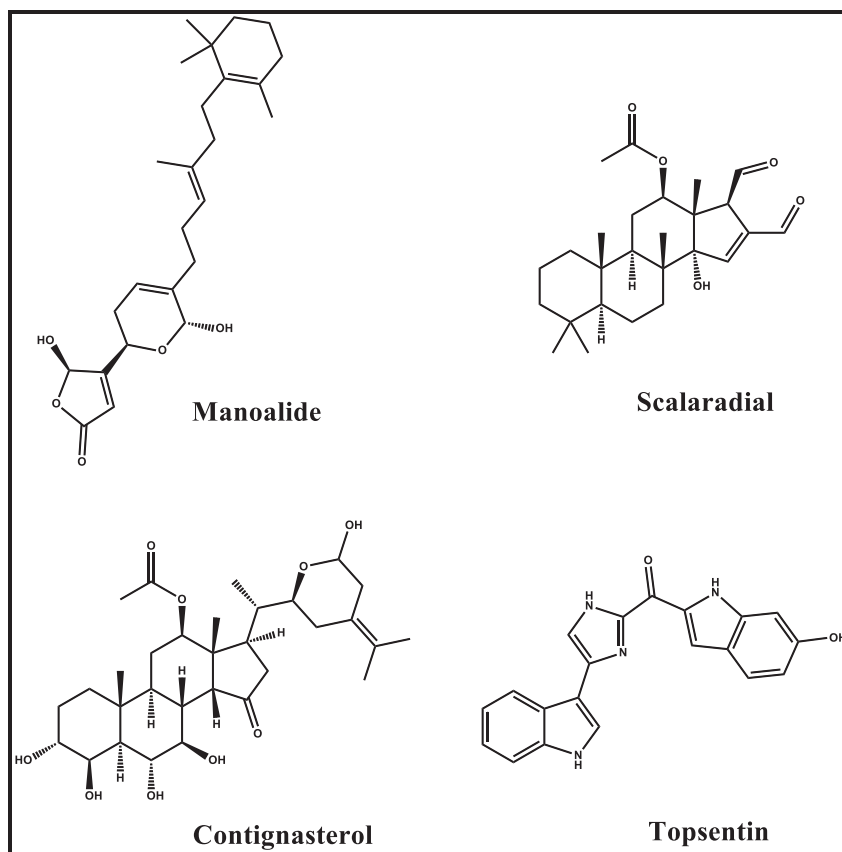
Figure 1.1: Anti-inflammatory marine natural products

1.2.2. Antitumor marine natural products

Cancer is the rapid formation of abnormal cells that grow beyond their natural boundaries, and which can then occupy adjacent parts of the body and spread to other organs (Stewart and Wild, 2014). This progression is referred to as metastasis, which is the main cause of death from cancer (Stewart and Wild, 2014). Natural products and their derivatives have been the mainstay of cancer therapy for the past 40 years. The relevance of the sea as a tool to discover novel bioactive compounds was corroborated by the discovery and marketing approval of cytarabine (Ara-C) (Bergmann *et al.*, 1985). Cytarabine is a semi-synthetic derivative of spongothymidine, a pyrimidine nucleoside analogue, which was originally isolated from the Caribbean marine sponge *Tethya crypta* (Bergmann and Feeney, 1950). Cytarabine is intracellularly converted to cytosine arabinoside triphosphate, which competes with the physiological substrate deoxycitidine triphosphate, and thus acts as antimetabolite cytotoxic agent inhibiting the synthesis of DNA (Mayer *et al.*, 2010). Since then, three marine drugs have been approved as anticancer agents including ET-

743 (Yondelis, EU registered 2007), eribulin mesylate (Halaven, FDA approval 2010), and brentuximab vendotin (SGN-35, FDA approval 2011). Additionally there is an abundant pipeline of preclinical marine compounds to suggest their contimued application as antitumor drugs (Mayer *et al.,* 2010).

Plitidepsin (Aplidin™) is a macrocyclic depsipeptide, which was originally obtained from the Mediterranean tunicate *Aplidium albicans* (Rinehart *et al.*, 2000). Plitidepsin highly induces cell death (apoptosis) with IC_{50} values at submicromolar concentrations (Mayer *et al.,* 2010). Specifically, it causes rapid activation of apoptosis as a result of activation of p38-MAPK, EGF receptor, and Src protein kinases, as well as induction of oxidative stress (Garcia-Fernandez *et al.,* 2002).

Hemiasterlin is a tripeptide, which was originally isolated from the sponge *Hemiasterella minor* (Talpir *et al.*, 1994). Hemiasterlin exhibited remarkable cytotoxicity against several tumor cell lines with IC_{50} values in the nanomolar range (Coleman *et al.*, 1994). Mechanistic studies showed that the remarkable activity hemiasterlins is based on the induction of mitotic arrest in metaphase as described for the well-studied tubulin binders taxol and vincristine (Molinski *et al.*, 2009). Molecular modelling studies likewise suggested that binding takes place near the α/β interface of the vinca domain β-tubulin, which is a known target for the tubulin inhibitors phomopsin A and dolastatin 10 (Mitra *et al.*, 2004). In addition, it was shown that hemiasterlin A induces microtubule depolymerization at high concentrations (Molinski *et al.*, 2009). Interestingly, hemiasterlin is a poor substrate for P-glycoprotein transporters, whereas it maintains toxicity against multidrug resistant tumor cell lines, thus hinting at its potential as a lead structure for the development of novel anticancer drugs (Loganzo *et al.,* 2003).

(+)-Discodermolide was isolated from the deep-water marine sponge *Discodermia dissoluta* (Gunasekera *et al.*, 1990). (+)-Discodermolide induces G2/M phase cell-cycle arrest in lymphoid and non-lymphoid cells with IC_{50} values at nanomolar concentrations (De Souza *et al.*, 2004). In addition, (+)-discodermolide displayed immunosuppressant activity (Longley *et al.,* 1991). Interestingly, the enantiomer (–)-discodermolide prepared by total synthesis showed less cytotoxicity than the natural (+)-discodermolide (Nerenberg *et al.*, 1993). Mechanistic studies showed that (+)-discodermolide stabilized microtubules with even higher affinity than that reported for taxol (Hung *et al.*, 1996). However, despite their competitive

inhibitory activity, both compounds showed strongly synergistic activity (Martello *et al.*, 2000), signifying the potential use of (+)-discodermolide in combination therapy.

Kahalalide F is a depsipeptide, which was originally isolated from the sacoglossan (sea slug) *Elysia rufescens*, an herbivorous opisthobranch. *E. rufescens* feeds on the alga *Bryopsis* sp. (Hamann *et al.*, 1993), and thus the latter is considered to be the the original source of kahalalide F. However, in *E. rufescens* the observed concentration of kahalalide F is higher (1%) compared with *Bryopsis* sp. (0.0002%), indicating that *E. rufescens* accumulates this compound as a chemical defense against predators (Becerro *et al*., 2001). Studies on the mode of action of kahalalide F showed that it disrupts lysosomal membranes, which is in accordance with the high concentration of lysosomal proteins found on prostate cells (Garcia-Rocha *et al.*, 1996). Moreover, kahalalide F induced oncotic cell death (necrosis associated with karyolysis) in human prostate cancer cells (Suarez *et al.*, 2003). In addition, kahalalide F induces channel formation and subsequent cell membrane permeability in HepG2 cells (Sewell *et al.*, 2005).

Plitidepsin

Hemiasterlin

(+)-Discodermolide

Kahalalide F
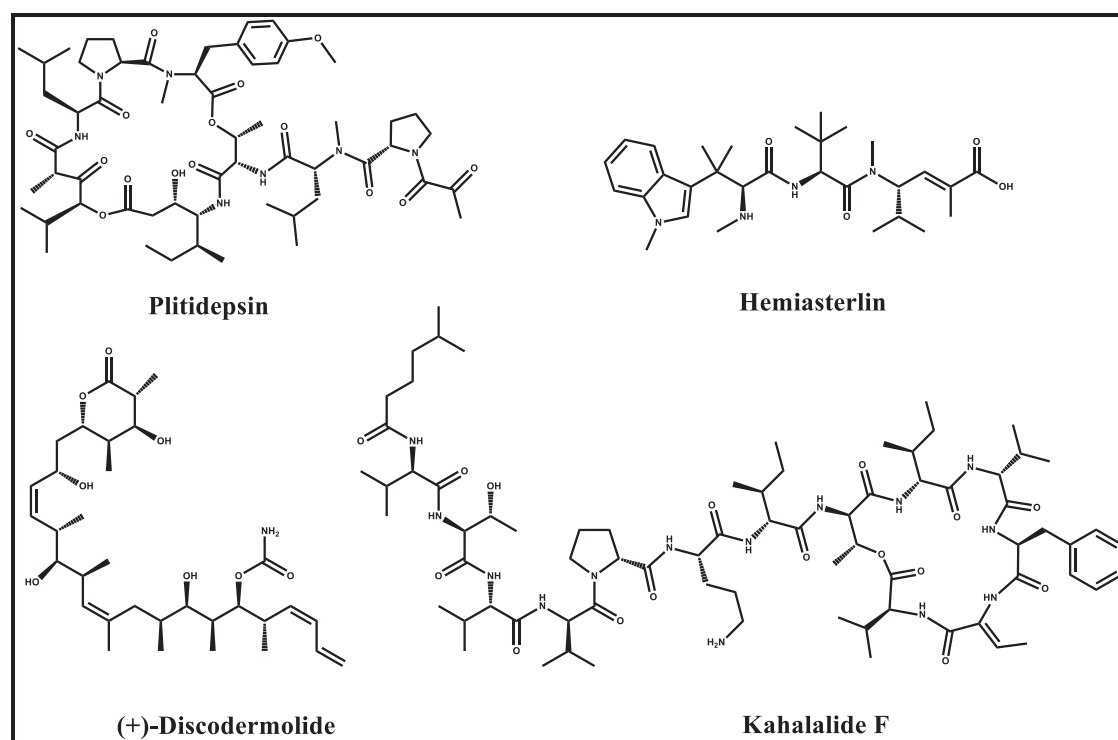
Figure 1.2: Antitumor marine natural products

1.2.3. Protein kinase inhibitors

A fundamental mechanism of cell communication in multicellular organisms is via binding of ligands to cell surface receptors with kinase catalytic activity. Protein kinases (PKs) are enzymes in that catalyze the transfer of a phosphate moiety from a high-energy molecule, commonly adenine triphosphate (ATP), to another substrate (Skropeta *et al.*, 2011). Phosphorylation mostly results in a functional modification of the target protein by altering enzyme activity, and/or association with other proteins (Hubbard and Till, 2000). The human genome comprises a total of 518 protein kinases, including 478 classical PKs and 40 atypical PKs. The former consist of 388 serine/threonine kinases and 90 tyrosine kinases, as well as 50 sequences lacking a functional catalytic site (Manning *et al.*, 2002). Serine/threonine kinases transfer a phosphate group to a serine or threonine amino acid residue, whereas tyrosine protein kinases recognise and phosphorylate a protein at a tyrosine moiety (Skropeta *et al.*, 2011).

PKs mediate a plethora of signaling pathways within cells and play a central role in various biological processes, including control of cell growth, metabolism, cell cycle progression, and apoptosis (Manning *et al.*, 2002). Thus, the development of selective protein kinase inhibitors that can impede or modulate diseases associated with abnormalities in these specific signaling pathways is extensively considered as a promising approach for drug development (Fabbro *et al.*, 2002). Numerous natural products of marine origin have been reported to inhibit protein kinases (*Bharate et al.*, 2013).

Bryostatin 1 is a macrocyclic lactone, originally isolated from the marine bryozoan *Bugula neritina* (Pettit *et al.,* 1982). It features a polyacetate carbon backbone skeleton bearing 11 stereocenters, which is unprecedented among natural products (Molinski *et al.*, 2009). Mechanistic studies showed that bryostatin 1 causes significant downregulation of protein kinase C (PKC). PKC is a tumor promoting receptor and as a result bryostatin 1 leads to inhibition of tumor cell growth (Hennings *et al.,* 1987). Moreover, this compound inhibits the growth of murine P388 leukemia cells at subnanomolar concentrations (Brown *et al.,* 2000). However, the positive effects of bryostatin are obtained only when combined with other anticancer agents, including taxol, vincristine, and dolastatin, among others (Mutter *et al.,* 2000).

Hymenialdisine is a marine component that has been isolated from many marine sponges belonging to the genera *Acanthella*, *Axinella* and *Hymeniacidon*

(Mattia *et al.*, 1982; Cimino *et al.*, 1982; Kitagawa *et al.*, 1983). Hymenialdisine is a potent (IC_{50}=10 $-$ 40 nM) inhibitor of the protein serine/threonine kinases CDK5, mitogen-activated protein kinase-1, and casein kinase 1, which regulate several vital cellular functions such as gene expression, cellular proliferation, membrane transport and apoptosis (Meijer *et al.*, 2000). In addition, hymenialdisine inhibited several pro-inflammatory cytokines (IL-1, IL-2, IL-6, and NO), through inhibition of the NF-kB signalling pathway that is potentially effective for treatment of various inflammatory diseases such as rheumatoid arthritis and osteoarthritis (Sharma *et al.*, 2004).

Aeroplysinin-1 is a bromotyrosine metabolite isolated from the sponges of the genus *Aplysina* (Proksch *et al.*, 2002). All *Aplysina* sponges accumulate isoxazoline bromoalkaloids, such as isofistularin-3, aplysinamisin-1, and aerophobin-2 (Ebel *et al.*, 1997). However, following disruption of the sponge tissue, these alkaloids are transformed through enzyme-mediated catalysis to aeroplysinin-1 (Proksch *et al.*, 2002). Despite the fact that the isoxazoline precursors exhibit no or only weak antibiotic activity, aeroplysinin-1 shows potent activity against numerous marine and terrestrial bacteria, and hence the formation of aeroplysinin-1 has been proposed to be implicated in the chemical defense of sponges against invading pathogenic bacteria (Weiss *et al.*, 1996). Moreover, aeroplysinin-1 was found to inhibit epidermal growth factor (EGF) receptor, followed by suppression of angiogenesis *in vivo* and of proliferation of cancer cell lines (Hinterding *et al.*, 1998; Haefner *et al.*, 2003).

Halenaquinone is a polyketide isolated from the Okinawan sponge *Xestospongia exigua* (Roll and Scheuer, 1983). Halenaquinone was shown to inhibit the tyrosine kinase activity of EGF and pp60[V-SRC] receptors in the low micromolar range. As a result, it inhibits the proliferation of several cell lines, including those transformed by oncogenic PTKs (Lee *et al.*, 1992; Skropeta *et al.*, 2011). Apart from its cytotoxicity, halenaquinone was also shown to possess antibiotic and cardiotonic effects (Schmitz and Bloor, 1988), which initiated further interest for several structure activity relationship studies (Nobuyuki *et al.*, 1988; Toyooka *et al.*, 1992).
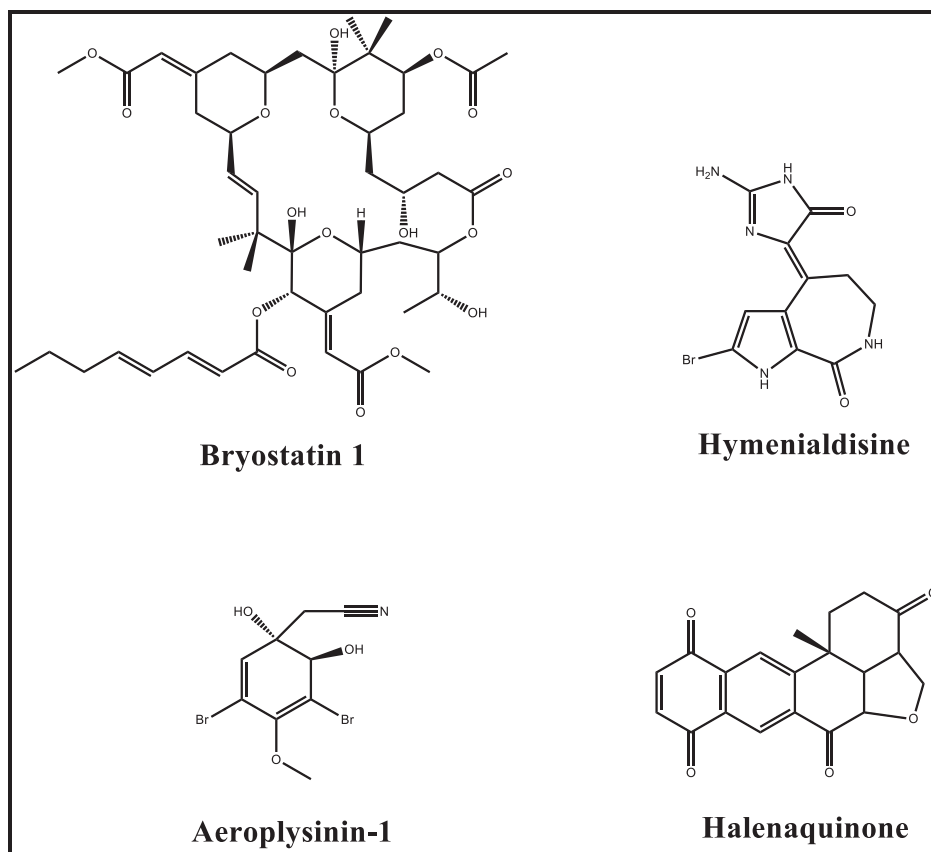
Figure 1.3: Marine Protein kinase inhibitors

1.2.4. Antiviral marine natural products

Marine sponges are rich sources of potent antiviral agents that have been advanced to clinical studies, with most of them screened toward human immunodeficiency virus (HIV) and Herpes simplex virus (HSV) (Sagar *et al.*, 2010). An example of sponge-derived antiviral metabolite that has successfully entered the pharmaceutical market is the nucleoside vidarabine (Ara-A). Vidarabine was synthetically developed from spongouridine, a nucleoside analogue from the Caribbean sponge *Tethya crypta* (Bergmann and Feeney, 1950). Mechanistic studies showed that it is readily transformed to adenine arabinoside triphosphate, followed by inhibition of the viral DNA polymerase (Mayer *et al.,* 2010). Vidarabine has been used herpes virus infection treatment, although it was discontinued in the USA by June 2001, probably due to its low therapeutic window with regard to antiviral compounds currently on the market (Newman and Cragg, 2004).

A number of sponge-derived lead compounds have been discovered that have the potential as promising antiviral agents (Sagar *et al.*, 2010).

Avarol, originally isolated from the marine sponge *Dysidea avara*, is a sesquiterpene quinol, possessing an unusual rearranged drimane skeleton (Minale *et al.*, 1974). Interestingly, avarol showed inhibitory activity toward HIV and human T-lymphotropic retrovirus (HTLV III) in human H9 cells at submicromolar concentrations (Sarin *et al.*, 1987). The antiviral activity of avarol was caused by an enhancement in the intracellular concentration levels of superoxide radicals, including glutathione peroxidases and dismutases (Batke *et al.*, 1988; Sagar *et al.*, 2010). Moreover, avarol completely inhibited glutamine tRNA, which is important for viral protease synthesis required for viral proliferation (Müller *et al.*, 1988). The antiviral activity of the quinone structural analogue of avarol, namely **avarone**, from the marine sponge *Dysidea avara* has likewise been reported (Sarin *et al.*, 1987).

Papuamides A and **B** are cyclic depsipeptides, originally isolated from the Papua New Guinea marine sponge of the genus *Theonella* (Ford *et al.*, 1999). Both compounds were tested toward CEM-SS T-cells and were found to possess remarkable activity at nanomolar concentrations (Xie *et al.*, 2008). Papuamides A and B are assumed to interact with the phospholipid phosphatidylserine, which is expressed on the viral membrane and is responsible for the antiviral activity of papuamides (Andjelic *et al.*, 2008). Interestingly, the antiviral activity of these peptides was independent of chemokine co-receptors that are known to be involved in the process of recognition and viral cell entry (Esté *et al.*, 2007).

4-Methylaaptamine is an alkaloid, originally isolated from a marine sponge of the genus *Aaptos*. (Coutinho *et al.*, 2002). Interestingly, 4-methylaaptamine displayed inhibition of HSV-1 in Vero cells with an IC_{50} value of 2.4 μM, which is more potent than that of the positive control acyclovir (8.6 μM) (Souza *et al.*, 2007) Subsequent mechanistic studies indicated that 4-methylaaptamine inhibited HSV-1 replication, by impeding viral entry into the host cells as well as by reducing ICP27 expression (Souza *et al.*, 2007). Moreover, 4-methylaaptamine was found to be not cytotoxic, and thus this alkaloid could be considered as a potential antiviral agent toward HSV-1 (Souza *et al.*, 2007).

Mycalamide A is a heterocyclic compound, possessing a trioxadecalin ring system, originally isolated from a marine sponge of the genus *Mycale* (Perry *et al.*, 1988). Mycalamide A was active toward A59 corona, herpes simplex type I, and polio type I viruses at submicromolar concentrations (1–2 ng/disc) (Perry *et al.*, 1990). The mode of action of mycalamide A was investigated and it was shown that it inhibits

protein biosynthesis. (Burres and Clement, 1990). In a subsequent study, the mode of action of mycalamide A was likewise investigated and it was shown that it binds to the large ribosomal subunit of *Haloarcula marismortui* followed by inhibition of RNA translation into protein, which is in agreement with the previously reported results (Gurel *et al.*, 2009). Moreover, mycalamide A analogues have been described to inhibit multiplication of influenza virus via interaction with nucleoproteins (NPs) (Hagiwara *et al.*, 2010). Therefore, the antiviral effect of mycalamide A may be attributed to its property as a protein synthesis inhibitor (Sagar *et al.*, 2010).
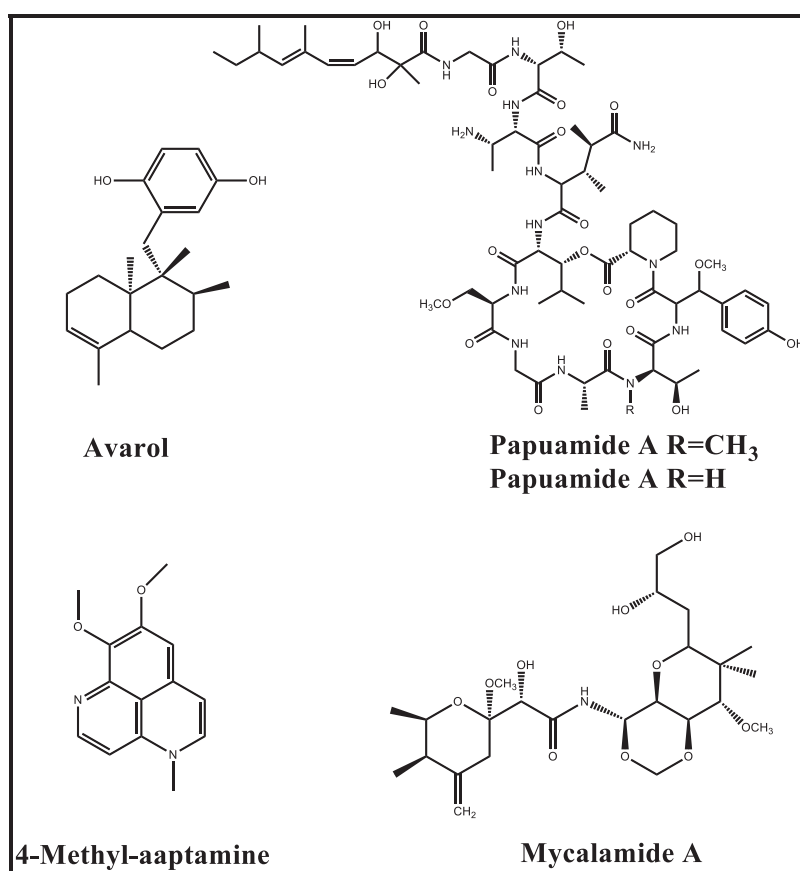
Figure 1.4: Antiviral marine natural products

1.2.5. Antitubercular marine natural products

Mycobacterium tuberculosis, the major causative agent of tuberculosis (TB), is one of the primary reasons of human mortality caused by infective microorganisms (Smith, 2003; Daletos *et al.*, 2015). At present, one third of the world's population is infected with *M. tuberculosis* and around 9 million new cases of tuberculosis are described every year (García *et al.*, 2012; Daletos *et al.*, 2015, WHO report 2015). In

addition, TB treatment is gradually facing serious obstacles due to the increased incidence of multidrug-resistant (MDR) and extensively drug-resistant (XDR) *M. tuberculosis* strains as well as due to the emergence of TB associated with viral infections such as HIV (Nora de Souza *et al.*, 2009). Thus, there is an urgent call for new antitubercular (anti-TB) drugs (Daletos *et al.*, 2015). Marine sponges producing unique and wide range of bioactive metabolites, emerge as prolific sources of new antituberculosis agents (Laport *et al.,* 2009).

Halicyclamine A is a tetracyclic alkaloid, originally obtained from the marine sponge *Haliclona* sp. (Jaspars *et al.*, 1994). Halicyclamine A was found to inhibit *M. tuberculosis* H37Ra with a MIC of 5.0 µg/ml under both aerobic and hypoxic conditions (Arai *et al.*, 1994). Moreover, it did not show cross-resistance with the anti-tuberculosis drugs ethambutol, isoniazid or rifampicin,. Interestingly, the mode of action of halicyclamine A was considered to be through inhibition of inosine 5′-monophosphate dehydrogenase (IMPDH) (Jaspars *et al.*, 1994). However, it displayed similar MIC values against the wild-type and IMPDH over-expressing *M. tuberculosis* strains, thus suggesting that IMPDH is not the target molecule of the anti-mycobacterial activity of halicyclamine A (Arai *et al.*, 1994).

Heteronemin is a scalarane-type sesterterpene that was originally isolated from the sponge *Heteronema erecta* (Arai *et al.*, 1994). It showed inhibition of *M. tuberculosis* (H37Rv) with an MIC of 6.25 µg/mL (Wonganuchitmeta *et al.*, 2004). Interestingly, this was the first report of anti-TB activity for this intriguing class of compounds. Furthermore, in a study investigating the mechanism of action of heteronemin, it was shown that it inhibited proteasome inhibition and TNF-α-induced NF-κB activation, thus inducing apoptotic cell death (Schumacher *et al.*, 2010).

1.2.6. Antimalarial marine natural products

Malaria is an exceptionally serious disease in sub-Saharan Africa, as well as a serious public health issue in certain Southeast Asia and South America regions of (Snow *et al.*, 2005). Around 40% of the world population lives in endemic areas and 350–500 million clinical incidences occur each year, causing more than 2.0 million deaths (Snow *et al.*, 2005). Protozoa from the genus *Plasmodium* (i.e. *P. falciparum*, *P. ovale*, and *P. malariae*) are the cause of malaria, with *P. falciparum* being the prominent agent responsible for most fatal cases (Mishra *et al.*, 1999). Removal of the vector of transmission (the *Anopheles* mosquito) is not feasible, and thus new

antimalarial agents with novel modes of action are urgently needed to combat resistance to the current antimalarial drugs, including quinolines and artemisinins (Fidock *et al.*, 2004).

Manzamine A is an unusual polycyclic β-carboline alkaloid originally obtained from an Okinawan marine sponge of the genus *Haliclona* (Sakai *et al.*, 1986). Manzamine A strongly inhibited the growth of *P. falciparum* at submicromolar concentrations both *in vitro* (IC_{50} = 5.0 ng/mL) and *in vivo* (at the same concentration as the positive control artemisinin) (Ang *et al.*, 2000). Moreover, manzamine A analogues have also displayed, antifungal, antibacterial and antitubercolosis effects, as well as activity against HIV/AIDS opportunistic infections (e.g. the protozoan *Toxoplasma gondii*) (Rao *et al.*, 2003, Yousaf *et al.*, 2004). Therefore, manzamine A is a potential candidate for further development as a promising lead against malaria and other serious infectious diseases.

Plakortin is a 1,2-dioxane polyketide metabolite, originally isolated from the marine sponge *Plakortis halichondroides* (Higgs *et al.*, 1978) and later obtained in large amounts from the marine sponge .*P. simplex* (Cafieri *et al.*, 1999). This compound displayed remarkable activity toward chloroquine-resistant strains of *P. falciparum*, whereas it was devoid of cytotoxicity (Campagnuolo *et al.*, 2005). Structure-activity relationship studies indicated that the endoperoxide functionality plays an important role for the antimalarial activity of plakortin, given that the respective diol was totally inactive (Fattorusso *et al.*, 2006). Remarkably, plakortin is thought to be produced by a bacterial symbiot of the sponge *Plakortis simplex* (Laroche *et al.*, 2006). Therefore, identification of the respective gene cluster could allow the production of plakortin by bacterial fermentation, overcoming the supply problem that is commonly encountered in marine natural products research. (Fattorusso and Taglialatela-Scafati, 2009).

Halicyclamine A

Heteronemin

Manzamine A

Plakortin A
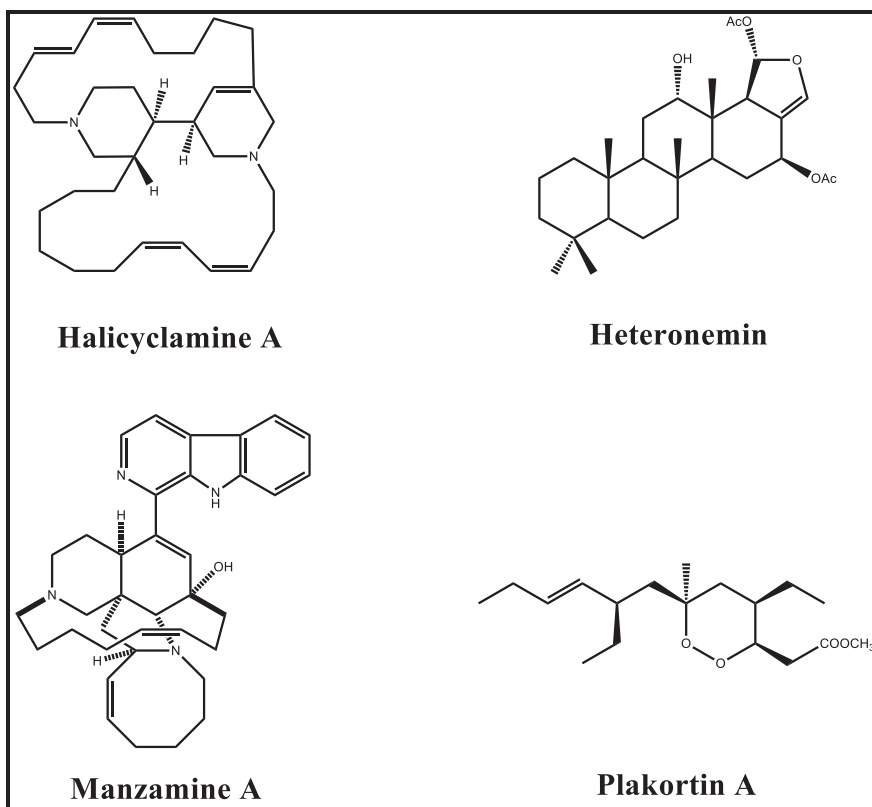
Figure 1.5: Antitubercular and antimalarial marine natural products

1.3. The current status of marine natural products research

Marine sponges are one of the most prolific sources of biologically active compounds occurring in the marine environment (Sagar *et al.*, 2010). The global marine preclinical and clinical pharmaceutical pipelines remain astonishingly active with a plethora of marine-derived metabolites entering clinical studies (Mayer *et al.*, 2013; Martins *et al.*, 2014). In 2004, the only FDA/EMEA approved drugs were cytarabine, vidarabine, ziconotide and omega-3 fatty acids. However, in 2013, the number of FDA/EMEA approved marine drugs doubled (Table 1.1), indicating the value of marine natural products as remarkably interesting candidates aimed at drug discovery and development (Martins *et al.*, 2014).

Eribulin mesylate (Halaven®, FDA-approved 2010), a synthetic analogue of halichondrin B, originally derived from the marine sponge *Halichondria okadai*, is a noteworthy example of approved marine-derived drugs. It is a tubulin-targeting chemotherapeutic drug that inhibits the proliferation of numerous cancer cell lines (Ortega and Cortés, 2012). Mechanistic studies showed that eribulin exerts its cytotoxicity via a novel action on tubulin, principally by binding to a small number of high affinity sites at the plus ends of microtubules (Smith *et al.*, 2012).

Brentuximab vedotin (Adcetris®, FDA-approved 2011) is currently the latest example of a marine drug that has successfully entered the market (Martins *et al.*, 2014). This drug was approved for the treatment of Hodgkin and systemic anaplastic large cell lymphoma (Senter and Sievers, 2012). Its structure is based on a synthetic analog of dolastatin 10, monomethyl auristatin E, connected to an anti-CD30 antibody (Martins *et al.*, 2014). It should be noted that dolastatins, originally isolated from the sea hare *Dolabella auricularia*, have shown remarkable cytotoxicity *in vitro*, but phase I and II clinical studies were unsuccessful due to presence of side effects. However, taking advantage of the progress on the development of antibody-drug conjugates (ADCs), connecting monomethyl auristatin E to an antibody that targets the cell membrane protein CD30 (brentuximab vendotin), yielded an effective agent with favorable safety profile (Bauer and Bronstrup, 2013).

The development of new drugs from marine natural products is undoubtedly on the horizon. Recent advances in sampling strategies and in NMR methodologies, such as nanoscale-NMR techniques for structure determination, are foundamental for the discovery of novel marine natural products as leads in drug development (Liu *et al.*, 2012).

Table 1.1: Selected marine natural products in clinical and preclinical trials (Martins *et al.*, 2014)

Name	Source	Therapeutic area	Status (2013)
Spongothymidine	*Cryptotethya crypta*	Cancer	Approved
Spongouridine	*Cryptotethya crypta*	Viral infection	Discontinued
Omega-3-fatty acids	Fish	Hypertriglyceridemia	Approved
ω-Conotoxin	*Conus magus*	Neuropathic Pain	Approved
Ecteinascidin 743	*Ecteinascidia turbinate*	Cancer	EU-approved
Halichondrin B	*Halichodria okadai*	Cancer	Approved
Dolastatin 10	*Dolabella auricularia*	Cancer	Approved
Pliditepsin	*Aplidium albicans*	Cancer	Phase II/III
Tetrodotoxin	Pufferfish	Pain: Chronic Pain	Phase II/III
Bryostatin I	*Bugula neritina*	Cancer	Phase I/II

1.4. Aim and scope of the study

Sponges are hitherto the most prolific sources of bioactive and structurally unique secondary metabolites in the marine environment with a vast medicinal potential, predominantly in the area of cancer, anti-inflammatory and analgesy (Proksch *et al.*, 2002).

The aim of this study was the isolation and structure elucidation of novel bioactive secondary metabolites from several sponge extracts, as well as the preliminary evaluation of their biological properties and pharmaceutical potential. Six marine sponges, *Dactylospongia metachromia*, *Callyspongia aerizusa*, *Acanthostrongylophora ingens*, *Sarcotragus spinosulus*, *Dysidea avara*, and *Agelas oroides* were investigated as biological objects of this study.

Bioassay-guided isolation of secondary metabolites was achieved through solvent extraction of marine sponges followed by various chromatographic techniques, such as column chromatography and semipreparative HPLC. Afterwards, the obtained fractions were analysed by HPLC for their purity and by LC-ESI-MS for their molecular weight and fragmentation patterns and monitored by bioactivity assays. The structures of the isolated compounds were unequivocaly elucidated by one- and two-dimensional NMR and by MS (HRESIMS) analysis, as well as by comparison with the literature. In addition, selected chiral compounds were derivatized to establish their absolute stereochemistry.

Chromatographic fractions and pure compounds were subjected to selected bioassays to evaluate their pharmaceutical potential, including cytotoxicity (MTT), antimycobacterial and protein kinase inhibitory activities. The assays were conducted in cooperation with Prof. W. E. G. Müller, Mainz, Dr. Rainer Kalscheuer, Düsseldorf, and ProQinase, Freiburg, respectively.

2. Materials and Methods

2.1. Biological materials

Sponge specimens were collected by scuba diving in three different collection sites in Indonesia (Makassar, S. Sulawesi; Lembeh, N. Sulawesi; Ambon, Maluku) and the Mediterranean Sea (Fethiye, Turkey). The specimens were preserved in a mixture of EtOH and H_2O (70:30) and stored in a −20 °C freezer until extraction. The voucher specimens were identified by Dr. Nicole de Voogd (Netherlands Centre for Biodiversity Naturalis, P.O. Box 9517, 2300 RA Leiden, the Netherlands) (Daletos *et al.,* 2014; Daletos *et al.,* 2015).

2.1.1. Sponges

Sponges are animals belonging to the phylum Porifera that literally means "bearing pores" (Kingdom Animalia). They are the oldest metazoans present at all water depths, from the tidal zone to the deepest regions (abyssal zone) (Müller, 1998). Calcarea and Demospongiae sponges are found in sublittoral rocky-bottom habitats, whereas Hexactinellida sponges are mainly found in muddy-bottom habitats of the deepest parts of the oceans (Van Soest *et al.,* 2015). Interestingly, sponges of the family Spongillidae (class Demospongiae) are adapted to the fresh waters of rivers and lakes. Currently, there are 8.603 valid species recognized (Van Soest *et al.*, 2015).

The outer surface of sponges is covered with tiny pores, which filter ambient water into the sponge body (Van Soest *et al.,* 2015). These pores lead to a system of internal canals, in which a continuous water flow is maintained by specialized collar cells providing oxygen and nutrients to the sponge. Lining these canals are special, which maintain a continuous water flow through the sponge to obtain and to remove carbon dioxide and waste (Müller, 1998).

The body of sponges is composed of a jelly-like mesohyl between a layer of conical cells (choanocytes) and a layer of flattened cells (pinacocytes), which are responsible for maintaining their structure and size (Müller, 1982). Remarkably, sponges lack nervous, digestive, or circulatory systems (Müller, 1998). Their skeleton consists of mineralized substances (calcareous or siliceous) or a collagen-type protein called spongin. Spicules are units of mineralized substances that are scattered throughout the sponge and their function is to aid protection or support (Uriz1 *et al.*, 2003). Notably, the skeleton is of great taxonomic significance and according to its composition, sponges are hitherto divided into Demospongiae, Calcarea,

Hexactinellida, and Homoscleromorpha (Müller, 2006). Demospongiae and Hexactinellida (or glass sponges) have siliceous spicules with the latter forming six fused rays as denoted by their names (Bergquist *et al.*, 2002). On the other side, Calcarea have skeletons made of calcite, which is a form of calcium carbonate (Bergquist *et al.*, 2002). Homoscleromorpha were previously considered as members of the class of Demospongiae. However, on the basis of recent molecular phylogenetic studies, they have recently been recognized as a new class of sponges (Gazave *et al.*, 2012). In contrast to Demospongiae, the skeleton of Homoscleromorpha is amorphous and not well organized indicative of the absence of a tertiary protein structure (Gazave *et al.*, 2012).

2.1.1.1. *Dactylospongia metachromia*

A specimen of *Dactylospongia metachromia* (Phylum: Porifera, Class: Demospongiae, Order: Dictyoceratida, Family: Thorectidae) (Fig. 2.1) was collected at Ambon, Indonesia, in August 1996 by Dr. Elisabeth Ferdinandus (University Pattimura, Ambon). A voucher specimen is kept in ethanol under registration number ZMAPOR 19107 at the Zoological Museum, Amsterdam, The Netherlands.

2.1.1.2. *Callyspongia aerizusa*

In this study we examined four separate collections of *Callyspongia aerizusa* (Phylum: Porifera, Class: Demospongiae, Order: Haplosclerida, Family: Callyspongiidae) (Fig. 2.2) obtained from three different regions in Indonesia as indicated: Makassar, S. Sulawesi (TF23, TF90); Lembeh, N. Sulawesi (SP3); and Ambon, Maluku (TF40). The collection was made by Dr. Elisabeth Ferdinandus (University Pattimura, Ambon) and Prof. Dr. Sumali Wiryowidagdo (University Hassanudin, Makassar) (Hooper, *et al.*, 2002). Voucher specimens are deposited at the Zoological Museum, Amsterdam, The Netherlands, under the registration numbers RMNH POR.6169 (TF23), RMNH POR.6170 (TF40), and RMNH POR.6171 (TF90).

2.1.1.3. *Acanthostrongylophora ingens*

A specimen of *Acanthostrongylophora ingens* (Phylum: Porifera, Class: Demospongiae, Order: Dictyoceratida, Family: Thorectidae) (Figure 2.3) was collected at Ambon, Indonesia, in August 1996 by Dr. Elisabeth Ferdinandus (University Pattimura, Ambon). A voucher specimen is kept in ethanol under

registration number RMNH POR.6172 at the Zoological Museum, Amsterdam, The Netherlands.

2.1.1.4. *Sarcotragus spinosulus*

A specimen of *Sarcotragus spinosulus* (Phylum: Porifera, Class: Demospongiae, Order: Dictyoceratida, Family: Thorectidae) (Figure 2.4, photo: G. Corriero, 1996) was collected in Fethiye, Turkey, in August 2006. A voucher specimen is kept in ethanol under registration number RMNH POR.6173 at the Zoological Museum, Amsterdam, The Netherlands.

2.1.1.5. *Dysidea avara*

A specimen of *Dysidea avara* (Phylum: Porifera, Class: Demospongiae, Order: Dictyoceratida, Family: Dysideidae) (Figure 2.5, De Caralt *et al.*, 2010) was collected in Ayvalic, Turkey, in August 2012. The sponge is rosy to violet similar to the common Mediterranean species *Dysidea fragilis* (Carballo *et al.,* 1994). A voucher specimen is kept in ethanol under registration number RMNH POR.6174 at the Zoological Museum, Amsterdam, The Netherlands.

2.1.1.6. *Agelas oroides*

A specimen of *Agelas oroides* (Phylum: Porifera, Class: Demospongiae, Order: Dictyoceratida, Family: Dysideidae) (Figure 2.6, photo: M.J. de Kluijver, 2012) was collected in Ayvalic, Turkey, in August 2012. A voucher specimen is kept in ethanol under registration number RMNH POR.6175 at the Zoological Museum, Amsterdam, The Netherlands.
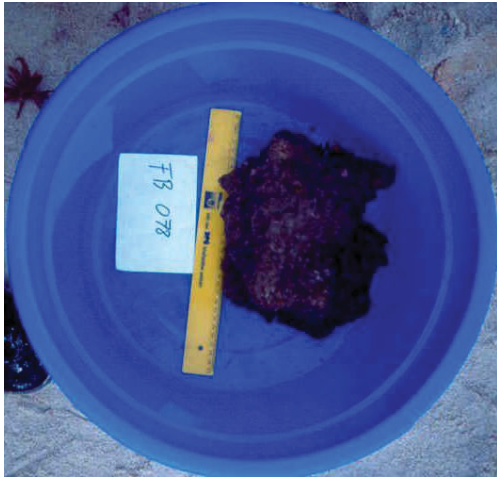
Fig. 2.1. *Dactylospongia metachromia*
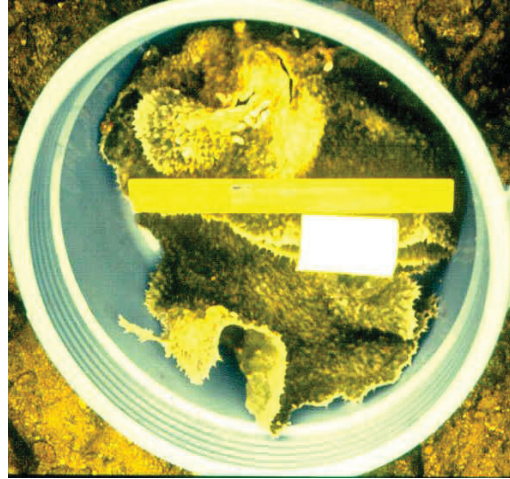
Fig. 2.2. *Callyspongia aerizusa*
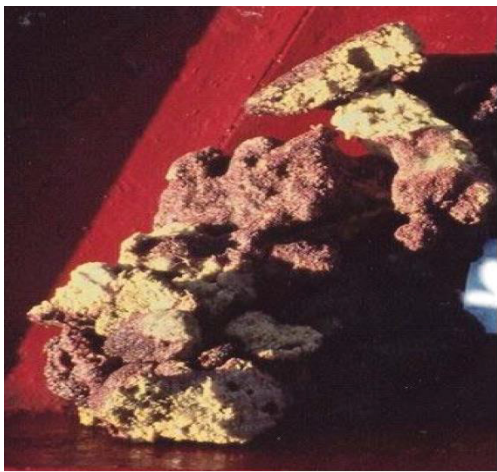
Fig. 2.3. *Acanthostrongylophora ingens*

Fig. 2.4. *Sarcotragus spinosulus*[1]
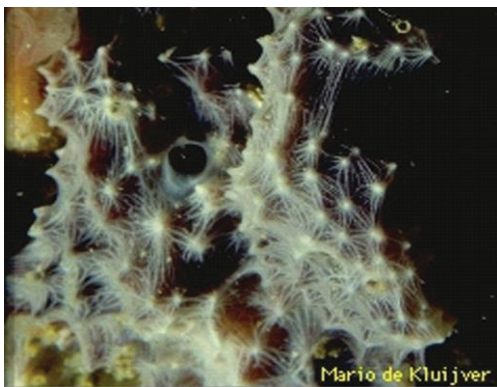
Fig. 2.5. *Dysidea avara*[2]

Fig. 2.6. *Agelas oroides*[3]

[1] http://species-identification.org/species.php?species_group=sponges&menuentry=soorten&id=402&tab=classificatie
(Photo G. Corriero)

[2] http://species-identification.org/species.php?species_group=sponges&menuentry=soorten&id=213&tab=classificatie
(Photo Mario de Kluiver)

[2] http://www.marinespecies.org/porifera/porifera.php?p=image&pic=48507 (Rob van Soest *et al.*, 2016)
(Photo Mario de Kluiver)

2.2. Chemicals

2.2.1. General laboratory chemicals

Anisaldehyde (4-methoxybenzaldehyde)	Merck
(-)-2-Butanol	Merck
Dimethylsulfoxide	Merck
Formaldehyde	Merck
Hydrochloric acid	Merck
Potassium hydroxide	Merck
Pyridine	Merck
Concentrated sulphuric acid	Merck
Ninhydrin	Merck
Formic acid	Merck
Trifloroacetic acid (TFA)	Merck
Concentrated ammonia solution	Fluka
Formic acid	Merck
N-(5-fluoro-2,4-dinitrophenyl)-L-Alaninamide	Merck
Amino acids standards	Sigma
Sodium hydrogen carbonate	Sigma

2.2.2. Chromatography

2.2.2.1. Stationary phases

Pre-coated TLC plates, Silica Gel 60 F_{254}, layer thickness 0.2 mm	Merck
Precoated TLC plates, Diol, F254 S, layer thickness 0.25 mm	Merck
Silica Gel 60, 0.04 – 0.063 mm mesh size	Merck
RP-18, 0.04 – 0.0.63 mm mesh size	Merck
Sephadex LH-20, 0.25 – 0.1 mm mesh size	Merck
LiChroprep Diol (40–63 mm) for liquid chromatography	Merck

2.2.2.2. Spray reagents

The reagents were stored in amber-colored bottles and kept refrigerated until being used. TLC was used to monitor the identity of each of the fractions and the qualitative purity of the isolated compounds.

Anisaldehyde/H₂SO₄ spray reagent

Methanol	85 mL
Glacial acetic acid	10 mL
Conc. H_2SO_4	5 mL (added slowly)
Anisaldehyde	0.5 mL

Ninhydrin spray reagent

Ninhydrin	0.2 g
Acetic acid	0.5 mL
H_2O	4.5 mL
Methanol	100 mL

2.2.3. Solvents

2.2.3.1. General solvents

Methanol, ethanol, acetone, ethyl acetate, acetonitrile, dichloromethane, and n-hexane, and were used for chromatographic separations and they were purchased from the Institute of Chemistry, Heinrich-Heine University, Duesseldorf. They were distilled before use and spectroscopic grade was employed for spectroscopic measurements (Daletos *et al.*, 2014).

2.2.3.2. Solvents for HPLC

Methanol	HPLC grade (Merck)
Acetonitrile	HPLC grade (Merck)
Nanopure water	Distilled water passed through ion exchange filter cells (Barnstead, France).

2.2.3.3. Solvents for optical rotation

| Chloroform | Spectroscopic grade (Sigma) |
| Methanol | Spectroscopic grade (Sigma) |

2.2.3.4. Solvents for NMR

Chloroform-*d*	Merck
DMSO-*d₆*	Merck
Methanol-*d₄*	Merck
Acetone-*d₆*	Merck

2.3. Methods

2.3.1. Isolation and purification of secondary metabolites

2.3.1.1. Isolation of secondary metabolites from *Dactylospongia metachromia*

```
┌─────────────────────────────────────────────┐
│        Dactylospongia metachromia            │
│   Sponge raw material (wet weight 600 g)     │
└─────────────────────────────────────────────┘
              │  MeOH ( 2L×2),
              │  MeOH.CH2Cl2 (1:1; 2L×2),
              │  room temperature
              ▼
      ┌─────────────────────┐
      │  Crude extract (6.7 g) │
      └─────────────────────┘
              │  Liquid-liquid extraction
```

| n-hexane crude extract (2.0 g) | CH$_2$Cl$_2$ crude extract (1.8 g) | EtOAc crude extract (617 mg) | n-BuOH crude extract (1.2 g) |
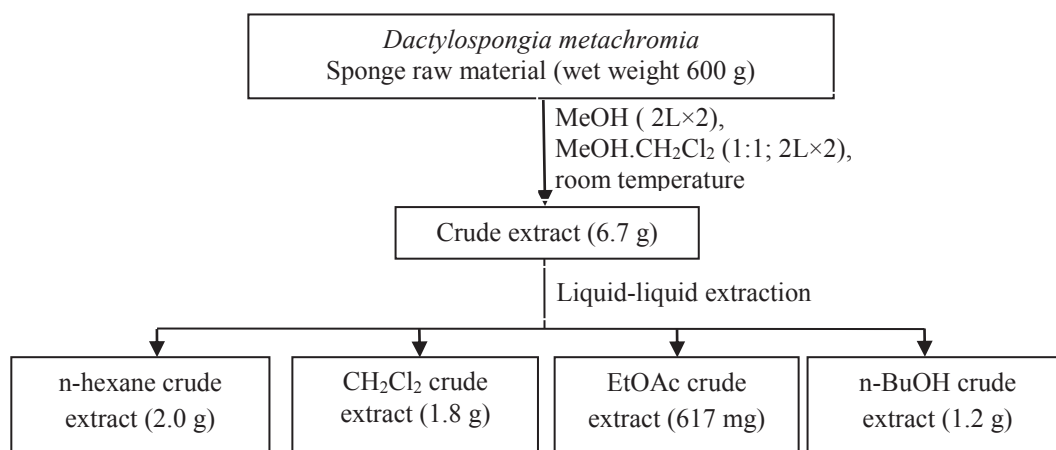
Figure 2.7: Fractionation scheme of *Dactylospongia metachromia*

```
      ┌──────────────────────────────┐
      │  CH2Cl2 crude extract (1.8 g)  │
      └──────────────────────────────┘
              │  VLC, silica gel (n-
```

| Fraction 3 (40% EtOAc in n-hexane), 110 mg | Fraction 4 (40% n-hexane in EtOAc), 60 | Fraction 6 (100% EtOAc), 85 mg |

| Sephadex LH-20, CH$_2$Cl$_2$/MeOH | Sephadex LH-20, CH$_2$Cl$_2$/MeOH | Sephadex LH-20, CH$_2$Cl$_2$/MeOH |

| DMD 3.3, 25 mg | DMD 4.5, 21 mg | DMD 6.8, 17 mg |

| semiprep. HPLC | semiprep. HPLC | semiprep. HPLC |

| **18-Hydroxy-5-*epi*-hyrtiophenol (8)**, 10 mg | **5-*epi*-Nakijiquinone Q**, 8 mg
 5-*epi*-Nakijiquinone N, 5 mg | **5-*epi*-Nakijiquinone S**, 4 mg
 5-*epi*-Nakijiquinone T, 2.5 mg
 5-*epi*-Nakijiquinone U, 2 mg |

Figure 2.8: Isolation scheme of *Dactylospongia metachromia* (CH$_2$Cl$_2$ fraction)

24
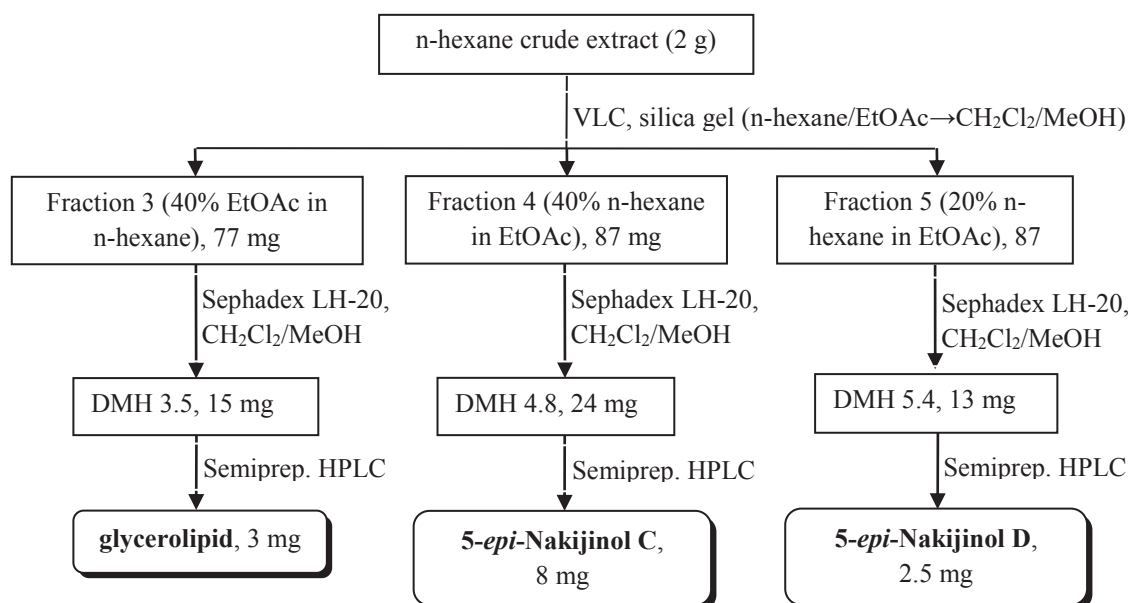
Figure 2.9: Isolation scheme of *Dactylospongia metachromia* (n-hexane fraction)

2.3.1.2. Isolation of secondary metabolites from *Callyspongia aerizusa*
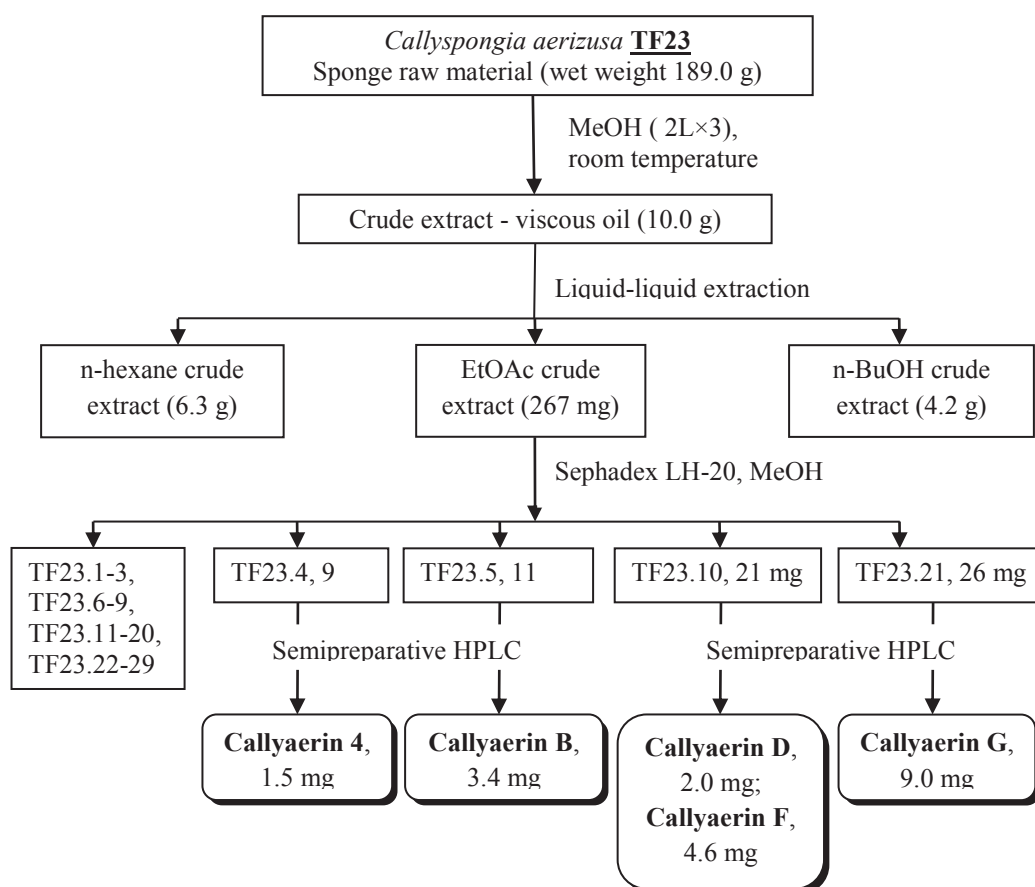
Figure 2.10. Isolation scheme of *Callyspongia aerizusa* (TF23)
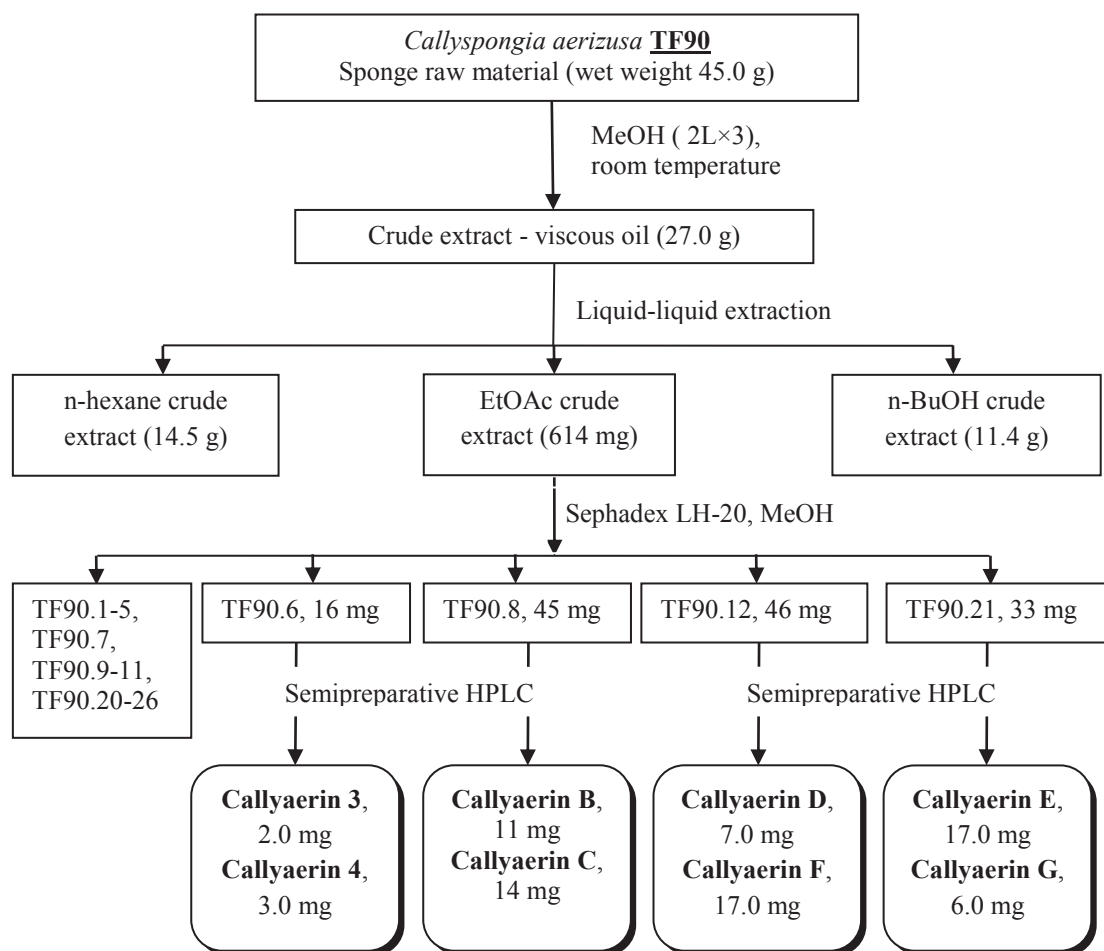
Figure 2.11. Isolation scheme of *Callyspongia aerizusa* (TF90)
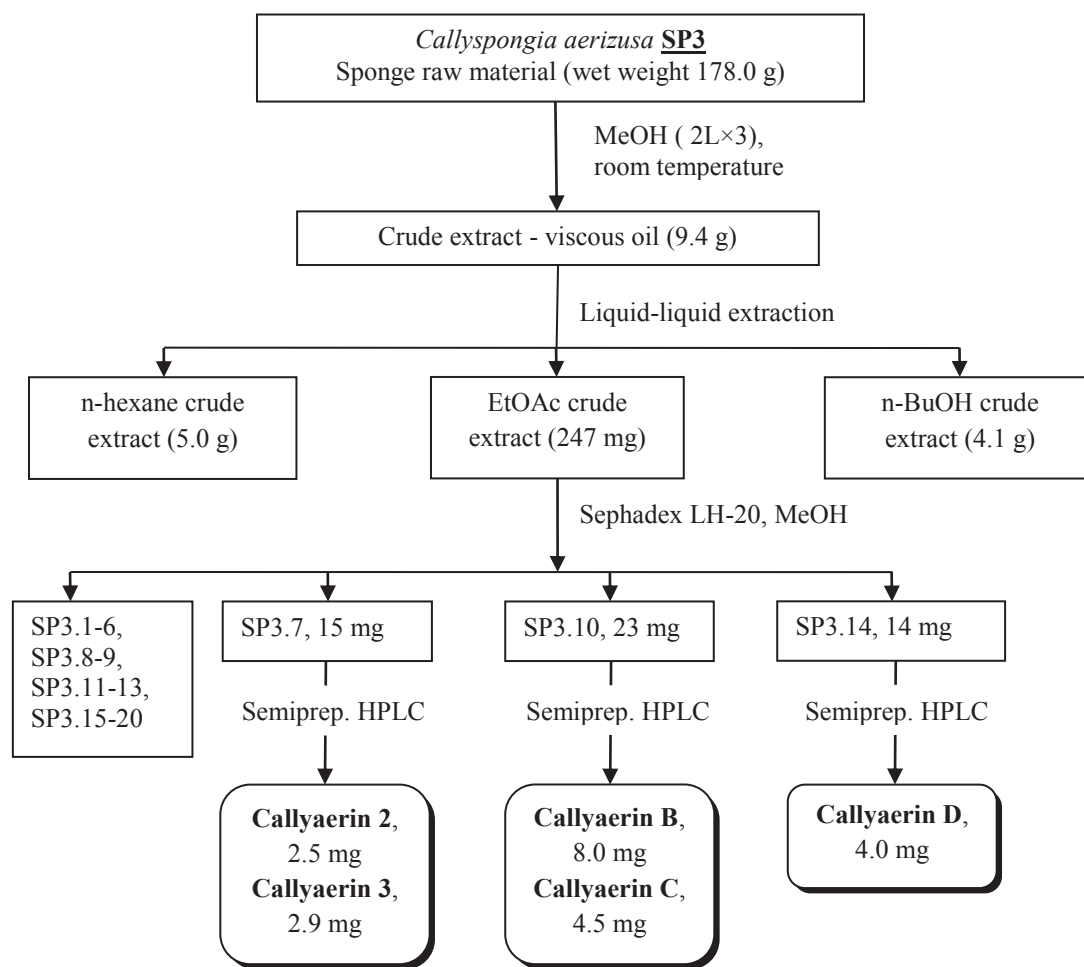
Figure 2.12. Isolation scheme of *Callyspongia aerizusa* (SP3)
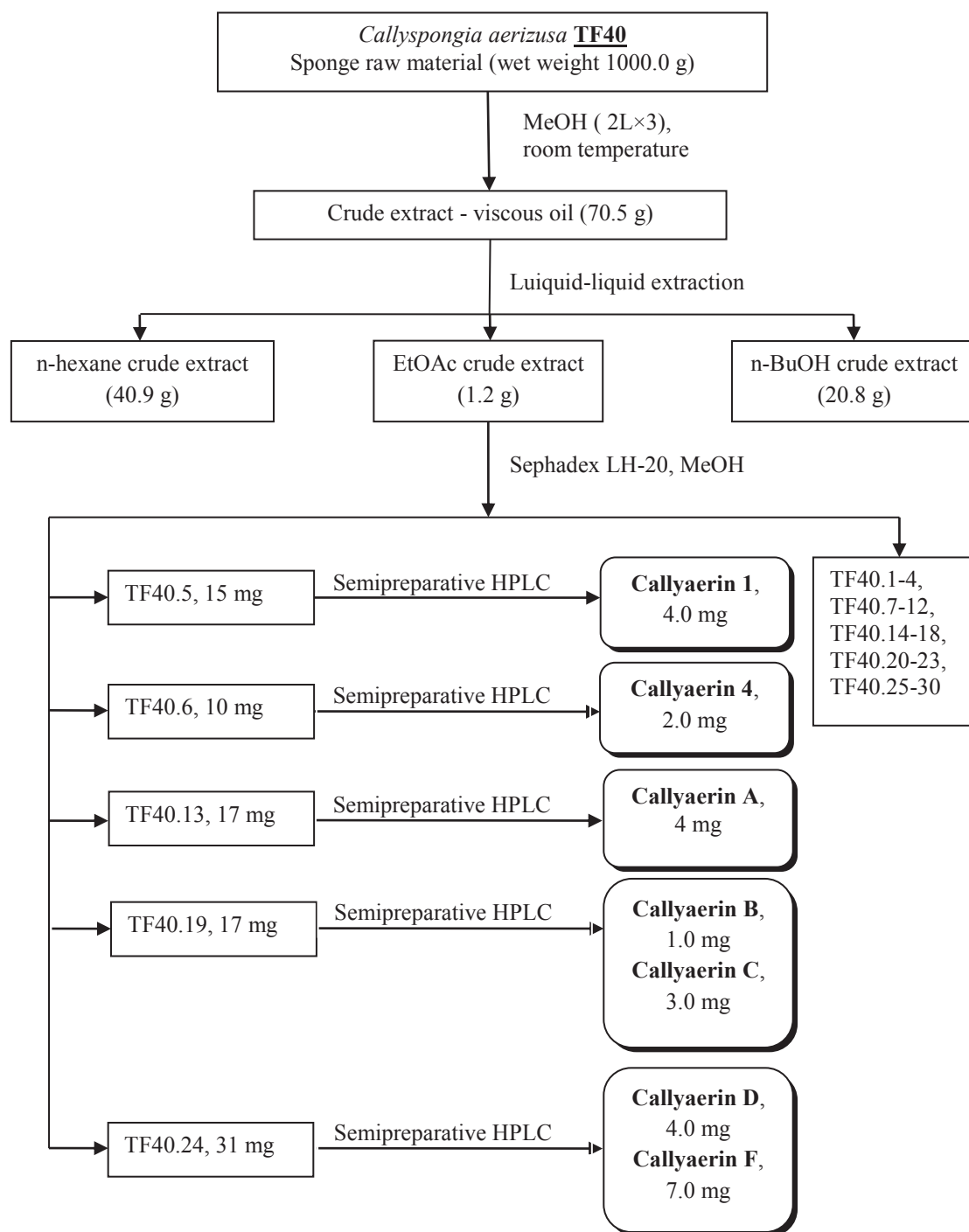
Figure 2.13: Isolation scheme of *Callyspongia aerizusa* (TF40)

2.3.1.3. Isolation of secondary metabolites from *Acanthostrongylophora ingens*
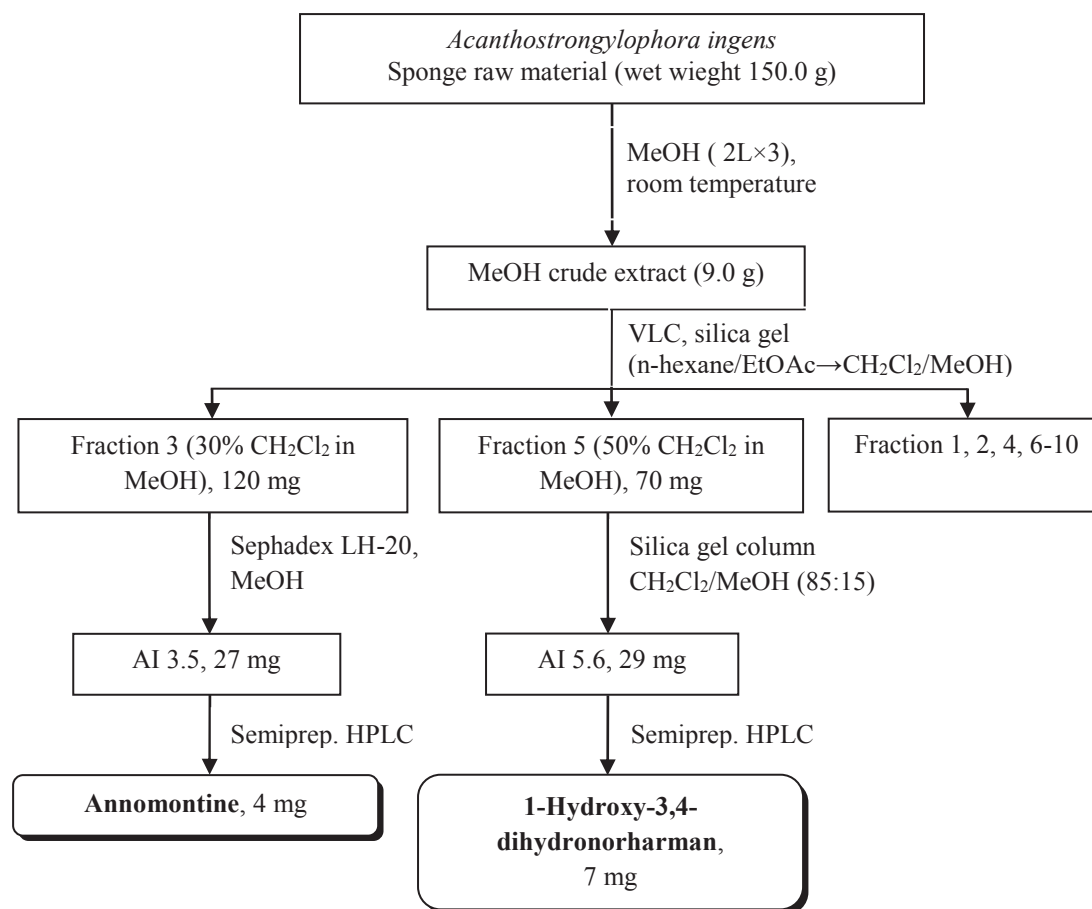
Figure 2.14: Isolation scheme of *Acanthostrongylophora ingens*

2.3.1.4. Isolation of secondary metabolites from *Sarcotragus spinosulus*.

```
┌─────────────────────────────────────────┐
│         Sarcotragus spinosulus           │
│  Sponge raw material (wet weight 100.0 g)│
└─────────────────────────────────────────┘
                    │ MeOH ( 2L×3),
                    │ room temperature
                    ▼
┌─────────────────────────────────────────┐
│     Crude extract - viscous oil (6.4 g)  │
└─────────────────────────────────────────┘
                    │ Liquid-liquid extraction
      ┌─────────────┼─────────────────┐
      ▼             ▼                 ▼
┌───────────┐ ┌───────────┐   ┌─────────────────┐
│n-hexane   │ │EtOAc crude│   │n-BuOH crude     │
│crude      │ │extract    │   │extract          │
│extract    │ │(370 mg)   │   │(2.0 g)          │
│(2.0 g)    │ └───────────┘   └─────────────────┘
└───────────┘      │ Sephadex LH-20, MeOH
      ┌────────────┴────────────┐
      ▼                         ▼
┌───────────┐           ┌─────────────┐
│SS1-7,     │           │ SS8, 19 mg  │
│SS8-25     │           └─────────────┘
└───────────┘                  │ Semipreparative HPLC
                               ▼
                      ┌──────────────────┐
                      │Ircinin 1,2 (3:1), │
                      │6mg                │
                      └──────────────────┘
```
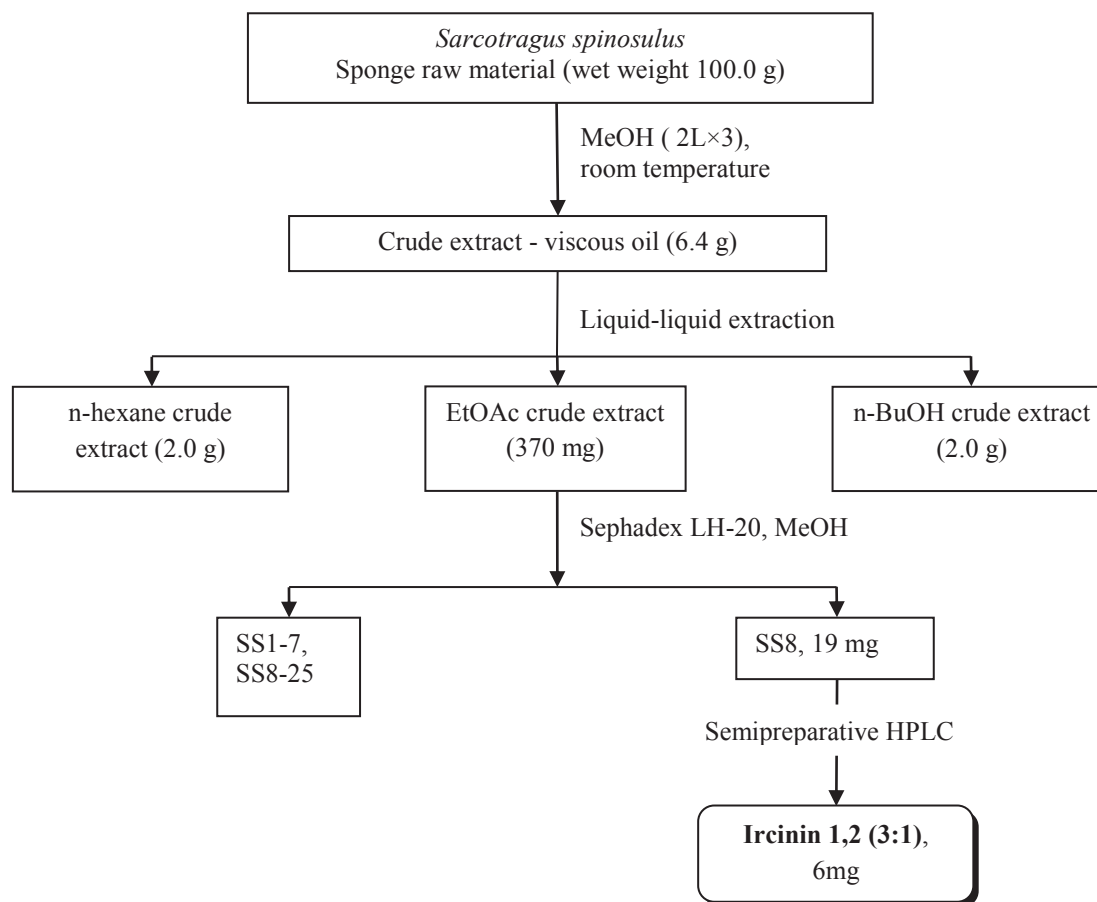
Figure 2:15: Isolation scheme of *Sarcotragus spinosulus*

2.3.1.5. Isolation of secondary metabolites from *Dysidea avara*.
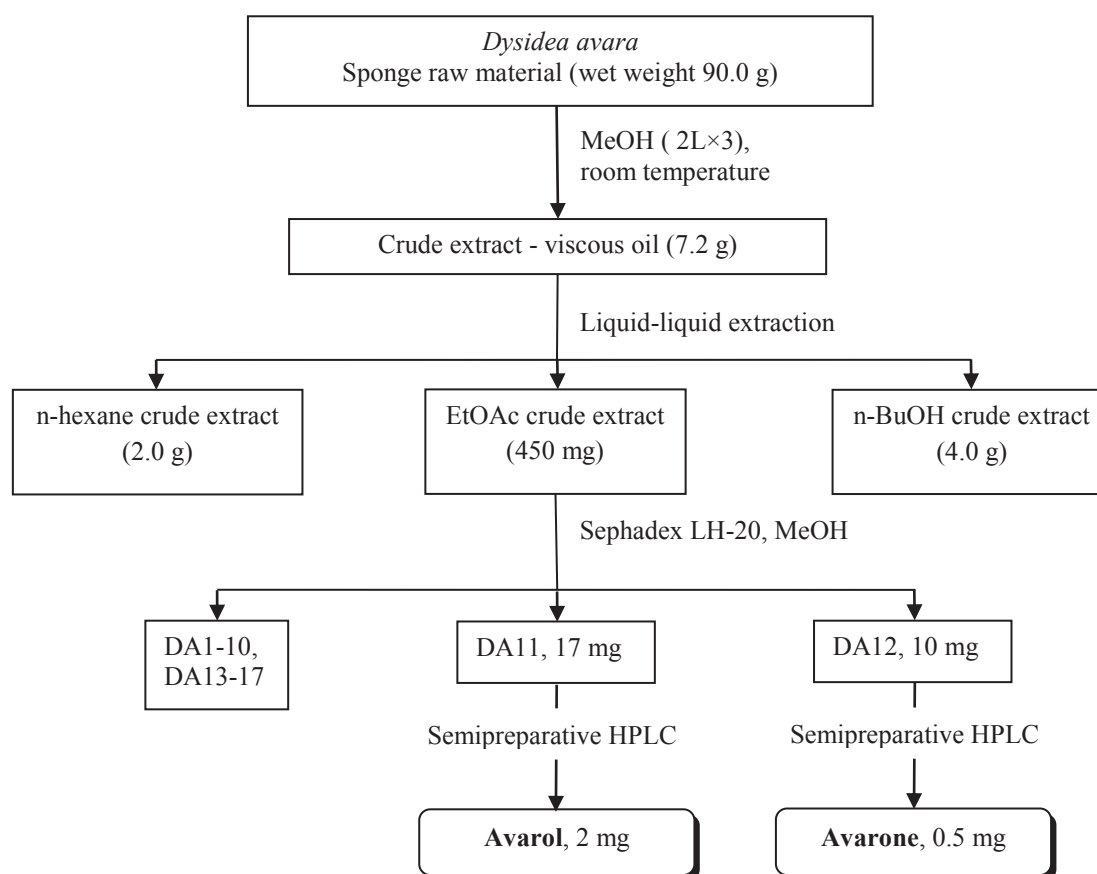
Figure 2.16: Isolation scheme of *Dysidea avara*

2.3.1.6. Isolation of secondary metabolites from *Agelas oroides*.
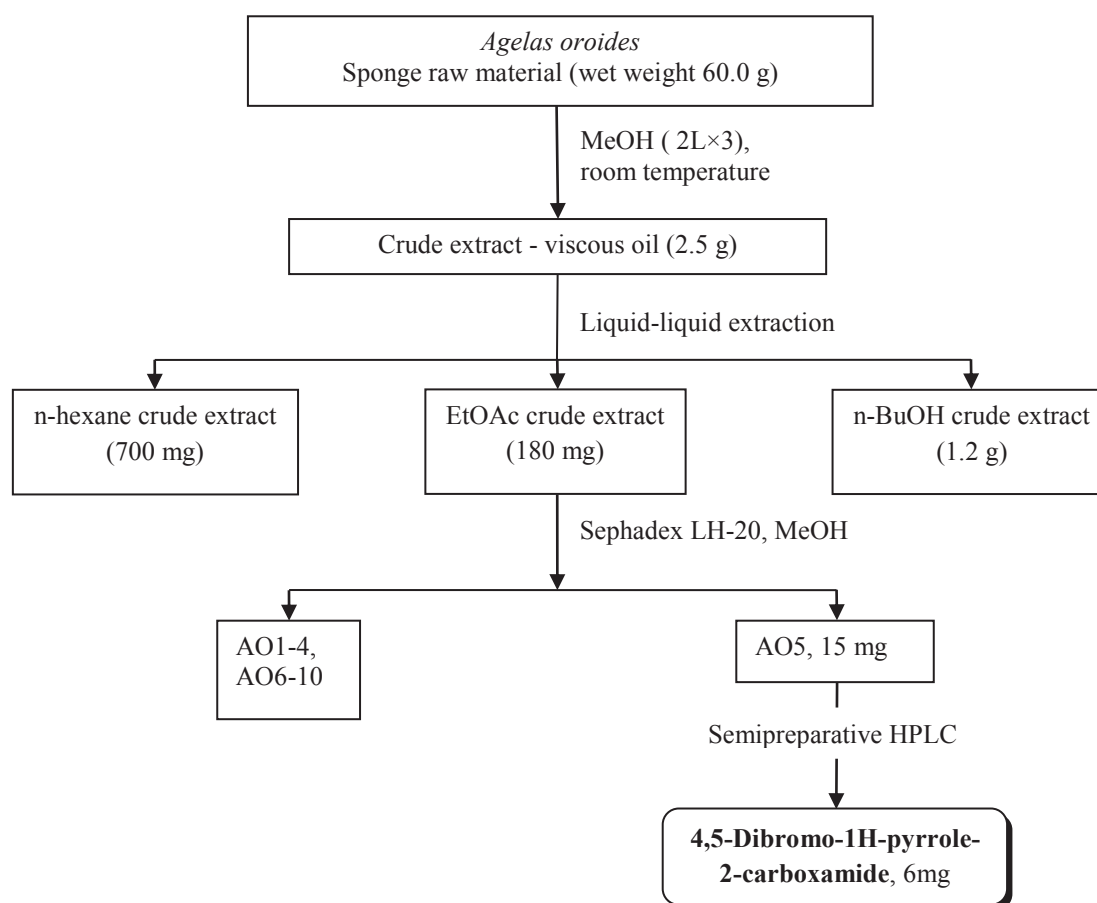
Figure 2.17: Isolation scheme of *Agelas oroides*

2.3.2. Chromatographic methods

2.3.2.1. Thin layer chromatography (TLC)

In thin layer chromatography the components move at different rates based on their polarity index. TLC was performed on pre-coated TLC plates with silica gel 60 F254 (layer thickness 0.2 mm, E. Merk, Darmstadt, Germany), using the following eluents:

For polar or semi-polar compounds   DCM:MeOH (95:5, 90:10, or 80:20)

For non-polar compounds   n-Hexane:EtOAc (90:10 or 80:20)

Pre-coated TLC plates with silica gel F254 (Merck) were used to monitor fractions (DCM:MeOH or n-Hexane:EtOAc mixtures as developing systems), and detection was by UV absorption at 254 and 366 nm or by spraying the TLC plates with anisaldehyde or with ninhydrin reagent (Daletos *et al.*, 2014; Ebada *et al.*, 2008).

2.3.2.2. Vacuum liquid chromatography (VLC)

Vacuum liquid chromatography (VLC) is mainly employed for the initial separation of crude extracts. The bioactive sponge extract was concentrated under vacuum and was mixed with a small part of the stationary phase (silica gel 60) using DCM/MeOH (1:1, v/v). After letting the sample dry, it was submitted to VLC on silica gel 60 using a step gradient of a non-polar mobile phase (e.g. n-hexane/EtOAc), followed by an increasing amount of polar mobile phase (e.g. DCM/MeOH), to yield 10 to 12 fractions (Daletos *et al.*, 2014; Ebada *et al.*, 2008).

2.3.2.3. Column chromatography

Fractions resulting from VLC were further purified by column chromatography. The following stationary phases were employed:

1. Silica gel 60 or Diol using a non-polar mobile phase (e.g. n-Hexane, DCM or EtOAc) As a result, non-polar compounds elute earlier than polar compounds (Daletos *et al.*, 2014; Ebada *et al.*, 2008).

2. Sephadex LH-20 using MeOH or MeOH:DCM (1:1, v/v). The chromatographic separation is based on the molecular size of analyzed compounds (size-exclusion chromatography). Compounds with larger molecular diameters elute

first, while compounds with smaller molecular diameters will enter the small-sized pores and elute later (Ebada *et al.*, 2008; Daletos *et al.*, 2014).

3. Diaion HP-20 using a polar phase (e.g. H_2O/MeOH). The sample components are separated based on their different electrical affinities (ion-exclusion chromatography) (Daletos *et al.*, 2014; Ebada *et al.*, 2008).

2.3.2.4. Semipreparative high-performance liquid chromatography (HPLC)

Semipreparative reversed-phase HPLC is used for final purification of compounds using an eluting gradient of MeOH/H_2O or CH_3CN/H_2O (with 0.01% HCOOH). Polar compounds elute earlier than non-polar compounds. The desired concentration of the sample was 1-3 mg per 100 μL (injection volume) and the solvent system rate was adjusted to 5 mL/min. Semipreparative purification was accomplished on a Merck Hitachi system consisting of an L-7400 UV detector and an L-7400 UV detector and an L-7100 pump connected with a Kipp & Zonen flatbed recorder. The attached column was a Knauer VertexPlus C18 column (Eurospher 100-10, 300 × 8 mm, L × i.d.) (Daletos *et al.*, 2014, 2015).

Semi-preparative HPLC system specifications:

Pump	Merk Hitachi L-7100
Detector	Merk Hitachi L-7400 UV detector
Column	Knauer VertexPlus C18 column
	(Eurospher 100-10, 300 × 8 mm, L × i.d.)

2.3.2.5. Analytical high-performance liquid chromatography (HPLC)

HPLC analysis was employed to obtain the chromatograms of extracts or fractions, and to evaluate the purity of obtained compounds. HPLC analysis was performed using a Dionex Ultimate 3000 System coupled to a photodiode array detector (DAD300RS). The separation column (125 × 4 mm, L × i.d.) was prefilled with Eurospher-10 C18 (Knauer, Germany), and the following gradient was used (MeOH, 0.1% HCOOH in H_2O): 0 min, 10% MeOH; 5 min, 10% MeOH; 35 min, 100% MeOH; 45 min, 100% MeOH. Routine detection was at 235, 254, 280, and 340 nm (Daletos *et al.*, 2014; Ebada *et al.*, 2008).

HPLC system specifications:

System	Dionex Ultimate 3000
Detector	Dionex Photodiode Array Detector DAD300RS
Column thermostat	STH 585
Autosampler	ASI-100T
HPLC Program	Chromeleon (V. 6.3)
Column	Knauer (125 X 4 mm, ID), pre-packed with Eurosphere 100–5 C18, with integrated pre-column

2.3.3. Structure elucidation of isolated secondary metabolites

2.3.3.1. Mass spectrometry (MS)

A mass spectrometer is an analytical instrument consisting of an ion source, a mass analyzer and an ion detector. Mass spectrometers generate ions from molecules under high-vacuum conditions and separate them according to their mass-to-charge ratio (m/z). Then, the signals obtained from the ion detector are transmitted to a data system and the respective mass spectrum is recorded. Thus, mass spectrometry is a powerful tool for obtaining molecular weight and structural information of analyzed compounds. In this study, several mass spectrometric techniques were used to establish the molecular weight of the isolated compounds (Ebada *et al.*, 2008).

2.3.3.1.1. Liquid chromatography / Mass spectrometry (LC / MS)

Electrospray ionization mass spectrometry (ESI-MS) is an important method for analyzing non-volatile, high molecular weight compounds. A solution of the sample is passing through a metal capillary and sprayed at a high voltage, thus producing electrostatically charged droplets that can be further detected (Ebada *et al.*, 2008). ESI-MS is commonly interfaced with LC (LC/ESI-MS) as a powerful tool for MS analysis of sample mixtures. HPLC/ESI-MS spectra were measured on a Thermoquest Finnigan LCQDeca mass spectrometer connected to an Agilent 1100 series LC. The samples were dissolved in MeOH and injected to HPLC/ESI-MS. The analytical column (100 × 2 mm, L × i.d.) was prefilled with Eurospher 100-3 C18 (Knauer), and the following gradient was used (MeOH, 0.1% HCOOH in H_2O): 0 min, 10% MeOH; 2 min, 10% MeOH; 35 min, 100% MeOH; 50 min, 100% MeOH,

51 min, 10% MeOH; 60 min, 10% MeOH at a flow rate of 0.25 mL/min, monitoring from 210 to 400 nm (Daletos *et al.*, 2015; Ebada *et al.*, 2008).

HPLC/ESI-MS system specifications:

HPLC system	Agilent 1100 series
MS spectrometer	Thermoquest Finnigan LCQDeca
Column	Knauer, (100 × 2 mm, L × i.d.), prefilled with Eurospher 100-3 C18 (Knauer), with integrated pre-column

2.3.3.1.2. Electron impact mass spectrometry (EI-MS)

Electron impact mass spectrometry (EI-MS) involves vaporizing a compound and then bombarding with electrons. It is a high energy method, generating extensive fragmentation patterns that may provide useful information for the molecule. It is not recommended for high-molecular weight compounds, such as peptides. EI-MS was measured on a Thermo Finnigan TCQ 7000 mass spectrometer. Measurements were held by Dr. Peter Tommes, Institute for Inorganic and Structural Chemistry, Heinrich-Heine University, Duesseldorf (Daletos *et al.*, 2014; Ebada *et al*., 2008).

2.3.3.1.3. Matrix Assisted Laser Desorption Ionisation-Time of Flight mass spectrometry (MALDI-TOF-MS)

Matrix Assisted Laser Desorption Ionisation (MALDI) is successfully applied for the analysis of high molecular weight compounds, such as peptides, oligosaccharides or oligonucleotides. A matrix is used (e.g. 4-aminoquinaldine) that absorbs energy produced by a laser followed by ionization of the sample. The analyser separates ions based on their mass-to-charge (*m/z*) ratios by measuring the time it takes for them to "travel" through the field (time-of-flight; TOF). MALDI-TOF-MS spectra were measured on a MALDI-TOF Ultraflex (Bruker Daltonics) mass spectrometer using nitrogen laser (337 nm). Measurements were carried out by Dr. Peter Tommes, Institute for Inorganic and Structural Chemistry, Heinrich-Heine University, Duesseldorf (Daletos *et al.*, 2014; Ebada *et al.*, 2008).

2.3.3.1.4. High-resolution mass spectrometry (HR-MS)

High-resolution mass spectrometry (HR-MS) measures ion masses with high accuracy, thus allowing the determination of the atomic composition of the detected

molecular ions. High-resolution ESI mass spectra were recorded on a Micromass Qtof 2 mass spectrometer at Helmholtz Centre for Infection Research, Braunschweig as well as on a UHR-QTOF maXis 4G (Bruker Daltonics, Bremen) mass spectrometer, Heinrich-Heine University, Duesseldorf (Daletos *et al.*, 2014; Ebada *et al.*, 2008).

2.3.3.2. Nuclear magnetic resonance spectroscopy (NMR)

Nuclear magnetic resonance (NMR) spectroscopy is a powerful method for determining the chemical structure of a molecule. In this study, the structures of all isolated compounds were unambiguously established on the basis of one-dimensional (i.e. ^1H, ^{13}C) and two-dimensional techniques (i.e. COSY, TOCSY, ROESY, HSQC, and HMBC). The samples were dissolved in different deuterated solvents (i.e. DMSO-d_6, CDCl$_3$ and CD$_3$OD), according to their solubility. Residual solvent signals were used as reference signals and chemical shift (δ) values were provided in ppm (Daletos *et al.*, 2014; Ebada *et al.*, 2008). NMR spectra were recorded at 300° K on a Bruker AVANCE DMX 600 by Prof. Dr. Klaus Schaper, Institute for Inorganic and Structural Chemistry, Heinrich-Heine University, Duesseldorf. Some measurements were also performed by Dr. Victor Wray, Helmholtz Centre for Infection Research, Braunschweig, using Bruker DMX 600, Bruker ARX 400, and Bruker DPX 300 spectrometers, as well as by Dr. Rudolf Hartmann, Institute of Complex Systems: Strukturbiochemie, Forschungszentrum Juelich, using a Bruker AVIII HD 700 NMR spectrometer. The 2D-NMR experiments for assignment of spin systems and structure elucidation (HH-COSY, HH-TOCSY, HH-ROESY, HC-HSQC and HC-HMBC) were measured with standard Bruker pulse-sequences on a Bruker AVIII HD 600 spectrometer, equipped with a QXI/QCI cryo-probe at 303K. The sweep width for the homonuclear experiments (COSY, TOCSY, ROESY) in F2 and in F1 was 7200 Hz. Quadratur detection was used in both dimensions. 2K data points were collected in F2 and 512 data points were collected in F1 each with 8 scans per increment. The TOCSY mixing time was set to 80 ms and a spin lock field of approximately 12 kHz and ROESY with 450 ms mixing time and a spin lock field of approximately 5 kHz. The sweep width for the heteronuclear experiments was set to 7200 Hz in F2 and 26.400 Hz in F1 for the HSQC and 27.900 Hz for the HMBC experiments. 4K data points were collected in F2 and 512 data points were collected in F1 each with 4 scans per increment (HSQC) or 64 scans per increment (HMBC) (Daletos *et al.*, 2014; 2015).

2.3.3.3. Optical activity

Optical activity is the rotation of the plane of polarized light that arises when passing through chiral molecules Optical rotation was determined on a JASCO P-2000 polarimeter. The chiral compound was subjected to a sample chamber (0.5 mL). The specific optical rotation was measured at 589 nm employing a sodium lamp as a light source at room temperature (25 °C) (Daletos *et al.*, 2014; Ebada *et al.*, 2008).

2.3.3.4. Determination of absolute stereochemistry by Marfey's analysis

The absolute configurations of the individual amino acid constituents of the isolated peptides were determined by acid hydrolysis and consecutive analysis of the hydrolysates using the Marfey's method (Marfey, 1984). LC-MS analyses of the resulting (Nα- (2,4-dinitro-5-fluorophenyl)-L-alaninamide) derivatives and comparison with authentic amino acids prepared as standards led to the assignment of the L or D configuration of the amino acid residues (Daletos *et al.*, 2015).

2.3.3.4.1. Hydrolysis of peptide

Each of the isolated peptides (0.5−1 mg) was dissolved in 1−2 mL of 6 N HCl in a sealed ampule and heated at 110 °C for 24 h under a N2 atmosphere. After cooling, the reaction mixture was concentrated in vacuo to dryness (Daletos *et al.*, 2015).

2.3.3.4.2. Derivatization of the amino acids

To 50 μL of ~50 μM of each hydrolysate, 100 μL of FDAA (1% Nα-(2,4-dinitro-5-fluorophenyl)-L-alaninamide in acetone) and 20 μL of 1 M NaHCO3 were added. The mixture was heated over a hot plate at 40 °C for 1 h with frequent mixing. The reaction was stopped by addition of 10 μL of 2 M HCl, and the derivatized product dried in a freeze-dryer and redissolved in MeOH. Commercially available standard amino acids (L- or D-configuration) that are of interest were treated separately with FDAA in the same manner. The derivatized amino acids obtained following hydrolysis of the peptide were analyzed using LC-ESIMS by comparison of the retention time and molecular weight with those of the derivatized standard amino acids (Daletos *et al.*, 2015).

2.3.4. Biological test methods:

2.3.4.1. Antimicrobial assay

2.3.4.1.1. Agar diffusion assay

The antimicrobial assay was carried out according to the Bauer-Kirby-Test, under aseptic conditions using microtiter 96 well plates (Bauer *et al.*, 1966). After adding the tested substance (or extract) on agar plate, the diameter of inhibition zone was measured.

The inhibitory activity of isolated substances or extracts was evaluated toward the following strains:

Gram-positive bacteria	*Staphylococcus aureus* (ATCC 29213)
Gram-negative bacteria	*Esherichia coli* (ATCC 25922)
	Pseudomonas aeruginosa (ATCC 27853)

2.3.4.1.2. Antibacterial assay

Susceptibility discs were impregnated with 200 μg of crude extracts and placed on agar plates that were inoculated with the bacterial strains *S. aureus*, *E. coli*, and *P. aeruginosa*. The plates were incubated at 37°C and checked for inhibition zones after 24 h. All isolated compounds were evaluated for their activity against the aforementioned bacterial strains, following the broth microdilution method and according to the recommendations of the Clinical and Laboratory Standards Institute (CLSI). For assay validation, gentamicin and rifampicin were used as positive controls. The direct colony suspension method was used for preparation of the inoculum with 5 x 10^5 colony forming units/mL after the last dilution step. The tested substances were added from stock solution (10 mg/mL in DMSO), resulting in a DMSO amount of 0.64% for the highest antibiotic concentration tested (64 μg/mL). Antibiotics addressing different bacterial targets, including ciprofloxacin, rifampicin, tetracycline, and vancomycin were employed as positive controls (Ancheeva e*t al.*, 2015, Daletos *et al.*, 2015).

2.3.4.1.3. Experiments with *Mycobacterium tuberculosis*

Growth inhibition of *M. tuberculosis* was tested using a metabolic activity assay employing the resazurin dye reduction method. *M. tuberculosis* cells were grown aerobically at 37 °C in Middlebrook 7H9 media supplemented with 0.5% (v/v)

glycerol, 0.05% (v/v) Tyloxapol and 10% (v/v) ADS enrichment (5%, w/v, bovine serum albumin fraction V; 2%, w/v, glucose; 0.85%, w/v, sodium chloride). Bacteria were precultured until log-phase (OD 600 nm ~ 1) and then seeded at 1×10^5 cells per well in a total volume of 100 µl in 96-well round bottom microtiter plates and incubated with test substances for 6 days. For viability determination, 10 µl resazurin solution (100 µg/ml, Sigma-Aldrich) was added per well and incubated for ca. 8 h. Then cells were fixed at room temperature for 30 min after addition of formalin (5%, v/v, final concentration), and fluorescence was measured using a microplate reader (excitation 540 nm, emission 590 nm). Residual growth was calculated relative to rifampicin treated (0% growth) and DMSO treated (100% growth) controls (Daletos *et al.*, 2015).

2.3.4.2. Cytotoxicity assays
2.3.4.2.1. Microculture tetrazolium (MTT) assay

Cytotoxicity assays were carried out by Prof. Dr. W. E. G. Müller, Institute for Physiological Chemistry and Pathobiochemistry, University of Mainz, Mainz. Cytotoxicity was tested against L5178Y mouse lymphoma cells grown in Fischer's medium using a microculture tetrazolium (MTT) assay and compared to that of untreated controls. Experiments were repeated three times and carried out in triplicate. As negative controls, media with 0.1% EGMME-DMSO were included in the experiments. Kahalalide F was used as positive control (IC$_{50}$ 4.3 μM) (Daletos *et al.*, 2014).

2.3.4.2.2. Resazurin cell viability assay

In vitro cytotoxicity studies were performed using the human monocytic cell line THP-1 (Deutsche Sammlung von Mikroorganismen und Zellkulturen GmbH) and the human fetal lung fibroblast cell line MRC-5 (American Type Culture Collection). THP-1 cells were cultured in RPMI 1640 medium with stable glutamine (Biochrom AG) containing 10% fetal bovine serum (FBS, Life Technologies) and MRC-5 cells in Dulbecco´s Modified Eagles Medium (DMEM, Life Technologies) containing 10% FBS, respectively, at 37 °C in a humidified atmosphere of 5% CO_2. Cells were seeded at ca. 5×10^4 cells per well in a total volume of 100 μL in 96-well flat bottom microtiter plates and incubated with tested substances for 48 h. For viability determination, 10 μL resazurin solution (100 μg/mL) was added per well and

incubated for further ca. 3 h after which fluorescence was quantified using a microplate reader (excitation 540 nm, fluorescence 590 nm). Residual growth was calculated relative to uninoculated (0% growth) and untreated (100% growth) controls, respectively (Daletos *et al.*, 2015).

2.3.4.2.2. Protein kinase assay

The inhibitory profiles of the compounds were determined using 16 protein kinases, namely, AKT1, ALK, ARK5, Aurora-B, AXL, FAK, IGF1-R, MEK1 wt, METwt, NEK2, NEK6, PIM1, PLK1, PRK1, SRC, and VEGF-R2. A radiometric protein kinase assay (^{33}PanQinase activity assay) was used for measuring the kinase activity of the 16 protein kinases as previously described.56 Briefly, recombinant protein kinases were incubated with a mixture of [γ-^{33}P]-labeled ATP, unlabeled ATP, and kinase substrate. After kinase reaction, incorporation of labeled ATP on the substrate was measured using 96-well FlashPlates from Perkin-Elmer/NEN. Protein kinase assay was carried out by Dr. Michael Kubbutat (ProQinase GmbH, Freiburg, Germany) (Daletos *et al.*, 2014).

Table 2.1: Relevance of the tested protein kinases to the regulation of tumor growth and metastasis (Daletos *et al.*, 2014).

Kinase	Deregulation in tumors	Relevant cancers
AKT1	deregulation of upstream effectors	many human cancers
ALK	expression of fusionproteins, mutations, gene amplification	ALCL, neuroblastoma
ARK5	overexpression	hepatocellular carcinoma
Aurora-B	overexpression	many human cancers
AXL	overexpression	many human cancers
FAK	overexpression, deregulation of upstream effectors	many human cancers
IGF1-R	overexpression of ligands	breast cancer
MEK1	mutation of upstream B-Raf	melanoma and all cancers
MET	gene amplification, mutations	many human cancers
NEK2	overexpression	breast cancer
NEK6	overexpression	most human cancers

PIM1	overexpression	hematopoietic malignancies/prostate cancer
PLK1	overexpression, mutations	many human cancers
PRK1	overexpression	androgen-dependent prostate cancer
SRC	overexpression, deregulation of upstream effectors	many human cancers
VEGF-R2	activated by tumor cells	solid tumors

2.3.5. General laboratory equipment

Balances	Mettler 200, Mettler AT 250, Mettler PE 1600, Sartorious MCI AC210S
Centrifuge	Biofuge pico, Heraeus
Cleanbench	HERAsafe, Heraeus
Digital pH meter	420Aplus, Orion
Drying Ovens	Kelvitront, Heraeus
Fraction collector	Cygnet, ISCO
Freeze dryer	Lyovac GT2, Steris
-80°C Freezer	Forma Scientific, 86-Freezer
Hot plate	Camag
Magnetic stirrer	Combi Mag, IKA
Rotary evaporator	Vacuubrand, IKA
Sonicator	Sonorex RK 102, Bandelin
Syringes	Hamilton
Ultra Turrax	T18 basic, IKA
UV lamp	Camag (254 and 366)
Vacuum centrifuge	SpeedVac SPD 111V, Savant

3. Results

3.1. Isolated compounds from the sponge *Dactylospongia metachromia*

In this study, we investigated a specimen of *Dactylospongia metachromia* collected at Ambon, Indonesia, in August 1996, and subsequently identified by Dr. Nicole de Voogd, National Museum of Natural History, Leiden, the Netherlands. The thawed sponge material was cut into small pieces and exhaustively extracted with MeOH (1L x 2) followed by MeOH:DCM (1:1, 1L x 2) at room temperature. Total methanolic extract of the sponge was subjected to liquid liquid partition technique against n-Hexane, DCM, EtOAc, and *n*-BuOH. The bioactive DCM fraction was further subjected to vacuum liquid chromatography (VLC) on silica gel using a stepwise gradient system from 100% n-Hexane to 100 % EtOAc, and from 100% DCM to 100% MeOH. Each fraction was purified by column chromatography using Sephadex LH-20 as a stationary phase and either MeOH or DCM:MeOH (1:1) as a mobile phase followed by semi-preparative reversed phase HPLC (C18 Eurosphere 100) for final purification using an eluting gradient of MeOH:H_2O or CH_3CN:H_2O. This afforded three new sesquiterpene aminoquinones in addition to one known sesquiterpene quinol. Following the same procedure, column chromatography of the *n*-hexane fraction followed by purification using semi-preparative HPLC afforded two new sesquiterpene benzoxazoles. In this part, we report the isolation and structure elucidation of the isolated compounds, as well as bioassay results employing the L5178Y mouse lymphoma cell line and a panel of protein kinases (Daletos *et al.*, 2014).

3.1.1. 5-*epi*-Nakijiquinone S (1, new natural product)

5-*epi*-Nakijiquinone S	
Sample code	G2-25
Biological source	*Dactylospongia metachromia*
Sample amount	4.0 mg
Physical description	red amorphous solid
Molecular formula	$C_{29}H_{37}NO4$
Molecular weight	463 g/mol
Optical rotation $[\alpha]_D^{20}$	-23 (*c* 0.05, MeOH)
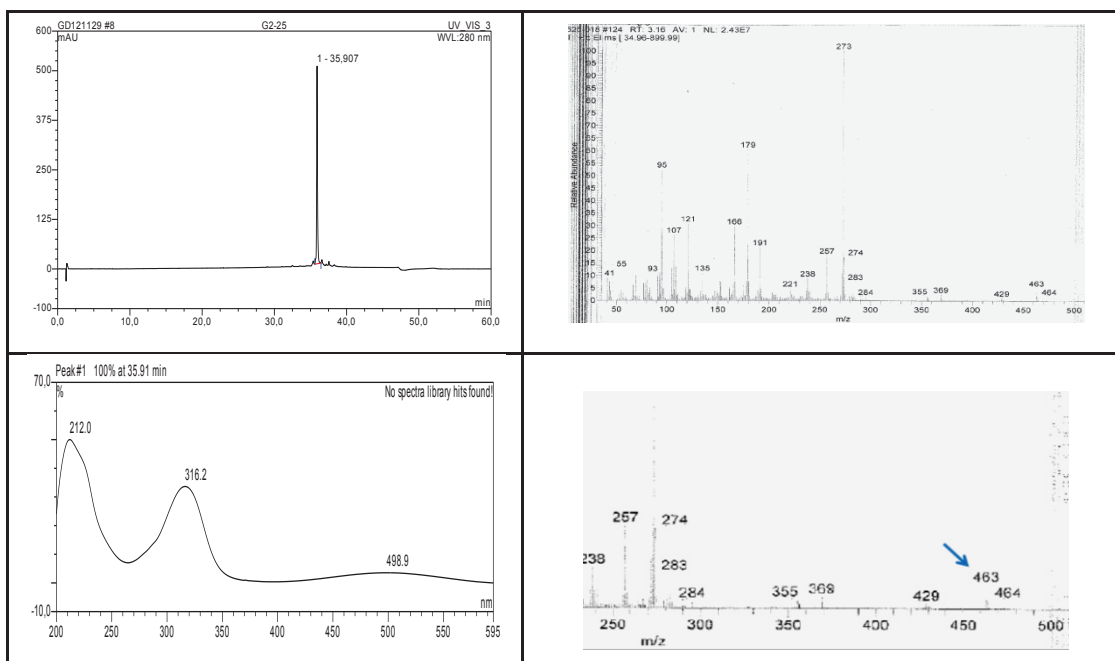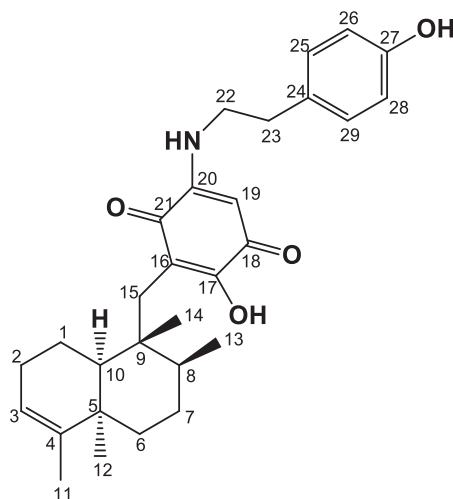
Compound **1** was obtained as a red amorphous solid. The HRESIMS spectrum exhibited a prominent peak at *m/z* 464.2792 [M+H]$^+$ consistent with the molecular formula $C_{29}H_{37}NO_4$. The UV spectrum, revealing absorbances at λ_{max} 319 and 490 nm, suggested the presence of a quinone chromophore in the molecule. The ^{1}H NMR spectrum (Table 3.1) indicated the presence of one NH proton resonating at δ_H 6.46 ppm, two olefinic protons at δ_H 5.30 and 5.38 ppm (H-3 and H-19, respectively), a *para* substituted aromatic ring (H-25/29 and H-26/28), an olefinic methyl group at δ_H 1.62 ppm (H_3-11), a secondary methyl group split to a doublet at δ_H 0.88 ppm (H_3-13), and two tertiary methyl signals at δ_H 0.88 and 0.93 ppm (H_3-14 and H_3-12, respectively). The ^{13}C NMR (Table 3.1) and HMQC spectra confirmed the corresponding carbon signals and revealed in addition eight sp^2 quaternary carbons, including two carbonyl groups at δ_C 178.6 and 183.1 ppm (C-18 and C-21, respectively), two sp^3 quaternary carbons, two sp^3 methines, and seven sp^3 methylene groups (Daletos *et al.*, 2014).

Thorough inspection of the 2D NMR spectra disclosed the presence of a sesquiterpenoid and an aminoquinone moiety in the structure of **1**, thus revealing a nakijiquinone core structure. The sesquiterpenoid moiety comprised two continuous spin systems, $CH(10)CH_2(1)CH_2(2)CH(3)$ and $CH_2(6)CH_2(7)CH(8)CH_3(13)$, as indicated by the COSY spectrum. The corresponding HMBC correlations (Figure 3.1) confirmed the sesquiterpenoid substructure as identical to that found in 18-hydroxy-5-*epi*-hyrtiophenol (**8**). This was further corroborated by the prominent fragment ion peak at *m/z* 191, characteristic of the decalin moiety ($C_{14}H_{23}$) that was observed in the mass spectrum of **1**. Further HMBC correlations of H_2-15 to C-16, C-17 and C-21, of H-19 to C-17 and C-21, and the downfield shifted signal of C-17 (δ_C 157.2 ppm) established the 17-hydroxyquinone subunit and its connection to the sesquiterpenoid moiety at C-16. The chemical shift of C-20 (δ_C 150.3 ppm) suggested its attachment to an amino substituent, the HMBC correlations of the 20-NH to C-19, C-21 and C-22 confirmed the presence of the amino substituent on C-20, and the upfield chemical shift of H-19 (δ_H 5.38 ppm) was consistent with location *ortho* to an amino group. All remaining signals were assigned to a tyramine unit, which included the $NHCH_2(22)CH_2(23)$ substructure and the AA'BB' spin system observed in the COSY spectrum. This was further corroborated by HMBC correlations of CH_2-22 to C-20, C-23 and C-24, of CH_2-23 to C-22, C-24 and C-25/29, of H-25/29 to C-23 and C-27, and of H-26/28 to C-24 and C-27 (Daletos *et al.*, 2014).

The relative configuration of the sesquiterpenoid unit in **1** was deduced from analysis of the ROESY spectrum. Key correlations were observed from H_2-15 to both H-8 and H-10, as well as from H-10 to H_3-12, indicating their cofacial orientation. According to the literature, the ^{13}C signals of CH_3-12 in *trans*-decalin moieties of structural analogues resonate upfield from those in *cis*-decalins (Δ ca. 10 ppm). Thus, the deshielded resonance of C-12 (δ_C 32.5 ppm) in **1** offered additional evidence and confirmed a *cis* rather than *trans* junction of the decalin ring. Hence, the structure of **1** was assigned representing a new natural product named 5-*epi*-nakijiquinone S (Daletos *et al.*, 2014).
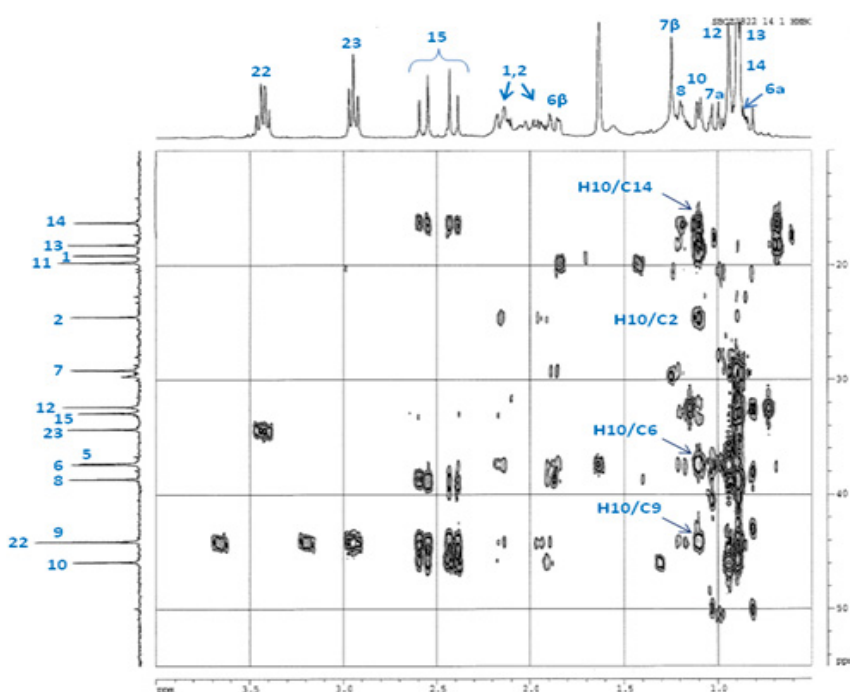
Figure 3.1: HMBC spectrum of **1**.

Table 3.1: NMR data of **1** at 600 (^{1}H) and 150 (^{13}C) MHz (CDCl$_3$, δ in ppm)

Nr.	δ_C, type	δ_H (J in Hz)	COSY	HMBC
			5-*epi*-nakijiquinone S	
1	19.3, CH$_2$	1.94, m	1a, 2, 10	2, 3, 9, 10
		2.15, m	1b, 2, 10	2, 3, 5, 9, 10
2	24.7, CH$_2$	2.01, m	1, 2a, 3	
		2.15, m	1, 2b, 3	
3	124.1, CH	5.30, brs	2, 11	1, 2, 5
4	139.2, C			
5	37.5, C			
6	37.6, CH$_2$	0.91^a	6a, 7	4, 5, 7, 8
		1.86, ddd (13.4, 3.9, 1.8)	6b, 7	7, 8, 10
7	29.3, CH$_2$	1.01, m	6, 7a, 8	5, 6, 9, 13
		1.22, m	6, 7b	5, 6
8	38.9, CH	1.19, m	7b, 13	6, 9, 10, 13, 14, 15
9	44.3, C			
10	46.1, CH	1.09, brd (6.3)	1	1, 2, 4, 5, 6, 9, 12, 14, 15
11	20.0, CH$_3$	1.62, d (1.1)	3	3, 4, 5
12	32.5, CH$_3$	0.93, s		4, 5, 6, 10
13	18.4, CH$_3$	0.88, d (6.2)	8	7, 8, 9
14	16.5, CH$_3$	0.88, s		8, 9, 10, 15
15	33.1, CH$_2$	2.40, d (13.8)	15a	8, 9, 10, 14, 16, 17, 21
		2.56, d (13.8)	15b	8, 9, 10, 14, 16, 17, 21
16	114.3, C			
17	157.2, C			
18	178.6, C			
19	92.0, CH	5.38, s		17, 21
20	150.3, C			
21	183.1, C			
22	44.5, CH$_2$	3.37, td (7.0, 6.7)	23, 20-NH	20, 23, 24
23	33.6, CH$_2$	2.86, t (7.0)	22	22, 24, 25/29
24	129.8, C			
25	130.0, CH	7.03, d (8.3)	26	23, 27, 29
26	116.0, CH	6.77, d (8.3)	25	24, 27, 28
27	154.8, C			
28	116.0, CH	6.77, d (8.3)	29	24, 26, 27
29	130.0, CH	7.03, d (8.3)	28	23, 25, 27
17-OH		8.27, brs		
20-NH		6.46, brt	22	19, 21, 22
27-OH		4.86, brs		

3.1.2. 5-*epi*-Nakijiquinone Q (2, new natural product)

5-*epi*-Nakijiquinone Q	
Sample code	G2-5
Biological source	*Dactylospongia metachromia*
Sample amount	8.0 mg
Physical description	red amorphous solid
Molecular formula	$C_{29}H_{37}NO_3$
Molecular weight	447 g/mol
Optical rotation $[\alpha]_D^{20}$	-18 (*c* 0.05, MeOH)
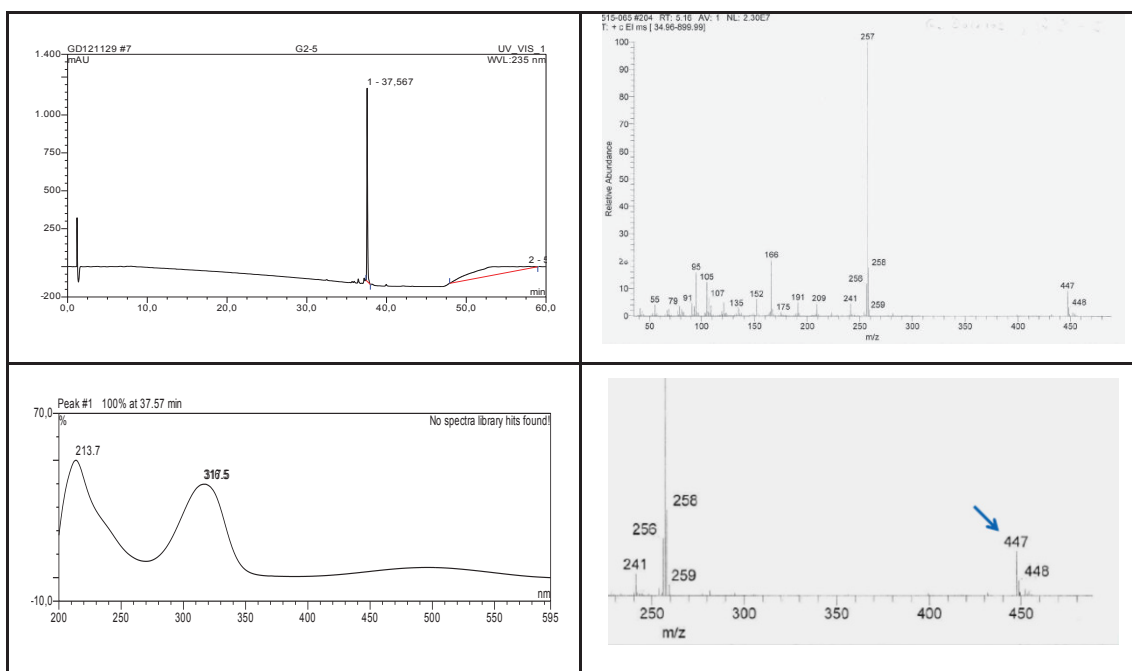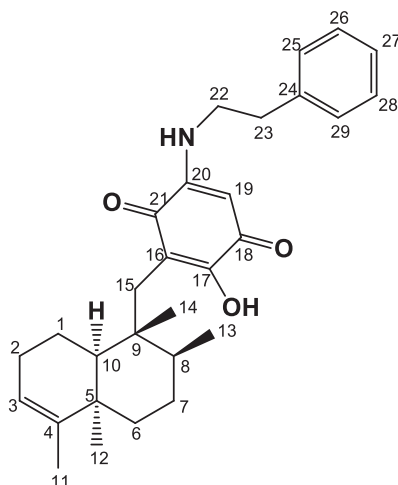
Compound **2** was obtained as a red amorphous solid. UV spectra of **2** were almost the same as those of 5-*epi*-nakijiquinone S (**1**), suggesting that **2** was an analog of **1**. The molecular formula was established to be $C_{29}H_{37}NO_3$ from the prominent ion peak at *m/z* 448.2844 for the protonated molecule $[M+H]^+$ in the HRESIMS spectrum, thus revealing a 16 amu decrease in the molecular weight compared to **1**. The ^{1}H and ^{13}C NMR data of **2** were similar to those of **1** except for the loss of the hydroxy group at C-27, which accounts for the molecular weight difference between both compounds. Furthermore, comparison of **2** to the data reported for the known nakijiquinone Q (Takahashi *et al.*, 2010) indicated that both compounds are epimers with different configurations at the stereogenic center C-5. This was corroborated by interpretation of ROESY spectra and the downfield chemical shift of C-12 (δ_C 32.5 ppm), establishing a *cis* junction of the decalin ring as in **1**, in contrast to the *trans* junction as reported for nakijiquinone Q (Figure 3.2). Thus, the structure of **2** was identified and the trivial name 5-*epi*-nakijiquinone Q is proposed (Daletos *et al.*, 2014).
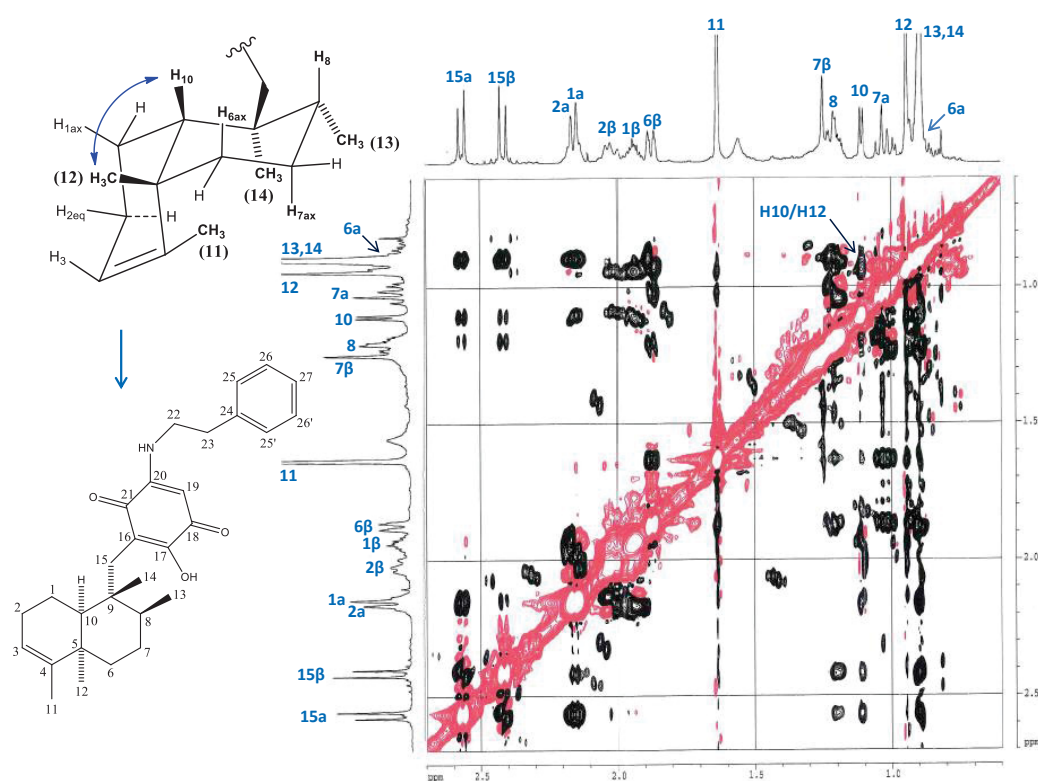
Figure 3.2: ROESY spectrum of **2**

Table 3.2: NMR data of **2** 600 (^{1}H) and 150 (^{13}C) MHz (CDCl$_3$, δ in ppm)

Nr.	δ_C, type	δ_H (J in Hz)	COSY	HMBC
		5-*epi*-nakijiquinone Q		
1	19.3, CH$_2$	1.94, m	1a, 2, 10	2, 3, 9, 10
		2.15, m	1b, 2, 10	2, 3, 5, 9, 10
2	24.7, CH$_2$	2.00, m	1, 2a, 3	
		2.15, m	1, 2b, 3	
3	124.1, CH	5.30, brs	2, 11	1, 2, 5
4	139.2, C			
5	37.5, C			
6	37.6, CH$_2$	0.92^a	6a, 7	4, 5, 7, 8
		1.86, brdd (13.3, 3.5)	6b, 7	7, 8, 10
7	29.3, CH$_2$	1.01, m	6, 7a, 8	5, 6, 13
		1.22, m	6, 7b	5, 6
8	38.9, CH	1.19, m	7b, 13	6, 9, 10, 13, 14, 15
9	44.3, C			
10	46.1, CH	1.10, brd (6.3)	1	1, 2, 4, 5, 6, 9, 12, 14, 15
11	20.0, CH$_3$	1.62, d (1.1)	3	3, 4, 5
12	32.5, CH$_3$	0.93, s		4, 5, 6, 10
13	18.4, CH$_3$	0.88, d (6.2)	8	7, 8, 9
14	16.5, CH$_3$	0.88, s		8, 9, 10, 15
15	33.1, CH$_2$	2.41, d (13.8)	15a	8, 9, 10, 14, 16, 17, 21
		2.56, d (13.8)	15b	8, 9, 10, 14, 16, 17, 21
16	114.3, C			
17	157.2, C			
18	178.7, C			
19	92.1, CH	5.40, s		17, 21
20	150.2, C			
21	183.1, C			
22	44.3, CH$_2$	3.42, td (7.0, 6.7)	23, 20-NH	20, 23, 24
23	34.5, CH$_2$	2.94, t (7.0)	22	22, 24, 25/29
24	137.7, C			
25	128.8, CH	7.17, d (7.4)	26	23, 27, 29
26	129.1, CH	7.31, dd (7.4, 7.5)	25, 27	24, 28
27	127.3, CH	7.24, t (7.5)	26/28	25/29
28	129.1, CH	7.31, dd (7.4, 7.5)	27, 29	24, 26
29	128.8, CH	7.17, d (7.4)	28	23, 25, 27
17-OH		8.29, brs		
20-NH		6.47, brt	22	

3.1.3. 5-*epi*-Nakijiquinone T (3, new natural product)

5-*epi*-Nakijiquinone T	
Sample code	G2-27
Biological source	*Dactylospongia metachromia*
Sample amount	2.5 mg
Physical description	red amorphous solid
Molecular formula	$C_{31}H_{38}N_2O_3$
Molecular weight	486 g/mol
Optical rotation $[\alpha]_D^{20}$	-17 (*c* 0.05, MeOH)
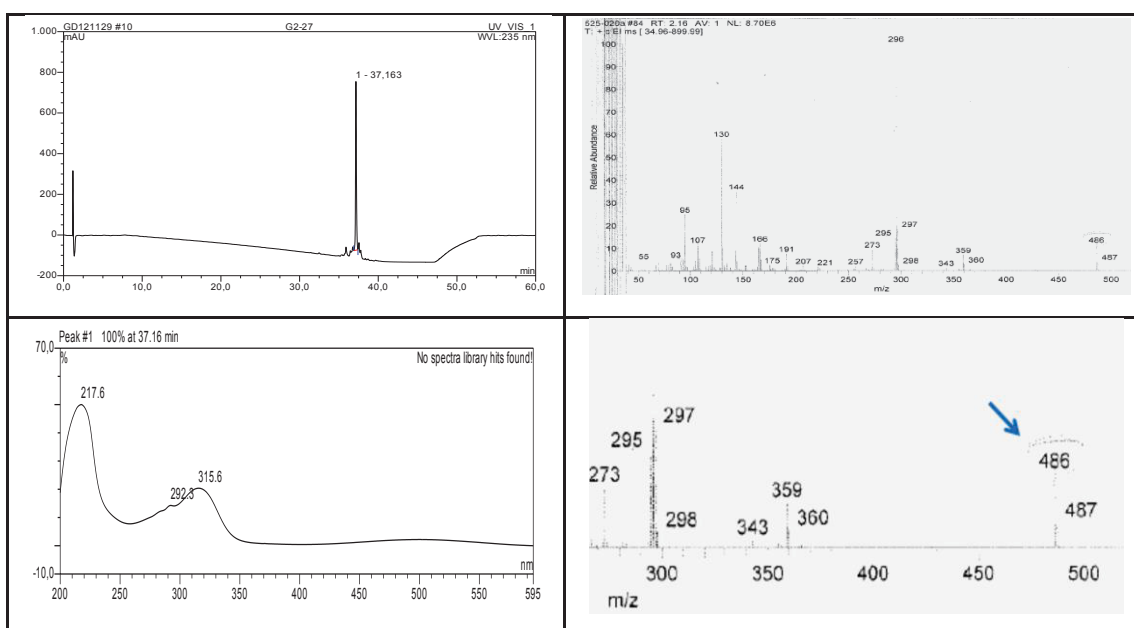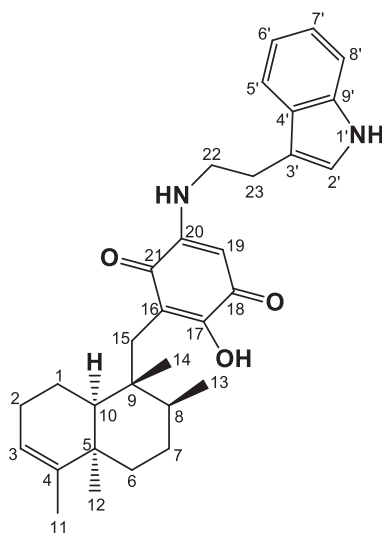
Compound **3** was obtained as a red amorphous solid. The molecular formula $C_{31}H_{38}N_2O_3$ was established by HRESIMS, in accordance with the signal observed at *m/z* 487.2953 [M+H]$^+$. UV absorptions at 315 and 500 nm suggested the presence of a quinone chromophore. The spectroscopic data of **3** had some features in common with those of **1** and **2**, suggesting the same sesquiterpenoid aminoquinone core structure, but a different amine function connected to C-20. ^{1}H NMR and COSY spectra revealed an aminoethyl residue, an additional NH proton resonating at δ_H 8.04 ppm, which is coupled to an aromatic proton at δ_H 7.04 ppm (H-2'), and an aromatic ABCD spin system (H-5' to H-8'). Hence, the last two spin systems revealed an indole moiety. This was confirmed by HMBC cross-peaks detected from H-2' to C-3', C-4' and C-9', from H-5' to C-3', C-7' and C-9', and from H-8' to C-4' and C-6' (Figure 3.3). In addition, HMBC correlations of H$_2$-23 to C-2', C-3', C-4' and C-22, as well as of H$_2$-22 to C-3' and C-23, established the connection of the indole ring with the aminoethyl unit at C-3' (Figure 3.3), thus indicating a tryptamine unit. Accordingly, the structure of **3** was elucidated and designated as 5-*epi*-nakijiquinone T (Daletos *et al.*, 2014).
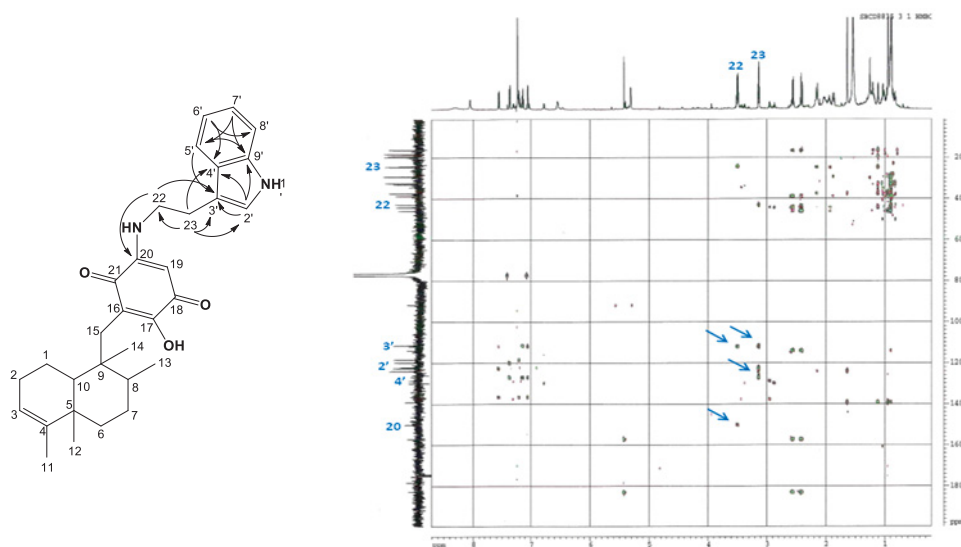
Figure 3.3: HMBC spectrum of **3**

Table 3.3: NMR data of **3** 600 (^{1}H) and 150 (^{13}C) MHz (CDCl$_3$, δ in ppm)

5-*epi*-nakijiquinone T				
Nr.	$\delta_C,^a$ type	δ_H^b (*J* in Hz)	COSY	HMBC
1	19.3, CH$_2$	1.92, m	1a, 2, 10	2, 3, 9, 10
		2.15, m	1b, 2, 10	2, 3, 5, 9, 10
2	24.7, CH$_2$	2.00, m	1, 2a, 3	
		2.14, m	1, 2b, 3	
3	124.1, CH	5.30, brs	2, 11	1, 2, 5
4	139.2, C			
5	37.5, C			
6	37.5, CH$_2$	0.89^d	6a, 7	4, 5, 7, 8
		1.85, ddd (13.3, 4.0, 1.7)	6b, 7	7, 8, 10
7	29.3, CH$_2$	1.00, m	6, 7a, 8	5, 6, 9, 13
		1.24, m	6, 7b	5, 6
8	38.8, CH	1.18, m	7b, 13	6, 9, 10, 13, 14, 15
9	44.3, C			
10	46.0, CH	1.10, brd (6.3)	1	1, 2, 4, 5, 6, 9, 12, 14, 15
11	20.0, CH$_3$	1.62, d (1.1)	3	3, 4, 5
12	32.5, CH$_3$	0.93, s		4, 5, 6, 10
13	18.4, CH$_3$	0.87, d (6.2)	8	7, 8, 9
14	16.5, CH$_3$	0.88, s		8, 9, 10, 15
15	33.1, CH$_2$	2.40, d (13.8)	15a	8, 9, 10, 14, 16, 17, 21
		2.55, d (13.8)	15b	8, 9, 10, 14, 16, 17, 21
16	114.2, C			
17	157.3, C			
18	178.6, C			
19	91.9, CH	5.41, s		17, 21
20	150.3, C			
21	183.1, C			
22	43.1, CH$_2$	3.49, td (6.9, 6.3)	23, 20-NH	20, 23, 3'
23	24.4, CH$_2$	3.12, t (6.9)	22	22, 2', 3', 4'
24				
25				
17-OH		8.29, brs		
20-NH		6.54, brt	22	
NH-1'		8.04, brs	2'	
2'	122.4, CH	7.04, d (1.7)	NH-1'	3', 4', 9'
3'	112.0, C			
4'	127.1, C			
5'	118.6, CH	7.56, brd (7.8)	6'	3', 7', 9'
6'	120.0, CH	7.13, dd (7.8, 7.4)	5', 7'	4', 8'
7'	122.8, CH	7.21, dd (8.0, 7.4)	6', 8'	5', 9'
8'	111.6, CH	7.37, brd (8.0)	7'	4', 6'
9'	136.7, C			

3.1.4. 5-*epi*-Nakijiquinone U (4, new natural product)

5-*epi*-Nakijiquinone U	
Sample code	G2-28
Biological source	*Dactylospongia metachromia*
Sample amount	2.0 mg
Physical description	red amorphous solid
Molecular formula	$C_{25}H_{37}NO_3S$
Molecular weight	431 g/mol
Optical rotation $[\alpha]_D^{20}$	-54 (*c* 0.1, MeOH)
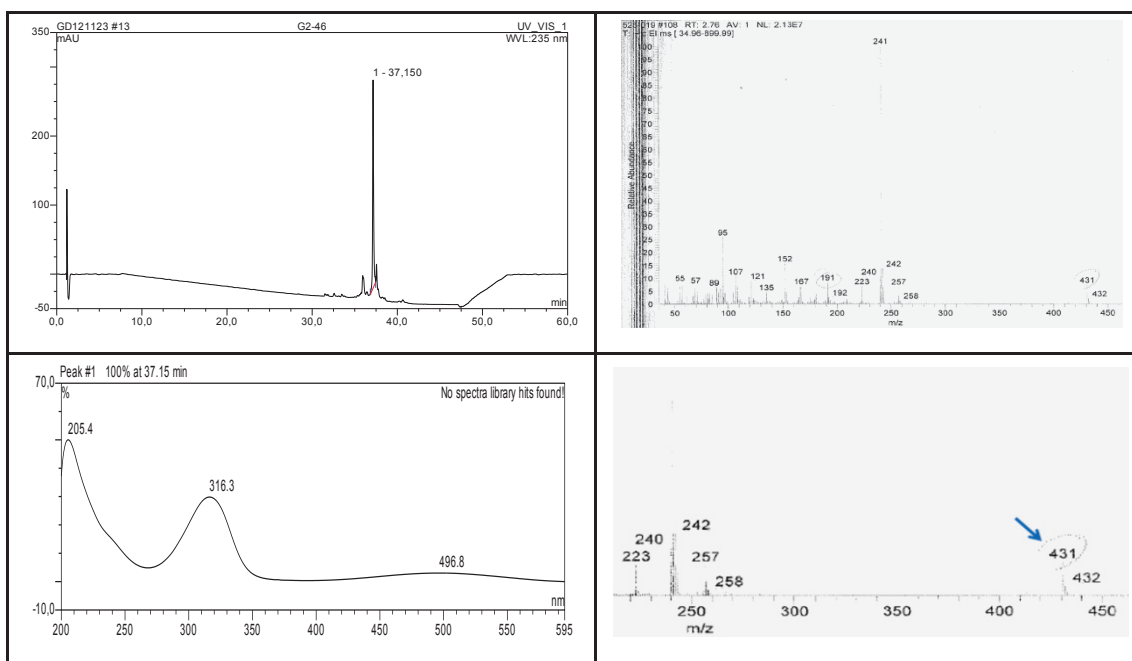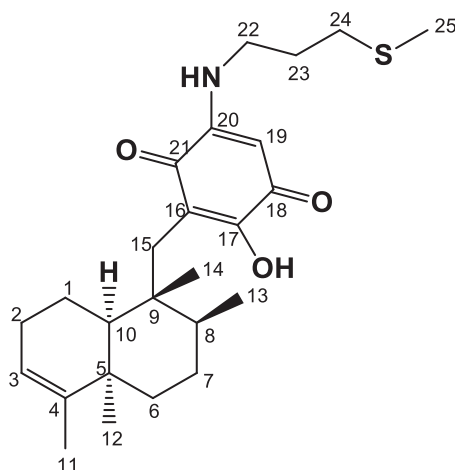
Compound **4** was obtained as a red amorphous solid. HRESIMS showed an ion peak at *m/z* 432.2567 [M+H]$^+$ indicating the molecular formula $C_{25}H_{37}NO_3S$. NMR data denoted the same sesquiterpenoid aminoquinone basic structure as in **1-3**. It displayed UV absorbances at λ_{max} (MeOH) 204.5, 327.8, and 493.9 nm, showing high similarity to UV spectra typical for nakijiquinone derivatives. In addition, ^{1}H NMR and COSY spectra (Table 3.4) showed an aminopropyl spin system including three methylene groups resonating at δ_H 3.30, 1.95 and 2.56 ppm (H$_2$-22, H$_2$-23 and H$_2$-24, respectively), and one methyl group singlet at δ_H 2.09 (H$_3$-25). The downfield chemical shifts of the methyl group and of CH$_2$-24 at δ_H 2.09 (δ_C 15.8) and 2.56 (δ_C 31.7) ppm, as well as the presence of one sulfur atom in the molecule, as indicated by HRESIMS, suggested the attachment of the methyl group to CH$_2$-24 through sulfur. This was further confirmed by the observed HMBC correlation of the methyl group to C-24 (Figure 3.4). Further HMBC correlations were observed from H$_2$-22 to C-20, C-23 and C-24, from H$_2$-23 to C-22 and C-24, and from H$_2$-24 to C-22, C-23 and C-25. Thus, **4** was identified as the new natural product 5-*epi*-nakijiquinone U. Based on ROESY and ^{13}C NMR spectra interpretation, the relative configuration of the sesquiterpenoid unit in **3** and **4** was found to be identical to that observed for **1** and **2** (Daletos *et al.*, 2014).
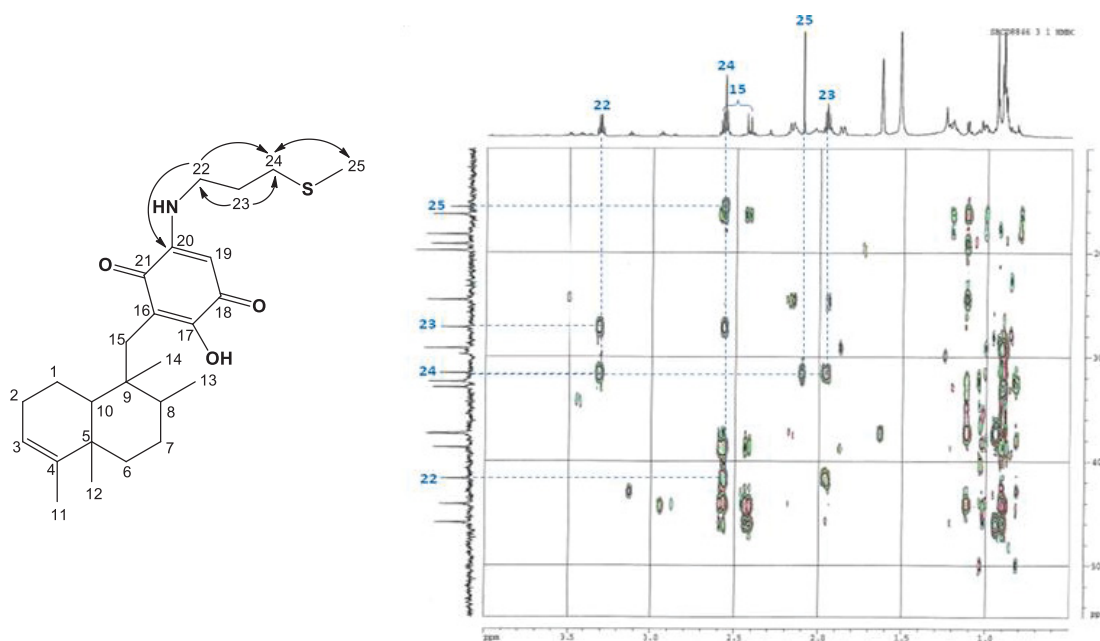
Figure 3.4: ROESY spectrum of **4**

Table 3.4: NMR data of **4** 600 (^{1}H) and 150 (^{13}C) MHz (CDCl$_3$, δ in ppm)

Nr.	$\delta_C,^a$ type	$\delta_H{}^b$ (J in Hz)	COSY	HMBC
1	19.3, CH$_2$	1.93, m	1a, 2, 10	2, 3, 9, 10
		2.17, m	1b, 2, 10	2, 3, 5, 9, 10
2	24.7, CH$_2$	2.00, m	1, 2a, 3	
		2.15, m	1, 2b, 3	
3	124.1, CH	5.30, brs	2, 11	1, 2, 5
4	139.2, C			
5	37.5, C			
6	37.5, CH$_2$	0.89^d	6a, 7	4, 5, 7, 8
		1.86, ddd (13.4, 4.5, 3.2)	6b, 7	7, 8, 10
7	29.3, CH$_2$	1.01, m	6, 7a, 8	5, 6, 9, 13
		1.24, m	6, 7b	5, 6
8	38.8, CH	1.20, m	7b, 13	6, 9, 10, 13, 14, 15
9	44.3, C			
10	46.1, CH	1.11, brd (5.9)	1	1, 2, 4, 5, 6, 9, 12, 14, 15
11	20.0, CH$_3$	1.62, d (1.1)	3	3, 4, 5
12	32.5, CH$_3$	0.93, s		4, 5, 6, 10
13	18.4, CH$_3$	0.90, d (6.2)	8	7, 8, 9
14	16.5, CH$_3$	0.89, s		8, 9, 10, 15
15	33.1, CH$_2$	2.41, d (13.8)	15a	8, 9, 10, 14, 16, 17, 21
		2.56, d (13.8)	15b	8, 9, 10, 14, 16, 17, 21
16	114.2, C			
17	157.3, C			
18	178.6, C			
19	92.0, CH	5.41, s		17, 21
20	150.4, C			
21	183.1, C			
22	41.8, CH$_2$	3.30, td (6.9, 6.5)	23, 20-NH	20, 23, 24
23	27.3, CH$_2$	1.95, q (6.9)	22, 24	22, 24
24	31.7, CH$_2$	2.56, t (6.9)	23	22, 23, 25
25	15.8, CH$_3$	2.09, s		24
17-OH		8.27, brs		
20-NH		6.51, brt	22	

56

3.1.5. 5-*epi*-Nakijiquinone N (5, new natural product)

5-*epi*-Nakijiquinone N	
Sample code	G2-13
Biological source	*Dactylospongia metachromia*
Sample amount	5.0 mg
Physical description	red amorphous solid
Molecular formula	$C_{26}H_{40}NO_3$
Molecular weight	413 g/mol
Optical rotation $[\alpha]_D^{20}$	-26 (*c* 0.05, MeOH)
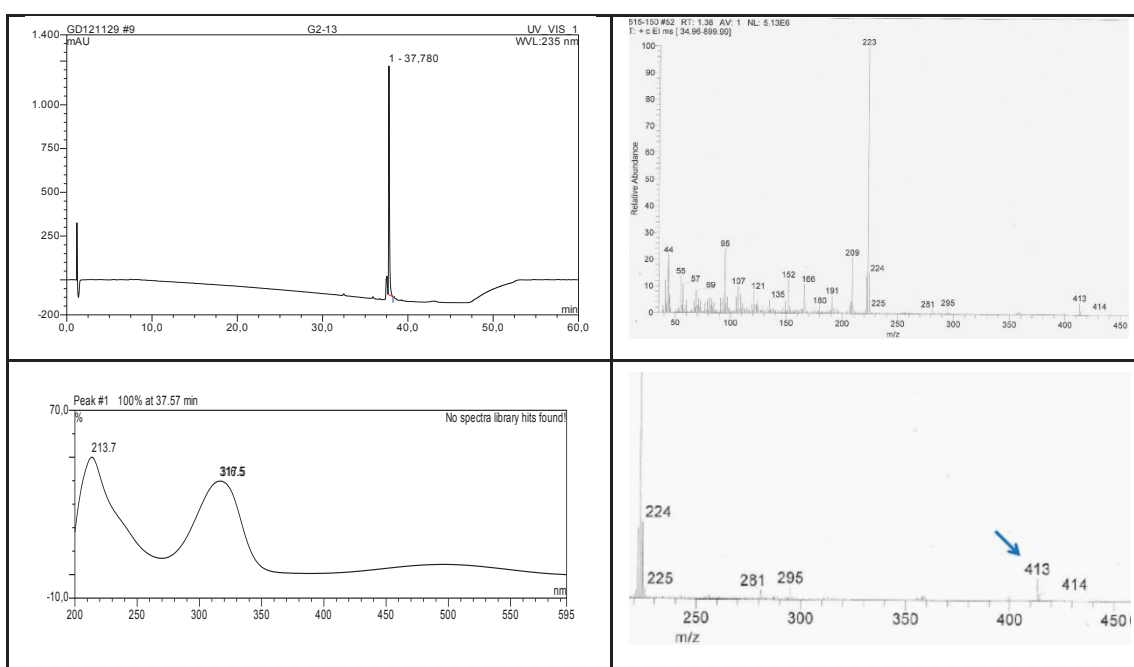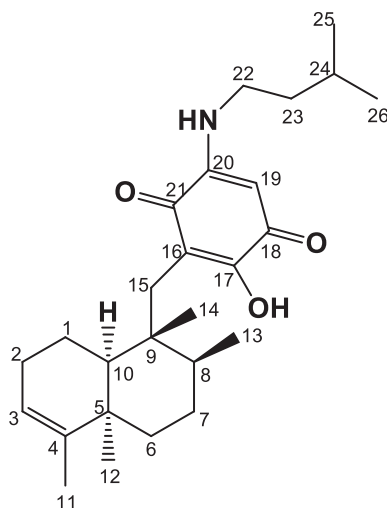
Compound **5** was obtained as a red amorphous solid. The molecular formula $C_{26}H_{39}NO_3$ was established by HRESIMS analysis (*m/z* 414.3006 $[M+H]^+$). It exhibited UV absorbances at λ_{max} (MeOH) 206.3, 322.2, and 495.1 nm. ^{1}H NMR and COSY spectra showed an isopentylamine spin system including two methylene groups resonating at δ_H 3.16, 1.55 ppm (H$_2$-22, H$_2$-23 respectively), one methine at δ_H 1.66 and two methyl groups at δ_H 0.93 (H$_3$-25, H$_3$-26). This was further confirmed by the observed HMBC correlations from H$_2$-23 to C-25, C-26 and C-22, from H$_2$-24 to C-22, C-25 and C-26, and from H$_3$-25/26 to C-23 and C-24. Close similarity of the ^{1}H and ^{13}C NMR data with those reported for nakijiquinone N (Takahashi *et al.*, 2010) indicated both compounds to be epimers differing in the configuration of C-5. In contrast to the *trans* fused decalin ring reported for nakijiquinone N, ROESY and ^{13}C NMR data indicated a *cis* fusion in **5**, by analogy with **1**-**4.** This was corroborated by interpretation of ROESY spectra and the downfield chemical shift of C-12 (δ_C 32.5 ppm), establishing a *cis* junction of the decalin ring as in **1**, in contrast to the *trans* junction as reported for nakijiquinone N. Thus, the structure of **5** was identified and the trivial name 5-*epi*-nakijiquinone N is proposed (Daletos *et al.*, 2014).
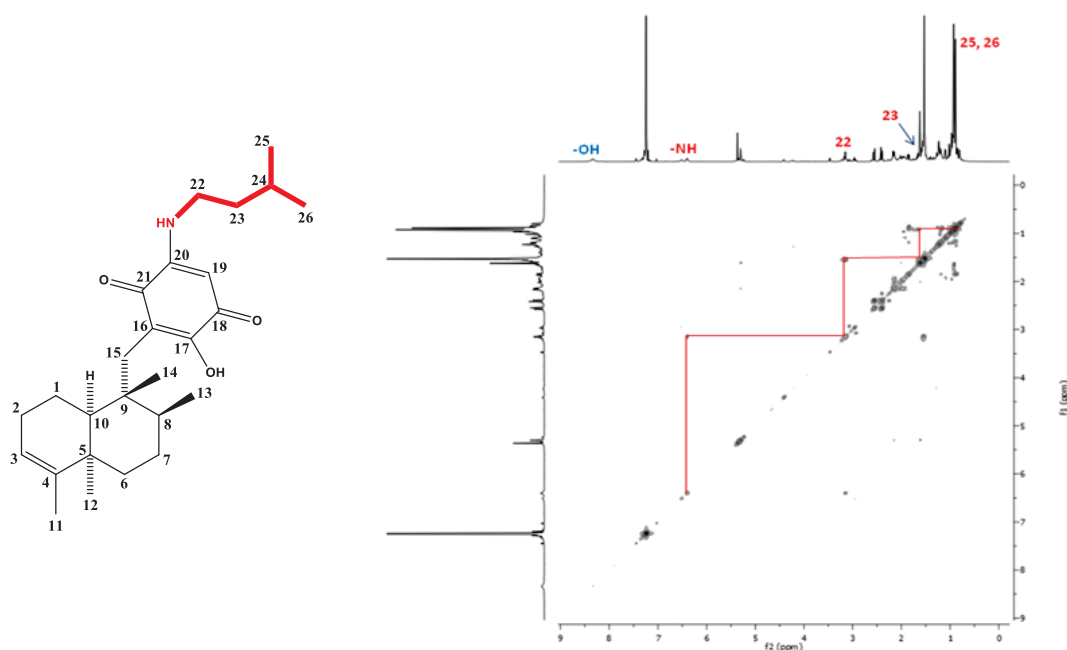
Figure 3.5: COSY spectrum of **5**

Table 3.5. NMR data of **5** 600 (^{1}H) and 150 (^{13}C) MHz (CDCl$_3$, δ in ppm)

Nr.	δc, type	δ_H (J in Hz)	COSY	HMBC
5-*epi*-nakijiquinone N				
1	19.3, CH$_2$	1.94, m	1a, 2, 10	2, 3, 9, 10
		2.17, m	1b, 2, 10	2, 3, 5, 9, 10
2	24.7, CH$_2$	2.00, m	1, 2a, 3	
		2.15, m	1, 2b, 3	
3	124.1, CH	5.30, brs	2, 11	1, 2, 5
4	139.2, C			
5	37.5, C			
6	37.5, CH$_2$	0.90^a	6a, 7	4, 5, 7, 8
		1.86, ddd (13.4, 3.7, 2.1)	6b, 7	7, 8, 10
7	29.4, CH$_2$	1.01, m	6, 7a, 8	5, 6, 13
		1.23, m	6, 7b	5, 6
8	38.8, CH	1.19, m	7b, 13	6, 9, 10, 13, 14, 15
9	44.2, C			
10	46.0, CH	1.11, brd (6.2)	1	1, 2, 4, 5, 6, 9, 12, 14, 15
11	20.0, CH$_3$	1.62, d (1.1)	3	3, 4, 5
12	32.5, CH$_3$	0.93, s		4, 5, 6, 10
13	18.4, CH$_3$	0.90, d (6.2)	8	7, 8, 9
14	16.5, CH$_3$	0.89, s		8, 9, 10, 15
15	33.1, CH$_2$	2.41, d (13.8)	15a	8, 9, 10, 14, 16, 17, 21
		2.56, d (13.8)	15b	8, 9, 10, 14, 16, 17, 21
16	114.0, C			
17	157.5, C			
18	178.4, C			
19	91.7, CH	5.37, s		17, 21
20	150.5, C			
21	183.2, C			
22	41.4, CH$_2$	3.16, td (8.0, 6.2)	23, 20-NH	20, 23, 24
23	37.1, CH$_2$	1.55, td (8.0, 7.1)	22, 24	22, 25/26
24	26.2, CH	1.66, m	23, 25, 26	23, 25/26
25	22.5, CH$_3$	0.93, d (6.5)	24	23, 24, 26
26	22.5, CH$_3$	0.93, d (6.5)	24	23, 24, 25
27				
28				
29				
17-OH		8.33, brs		
20-NH		6.39, brt	22	

3.1.6. 5-*epi*-Nakijinol C (6, new natural product)

5-*epi*-Nakijinol C	
Sample code	G2-37
Biological source	*Dactylospongia metachromia*
Sample amount	8.0 mg
Physical description	pale yellow amorphous solid
Molecular formula	$C_{24}H_{33}NO_3$
Molecular weight	483 g/mol
Optical rotation $[\alpha]_D^{20}$	-33 (*c* 0.1, MeOH)
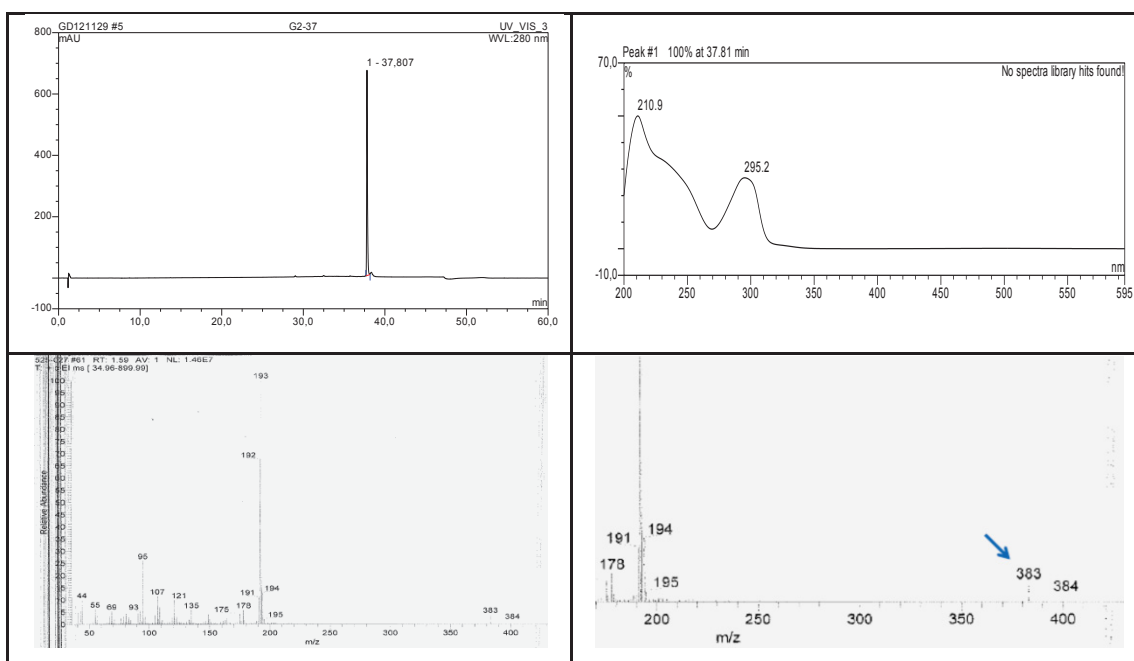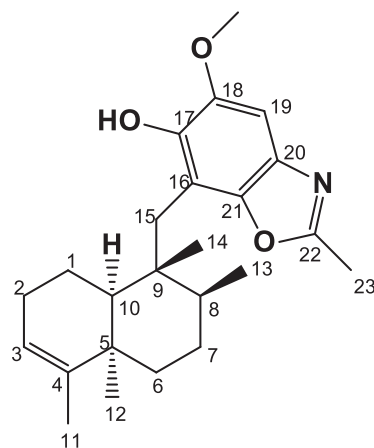
Compound **6** was obtained as a pale yellow amorphous solid. The molecular formula was determined to be $C_{24}H_{33}NO_3$ by HRESIMS (m/z 384.2532 [M+H]$^+$), indicating nine elements of unsaturation. It showed UV absorbances at λ_{max} (MeOH) 204.1, 227.4, and 294.0 nm. Thorough inspection of 1D and 2D NMR data disclosed the presence of the same sesquiterpenoid moiety as in **1-5**. In addition, the ^{1}H NMR spectrum revealed the presence of a hydroxy group resonating at δ_H 5.85 ppm, an aromatic proton at δ_H 6.98 ppm (H-19), a methoxy group at δ_H 3.91 ppm (18-OCH$_3$), and an olefinic methyl group at δ_H 2.54 ppm (CH$_3$-23). The ^{13}C NMR (Table 3.6) and HMQC spectra confirmed the corresponding carbon signals and revealed in addition six sp^2 quaternary carbons, four of which were oxygenated as indicated by their downfield chemical shifts at δ_C 162.1, 146.8, 144.6 and 143.7 ppm (C-22, C-17, C-18 and C-21, respectively) (Daletos *et al.*, 2014).

HMBC correlations of H-19 to C-17, C-18, C-20 and C-21 (Figure 3.6) established a pentasubstituted aromatic ring, which was connected to the sesquiterpenoid moiety at C-16 based on correlations observed for H$_2$-15 to C-16, C-17 and C-21. The methoxy group 18-OCH$_3$ was attached to C-18, as indicated by the respective HMBC correlation (Figure 3.7), as well as by its ROESY correlation to H-19. The downfield chemical shifts of C-20 (δ_C 132.5), C-21 (δ_C 143.7) and C-22 (δ_C 162.1), as well as the HMBC correlation observed for the methyl group H$_3$-23 to C-22, were indicative of a 2-methyloxazole moiety and hence accounted for the remaining two elements of unsaturation in the structure of **6**. This was further confirmed by the upfield chemical shift of C-23 at δ_C 14.6 ppm, which is characteristic for respective methyl substituents in structural analogues. Accordingly, **6** was identified as a new natural product and was given the name 5-*epi*-nakijinol C (Daletos *et al.*, 2014).
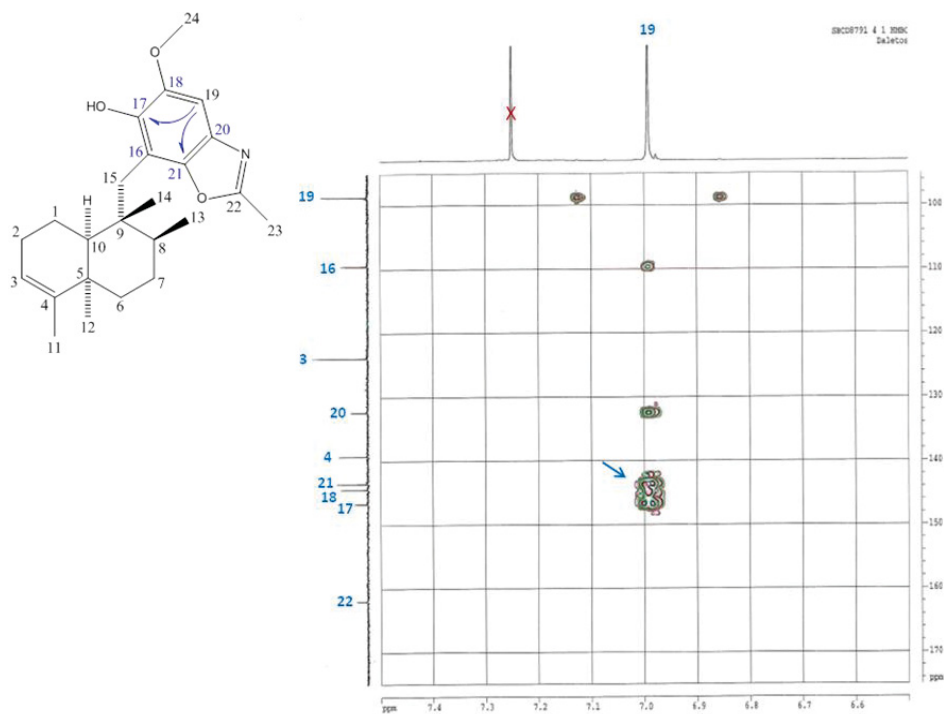
Figure 3.6: HMBC spectrum of **6**
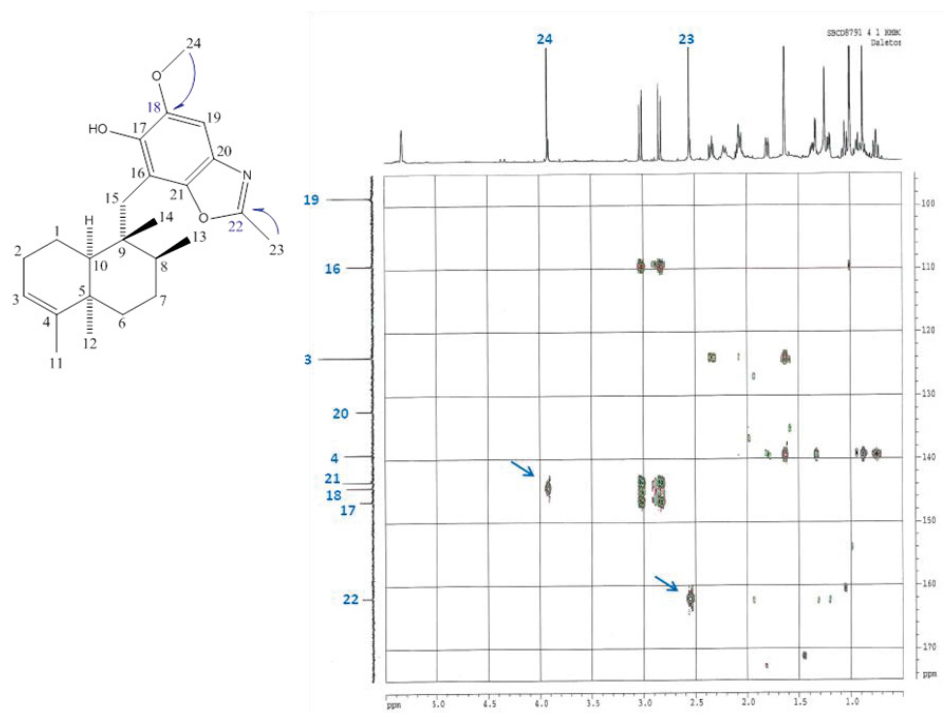
Figure 3.7: HMBC spectrum of **6**

Table 3.6. NMR data of **6** 600 (^{1}H) and 150 (^{13}C) MHz (CDCl$_3$, δ in ppm)

position	δ_C, type	δ_H (J in Hz)	COSY	HMBC
		5-*epi*-nakijinol C		
1	19.6, CH$_2$	2.05, m	1a, 2, 10	2, 9, 10
		2.32, brdd (13.3, 9.1)	1b, 2, 10	2, 3, 5, 9, 10
2	24.9, CH$_2$	2.06, m	1, 2a, 3	
		2.21, m	1, 2b, 3	
3	124.1, CH	5.32, brs	2, 11	1, 2, 5
4	139.4, C			
5	37.4, C			
6	37.3, CH$_2$	0.74, td (13.6, 2.8)	6a, 7	4, 5, 7, 8
		1.79, ddd (13.6, 3.5, 2.8)	6b, 7	7, 8, 10
7	29.4, CH$_2$	1.03, qd (13.3, 2.5)	6, 7a, 8	5, 6, 13
		1.19, dq (13.4, 3.5)	6, 7b	5, 6, 9, 13
8	38.1, CH	1.35, m	7b, 13	6, 7, 9, 13, 14, 15
9	44.2, C			
10	45.3, CH	1.32, brd (5.7)	1	1, 2, 4, 5, 6, 9, 12, 14, 15
11	20.0, CH$_3$	1.62, d (1.2)	3	3, 4, 5
12	32.4, CH$_3$	0.87, s		4, 5, 6, 10
13	18.7, CH$_3$	0.99, d (6.2)	8	7, 8, 9
14	16.7, CH$_3$	0.99, s		8, 9, 10, 15
15	34.9, CH$_2$	2.82, d (14.0)	15a	8, 9, 10, 14, 16, 17, 21
		3.01, d (14.0)	15b	8, 9, 10, 14, 16, 17, 21
16	109.7, C			
17	146.8, C			
18	144.6, C			
19	98.9, CH	6.98, s		17, 18, 20, 21
20	132.5, C			
21	143.7, C			
22	162.1, C			
23	14.6, CH$_3$	2.54, s		22
24				
25				
18-OCH$_3$	56.7, CH$_3$	3.91, s		18
17-OH		5.85, s		

3.1.7. 5-*epi*-Nakijinol D (7, new natural product)

5-*epi*-Nakijinol D	
Sample code	G2-46
Biological source	*Dactylospongia metachromia*
Sample amount	2.5 mg
Physical description	pale yellow amorphous solid
Molecular formula	$C_{25}H_{32}N_2O_2$
Molecular weight	393 g/mol
Optical rotation $[\alpha]_D^{20}$	-41 (*c* 0.1, MeOH)
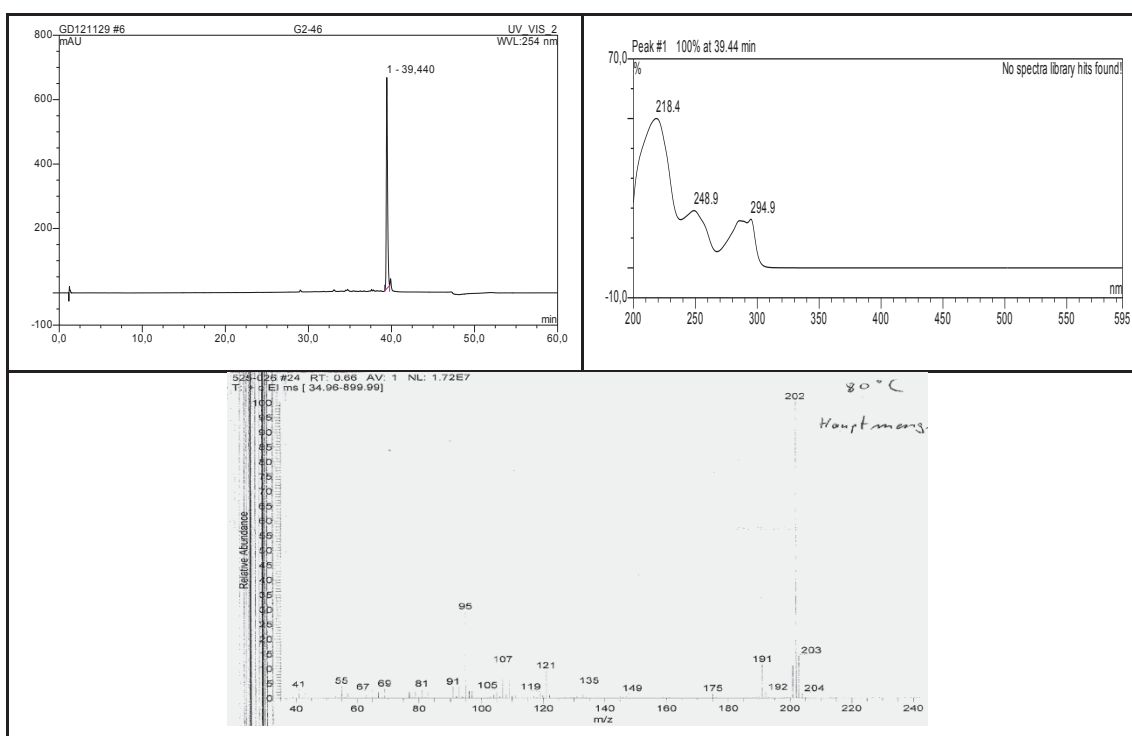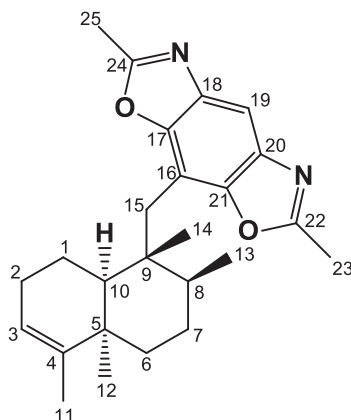
Compound **7** was obtained as a pale yellow amorphous solid. The molecular formula $C_{25}H_{32}N_2O_2$ was established by HRESIMS (m/z 393.2535 $[M + H]^+$), thus corresponding to 11 elements of unsaturation. It displayed UV absorbances at λ_{max} (MeOH) 219.0, 248.9, 284.1, 288.9, and 493.9 nm. NMR data of **7** revealed the presence of the same *cis*-4,9-friedodrim-3-ene subunit as for **1-6**. The remaining ^{1}H NMR signals (Table 3.7) included an aromatic proton at δ_H 7.71 ppm (H-19), and two overlapping olefinic methyl groups at δ_H 2.61 ppm (CH$_3$-23/25), both familiar features from the spectra of **6**. In addition to the corresponding carbon signals, only four out of seven expected *sp²* quaternary carbon signals were detected in the ^{13}C NMR spectrum. Accordingly, six carbons appeared as three pairs of overlapped signals (C-17/21, C-18/20 and C-22/24), suggesting a plane of symmetry in the structural subunit. HMBC correlations from H-19 to C-17/21 and C-18/20, from H$_3$-23/25 to C-22/24 (Figure 3.9), as well as comparison of ^{13}C chemical shifts of C-18/20 (δc 138.5), C-17/21 (δc 149.2) and C-22/24 (δc 163.9) with those detected in **6**, corroborated the presence of a 2,6-dimethyl-bisbenzoxazole moiety, rationalizing the remaining elements of unsaturation. The connection to the sesquiterpenoid moiety at C-16 was deduced from HMBC correlations of H$_2$-15 to C-16 and C-17/21 (Figure 3.8) by analogy with **6**. Moreover, the prominent fragment ion peaks detected at m/z 191 and 202, which are characteristic for the decalin ($C_{14}H_{23}$) and the 2,6,8-trimethyl-bisbenzoxazole ($C_{11}H_{10}N_2O_2$) subunits, respectively, offered further evidence. Thus, the structure of **7** was assigned and it was designated 5-*epi*-nakijinol D (Daletos *et al.*, 2014).
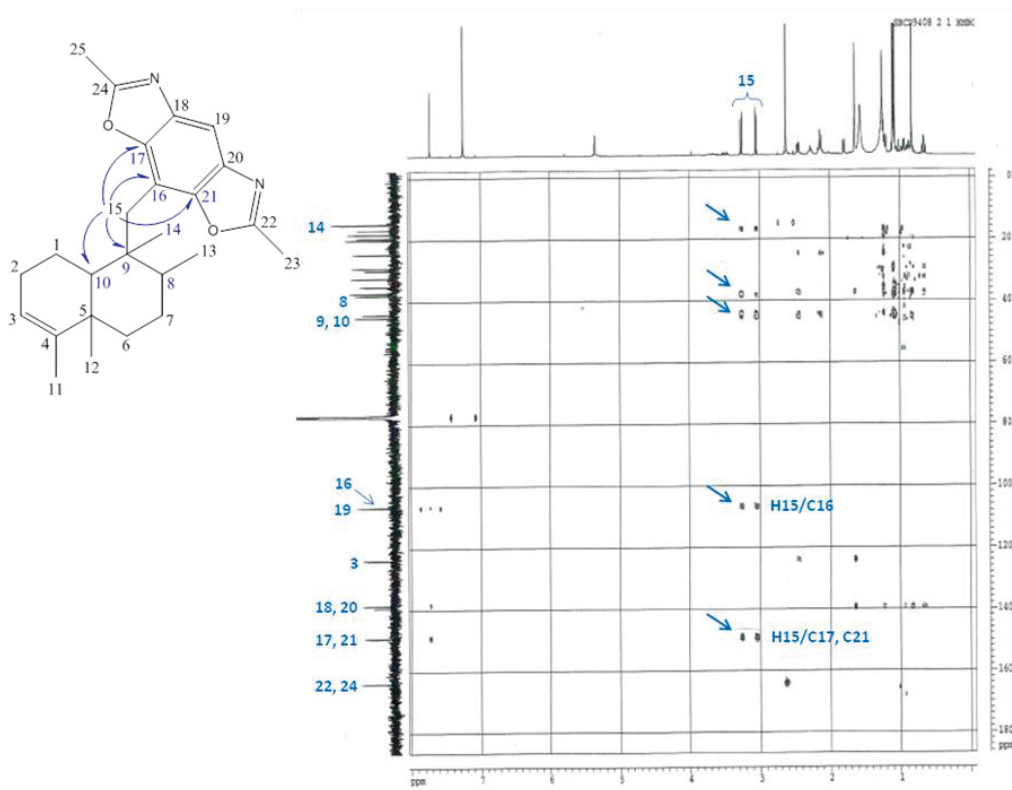
Figure 3.8: HMBC spectrum of **7**
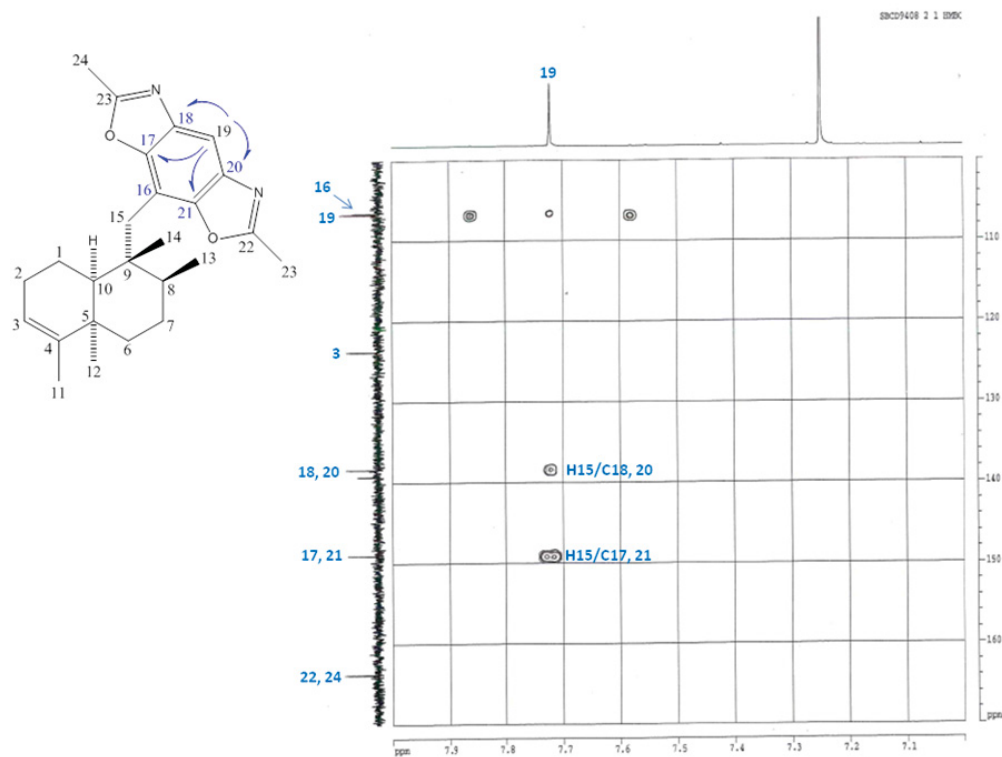
**Figure 3.9:** HMBC spectrum of **7**

66

Table 3.7: NMR data of **7** 600 (^{1}H) and 150 (^{13}C) MHz (CDCl$_3$, δ in ppm)

Nr.	δ_C, type	δ_H (J in Hz)	COSY	HMBC
		5-*epi*-nakijinol D		
1	19.3, CH$_2$	2.11, m	1a, 2, 10	2, 9, 10
		2.44, brdd (13.7, 9.8)	1b, 2, 10	2, 3, 5, 9, 10
2	24.7, CH$_2$	2.12, m	1, 2a, 3	
		2.26, m	1, 2b, 3	
3	123.9, CH	5.34, brs	2, 11	1, 2
4	139.4, C			
5	37.3, C			
6	37.2, CH$_2$	0.64, td (13.8, 3.0)	6a, 7	4, 5, 7, 8, 12
		1.78, brdt (13.8, 3.1)	6b, 7	4, 7, 8, 10
7	29.1, CH$_2$	1.08^a	6, 7a, 8	5, 6, 8
		1.19, m	6, 7b	8, 13
8	38.0, CH	1.25, m	7b, 13	9, 13, 14
9	44.2, C			
10	45.2, CH	1.22, m	1	1, 2, 4, 5, 6, 9, 12, 14, 15
11	19.9, CH$_3$	1.63, d (1.3)	3	3, 4, 5
12	32.4, CH$_3$	0.81, s		4, 5, 6, 10
13	18.1, CH$_3$	1.08, d (6.5)	8	7, 8, 9
14	16.7, CH$_3$	1.06, s		8, 9, 10, 15
15	35.2, CH$_2$	3.04, d (14.2)	15a	8, 9, 10, 14, 16, 17/21
		3.25, d (14.2)	15b	8, 9, 10, 14, 16, 17/21
16	106.7, C			
17	149.2, C			
18	138.5, C			
19	106.7, CH	7.71, s		17/21, 18/20
20	138.5, C			
21	149.2, C			
22	163.9, C			
23	14.9, CH$_3$	2.61, s		22
24	163.9, C			
25	14.9, CH$_3$	2.61, s		24

3.1.8. 18-Hydroxy-5-*epi*-hyrtiophenol (8, known natural product)

18-Hydroxy-5-*epi*-hyrtiophenol	
Sample code	G2-1
Biological source	*Dactylospongia metachromia*
Sample amount	10 mg
Physical description	white amorphous solid
Molecular formula	$C_{23}H_{32}O_4$
Molecular weight	372 g/mol
Optical rotation $[\alpha]_D^{20}$	-70 (*c* 0.1, MeOH)
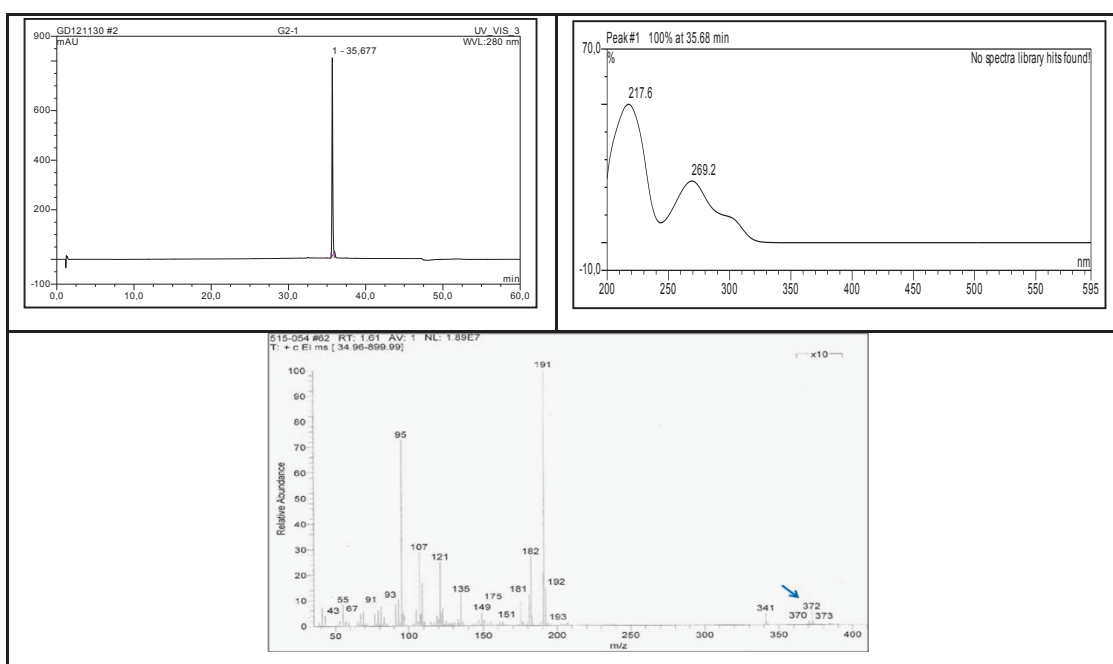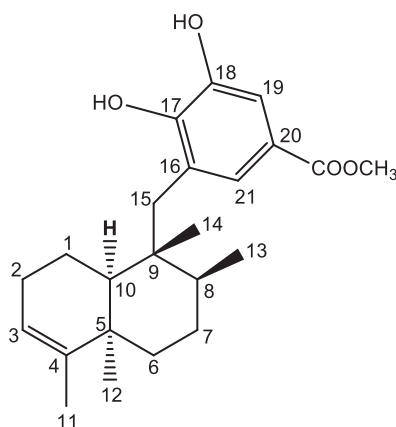
Compound **8** was obtained as a white amorphous solid. It displayed UV absorbances at λ_{max} 218 and 269 nm. The EIMS showed molecular ion peak at m/z 372 [M$^+$] indicating a molecular weight of 372 g/mol. The NMR spectral data revealed two substructures consisting of a sesquiterpene and a tetrasubstituted benzene moiety. The NMR ^{13}C and ^{1}H chemical shifts corresponding to the sesquiterpene substructure indicated among others the presence of a secondary methyl, two tertiary methyls, and a trisubstituted double bond bearing one further methyl group. Such a pattern, together with the presence in the mass spectrum of an intense fragment ion at *m/z* 191, is characteristic of the *cis*-4,9-friedodrim-3-ene subunit as for **1-7**. In addition, HMBC correlations from H-19 to C-17, C-21, and C-22, and from H-21 to C-17, C-19 and C-22 (Figure 3.10) established a 1,3,4,5-tetrasubstituted benzene ring, which was connected to the sesquiterpenoid moiety at C-16 based on correlations observed for H$_2$-15 to C-16, C-17, and C-21. The structure of **8** was further confirmed by comparison of its spectroscopic data (UV, MS, 1H and 13C NMR) with those reported for 18-Hydroxy-5-*epi*-hyrtiophenol from the sponge *Hyrtios tubulatus* (Salmoun *et al.*, 2000; Daletos *et al.*, 2014).
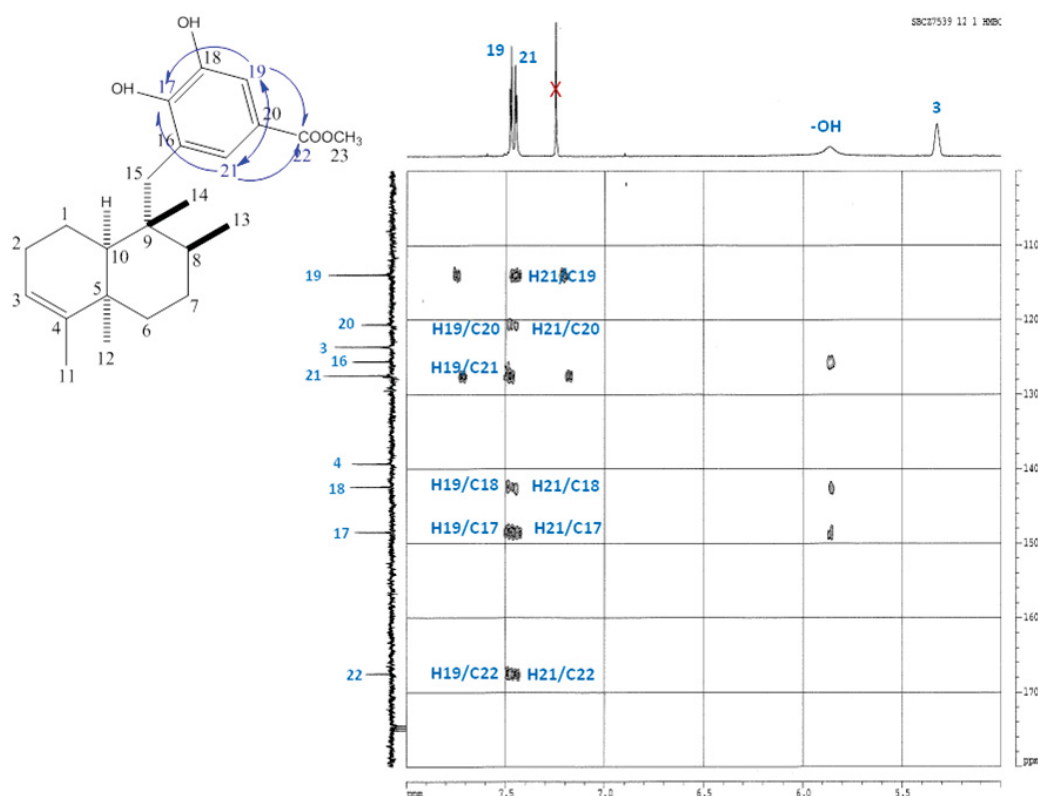
Figure 3.10: HMBC spectrum of **8**

3.1.9. 1,2-Propanediol, 3-[(13-methyltetradecyl)oxy]-, (2*S*)- (9, known natural product)

1,2-Propanediol, 3-[(13-methyltetradecyl)oxy]-, (2*S*)-	
Sample code	G2-6
Biological source	*Dactylospongia metachromia*
Sample amount	3 mg
Physical description	white amorphous solid
Molecular formula	$C_{18}H_{38}O_3$
Molecular weight	302 g/mol
Optical rotation $[\alpha]_D^{20}$	+10 (*c* 0.06, MeOH)
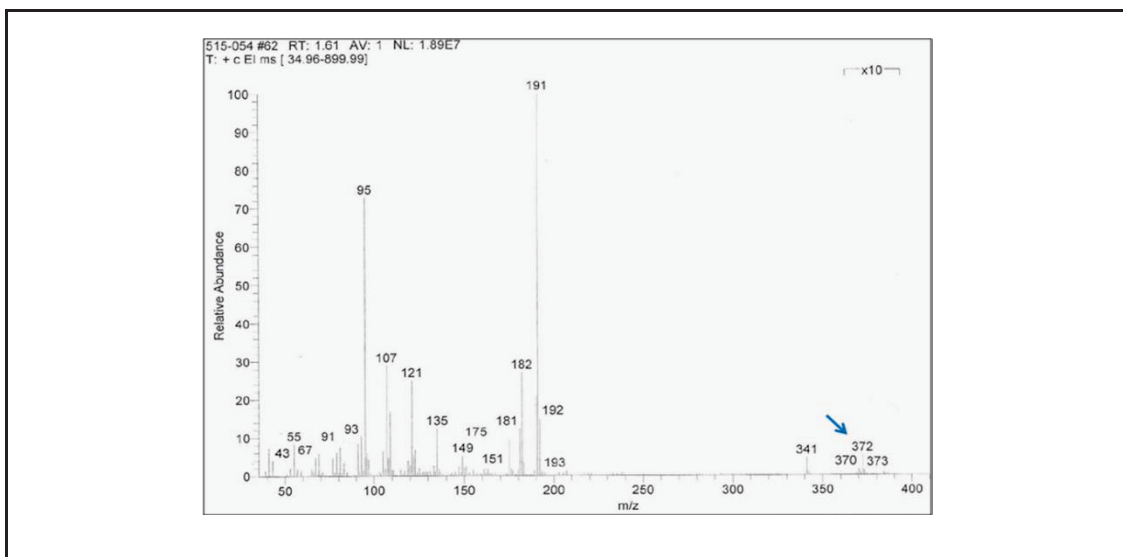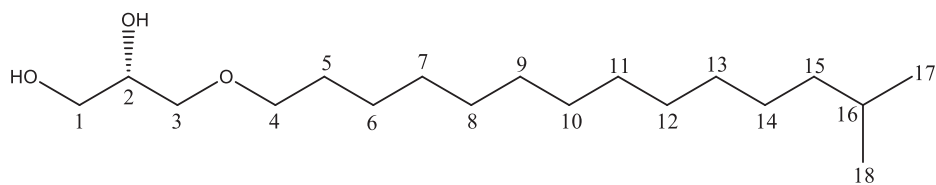
Compound **9** was isolated as a white amorphous solid. Its molecular formula was established as $C_{18}H_{38}O_3$ based on MS and NMR spectral analyses. The ^{1}H-NMR spectrum of **9** displayed a typical fatty acid spectrum, with an intense peak at δ_H 1.23, due to the methylenes in the fatty acyl chain. In addition proton signals for three pairs of oxymethylene protons and one oxymethine were observed [δ_H 3.94 (1H, brddd, 9.4, 5.5, 3.9, H-2), 3.71 (1H, dd, J = 11.4, 3.9 Hz, H-1a), 4.16 (1H, dd, J = 11.4, 5.5 Hz, H-1b), 3.51 (2H, m, H-3), 3.44 (2H, m, H-4)], representing typical signals for a glycerol monoether moiety. The remaining resonances of an aliphatic methine at δ_H 1.50 (1H, m, H-16) and two overlapping methyl groups at δ_H 1.50 (6H, d, J = 6.6, H_3-17 and H_3-18) were indicative of an isopropyl terminated aliphatic long chain, as confirmed by the strong COSY correlation from both methyl groups H_3-17 and H_3-18 to H-16. Thus, compound **9** was identified as 1,2-propanediol, 3-[(13-methyltetradecyl)oxy]- by comparison of its NMR and MS spectroscopic data with those reported in the literature (Liu *et al.*, 2006). Previous reports include the detection of the isolated glycerolipid in the Myxobacterium *Myxococcus xanthus* and its isolation from a *Sarcotragus* sp. (Dictyoceratida) sponge (Liu *et al.*, 2006). The S configuration was established from the positive specific rotation value ($[\alpha]^{20}_D$ +10, *c* 0.06, MeOH), which is a general feature of long-chain 1-O-alkyl-sn-glycerols (Baer and Fischer, 1941; Daletos *et al.*, 2014).

3.1.10. Indole-3-carboxyaldehyde (10, known natural product)

Indole-3-carboxyaldehyde	
Sample code	G2-22
Biological source	*Dactylospongia metachromia*
Sample amount	3 mg
Physical description	Yellowish white amorphous solid
Molecular formula	C_9H_7NO
Molecular weight	145 g/mol
Optical rotation $[\alpha]_D^{20}$	─

No ionization in (-)-ESI-MS
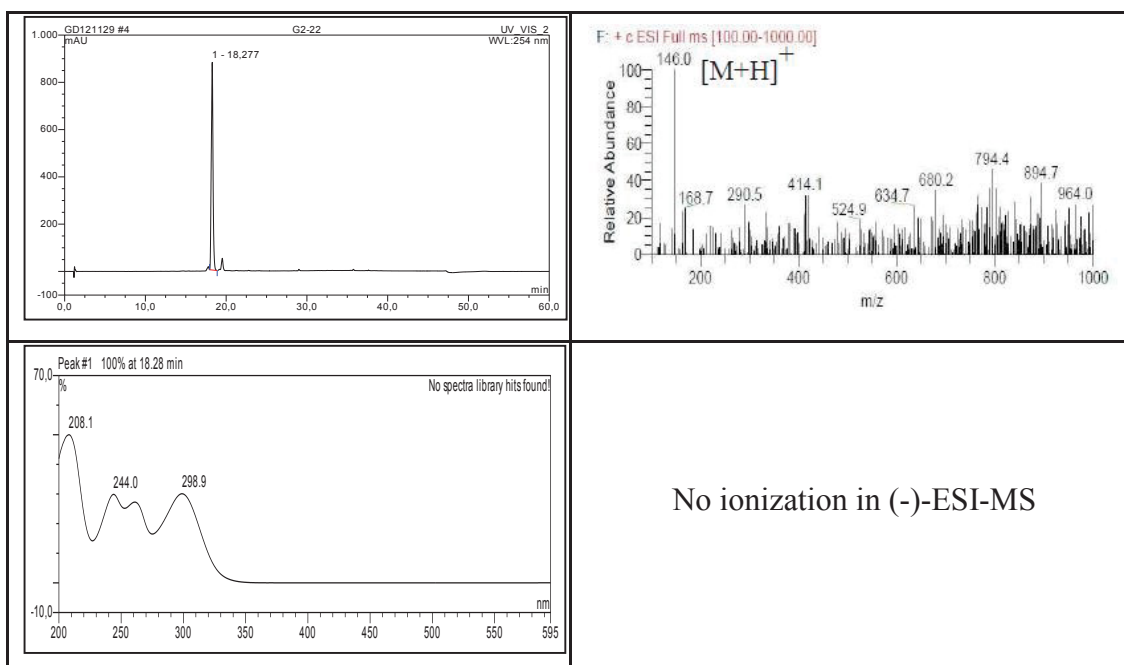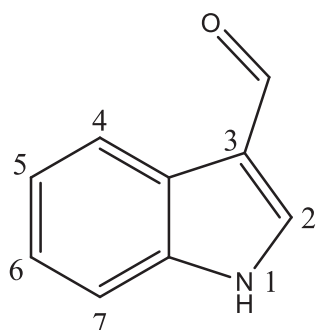
Compound **10** was isolated as a yellowish white amorphous The UV spectrum revealing absorbances at λ_{max} (MeOH) 208, 244, 260, and 299 nm, indicating the presence of an indole chromophore. The (+)-ESI-MS spectrum exhibited a molecular ion peak at *m/z* 146.0 [M+H]$^+$ (base peak), suggesting a molecular weight of 145 g/mol. The ^{1}H NMR spectrum revealed the presence of a a ABCD spin system, including a doublet at δ_H 8.16 (1H, d, J = 7.8 Hz, H-4), two doublets of triplets in the downfield region at δ_H 7.24 (1H, dt, *J* = 7.8, 1.1 Hz, H-5) and δ_H 7.28 (1H, d, J = 8.1, 1.3 Hz, H-6), and one doublet at δ_H 7.48 (1H, d, J = 8.1 Hz, H-7) (Figure 3.11), hence suggesting an ortho-disubstituted benzene ring. The other singlet signal at δ_H 8.09 (1H, s, H-2) in addition to the above mentioned signals were assigned to a C3-substituted indole moiety. Moreover, the downfield signal at δ_H 9.88 (1H, s), which was not exchangeable indicated the presence of an aldehyde group. The above data were identical to those in the literature for indole-3-carboxyaldehyde (Aldrich, 1992; Daletos *et al.*, 2014).
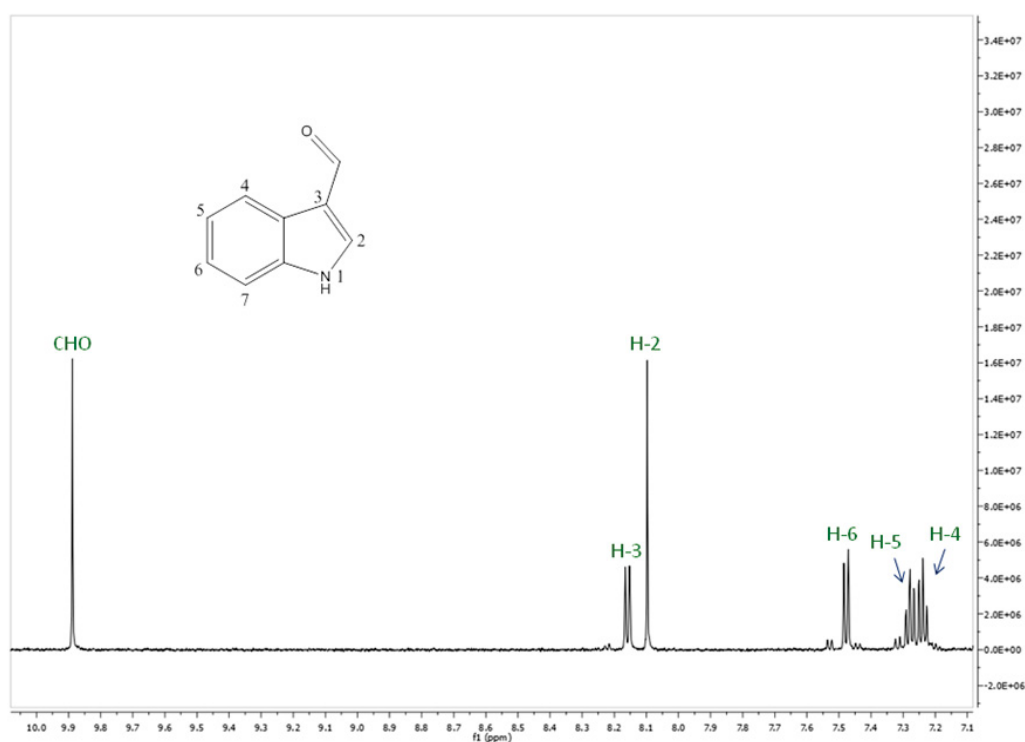
Figure 3.11: ^{1}H NMR spectrum of **10**

3.1.11. Bioactivity of compounds isolated from the marine sponge *D. metachromia*

The isolated compounds were subjected to bioassays aimed to determine their cytotoxicity and their protein kinase inhibitory profiles. The results are shown in Tables 3.8 amd 3.9. Compounds **1-5** showed potent cytotoxicity against the mouse lymphoma cell line L5178Y with IC_{50} values ranging from 1.1 to 3.7 μM. When tested *in vitro* for their inhibitory potential against 16 different protein kinases, compounds **5**, **6** and **8** exhibited the strongest inhibitory activity against ALK, FAK, IGF1-R, SRC, VEGF-R2, Aurora-B, MET wt and NEK6 kinases (IC_{50} 0.97-8.62 μM) Daletos *et al.*, 2014).

Table 3.8: Cytotoxic activities of **1-8**

Compound	IC_{50} $(\mu M)^a$
1	1.7
2	1.1
3	3.7
4	1.8
5	1.3
6	> 10.0
7	> 10.0
8	> 10.0
Kahalalide F	4.30

^{a}Only IC_{50} values < 10.0 μM are reported.

Table 3.9: IC_{50} values of **5**, **6** and **8** against 16 different protein kinases

							IC_{50} [μM]									
#	AKT1	ALK	ARK5	Aurora-B	AXL	FAK	IGF1-R	MEK1 wt	MET wt	NEK2	NEK6	PIM1	PLK1	PRK1	SRC	VEGF-R2
5	73.2	0.97	>100	61.0	>100	3.03	1.94	>100	40.3	29.9	90.8	62.6	100.0	>100	2.20	2.22
6	>100	3.38	>100	>100	14.7	7.78	3.31	>100	>100	>100	>100	>100	>100	>100	19.7	3.66
8	48.4	2.19	29.4	3.89	13.1	4.56	11.8	>100	3.12	14.7	7.72	20.3	21.7	>100	8.62	4.81

3.2. Isolated compounds from the sponge *Callyspongia aerizusa*

In this study, we investigated four separate collections of *Callyspongia aerizusa* obtained from three different regions in Indonesia. Total methanolic extract of the sponge was subjected to liquid-liquid partition technique against n-Hexane, EtOAc, and BuOH. The bioactive EtOAc fractions were subjected to consecutive column chromatography on Sephadex LH-20, using MeOH as a mobile phase. Further purification was achieved by semi-preparative reversed phase HPLC (C18 Eurosphere 100) using an eluting gradient of MeOH:H_2O. This afforded five new cyclic peptides callyaerins I-M, along with the known callyaerins A-G. The structures of the new compounds were unambiguously elucidated on the basis of one- and two-dimensional NMR spectroscopy and mass spectrometry. In addition the structures of callyaerin D, F, and G, previously available in only small amounts, have been reinvestigated and revised. All compounds were tested *in vitro* against *M. tuberculosis*, as well as against THP-1 (human acute monocytic leukemia), and MRC-5 (human fetal lung fibroblast) cell lines in order to assess their general cytotoxicity. In this part, the results of the chemical investigation of the secondary metabolites produced by *C. aerizusa* are presented (Daletos *et al.*, 2015).

3.2.1. Callyaerin I (11, new natural product)

Callyaerin I	
Sample code	G4-1
Biological source	*Callyspongia aerizusa*
Sample amount	4.0 mg
Physical description	white amorphous powder
Molecular formula	$C_{69}H_{94}N_{13}O_{12}$
Molecular weight	1295 g/mol
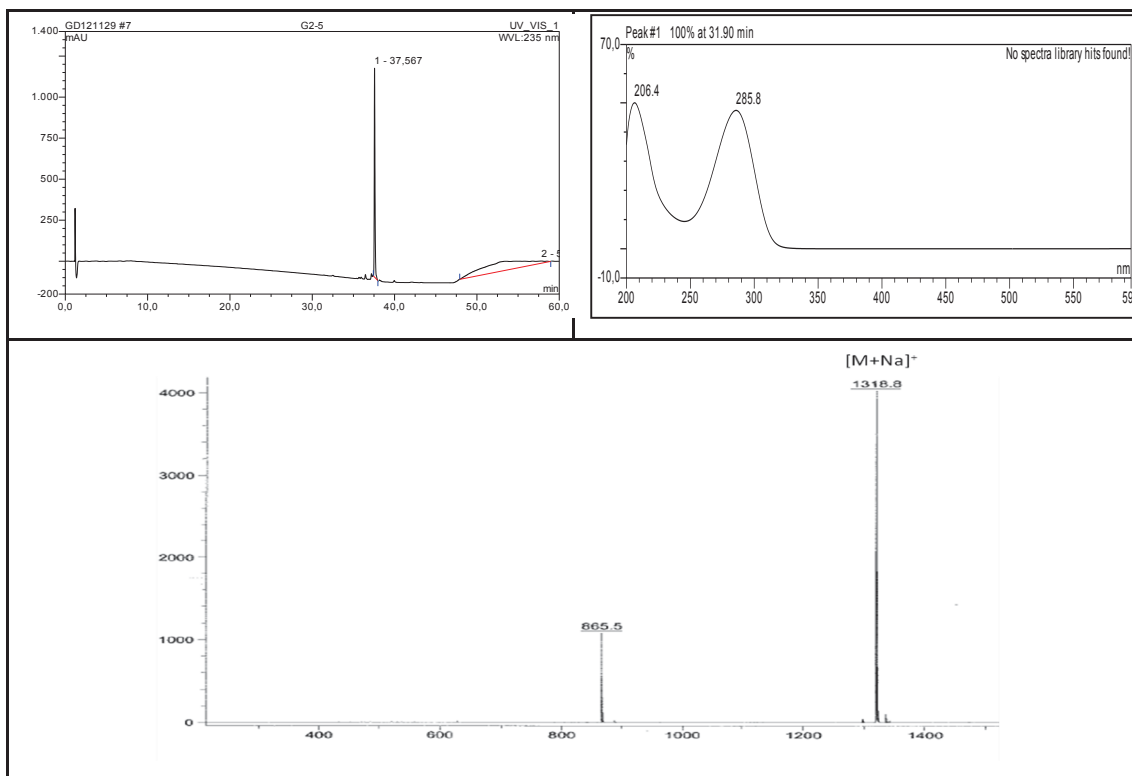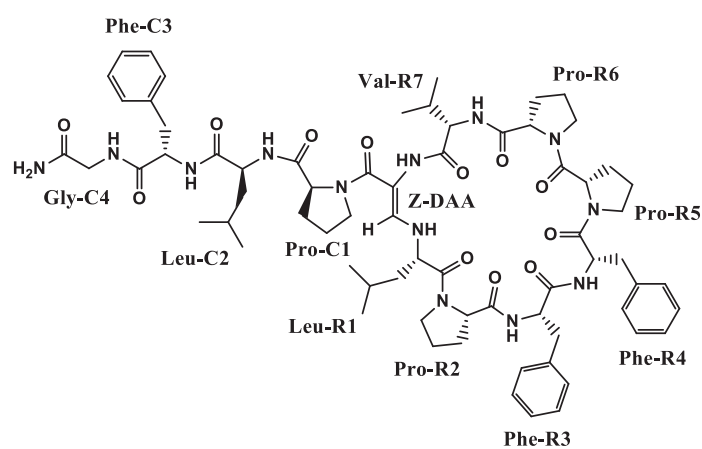
Compound **11** was obtained as a white amorphous solid. The HRESIMS spectrum exhibited the prominent ion peak at *m/z* 1296.7139 [M+H]$^+$ consistent with the molecular formula $C_{69}H_{93}N_{13}O_{12}$, accounting for thirty degrees of unsaturation. The peptidic nature of **11** was evident from the abundance of signals in the amide NH region (δ_H 8.45-5.36), from the α-amino protons (δ_H 4.63-3.52) in the ^{1}H NMR spectrum and from the presence of carbonyl carbons (δ_C 174.1-168.3), as deduced from the HMBC spectrum. Additionally, a cluster of aliphatic primary and secondary methyl groups indicated the presence of lipophilic amino acid residues. In particular, the region between 5.36 and 7.78 ppm of the ^{1}H spectrum of **11** accounted for 9 deshielded amide NH resonances. Extensive analysis of the 2D NMR data of **11**, including COSY, TOCSY, HSQC, and HMBC spectra, enabled the assignment of eleven spin systems, seven of which originated from the amidic protons of one Gly, two Leu, three Phe and one Val residues. In addition, an uncommon spin system of one NH proton resonating at δ_H 8.45 (brs, NH), which is coupled to an olefinic proton at δ_H 7.43 (d, J=13.5 Hz, *β*-H), in association with their HMBC correlations to δ_C 98.1 (DAA-α) and 168.3 (DAA-CO), indicated the presence of an unusual (*Z*)-2,3-diaminoacrylic acid (DAA) moiety, characteristic of the callyaerin series of peptides. The remaining three spin systems showed no correlations to any amide proton and were indicative of three proline residues. Finally, two NH protons at δ_H 7.21 and 7.10 were attributed to the terminal NH$_2$ group. The HMBC and HSQC NMR spectra supported the presence of 11 amino acids along with the DAA unit, as indicated by the 12 carbonyl signals at δ_C 174.1-168.3 and 11 α-carbon signals of amino acids in the region δ_C 42.1-63.4. These residues accounted for 29 of the 30 degrees of unsaturation, indicating that the final degree of unsaturation must arise from the cyclic nature of **11** (Daletos *et al.*, 2015).

HMBC and ROESY NMR data established the connectivity and the sequence of the amino acids for **11**. Key ROESY correlations were observed between Pro^{C1}-Hα/Leu^{C2}-NH, Leu^{C2}-Hα/Phe^{C3}-NH, Phe^{C3}-Hα/Gly^{C4}-NH, and Gly^{C4}-Ha/terminal-NH$_2$, as well as between the amide protons of adjacent residues Leu^{C2}-NH/Phe^{C3}-NH/Gly^{C4}-NH, corresponding to the peptide fragment Pro^{C1}-Leu^{C2}-Phe^{C3}-Gly^{C4}-NH$_2$. This was further corroborated by the HMBC correlations of NH signals at 7.21/7.10, 7.53, 7.66 and 7.78 for terminal-NH$_2$, Gly^{C4}, Phe^{C3} and Leu^{C2}, respectively, to their neighboring vicinal (^{2}J) carbonyls of Gly^{C4} (δ_C 170.6), Phe^{C3} (δ_C 170.7), Leu^{C2} (δ_C 171.5), and Pro^{C1} (δ_C 174.1), respectively (Daletos *et al.*, 2015).

Further ROESY correlations between Phe^{R3}-NH/Phe^{R4}-NH, and DAA-NH/Val^{R7}-Hα, Val^{R7}-NH, along with the HMBC correlations between Phe^{R4}-Hα/ Phe^{R3}-CO (δ_C 170.9), and DAA-NH/ Val^{R7}-CO (δ_C 171.8), established the partial structures Phe^{R3}-Phe^{R4} and DAA-Val^{R7}, respectively. The positions of the proline residues Pro^{R2} and Pro^{R5} were apparent from the ROESY correlations of their δ proton signals with the preceding residues Leu^{R1}-Hα and Phe^{R4}-Hα, respectively (Figure 3.12). In addition, HMBC correlations from the amide protons to adjacent carbonyls allowed the assignment of connections between Phe^{R3}-NH/Pro^{R2}-CO and between Val^{R7}-NH/Pro^{R6}-CO. This assignment was also evident from the ROESY cross-peaks between Phe^{R3}-NH/Pro^{R2}-Hα and Val^{R7}-NH/Pro^{R6}-Hβ, respectively, thus leading to the overall substructure Leu^{R1}-Pro^{R2}-Phe^{R3}-Phe^{R4}-Pro^{R5}-Pro^{R6}-Val^{R7}-DAA (Daletos *et al.*, 2015).

Moreover, the ROESY correlations observed for DAA-βH to Leu^{R1}-Hα and Leu^{R1}-NH, in addition to its COSY correlation to Leu^{R1}-NH, established the nature of the cyclization of compound **11** via the connection of the DAA unit with Leu^{R1}, fulfilling the degrees of unsaturation (Figure 3.13). Thus, the cyclic substructure was established as *cyclo*(Leu^{R1}-Pro^{R2}-Phe^{R3}-Phe^{R4}-Pro^{R5}-Pro^{R6}-Val^{R7}-DAA). Finally, the connectivity of the cyclic part of **9** (R1-R7) and the linear chain (C1-C4) was established through the ROESY correlation of DAA-NH/Pro^{C1}-Hδ, as well as by the HMBC correlation between Pro^{C1}-Hα/DAA-CO (Figure 3.14). Further support was provided by ESI and MALDI-TOF MS spectra, which gave a fragment ion at m/z 865 for [M-(Pro+Leu+Phe+Gly+NH$_2$)]$^+$, arising from the cleavage of the linear side chain. Interestingly, **9** comprises a cyclic part and a linear side chain identical to that found for callyaerin E and C, respectively, indicating a combinatorial biosynthesis of the non-ribosomal peptide synthetases (NRPSs), catalyzing the synthesis of these peptides (Daletos *et al.*, 2015).

A further attempt to confirm the sequence of the amino acids of **11** was made through an ESIMS/MS fragmentation experiment. However, this experiment only confirmed the nature of the linear side chain as elucidated by NMR, whereas the amino acid sequence of the cyclic part could not be unambiguously determined (Daletos *et al.*, 2015).

The absolute configurations of the individual amino acid constituents of compound **11** were determined by acid hydrolysis and consecutive analysis of the hydrolysates using the advanced Marfey's method. LC-MS analyses of the resulting

(N-(5-fluoro-2,4-dinitrophenyl)-L-leucinamide) derivatives and comparison with authentic amino acids prepared as standards led to the assignment of the L-configuration of all amino acid residues (Daletos *et al.*, 2015).
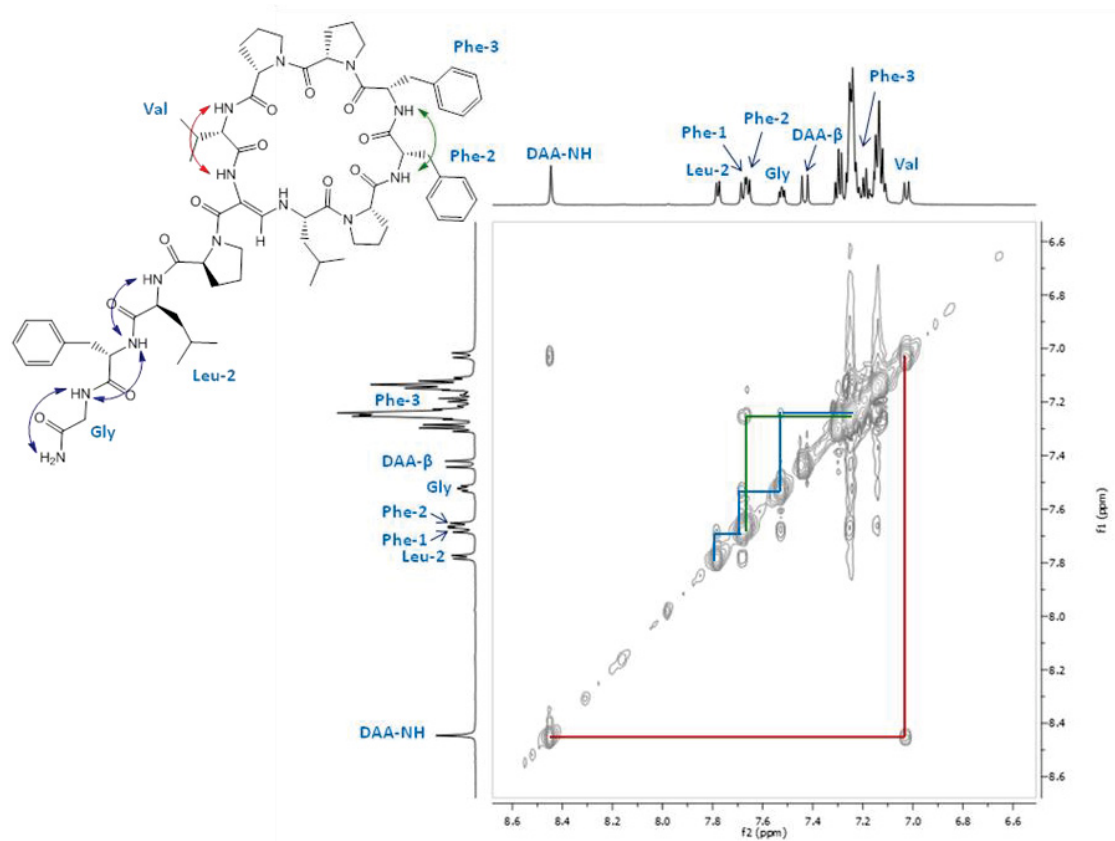
Figure 3.12: ROESY spectrum of **11**
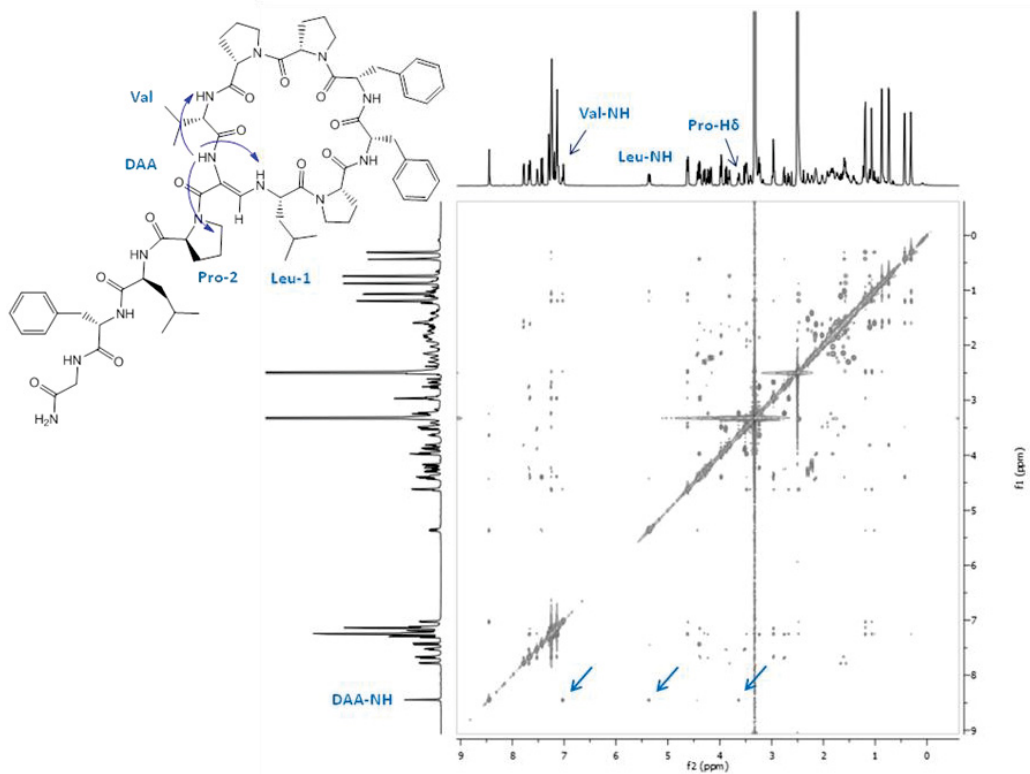
Figure 3.13: ROESY spectrum of **11**
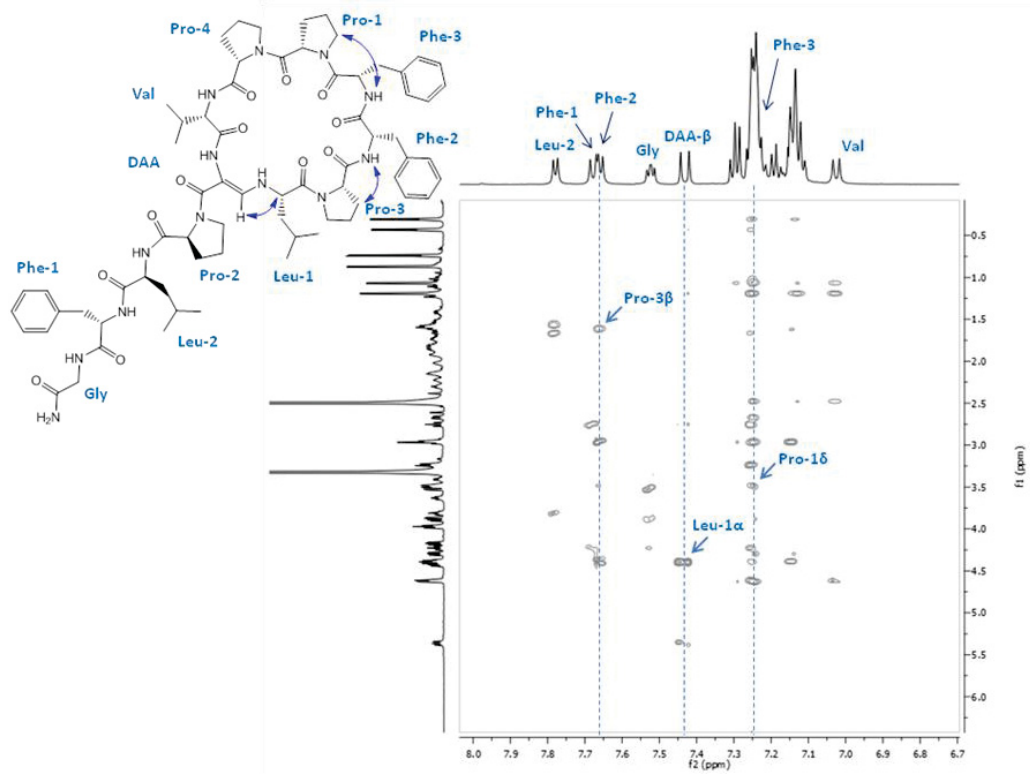
Figure 3.14: ROESY spectrum of **11**

Table 3.10: NMR data of **11** at 600 (^{1}H) and 150 (^{13}C) MHz (DMSO-d_6, δ in ppm)

unit	position	$\delta_C{}^a$, type	δ_H (J in Hz)	HMBC	ROESY[b]
DAA	NH		8.45 (brs)	DAA-α, DAA-CO, R7-CO	C1-δ, R1-α, R1-NH, R7-α, R7-NH
	CO	168.3, C			
	α	98.1, C			
	β	143.3, CH	7.43 (d, 13.5)	R1-α, DAA-α, DAA-CO	R1-α, R1-γ, R1-δ, R1-NH
R1 Leu	NH		5.36 (dd, 13.5, 9.8)	R1-α, DAA-α, DAA-β	R1-α, R7-γ, R7-γ', DAA-β, DAA-NH
	CO	173.4, C			
	α	57.4, CH	4.39^c	R1-β, R1-γ, DAA-β, R1-CO	R2-α, R2-δ, DAA-β, DAA-NH
	β	42.1, CH₂	1.59 (m); 1.02 (m)		
	γ	23.1, CH	1.21 (m)		DAA-β
	δ	19.6, CH₃	0.45 (d, 6.4)	R1-β, R1-γ, R1-δ'	DAA-β
	δ'	22.7, CH₃	0,32 (d, 6.7)	R1-β, R1-γ, R1-δ	
R2 Pro	CO	172.1, C			
	α	63.1, CH	3.98 (dd, 10.0, 7.3)	R2-β, R2-CO, R1-CO	R1-α, R3-NH
	β	28.3, CH₂	2.14 (m); 1.63 (m)		R3-NH
	γ	24.7, CH₂	2.02 (m); 1.82 (m)		
	δ	45.9, CH₂	3.96 (m); 3.48 (m)	R2-γ	R1-α, R3-NH
R3 Phe	NH		7.61 (d, 6.8)	R3-α, R3-β, R2-CO	R2-α, R2-β, R2-δ, R4-NH
	CO	170.9, C			
	α	53.7, CH	4.38^c	R3-β, R3-1, R2-CO, R3-CO	R4-NH
	β	35.0, CH₂	2.96 (m)	R3-CO, R3-α, R3-1, R3-2,6	
	Aromatic	1: 138.0, C			
		2: 128.3, CH	7.25^c	R3-β, R3-3/5, R3-4	
		3: 128.3, CH	7.15^c	R3-2/6, R3-4	
		4: 126.3, CH	7.18^c	R3-2/6, R3-3/5	
		5: 128.3, CH	7.15^c	R3-2/6, R3-4	
		6: 128.3, CH	7.25^c	R3-β, R3-3/5, R3-4	
R4 Phe	NH		7.25^c	R4-α, R4-β, R3-CO, R4-CO	R5-δ, R3-NH
	CO	169.1, C			
	α	52.7, CH	4.63^c	R4-β, R4-1, R4-CO, R3-CO	R5-Hδ
	β	35.8, CH₂	2.96 (m); 2.68 (dd, 13.4, 4.7)	R4-α, R4-CO, R4-1, R4-2,6	
	Aromatic	1: 137.8, C			
		2: 128.9, CH	7.25^c	R4-β, R4-3/5, R4-4	
		3: 128.1, CH	7.29^c	R4-2/6, R4-4	
		4: 126.4, CH	7.23^c	R4-2/6, R4-3/5	
		5: 128.1, CH	7.29^c	R4-2/6, R4-4	
		6: 128.9, CH	7.25^c	R4-β, R4-3/5, R4-4	
R5 Pro	CO	171.6, C			
	α	63.4, CH	4.44 (dd, 11.1, 7.6)	R5-β, R5-γ, R5-CO, R4-CO	
	β	26.9, CH₂	2.16 (m); 1.81 (m)		
	γ	24.0, CH₂	1.92 (m); 1.90 (m)		
	δ	46.1, CH₂	3.49 (m); 3.41 (m)	R5-β, R5-γ	R4-NH, R4-α
R6 Pro	CO	171.7, C			
	α	63.1, CH	4.18 (dd, 10.1, 7.4)	R6-β, R6-CO	R7-NH

81

	β	28.7, CH$_2$	2.23 (m); 1.42 (m)	R6-α, R6-γ, R6-δ	R7-NH
	γ	25.4, CH$_2$	1.75 (m); 1.59 (m)	R6-β, R6-δ	
	δ	46.5, CH$_2$	3.34 (m); 2.49 (m)	R6-α, R6-β, R6-γ	
R7 Val	NH		7.03 (d, 10.1)	R7-α, R7-CO, R6-CO	R6-α, R6-β, R6-δ, DAA-NH
	CO	171.8, C			
	α	56.6, CH	4.62 (dd, 10.2, 3.8)	R7-β, R7-γ, R7-γ', R7-CO	DAA-NH, C1-δ
	β	30.0, CH	2.48 (m)	R7-α, R7-γ, R7-γ'	
	γ	17.4, CH$_3$	1.19 (d, 7.0)	R7-α, R7-β, R7-γ'	R1-NH
	γ'	18.0, CH$_3$	1.06 (d, 7.0)	R7-α, R7-β, R7-γ	R1-NH
C1 Pro	CO	174.1, C			
	α	61.9, CH	4.30 (dd, 10.8, 7.1)	C1-β, C1-CO, DAA-CO	C2-NH
	β	29.2, CH$_2$	2.30 (dt, 12.1, 6.4); 1.52 m	C1-α, C1-γ, C1-δ	
	γ	25.7, CH$_2$	1.71 (m); 1.85 (m)	C1-α, C1-β, C1-δ	
	δ	48.5, CH$_2$	3.64 (dd, 11.0, 7.7); 3.24 (m)	C1-α, C1-β, C1-γ, DAA-CO	DAA-NH, C2-NH
C2 Leu	NH		7.78 (d, 7.0)	C2-α, C2-β, C1-CO	C1-α, C1-δ, C3-NH
	CO	171.5			
	α	52.6, CH	3.82 (ddd, 11.4, 7.0, 4.2)	C2-β, C2-γ, C2-CO, C1-CO	C3-NH
	β	38.0, CH$_2$	1.66 (m); 1.12 (ddd, 13.6, 9.3, 4.2)	C2-α, C2-γ, C2-δ, C2-δ', C1-CO	
	γ	24.4, CH	1.56 (m)	C2-α, C2-β, C2-δ, C2-δ'	
	δ	22.3, CH$_3$	0.87 (d, 6.6)	C2-β, C2-γ, C2-δ'	
	δ'	20.4, CH$_3$	0,74 (d, 6.6)	C2-β, C2-γ, C2-δ	
C3 Phe	NH		7.66 (d, 9.7)	C3-α, C3-β, C2-CO	C2-α, C2-NH, C4-NH
	CO	170.7, C			
	α	54.4, CH	4.23 (ddd, 12.4, 9.7, 2.9)	C3-β, C3-1, C3-CO, C2-CO	C4-NH
	β	37.5, CH2	3.24 (dd, 12.4, 2.9); 2.75 (t, 12.4)	C3-α, C3-CO, C3-1, C4-2,6	
	Aromatic	1: 138.2, C			
		2: 129.7, CH	7.25[c]	C3-β, C3-3/5, C3-4	
		3: 127.6, CH	7.12[c]	C3-2/6, C3-4	
		4: 125.9, CH	7.15[c]	C3-2/6, C3-3/5	
		5: 127.6, CH	7.12[c]	C3-2/6, C3-4	
		6: 129.7, CH	7.25[c]	C3-β, C3-3/5, C3-4	
C4 Gly	NH		7.53 (dd, 7.3, 5.0)	C4-α, C3-CO	C3-NH, Terminal-NH$_2$
	CO	170.6, C			
	α	42.1, CH$_2$	3.88 (dd, 17.0, 7.3); 3.52 (dd, 17.0, 5.0)	C3-CO, C4-CO	Terminal-NH$_2$
	NH$_2$		7.21 (brs), 7.10 (brs)	C4-α, C4-CO	C4-α, C4-NH

[a] Data extracted from HSQC and HMBC spectra. [b] Sequential NOEs. [c] Signal overlap prevents determination of couplings

3.2.2. Callyaerin J (12, new natural product)

Callyaerin J	
Sample code	G4-2
Biological source	*Callyspongia aerizusa*
Sample amount	2.5 mg
Physical description	white amorphous powder
Molecular formula	$C_{66}H_{95}N_{13}O_{12}$
Molecular weight	1262 g/mol
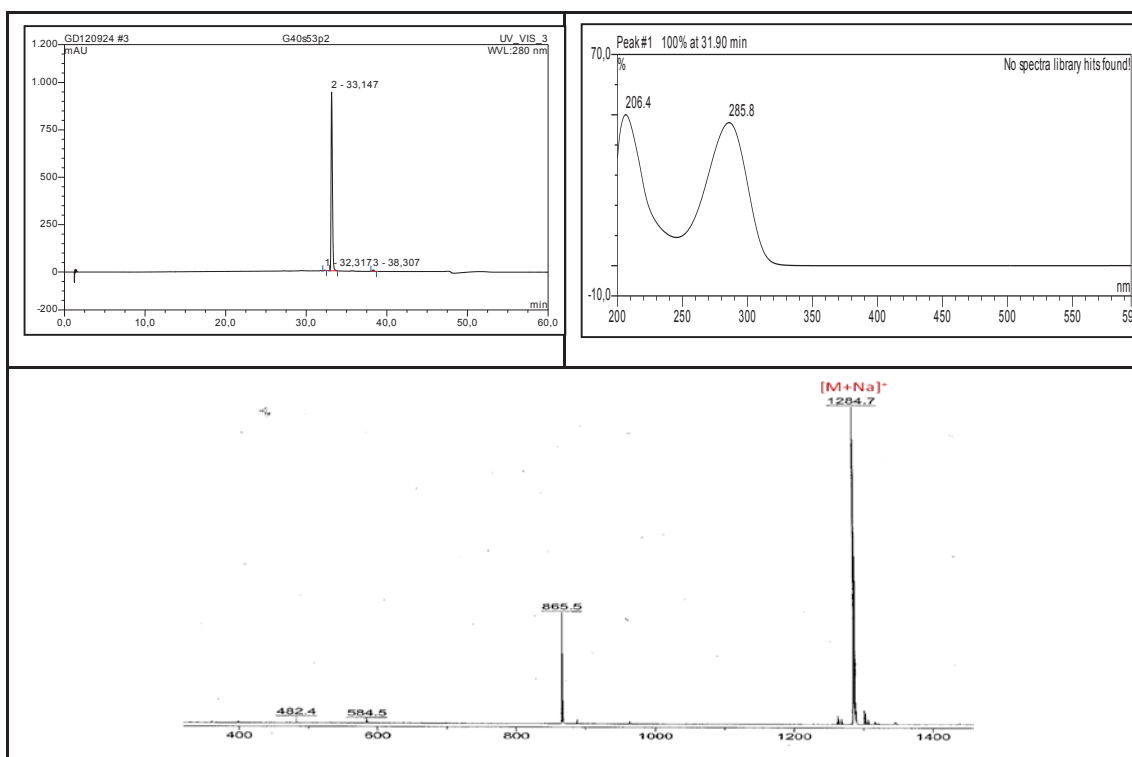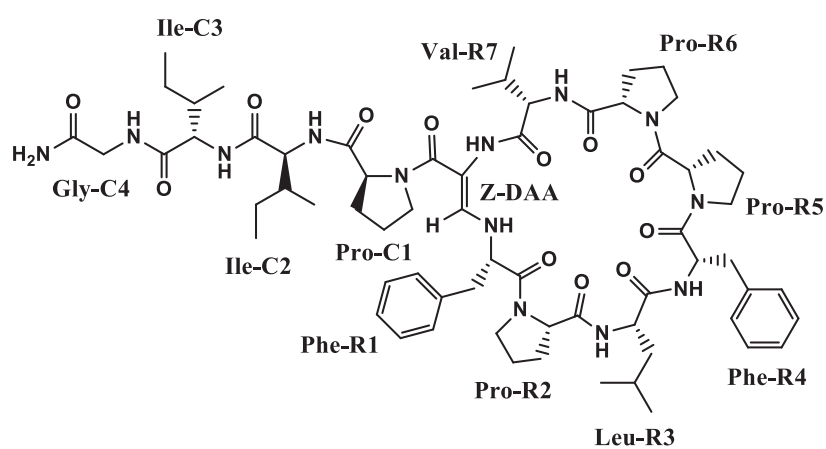
Compound **12** was obtained as a white amorphous solid. The HRESIMS spectrum showed a prominent ion peak at *m/z* 1262.7292 [M+H]$^+$ indicating the molecular formula $C_{66}H_{95}N_{13}O_{12}$, and accounting for twenty six degrees of unsaturation. The ^{1}H NMR spectrum of **12** exhibited dispersed amide (δ_H 5.44-8.21), α-amino protons (δ_H 3.50-4.60), and aliphatic signals, indicative of its peptidic nature. Interpretation of COSY and TOCSY spectra of **12** established the amino acid residues Gly, Leu, IIe (2X), Phe (2X), Val, and Pro (4X), which are identical to those of the known compound callyaerin E (Ibrahim *et al.*, 2010). However, significant differences were observed in the ^{1}H and ^{13}C NMR data for compound **12** and callyaerin E, suggesting that both compounds were isomers. The presence of DAA was indicated by signals at δ_H 8.21 (brs, NH) and δ_H 7.04 (d, J=13.4 Hz, *β*-H). Two downfield singlets at δ_H 7.01 and 7.04 were assigned to the terminal NH$_2$ group (Daletos *et al.*, 2015).

As described for **11**, the connectivities between the different amino acid residues in **12** were unambiguously identified by key HMBC and ROESY correlations. ROESY correlations between Pro^{C1}-Hα/IIe^{C2}-NH, IIe^{C2}-Hα/IIe^{C3}-NH, IIe^{C3}-Hα/Gly^{C4}-NH, and Gly^{C4}-Hα/terminal-NH$_2$, as well as between IIe^{C2}-NH/IIe^{C3}-NH/Gly^{C4}-NH/terminal NH$_2$, indicated the peptide fragment Pro^{C1}-IIe^{C2}-IIe^{C3}-Gly^{C4}-NH$_2$. This was supported by HMBC correlations between terminal NH$_2$/Gly^{C4}-CO (δ_C 170.9), Gly^{C4}-NH/IIe^{C3}-CO (δ_C 170.9), IIe^{C3}-NH/IIe^{C2}-CO (δ_C 171.1), and IIe^{C2}-NH/Pro^{C1}-CO (δ_C 172.9) (Table 3.15) (Daletos *et al.*, 2015).

Similarly, the observed ROESY correlation of Leu^{R3}-NH/Phe^{R4}-NH suggested the fragment Leu^{R3}-Phe^{R4}, which was confirmed by the HMBC correlation of Phe^{R4}-NH to Leu^{R3}-CO (171.9). The positions of the proline units Pro^{R2}, Pro^{R5} and Pro^{R6}, were found to be the same as in compound **11**, as indicated by the ROESY correlations of Phe^{R1}-Hα/Pro^{R2}-Hδ, Leu^{R4}-NH/Pro^{R5}-Hδ and Val^{R7}-NH/Pro^{R6}-Hα, together with the HMBC correlations between Leu^{R3}-NH/Pro^{R2}-CO (δ_C 172.0) and Val^{R7}-NH/Pro^{R6}-CO (δ_C 171.5). Additionally, ROESY correlations between DAA-βH/Phe^{R1}-Hα, Phe^{R1}-NH; and DAA-NH/Val^{R7}-Hα, Val^{R7}-NH, established the ring closure of **10** through the linkage of the DAA unit with Phe^{R1} and Val^{R7}, respectively (Table 3.16). These data corroborated the amino acid sequence of the cyclic part of **12** as *cyclo*(DAA-Phe^{R1}-Pro^{R2}-Leu^{R3}-Phe^{R4}-Pro^{R5}-Pro^{R6}-Val^{R7}). Finally, ROESY cross peak between DAA-NH/Pro^{C1}-Hδ, in association with the HMBC correlation between Pro^{C1}-Hα/DAA-CO, confirmed the linkage between the linear side chain (C1-C4) and

the cyclic part (R1-R7) of compound **12**. This was in agreement with the fragment ion at m/z 865 for $[M-(Pro+2IIe+Gly+NH_2)]^+$ that was observed in the ESI mass spectrum of **12**. Thus, compound **12** differs from the known callyaerin E by an exchange of the amino acids Phe and Leu at positions R1 and R3, respectively (Daletos *et al.*, 2015).

The absolute stereochemistries of the individual amino acid constituents of **12** were determined following acid hydrolysis of the parent peptide and consequent derivatization with Marfey´s reagent. Stereochemical assignments were made using LC-MS technique to compare the amino acids of **12** with appropriate standards (Fig. 3.10). The LC-MS analysis of the resulting 1-flouro-2,4-dinitrophenyl-5-L-leucinamide derivatives established the presence of the L-configuration of all amino acid residues (Daletos *et al.*, 2015).
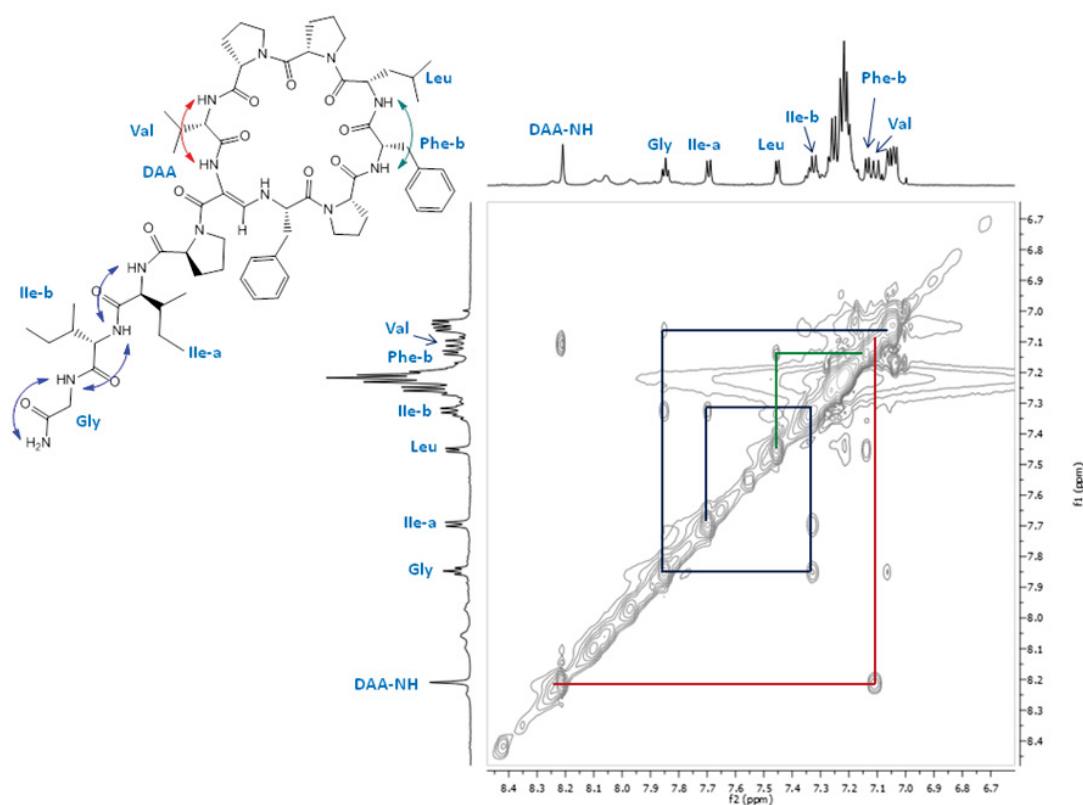
Figure 3.15: ROESY spectrum of **12**
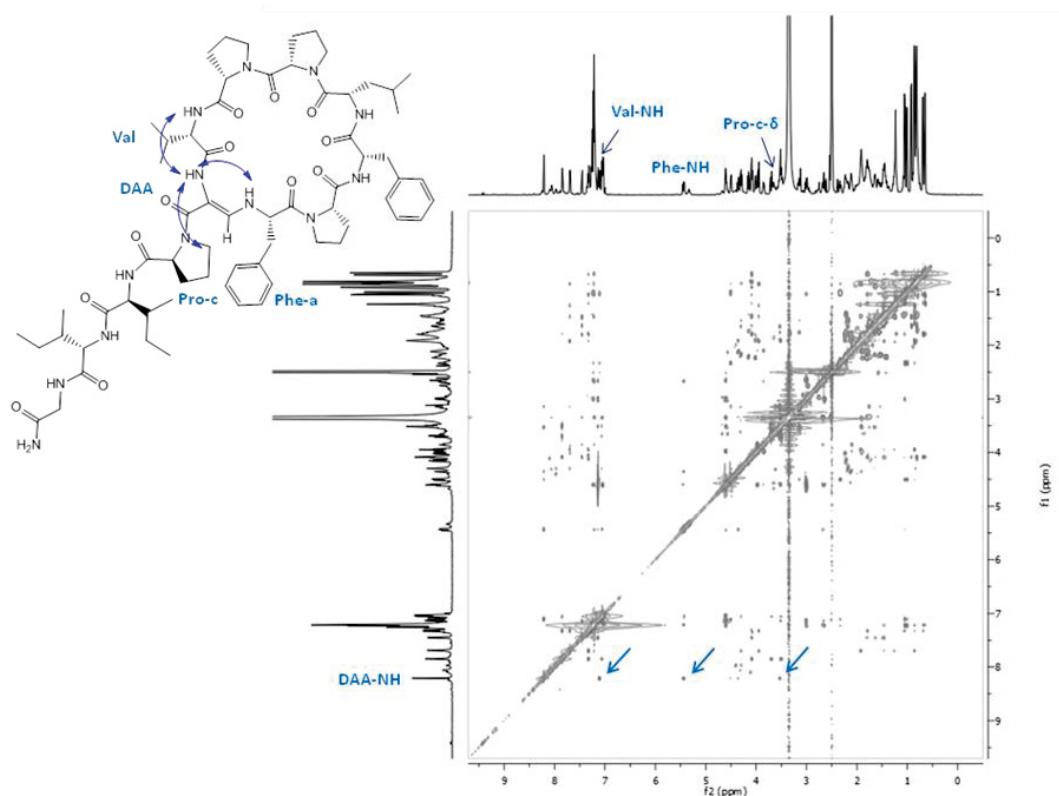
Figure 3.16: ROESY spectrum of **12**

Table 3.11: NMR data of **12** at 600 (^{1}H) and 150 (^{13}C) MHz (DMSO-d_6, δ in ppm)

Unit	position	δc^a, type	δ_H (*J* in Hz)	HMBC	ROESY^b
DAA	NH		8.21 (brs)	DAA-α, DAA-CO, R7-CO	R7-α, R7-NH, C1-δ, R1-NH
	CO	167.3, C			
	α	99.2, C			
	β	142.0, CH	7.04 (d, 13.4)	R1-α, DAA-α, DAA-CO	R1-α, R1-NH, R7-γ
R1 Phe	NH		5.44 (dd, 13.4, 9.7)	R1-α, DAA-α, DAA-β	DAA-NH, DAA-β
	CO	172.4, C			
	α	60.4, CH	4.60^c	R1-β, DAA-β, R1-CO	R2-δ, DAA-β
	β	38.7, CH$_2$	3.34 (dd, 14.2, 3.1); 2.67 (m)	R1-CO, R1-α, R1-1, R1-2,6	
	Aromatic	1: 136.0, C			
		2: 129.1, CH	7.21^c	R1-β, R1-3/5, R1-4	
		3: 128.2, CH	7.22^c	R1-2/6, R1-1	
		4: 126.5, CH	7.22^c	R1-2/6	
		5: 128.2, CH	7.22^c	R1-2/6, R1-1	
		6: 129.1, CH	7.21^c	R1-β, R1-3/5, R1-4	
R2 Pro	CO	172.0, C			
	α	63.4, CH	4.02 (dd, 10.5, 6.9)	R2-β, R2-γ, R2-CO	R3-NH
	β	28.8, CH$_2$	2.23 (m); 1.81 (m)	R2-α, R2-γ, R2-δ	
	γ	24.8, CH$_2$	2.10 (m); 1.90 (m)	R2-α, R2-β, R2-δ	
	δ	46.5, CH$_2$	3.97 (brt, 9.7); 3.85 (td, 9.7, 6.5)	R2-α, R2-β, R2-γ	R1-α
R3 Leu	NH		7.41 (d, 6.2)	R3-α, R3-β, R2-CO	R2-α, R2-β, R2-δ, R4-NH
	CO	171.9, C			

	α	51.8, CH	4.08[c]	R3-β, R3-γ, R3-CO	R4-NH
	β	38.9, CH$_2$	1.47 (m)	R3-α, R3-γ, R3-δ, R3-δ', R3-CO	
	γ	24.2, CH	1.63 (m)	R3-α, R3-β, R3-δ, R3-δ'	
	δ	22.4, CH$_3$	0.92 (d, 6.6)	R3-β, R3-γ, R3-δ'	
	δ'	21.0, CH$_3$	0.82 (d, 6.6)	R3-β, R3-γ, R3-δ	
R4 Phe	NH		7.13 (d, 6.5)	R4-α, R4-CO, R3-CO	R3-α, R3-β, R3-NH, R5-δ
	CO	169.1, C			
	α	52.5, CH	4.60[c]	R4-β, R4-1, R4-CO	R5-δ
	β	36.0, CH$_2$	3.01 (dd, 13.5, 8.9); 2.64 (dd, 13.5, 4.9)	R4-CO, R4-α, R4-1, R4-2,6	
	Aromatic	1: 138.0, C			
		2: 128.9, CH	7.24[c]	R4-β, R4-3/5, R4-4	
		3: 127.8, CH	7.26[c]	R4-2/6, R4-1	
		4: 126.2, CH	7.20[c]	R4-2/6	
		5: 127.8, CH	7.26[c]	R4-2/6, R4-1	
		6: 128.9, CH	7.24[c]	R4-β, R4-3/5, R4-4	
R5 Pro	CO	171.4, C			
	α	63.2, CH	4.36 (dd, 11.3, 7.6)	R5-β, R5-γ, R5-CO, R4-CO	R4-NH
	β	26.8, CH$_2$	2.11 (m); 1.80 (m)	R5-α, R5-γ, R5-δ	
	γ	24.1, CH$_2$	1.92 (m); 1.90 (m)	R5-α, R5-β, R5-δ	
	δ	46.3, CH$_2$	3.52 (m); 3.34 (m)	R5-α, R5-β, R5-γ	R4-α, R4-NH
R6 Pro	CO	171.5, C			
	α	62.8, CH	4.15 (dd, 9.8, 7.5)	R6-β, R5-CO	R7-NH
	β	28.6, CH$_2$	2.22 (m); 1.42 (m)	R6-α, R6-γ, R6-δ	R7-NH
	γ	25.2, CH$_2$	1.74 (m); 1.58 (m)	R6-α, R6-β, R6-δ	
	δ	46.4, CH$_2$	3.34 (m); 2.51 (m)	R6-α, R6-β, R6-γ	R7-NH
R7 Val	NH		7.10 (d, 10.2)	R7-α, R7-β, R6-CO	R6-α, R6-β, R6-δ, DAA-NH
	CO	170.9, C			
	α	56.7, CH	4.50 (dd, 10.2, 5.2)	R7-β, R7-γ, R7-γ', R7-CO	C1-δ, DAA-NH
	β	29.7, CH$_2$	2.33 (m)	R7-α, R7-γ, R7-γ'	
	γ	18.7, CH$_3$	1.06 (d, 6.9)	R7-α, R7-β, R7-γ'	
	γ'	18.3, CH$_3$	1.01 (d, 6.9)	R7-α, R7-β, R7-γ	
C1 Pro	CO	172.9, C			
	α	61.1, CH	4.30 (dd, 9.7, 7.4)	C1-β, C1-CO, DAA-CO	C2-NH
	β	29.0, CH$_2$	2.18 (m); 1.54 (m)	C1-α, C1-γ, C1-δ	
	γ	25.5, CH$_2$	1.76 (m); 1.65 (m)	C1-α, C1-β, C1-δ	
	δ	48.4, CH$_2$	3.53 (m); 3.14 (td, 11.3, 6.7)	C1-α, C1-β, C1-γ	DAA-NH, C2-NH, R7-Hα
C2 IIe	NH		7.68 (d, 7.5)	C2-α, C2-β, C1-CO	C3-NH, C1-α, C1-δ
	CO	171.1, C			
	α	58.5, CH	3.95 (t, 7.5)	C2-β, C2-γ, C2-γ', C2-CO	C3-NH
	β	35.1, CH	1.92 (m)	C2-α, C2-γ, C2-γ', C2-δ	
	γ	24.9, CH$_2$	1.46 (m); 1.26 (m)	C2-α, C2-β, C2-γ', C2-δ	
	γ'	15.4, CH$_3$	0.86 (d, 6.8)	C2-α, C2-β, C2-γ	
	δ	11.0, CH$_3$	0.86 (t, 7.4)	C2-β, C2-γ	
C3 IIe	NH		7.31 (d, 8.4)	C3-α, C3-β, C2-CO	C2-α, C2-NH, C4-NH
	CO	170.9, C			
	α	57.1, CH	4.08[b]	C3-β, C3-γ, C3-γ', C3-CO	C4-NH
	β	35.4, CH	1.78 (m)	C3-α, C3-γ, C3-γ', C3-δ	C4-NH
	γ	24.1, CH$_2$	1.23 (m); 1.06 (m)	C3-α, C3-β, C3-γ', C3-δ	
	γ'	15.3, CH$_3$	0.69 (d, 6.9)	C3-α, C3-β, C3-γ	
	δ	10.5, CH$_3$	0.65 (t, 7.4)	C3-β, C3-γ	
C4 Gly	NH		7.83 (dd, 6.5, 5.6)	C4-α, C3-CO	C3-NH, C3-α, C3-β, terminal-NH$_2$
	CO	170.9, C			
	α	42.1, CH$_2$	3.70 (dd, 16.7, 6.5) 3.50 (dd, 16.8, 5.6)	C4-CO	terminal-NH$_2$
	NH$_2$		7.04 (brs); 7.01 (brs)	C4-α, C4-CO	C4-α, C4-NH

[a] Data extracted from HSQC and HMBC spectra. [b] Sequential NOEs. [c] Signal overlap prevents determination of couplings

3.2.3. Callyaerin K (13, new natural product)

Callyaerin K	
Sample code	G4-3
Biological source	*Callyspongia aerizusa*
Sample amount	5.0 mg
Physical description	white amorphous powder
Molecular formula	$C_{77}H_{97}N_{13}O_{16}$
Molecular weight	1459 g/mol
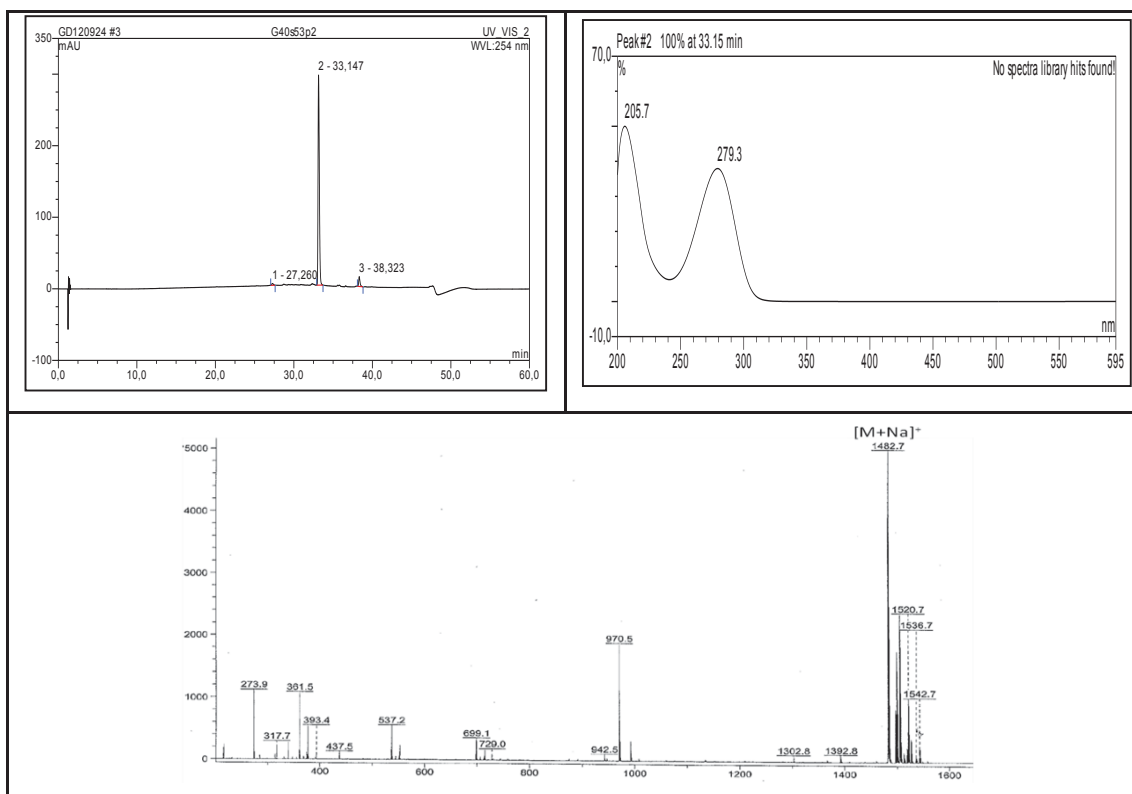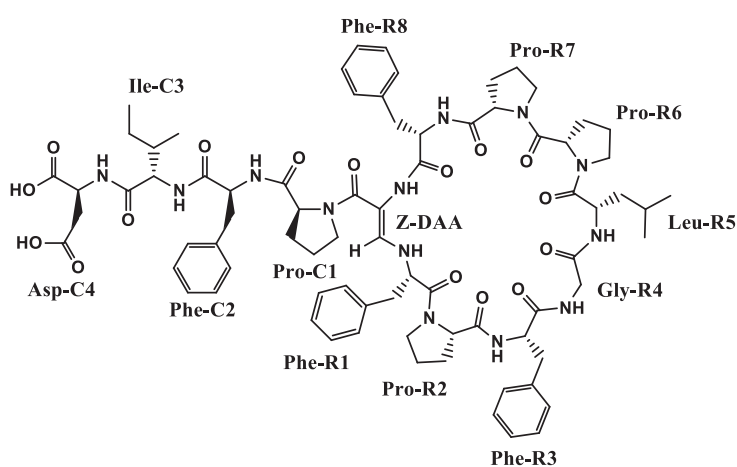
Callyaerin K (**13**) was obtained as a white amorphous solid. The HRESIMS spectrum showed the pseudomolecular ion peak at *m/z* 1460.7252 [M+H]$^+$ indicating the molecular formula $C_{77}H_{97}N_{13}O_{16}$, accounting for thirty six degrees of unsaturation. The ^{1}H NMR spectrum again suggested the peptidic nature of compound **13**, as indicated by the presence of a series of amide NH signals (δ_H 5.53-8.93) and α-amino protons (δ_H 3.24-5.11). Detailed analysis of the TOCSY and HMBC spectra allowed the assignment of twelve amino acid residues consisting of Pro (4X), Phe (4X), Gly, Leu, IIe, and Asp along with the DAA unit (Daletos *et al.*, 2015).

In the ^{1}H NMR spectrum of **13** the absence of terminal NH signals indicated that the terminal carboxyamide group of **11** and **12** was replaced by a carboxylic group, which is in accordance with the molecular formula of **13**. In addition, the presence of Asp explains the additional carbonyl signal (δ_C 171.9), as observed in the HMBC spectrum (Daletos *et al.*, 2015).

ROESY correlations between Pro^{C1}-Hα/Phe^{C2}-NH, Phe^{C2}-NH/IIe^{C3}-NH, and IIe^{C3}-NH/Asp^{C4}-NH (Table 3.17), indicated the sequence of the linear side chain as Pro^{C1}-Phe^{C2}-IIe^{C3}-Asp^{C4}-OH. The HMBC correlations of Asp^{C4}-NH/IIe^{C3}-CO (δ_C 170.2), IIe^{C3}-NH/Phe^{C2}-CO (δ_C 170.2), and Phe^{C2}-NH/Pro^{C1}-CO (δ_C 171.6) further supported the assignments made from the ROESY spectrum (Daletos *et al.*, 2015).

Additional ROESY correlations observed between Phe^{R8}-Hα/DAA-NH, Phe^{R3}-NH/Gly^{R4}-NH and Gly^{R4}-NH/Leu^{R5}-NH, established the partial peptide sequences Phe^{R8}-DAA and Phe^{R3}-Gly^{R4}-Leu^{R5} (Table 3.18). Key ROESY correlations between Phe^{R3}-NH/Pro^{R2}-Hα, Phe^{R8}-NH/Pro^{R7}-Hα and Pro^{R7}Hα/Pro^{R6}-Hα confirmed the assignments of the remaining proline residues Pro^{R2}, Pro^{R6}, and Pro^{R7}, respectively. The nature of the ring closure was corroborated by the ROESY correlations between DAA-βH/Phe^{R1}-Hα and Phe^{R1}-NH, indicating the sequence of the cyclic part of **13** as *cyclo*(DAA-Phe^{R1}-Pro^{R2}-Phe^{R3}-Gly^{R4}-Leu^{R5}-Pro^{R6}-Pro^{R7}-Phe^{R8}) (Daletos *et al.*, 2015).

The linkage of the linear side chain (C1-C4) with the cyclic part (R1-R7) of compound **13** was deduced from the ROESY correlation between DAA-NH/Pro^{C1}-Hδ, as well as from the HMBC correlation between Pro^{C1}-Hα/DAA-CO. This was in agreement with the fragment ion at *m/z* 970 for [M-(Pro+Phe+IIe+Asp+OH)]$^+$ that was observed in the ESI mass spectrum of **13** (Daletos *et al.*, 2015).

The absolute stereochemistries of the individual amino acid constituents of **13** were determined following acid hydrolysis of the parent peptide and consequent

treatment with Marfey´s reagent [Marfey, 1984]. This established the presence of the L-configuration of all amino acid residues (Daletos *et al.*, 2015).
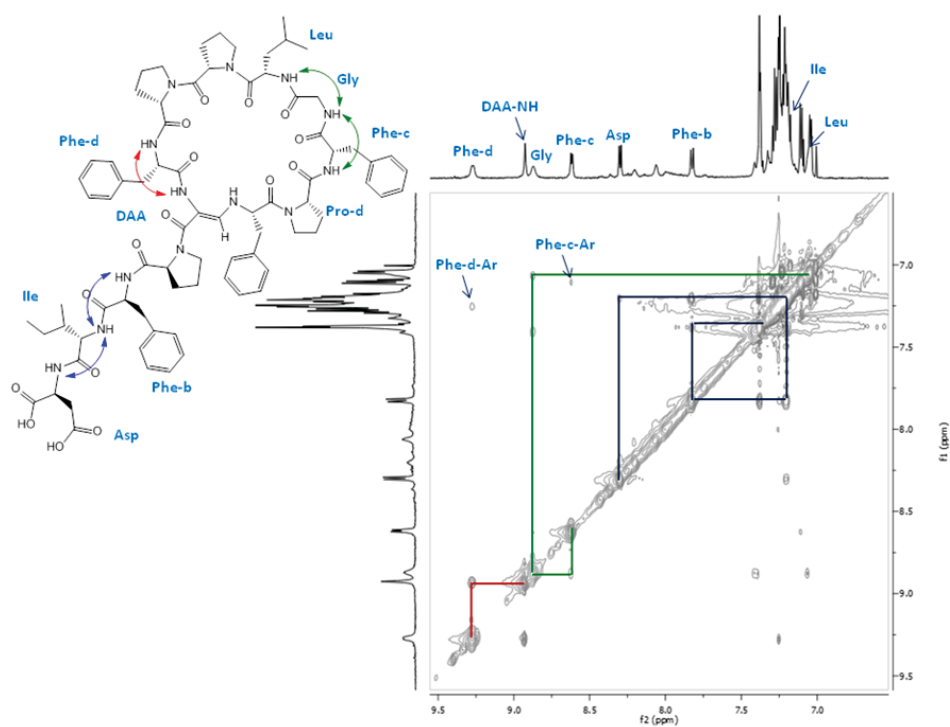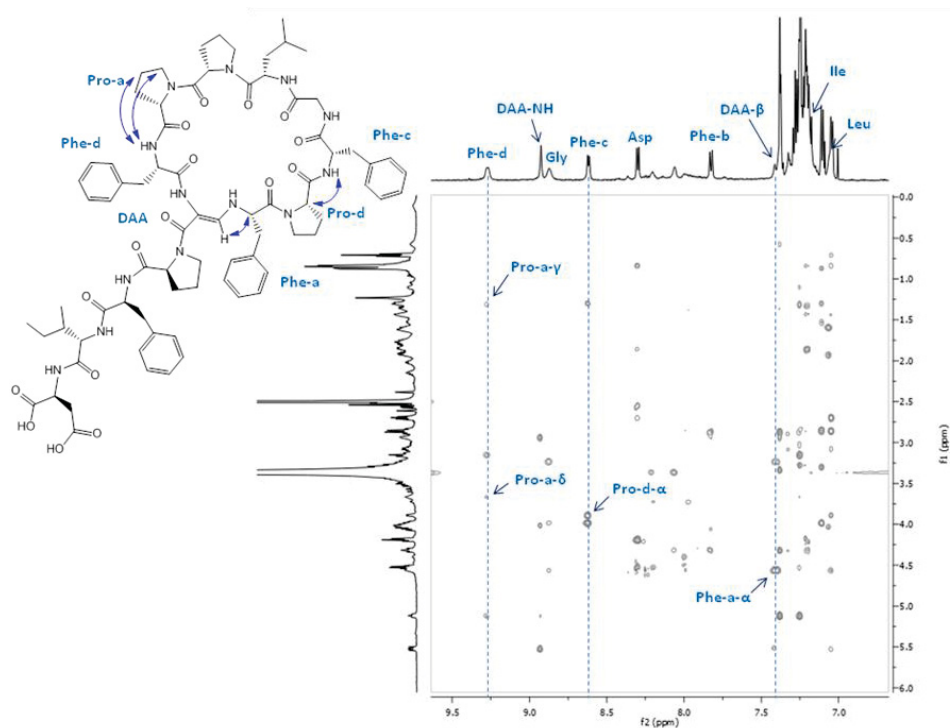

Figure 3.17: ROESY spectrum of **13**

Figure 3.18: ROESY spectrum of **13**

Table 3.12: NMR data of **13** at 600 (^{1}H) and 150 (^{13}C) MHz (DMSO-d_6, δ in ppm)

Unit	position	δc[a], type	δH (J in Hz)	HMBC	ROESY[b]
DAA	NH		8.93 brs	DAA-α, DAA-CO, R8-CO	C1-δ, R8-β, R8-α, R8-NH, R1-NH, DAA-β
	CO	168.1, C			
	α	101.1, C			
	β	139.1, CH	7.41[c]	DAA-α	R1-α, R1-β, R1-NH
R1 Phe	NH		5.53 (dd, 13.6, 8.5)	R1-α, R1-CO, DAA-α	DAA-β, DAA-NH
	CO	169.0, C			
	α	58.2, CH	4.54 (m)		R2-α, DAA-β
	β	42.8, CH2	2.87 (m); 2.68 (m)	R1-α, R1-CO, R1-1, R1-2/6	
	Aromatic	1: 135.6, C			
		2: 129.2, CH	7.05[c]	R1-β, R1-3/5, R1-4	
		3: 127.9, CH	7.24[c]	R1-2/6, R1-1	
		4: 126.4, CH	7.21[c]	R1-2/6	
		5: 127.9, CH	7.24[c]	R1-2/6, R1-1	
		6: 129.2, CH	7.05[c]	R1-β, R1-3/5, R1-4	
R2 Pro	CO	171.9, C			
	α	58.9, CH	3.89 (brd, 7.8)	R2-β, R2-γ, R2-δ, R2-CO	R1-α, R1-β, R3-NH
	β	31.2, CH$_2$	1.44 (m); 1.30 (m)		
	γ	21.0, CH$_2$	1.63 (m); 1.52 (m)	R2-β, R2-δ	
	δ	45.1, CH$_2$	3.43 (m); 3.08 (ddd, 11.4, 8.9, 7.4)	R2-α, R2-β, R2-γ	
R3 Phe	NH		8.61 (brs)		R2-α, R2-β, R4-NH
	CO	170.4, C			
	α	55.3, CH	3.97 (dd, 10.9, 5.4)	R3-β, R3-1, R3-CO	R4-NH
	β	34.4, CH$_2$	3.30 (m); 2.84 (m)	R3-α, R3-1, R3-2/6, R3-CO	
	Aromatic	1: 139.0, C			
		2: 129.0, CH	7.38[c]	R3-β, R3-3/5, R3-4	
		3: 128.1, CH	7.28[c]	R3-2/6, R3-1	
		4: 126.1, CH	7.21[c]	R3-2/6	
		5: 128.1, CH	7.28[c]	R3-2/6, R3-1	
		6: 129.0, CH	7.38[c]	R3-β, R3-3/5, R3-4	
R4 Gly	NH		8.83 (brs)		R3-α, R3-NH, R5-NH
	CO	169.5, C			
	α	42.6, CH$_2$	3.50 (m); 3.24 (m)	R4-CO, R3-CO	R5-α
R5 Leu	NH		7.05[c]		R4-NH
	CO	170.8, C			
	α	49.9, CH	4.04 (m)	R5-γ	
	β	38.9, CH$_2$	1.58 (m); 1.30 (m)	R5-α,R5-γ, R5-δ, R5-δ', R5-CO	
	γ	23.1, CH	1.93 (m)	R5-α, R5-β, R5-δ, R5-δ'	
	δ	22.6, CH$_3$	0.87 (d, 6.5)	R5-β, R5-γ, R5-δ'	R6-δ
	δ'	22.0, CH$_3$	0.85 (d, 6.5)	R5-β, R5-γ, R5-δ	R6-δ
R6 Pro	CO	169.6, C			
	α	58.1, CH	4.03 (m)	R6-β, R6-γ	R7-α
	β	27.5, CH$_2$	2.15 (m); 1.76 (m)	R6-α, R6-γ, R6-δ, R6-CO	R7-α
	γ	24.1, CH$_2$	1.90 (m); 1.78 (m)	R6-α, R6-β, R6-δ	
	δ	47.3, CH$_2$	4.02 (m); 3.45 (m)	R6-α, R6-β, R6-γ	
R7 Pro	CO	173.3, C			
	α	60.3, CH	4.18[c]	R7-β, R7-γ, R7-CO	R6-α, R6-β
	β	31.6, CH$_2$	2.02 (m); 1.10 (m)	R7-α, R7-γ, R7-CO	
	γ	21.3, CH$_2$	1.44 (m); 1.32 (m)	R7-α, R7-β, R7-δ	
	δ	47.1, CH$_2$	3.66 (m); 3.15 (m)	R7-α, R7-β, R7-γ	R8-NH
R8 Phe	NH		9.23 (brd, 8.1)		R7-a, R7-β, R7-γ, R7-δ, DAA-NH
	CO	171.7, C			
	α	55.9, CH	5.11 (ddd,11.8, 8.1, 3.2)	R8-β, R8-1, R8-CO	DAA-NH, DAA-β
	β	37.3, CH$_2$	3.27[c]; 3.15 (brd, 11.8)	R8-α, R8-1, R8-2/6, R8-CO	

	Aromatic	1: 138.1, C			
		2: 128.6, CH	7.11[c]	R8-β, R8-3/5, R8-4	
		3: 128.0, CH	7.25[c]	R8-2/6, R8-1	
		4: 126.3, CH	7.22[c]	R8-2/6	
		5: 128.0, CH	7.25[c]	R8-2/6, R8-1	
		6: 128.6, CH	7.11[c]	R8-β, R8-3/5, R8-4	
C1 Pro	CO	171.6, C			
	α	60.3, CH	4.07 (dd, 10.1, 7.7)	C1-β, C1-CO, DAA-CO	C2-NH
	β	28.5, CH_2	1.83 (m); 0.57 (m)	C1-γ, C1-δ	
	γ	24.6, CH_2	1.61 (m); 1.35 (m)		
	δ	48.1, CH_2	2.95 (m)	C1-α, C1-β, C1-γ	DAA-NH
C2 Phe	NH		7.83 (d, 9.3)	C2-α, C2-β, C1-CO	C1-α, C3-NH
	CO	170.2, C			
	α	53.7, CH	4.32 (ddd, 12.6, 9.3, 3.6)	C2-β, C2-1, C2-CO, C1-CO	C3-NH
	β	36.9, CH_2	3.33 (m); 2.87 (m)	C2-α, C2-1, C2-2,6	
	Aromatic	1: 138.4, C			
		2: 129.4, CH	7.32[c]	C2-β, C2-3/5, C2-4	
		3: 128.2, CH	7.25[c]	C2-2/6, C2-1	
		4: 126.0, CH	7.19[c]	C2-2/6	
		5: 128.2, CH	7.25[c]	C2-2/6, C2-1	
		6: 129.4, CH	7.32[c]	C2-β, C2-3/5, C2-4	
C3 IIe	NH		7.21[c]	C3-α , C3-β, C2-CO	C2-α, C2-NH, C4-NH
	CO	170.2, C			
	α	55.8, CH	4.19[c]	C3-β, C3-γ, C3-γ', C3-CO	C4-NH
	β	35.9, CH	1.84 (m)	C3-α , C3-γ, C3-γ', C3-δ	
	γ	24.1, CH_2	1.43 (m); 1.32 (m)	C3-α , C3-β, C3-γ', C3-δ	
	γ'	14.9, CH_3	0.82 (d, 6.8)	C3-α , C3-β, C3-γ	
	δ	10.1, CH_3	0.71 (t, 7.4)	C3-β, C3-γ	
C4 Asp	NH		8.26 (d, 7.7)	C4- α, C3-CO	C3-α, C3-β, C3-γ, C3-NH
	CO	172.1, C			
	CO(γ)	171.9, C			
	α	48.3, CH	4.52 (ddd, 7.7, 6.8, 6.3)	C4- β, C4-CO	
	β	35.7, CH_2	2.70 (dd, 6.3, 16.6); 2.55 (dd, 6.8, 16.6)	C4- α, C4- CO(γ)	

[a] Data extracted from HSQC and HMBC spectra. [b] Sequential NOEs. [c] Signal overlap prevents determination of couplings

3.2.4. Callyaerin L (14, new natural product)

Callyaerin L	
Sample code	G4-4
Biological source	*Callyspongia aerizusa*
Sample amount	5.0 mg
Physical description	white amorphous powder
Molecular formula	$C_{66}H_{101}N_{13}O_{15}$
Molecular weight	1316 g/mol
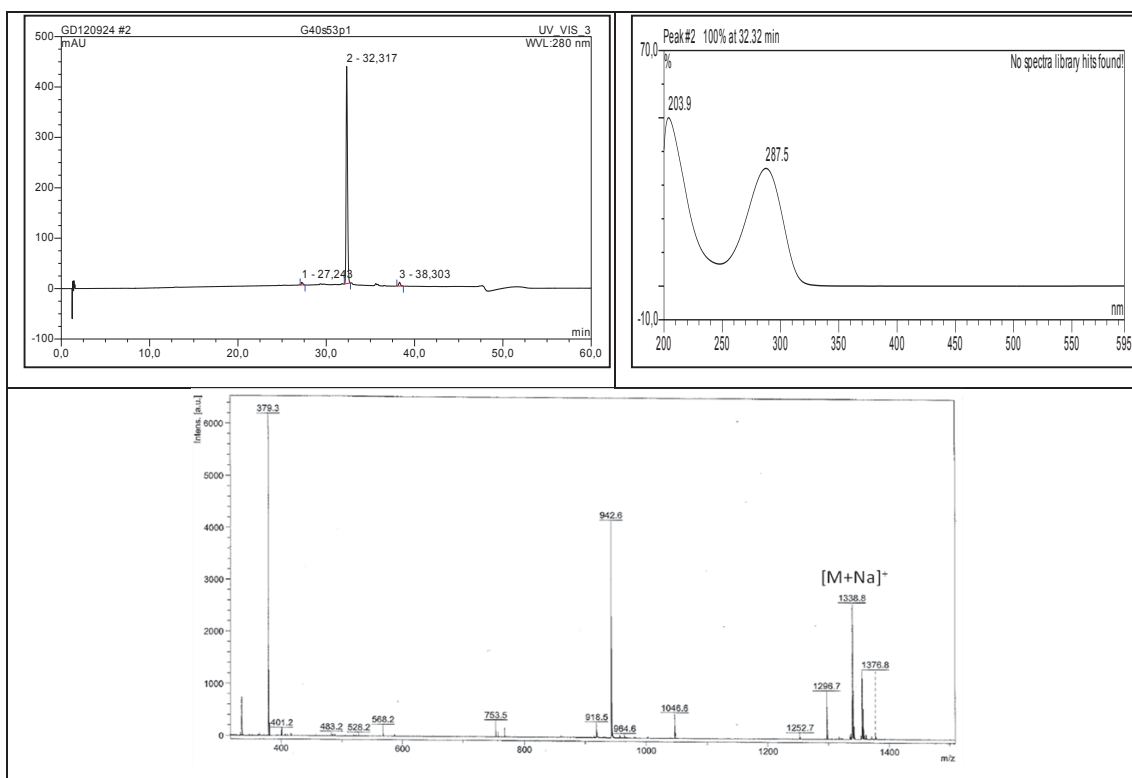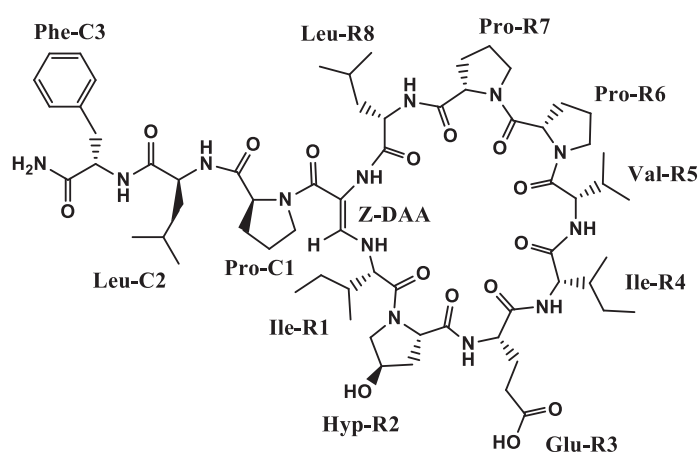
Compound **14** was obtained as a white amorphous solid. The HRESIMS spectrum showed the pseudomolecular ion peak at *m/z* 1316.7614 [M+H]$^+$, which was consistent with the molecular formula $C_{66}H_{101}N_{13}O_{15}$, accounting for 25 degrees of unsaturation. Inspection of the ^{1}H spectrum of **14** denoted its peptidic nature from the presence of a series of amide protons, as well as signals in the diagnostic region for α-amino protons. However, the amide protons of Glu^{R3} and Ile^{R4} were not observed in the ^{1}H NMR spectrum measured in DMSO-*d$_6$*. By employing CF$_3$CD$_2$OH/H$_2$O (1:1) as a solvent for the NMR measurements, it was possible to assign all exchangeable signals of the amino acids and hence CF$_3$CD$_2$OH/H$_2$O (1:1) was subsequently used as an alternative NMR solvent for a series of 1D and 2D NMR experiments (^{1}H, TOCSY, ROESY, HSQC, and HMBC) for the structure elucidation of compound **14**. Accordingly, interpretation of the 2D NMR data revealed the presence of ten amino acids as Ile(2X), Glu, Val, Pro(3X), Leu(2X), and Phe, together with the unusual amino acid γ-hydroxyproline (Hyp) and the DAA moiety. The amine protons at δ_H 6.94 and 7.27 were attributed to the terminal NH$_2$ group (Daletos *et al.*, 2015).

ROESY correlations between the α-protons and NH protons of adjacent amino acids allowed us to establish the sequence of the linear side chain as Pro^{C1}-Leu^{C2}-Phe^{C3}-NH$_2$ (C1-C3). This was further corroborated by inspection of the respective HMBC correlations (Table 3.13) (Daletos *et al.*, 2015).

In the same manner the cyclic part of **14** was found to be composed of two peptide fragments Leu^{R8}-DAA-Ile^{R1} and Glu^{R3}-Ile^{R4}-Val^{R5}. Key ROESY correlations between Glu^{R3}-NH/Hyp^{R2}-Hα, Val^{R5}-NH/Pro^{R6}-Hδ, and Leu^{R8}-NH/Pro^{R7}-Hα connected these two fragments, and accordingly the cyclic part of **14** was established as *cyclo*(DAA-Ile^{R1}-Hyp^{R2}-Glu^{R3}-Ile^{R4}-Val^{R5}-Pro^{R6}-Pro^{R7}-Leu^{R8}). The HMBC correlations of Val^{R5}-NH/Ile^{R4}-CO, and Leu^{R8}-NH/Pro^{R7}-CO supported the interpretation of the ROESY spectrum. Finally, the HMBC correlation between Pro^{C1}-Hα/DAA-CO and the ROESY correlation between DAA-NH/Pro^{C1}-Hδ established the linkage between the linear side chain and the cyclic part of compound **14**. Further support for the linkage was provided by the fragment ion at *m/z* 942 for [M-(Pro+Leu+Phe+NH$_2$)]$^+$ that was observed in the ESI mass spectrum of **14** (Daletos *et al.*, 2015).

The absolute stereochemistries of the individual amino acid constituents of **14** were determined following acid hydrolysis of the parent peptide and consequent treatment with Marfey´s reagent [Marfey, 1984]. This established the presence of the

L-configuration of all amino acid residues. In the same manner, the hydroxyproline unit was identified as *trans*-4-hydroxy-L-proline (Daletos *et al.*, 2015).

**Table 3.13**. NMR data of **14** at 700 (^{1}H) and 176 (^{13}C) MHz (CF$_3$CD$_2$OH/H$_2$O 1:1)

unit	position	δc[a], type	δH (*J* in Hz)	HMBC	ROESY[b]
DAA	NH		8.19 (brs)	DAA- α, DAA-CO, R8-CO	R8-α, R1-NH, R8-NH, C1-δ
	CO	171.4, C			
	α	102.3, C			
	β	145.4, CH	7.24 (d, 13.4)	R1-α, DAA-α, DAA-CO	R1-α, R1-γ, R1-NH, R2-δ
R1 IIe	NH		5.50 (dd, 13.4, 10.3)		DAA-β, DAA-NH
	CO	175.3, C			
	α	68.8, CH	3.73 (t, 10.3)	R1-β, R1-γ', R1-CO, DAA-α	R2-δ, DAA-β
	β	40.9, CH	1.50 (m)	R1-α, R1-γ, R1-γ', R1-δ	
	γ	26.8, CH$_2$	1.27 (m); 0.62 (m)	R1-α, R1- β, R1-γ', R1-δ	
	γ'	16.9, CH$_3$	0.81 (d, 6.5)	R1-α, R1-β, R1-γ	
	δ	11.7, CH$_3$	0.26 (t, 7.4)	R1-β, R1-γ	
R2 Hyp	CO	175.8, C			
	α	63.5, CH	4.23[c]	R2-β, R2-γ, R2-δ, R2-CO	R3-NH
	β	39.4, CH$_2$	2.35 (m); 2.05 (m)	R2-α, R2-δ, R2-CO	R3-NH
	γ	71.8, CH	4.62 (brs)	R2-α	
	δ	58.6, CH$_2$	4.01 (m); 3.77 (dd, 11.2, 1.5)	R2-α, R2-β, R2-γ	R1-α, R3-NH, DAA- β
R3 Glu	NH		8.92 (brs)		R1-δ, R2-α, R2-β, R2-δ, R4-NH
	CO	175.5, C			
	CO(γ)	182.0, C			
	α	59.3, CH	3.90[c]	R3- γ, R3-CO	
	β	28.3, CH$_2$	2.12 (m); 2.17 (m)		
	γ	35.1, CH$_2$	2.35 (m); 2.27 (m)	R3-α, R3-CO(γ)	
R4 IIe	NH		7.70 (brs)		R3-β, R3-NH
	CO	174.8, C			
	α	63.1, CH	4.24[c]	R4-β, R4-γ, R4-γ', R4-CO	R5-NH
	β	40.8, CH	1.45 (m)	R4-α, R4-γ, R4-γ', R4-δ	
	γ	26.9, CH$_2$	1.43 (m); 1.05 (m)	R4-α, R4-β, R4-γ', R4-δ	
	γ'	16.3, CH$_3$	0.90 (d, 6.6)	R4-α, R4-β, R4-γ	
	δ	11.1, CH$_3$	0.78 (t, 7.3)	R4-β, R4-γ	
R5 Val	NH		7.75 (d, 7.8)	R5-α, R5-β, R5-CO, R4-CO	R4-α, R4-γ, R4-γ', R4-δ, R6-δ
	CO	173.7, C			
	α	57.9, CH	4.58[c]	R5-β, R5-γ, R5-γ'	
	β	32.5, CH	2.21 (m)	R5-α, R5-γ, R5-γ'	
	γ,	21.1, CH$_3$	1.05 (d, 6.8)	R5-α, R5-β, R5-γ'	
	γ'	19.9, CH$_3$	1.01 (d, 6.8)	R5-α, R5-β, R5-γ	
R6 Pro	CO	176.0, C			
	α	66.8, CH	4.05[c]	R6-β, R6-CO	
	β	28.4, CH$_2$	2.44 (m); 1.99 (m)	R6-α, R6-γ	
	γ	26.9, CH$_2$	2.23 (m); 2.20 (m)	R6-β, R6-δ	
	δ	49.1, CH$_2$	3.57 (m); 3.52 (m)	R6-γ	R5-NH
R7 Pro	CO	176.1, C			
	α	65.4, CH	4.37[c]	R7-β, R7-γ, R7-CO	R8-NH
	β	30.8, CH$_2$	2.37 (m); 1.74 (m)	R7-α, R7-γ, R7-δ, R7-CO	
	γ	27.4, CH$_2$	2.00 (m); 1.96 (m)	R7-α, R7-β, R7-δ	
	δ	50.1, CH$_2$	3.60 (m); 3.34 (m)	R7-β, R7-γ	R6-β, R8-NH

Residue	Position	δC	δH	HMBC	NOE
R8 Leu	NH		7.00 (d, 9.8)	R8-α, R8-β, R7-CO	R7-α, R7-δ, DAA-NH
	CO	175.2, C			
	α	53.7, CH	4.75 (ddd, 11.7, 9.8, 3.8)	R8-β, R8-CO	C1-δ, DAA-NH
	β	43.2, CH₂	1.95 (m); 1.78 (m)	R8-α,R8-γ, R8-δ, R8-δ', R8-CO	
	γ	26.9, CH	1.62 (m)	R8-δ, R8-δ'	
	δ	24.1, CH₃	0.94 (d, 6.5)	R8-β, R8-γ, R8-δ'	
	δ'	21.6, CH₃	0.87 (d, 6.5)	R8-β, R8-γ, R8-δ	
C1 Pro	CO	178.4, C			
	α	65.1, CH	4.36ᶜ	C1-β, C1-CO, DAA-CO	C2-NH
	β	31.6, CH₂	2.38 (m); 1.60 (m)	C1-α, C1-δ	
	γ	28.0, CH₂	2.02 (m); 1.85 (dq, 12.2, 5.7)	C1-α, C1-β, C1-δ	
	δ	52.0, CH₂	3.54 (m); 3.35 (m)	C1-α, C1-β, C1-γ, DAA-CO	DAA-NH, C2-NH, R8-Hα
C2 Leu	NH		8.11 (d, 7.1)	C2-α, C2-β, C1-CO	C1-α, C1-β, C1-δ, C3-NH
	CO	177.4, C			
	α	55.7, CH	4.05ᶜ	C2-β, C2-CO	C3-NH
	β	41.1, CH₂	1.60 (m); 1.11 (m)	C2-α, C2-γ	
	γ	26.7, CH	1.56 (m)	C2-β	
	δ	24.2, CH₃	0.85 (d, 6.5)	C2-β, C2-γ, C2-δ'	
	δ'	21.7, CH₃	0.73 (d, 6.5)	C2-β, C2-γ, C2-δ	
C3 Phe	NH		7.81 (d, 9.1)	C3-α, C3-β, C2-CO	C2-β, C2-α, C2-NH, Terminal-NH₂
	CO	178.6, C			
	α	57.9, CH	4.40 (ddd, 12.0, 9.1, 3.1)	C3-β, C3-1, C3-CO	Terminal-NH₂
	β	40.0, CH2	3.28 (dd,13.7, 3.1); 2.73 (dd, 13.7, 12.0)	C3-α, R4-CO, C3-1, C3-2,6	
	Aromatic	1: 139.1, C			
		2: 131.7, CH	7.21ᶜ	C3-β, C3-4	
		3: 130.5, CH	7.13ᶜ	C3-1	
		4: 128.9, CH	7.13ᶜ	C3-2/6	
		5: 130.5, CH	7.13ᶜ	C3-1	
		6: 131.7, CH	7.21ᶜ	C3-β, C3-4	
	NH₂		7.27 (brs); 6.94 (brs)	C3-α, C3-CO	C3-α, C3-NH

ᵃ Data extracted from HSQC and HMBC spectra. ᵇ Sequential NOEs. ᶜ Signal overlap prevents determination of couplings

3.2.5. Callyaerin M (15, new natural product)

Callyaerin M	
Sample code	G4-5
Biological source	*Callyspongia aerizusa*
Sample amount	2.0 mg
Physical description	white amorphous powder
Molecular formula	$C_{64}H_{95}N_{15}O_{15}$
Molecular weight	1313 g/mol
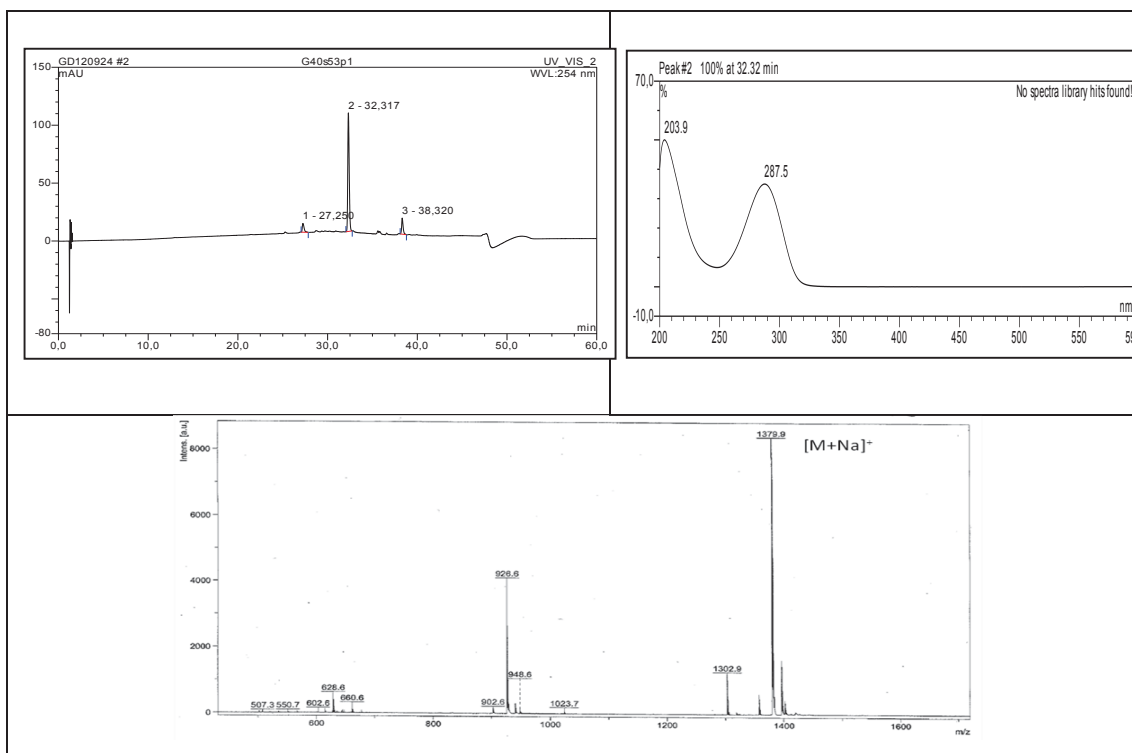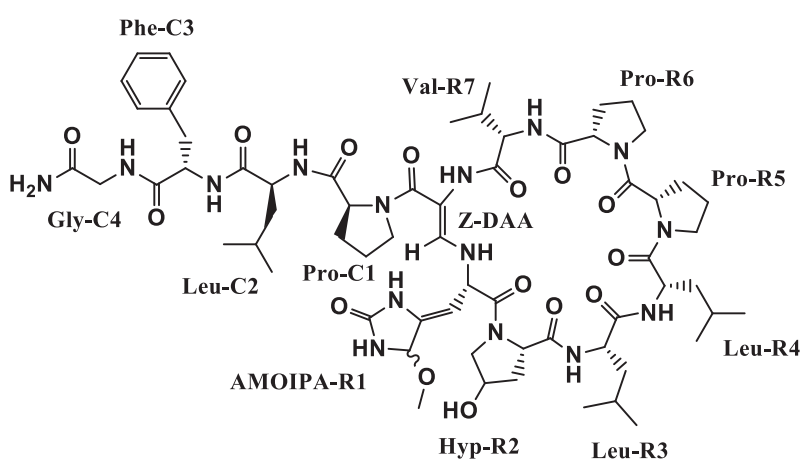
Compound **15** was obtained as a white, amorphous solid. The molecular formula was determined to be $C_{64}H_{95}N_{15}O_{15}$ by HRESIMS (m/z 1314.7202 [M+H]$^+$), and contained twenty five degrees of unsaturation. The ^{1}H NMR spectrum of **15** denoted the same callyaerin basic structure as in **11 − 14** (Table 3.14). Thorough inspection of 1D and 2D NMR data disclosed the presence of nine amino acid residues as Leu (3X), Pro (3X), Val, Gly, and Phe, together with two unusual amino acid moieties: γ-hydroxyproline (Hyp) and 2-amino-3-(5-methoxy-2-oxoimidazolidin-4-ylidene)propanoic acid (AMOIPA). The presence of DAA was indicated by signals at δ_H 8.40 (brs, NH) and δ_H 7.40 (d, J=13.7 Hz, β-H). In addition, the amine protons at δ_H 7.06 and 7.17 were attributed to the terminal NH$_2$ group. The previously unreported amino acid 2-amino-3-(5-methoxy-2-oxoimidazolidin-4-ylidene)propanoic acid (AMOIPA) was identified by long-range HMBC correlations of both NH(3) and NH(5) to C4 (δ_C 157.5), C2 (δ_C 83.5), and C1 (δ_C 140.1); of H-2 to C-1, C-4, and C-β (δ_C 94.1); and of 2-OMe to C2 (Table 3.14) (Daletos *et al.*, 2015).

The geometry of the double bond between C1 and C-β was deduced to be *Z*, on the basis of key ROESY cross-peaks detected from H-β to 2-OMe, and from NH(5) to AMOIPA^{R1}-Hα and DAA-β. However, analysis of the relative configuration of the stereocenter at C-2 of AMOIPA was not possible due to the limited amount of sample (Daletos *et al.*, 2015).

The connectivities between the amino acid residues in **15** were revealed by key HMBC and ROESY correlations (Table 3.14). Thus, compound **15** was deduced to have an overall callyaerin basic structure consisting of the linear side chain Pro^{C1}-Leu^{C2}-Phe^{C3}-Gly^{C4}-NH$_2$ (C1-C4) and the cyclic substructure *cyclo*(DAA-AMOIPA^{R1}-Hyp^{R2}-Leu^{R3}-Leu^{R4}-Pro^{R5}-Pro^{R6}-Val^{R7}) (R1-R7), connected through the DAA unit. This was also corroborated by the base peak at m/z 883 [M-(Pro+Leu+Phe+Gly+NH$_2$)]$^+$ that was observed in the ESI mass spectrum of **15**. Interestingly, compound **15** shares the same amino acid sequence with the known callyaerin C,[5] except for the amino acid moiety at position R1 in the cyclic part, where histidine has been replaced by the uncommon amino acid 2-amino-3-(5-methoxy-2-oxoimidazolidin-4-ylidene)propanoic acid (AMOIPA). Thus, it is suggested that this unusual amino acid is the oxidation product of histidine, followed by methylation and subsequent migration of the double bond into the linear region of the side chain. The upfield proton chemical shifts of Hβ (δ_H 3.83) and 2-OMe (δ_H 2.90) are unusual and suggest the possibility of anisotropy caused by the imidazolidin-2-one ring and/or by

the spatial proximity of the γ-hydroxyproline unit. It is well documented that proline analogues restrict the conformational mobility of the preceding residue, hence favoring steric and anisotropic effects. In the case of callyaerin C, the marked difference in the chemical shifts observed for the Hδ protons of the hydroxyproline unit (δ_H 3.54 and 1.81), further supported this assumption (Daletos *et al.*, 2015).

The absolute stereochemistries of the individual amino acid constituents of **15** were determined following acid hydrolysis of the parent peptide and consequent derivatization with Marfey´s reagent. LC-MS analyses of the resulting (N-(5-fluoro-2,4-dinitrophenyl)-L-leucinamide) derivatives and comparison with authentic amino acids prepared as standards led to the assignment of the L-configuration of all amino acid residues except for AMOIPA where no standard was available (Daletos *et al.*, 2015).

Table 3.14: NMR data of **15** at 600 (^{1}H) and 150 (^{13}C) MHz (DMSO-d_6, δ in ppm)

Unit	position	$\delta_C{}^a$, type	δ_H (*J* in Hz)	HMBC	ROESY[b]
DAA	NH		8.40 (brs)	DAA-α, DAA-CO, R7-CO	R1-NH, R7-α, R7-γ', R7-NH, C1-δ
	CO	167.8, C			
	α	99.6, C			
	β	141.0, CH	7.40 (d, 13.7)	R1-α, DAA-α, DAA-CO	R1-α, R1-NH, R1-NH(5)
R1 AMOIPA	NH		5.76 (dd, 13.9, 8.8)	R1-α, DAA-α	R1-α, R1-β, R7-γ, DAA-β, DAA-NH
	CO	171.0, C			
	α	56.5, CH	5.13 (dd, 10.8, 8.8)	R1-β, R1-1, DAA-β, R1-CO	R2-δ, DAA-β, R1-NH(5)
	β	94.1, CH	3.83 (dd, 10.8, 1.3)	R1-1, R1-2, R1-CO	R1-OCH₃, R1-α, R1-NH, R1-4
	1	140.1, C			
	2	83.5, CH	3.59 (brdd, 1.7, 1.3)	R1-β, R1-1, R1-4, R1-OCH₃	R1-OCH₃, R1-NH(3)
	4	157.5, C			
	-OCH₃	52.0, CH₃	2.90 (s)	R1-2	R1-2, R1-NH(3), R2-δ
	-NH(3)		7.60 (brt, 1.7)	R1-1, R1-2, R1-4	R1-OCH₃, R1-2
	-NH(5)		9.64 (brd, 1.7)	R1-1, R1-2, R1-4	R2-δ, R1-Hα, DAA-β
R2 Hyp	CO	171.6, C			
	α	61.3, CH	4.14^c	R2-β, R2-CO	R3-NH
	β	36.9, CH₂	2.04 (m); 1.92 (m)	R2-α, R2-γ, R2-δ	
	γ	68.7, CH	4.32 (m)		
	δ	54.8, CH₂	3.50 (m)	R2-α, R2-β, R2-γ	R1-Hα, R1-NH(5), R1-OCH₃
			3.40 (dd, 10.8, 3.9)		
	OH		5.20 (d, 4.2)	R2-β, R2-γ, R2-δ	
R3 Leu	NH		6.71 (d, 6.0)	R3-α, R3-β, R2-CO	R2-α, R4-NH
	CO	171.6, C			
	α	52.6, CH	3.96 (dt, 9.0, 6.0)	R3-β, R3-γ, R3-CO	R4-NH
	β	39.2, CH₂	1.48 (m); 1.47 (m)	R3-α, R3-γ, R3-δ, R3-δ', R3-CO	
	γ	24.1, CH	1.60 (m)	R3-δ, R3-δ'	
	δ	22.4, CH₃	0.86 (d, 6.6)	R3-β, R3-γ, R3-δ'	
	δ'	21.3, CH₃	0.80 (d, 6.6)	R3-β, R3-γ, R3-δ	

Residue	Position	^{13}C	^{1}H	HMBC[a]	NOE[b]
R4 Leu	NH		7.11 (d, 7.1)	R4-α, R4-CO, R3-CO	R5-δ, R3-α, R3-NH
	CO	170.2, C			
	α	48.5, CH	4.53 (q, 7.1)	R4-β, R4-γ, R4-CO	R5-δ
	β	40.2, CH$_2$	1.63 (m); 1.37 (m)	R4-α,R4-γ, R4-δ, R4-δ', R4-CO	
	γ	23.9, CH	1.47 (m)	R4-α, R4-β, R4-δ, R4-δ'	
	δ	22.7, CH$_3$	0.93 (d, 6.6)	R4-β, R4-γ, R4-δ'	
	δ'	21.9, CH$_3$	0.91 (d, 6.6)	R4-β, R4-γ, R4-δ	
R5 Pro	CO	171.7, C			
	α	63.8, CH	4.45 (d, 11.0, 7.6)	R5-β, R5-CO	
	β	26.4, CH$_2$	2.20 (m); 1.91 (m)	R5-α, R5-γ, R5-δ	
	γ	24.2, CH$_2$	2.00 (m)	R5-α, R5-β	
	δ	45.8, CH$_2$	3.58 (m); 3.51 (m)	R5-α, R5-β, R5-γ	R4-α
R6 Pro	CO	171.6, C			
	α	62.5, CH	4.29 (t, 8.3)	R6-β, R6-γ, R6-CO	R7-NH
	β	28.8, CH$_2$	2.30 (m); 1.62 (m)	R6-α, R6-γ, R6-δ, R6-CO	
	γ	25.3, CH$_2$	1.92 (m)	R6-α, R6-β, R6-δ	
	δ	46.8, CH$_2$	3.64 (m); 3.26 (m)	R6-β, R6-γ	R7-α
R7 Val	NH		7.34 (d, 10.2)	R7-α, R6-CO	R6-α, DAA-NH
	CO	171.4, C			
	α	56.7, CH	4.53 (dd, 10.2, 5.3)	R7-β, R7-γ, R7-γ', R7-CO	R6-δ, DAA-NH
	β	29.2, CH	2.46 (m)	R7-α, R7-γ, R7-γ'	
	γ	17.9 , CH$_3$	1.08 (d, 6.9)	R7-α, R7-β, R7-γ'	
	γ'	18.9, CH$_3$	0.98 (d, 6.9)	R7-α, R7-β, R7-γ	
C1 Pro	CO	174.2, C			
	α	62.1, CH	4.30[c]	C1-β, C1-CO, DAA-CO	C2-NH
	β	29.0, CH$_2$	2.30 (m); 1.53 (m)	C1-α, C1-γ, C1-δ, C1-CO	
	γ	25.6, CH$_2$	1.88 (m); 1.76 (m)	C1-α, C1-β, C1-δ	
	δ	48.3, CH$_2$	3.48 (m); 3.27 (m)	C1-β, C1-γ	DAA-NH
C2 Leu	NH		7.96 (d, 6.8)	C2-α, C2-β, C1-CO	C1-α, C3-NH
	CO	172.0, C			
	α	52.7, CH	3.77 (m)	C2-β, C2-γ, C2-CO	C3-NH
	β	37.8, CH$_2$	1.51 (m); 1.08 (m)	C2-α, C2-γ, C2-δ, C2-δ'	
	γ	24.1, CH	1.59 (m)	C2-α, C2-β, C2-δ, C2-δ'	
	δ	22.5, CH$_3$	0.82 (d, 6.6)	C2-β, C2-γ, C2-δ'	
	δ'	20.5, CH$_3$	0.71 (d, 6.6)	C2-β, C2-γ, C2-δ	
C3 Phe	NH		7.64 (d, 9.2)	C3-α, C3-β, C2-CO	C2-α, C4-NH, C2-NH
	CO	170.9, C			
	α	54.8, CH	4.14 (ddd, 13.1, 9.2, 3.0)	C3-β, C3-1, C3-CO	C4-NH
	β	36.4, CH2	3.19 (dd, 13.1, 3.0); 2.81 (t, 13.1)	C3-α, C3-CO, C3-1, C3-2,6	
	Aromatic	1: 138.2			
		2: 129.6	7.15[c]	C3-β, C3-4	
		3: 127.2	7.04[c]	C3-1	
		4: 125.3	7.07[c]	C3-2/6	
		5: 127.2	7.04[c]	C3-1	
		6: 129.6	7.15[c]	C3-β, C3-4	
C4 Gly	NH		7.46 (dd, 6.9, 5.5)	C4-α, C3-CO	C3-NH, Terminal –NH$_2$
	CO	170.5, C			
	α	42.0, CH$_2$	3.81 (dd, 17.0, 6.9); 3.55 (dd, 17.0, 5.5)	C3-CO, C4-CO	
	NH$_2$		7.17 (brs); 7.06 (brs)	C3-α, C3-CO	C3-α, C3-NH

[a] Data extracted from HSQC and HMBC spectra. [b] Sequential NOEs. [c] Signal overlap prevents determination of couplings

3.2.6. Callyaerin A (16, known natural product)

Callyaerin A	
Sample code	G4-6
Biological source	*Callyspongia aerizusa*
Sample amount	4.0 mg
Physical description	white amorphous powder
Molecular formula	$C_{69}H_{108}N_{14}O_{14}$
Molecular weight	1357 g/mol
Optical rotation $[\alpha]_D^{20}$	-80 (*c* 0.12, MeOH)
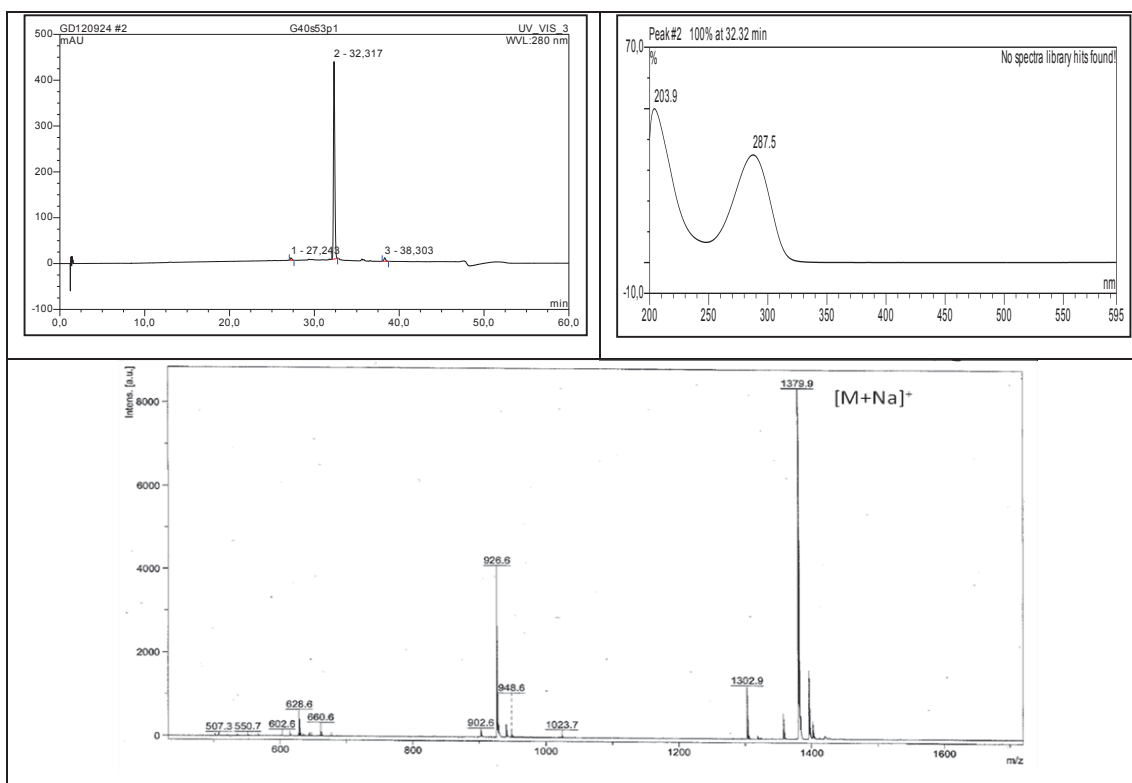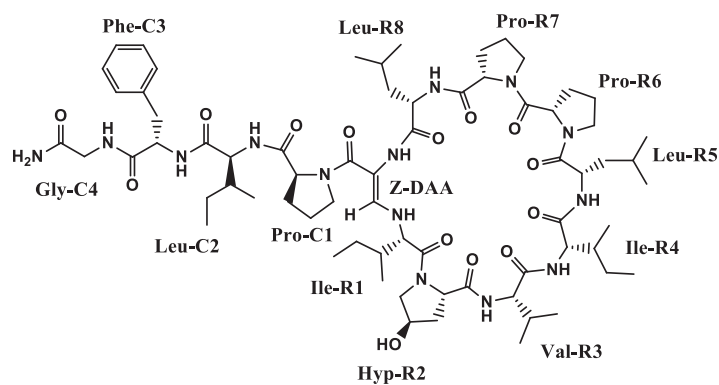
Compound **16** was obtained as a white amorphous solid. MALDI-TOF-MS showed molecular ion peak at *m/z* 1379.8 [M+Na]+ (base peak), respectively, indicating a molecular weight of 1356.8 g/mol. Particularly noteworthy were the numerous deshielded amide N*H* resonances, α-amino acid methines, aromatic protons, and aliphatic primary and secondary methyls, indicative of the peptidic nature of compound **16**. Careful inspection of TOCSY and COSY spectra showed the existence of eleven amino acid residues consisting of Pro (3X), Phe, Gly, Leu (2X), IIe (3X), and Val along with the DAA unit (Daletos *et al.*, 2015).

The sequence of amino acids, the position of the DAA, the terminal NH and the cyclic structure of callyaerin **16** were established by interpretation of HMBC and ROESY experiments. ROESY correlations between Pro^{C1}-Hα/Ile^{C2}-NH, Ile^{C2}-NH/Phe^{C3}-NH, and Phe^{C3}-NH/Gly^{C4}-NH, indicated the sequence of the linear side chain as Pro^{C1}-Ile^{C2}-Phe^{C3}-Gly^{C4}-NH$_2$. The HMBC correlations of Gly^{C4}-NH/Phe^{C3}-CO, Phe^{C3}-NH/Ile^{C2}-CO, and Ile^{C2}-NH/Pro^{C1}-CO further supported the assignments made from the ROESY spectrum (Daletos *et al.*, 2015).

Additional ROESY correlations observed between Leu^{R8}-Hα/DAA-NH, Val^{R3}-NH/Ile^{R4}-NH and Ile^{R4}-NH/Leu^{R5}-NH established the partial peptide sequences Leu^{R8}-DAA and Val^{R3}-Ile^{R4}-Leu^{R5}. Key ROESY correlations between Val^{R3}-NH/Hyp^{R2}-Hα, Leu^{R8}-NH/Pro^{R7}-Hα and Pro^{R7}Hα/Pro^{R6}-Hα confirmed the assignments of the remaining proline residues Pro^{R2}, Pro^{R6}, and Pro^{R7}, respectively. The nature of the ring closure was corroborated by the ROESY correlations between DAA-βH/Ile^{R1}-Hα and Ile^{R1}-NH, indicating the sequence of the cyclic part of **16** as *cyclo*(DAA-Ile^{R1}-Hyp^{R2}-Val^{R3}-Ile^{R4}-Leu^{R5}-Pro^{R6}-Pro^{R7}-Leu^{R8}) (Daletos *et al.*, 2015).

The linkage of the linear side chain (C1-C4) with the cyclic part (R1-R8) of compound **16** was deduced from the ROESY correlation between DAA-NH/Pro^{C1}-Hδ, as well as from the HMBC correlation between Pro^{C1}-Hα/DAA-CO. This was in agreement with the fragment ion at *m/z* 870 for [M-(Pro+Ile+Phe+Gly+NH$_2$)]$^{+}$ that was observed in the ESI mass spectrum of **16**. The obtained NMR and mass spectral data were found to be identical with published data for callyaerin A, previously reported from the sponge *C. aerizusa* (Ibrahim *et al.*, 2010; Daletos *et al.*, 2015).

3.2.7. Callyaerin B (17, known natural product)

Callyaerin B	
Sample code	G4-7
Biological source	*Callyspongia aerizusa*
Sample amount	10.0 mg
Physical description	white amorphous powder
Molecular formula	$C_{64}H_{95}N_{15}O_{15}$
Molecular weight	1280.6 g/mol
Optical rotation $[\alpha]_D^{20}$	-89 (*c* 0.2, MeOH)
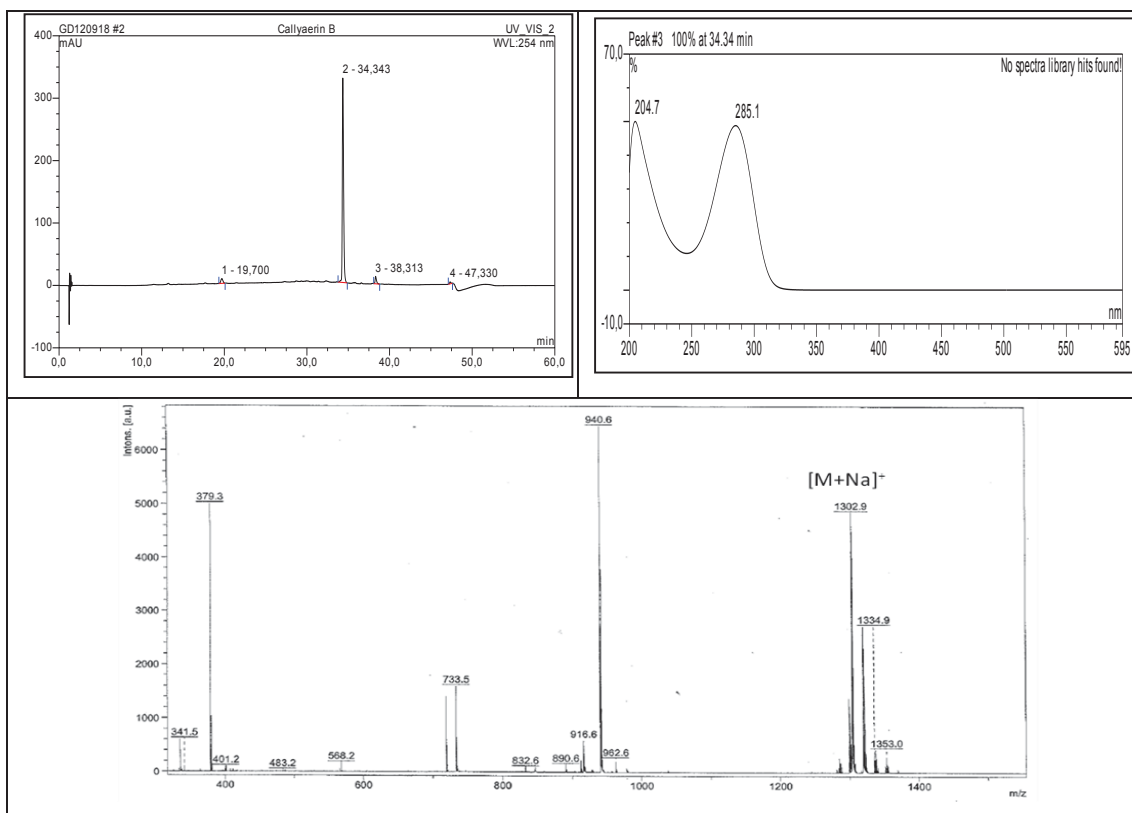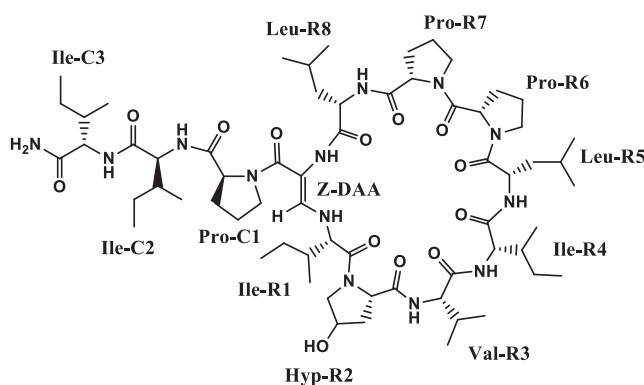
Compound **17** was obtained as a white amorphous solid. The MALDI-TOF-MS showed molecular ion peak at *m/z* 1302.6 [M+Na]+ (base peak), respectively, which was consistent with the molecular weight of 1280.6 g/mol. Interpretation of TOCSY and COSY spectra revealed the spin systems for nine amino acid residues consisting of Pro (3X), Leu (2X), IIe (3X), and Val along with the DAA unit. A detailed 1D and 2D NMR spectroscopic data analysis revealed that **17** had the same ring size as **14**, but differed in the length and sequence of the side chain. This was in agreement with the fragment ion at *m/z* 940.2 for [M-(Pro+2IIe+NH$_2$)]$^+$ that was observed in the MALDI-TOF mass spectrum of **17** (Daletos *et al.*, 2015).

In particular, the observed ROESY correlations between Leu^{R8}-Hα/DAA-NH, Val^{R3}-NH/Ile^{R4}-NH, Ile^{R4}-NH/Leu^{R5}-NH, Val^{R3}-NH/Hyp^{R2}-Hα, Leu^{R8}-NH/Pro^{R7}-Hα and DAA-βH/Ile^{R1}-Hα, corroborated the sequence of the cyclic part of **17** as *cyclo*(DAA-Ile^{R1}-Hyp^{R2}-Val^{R3}-Ile^{R4}-Leu^{R5}-Pro^{R6}-Pro^{R7}-Leu^{R8}), which is identical to that found in **16**. Moreover, ROESY correlations between Pro^{C1}-Hα/Ile^{C2}-NH, Ile^{C2}-Hα/Ile^{C3}-NH, and Ile^{C3}-Hα/terminal-NH$_2$, indicated the peptide fragment Pro^{C1}-Ile^{C2}-Ile^{C3}-NH$_2$. This was further supported by HMBC correlations between terminal NH$_2$/Ile^{C3}-CO (δ_C 172.7), Ile^{C3}-NH/IIe^{C2}-CO (δ_C 172.1), and IIe^{C2}-NH/Pro^{C1}-CO (δ_C 171.2) (Daletos *et al.*, 2015).

Finally, ROESY cross peak between DAA-NH/Pro^{C1}-Hδ, in association with the HMBC correlation between Pro^{C1}-Hα/DAA-CO, confirmed the linkage between the linear side chain (C1-C4) and the cyclic part (R1-R8) of compound **17**. Comparison of the NMR data and molecular weight of 15 with callyaerin B isolated from *C. aerizusa* indicated that both compounds were identical (Ibrahim *et. al.* 2010; Daletos *et al.*, 2015).

3.2.8. Callyaerin C (18, known natural product)

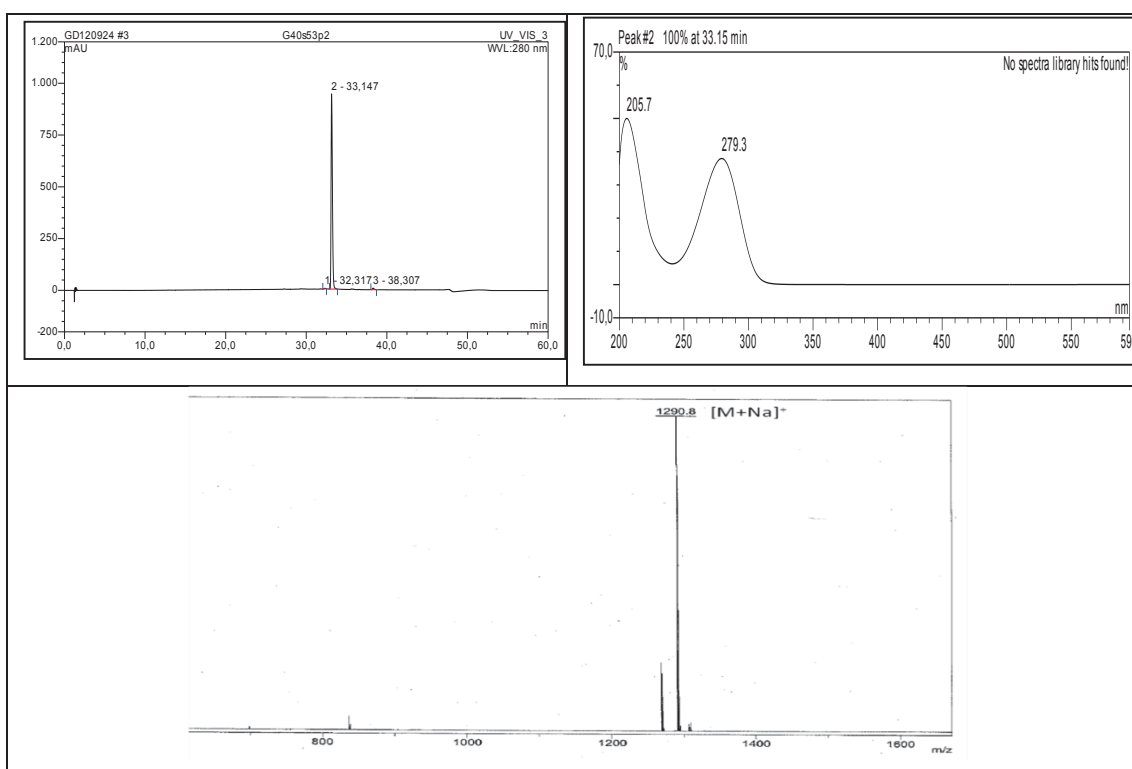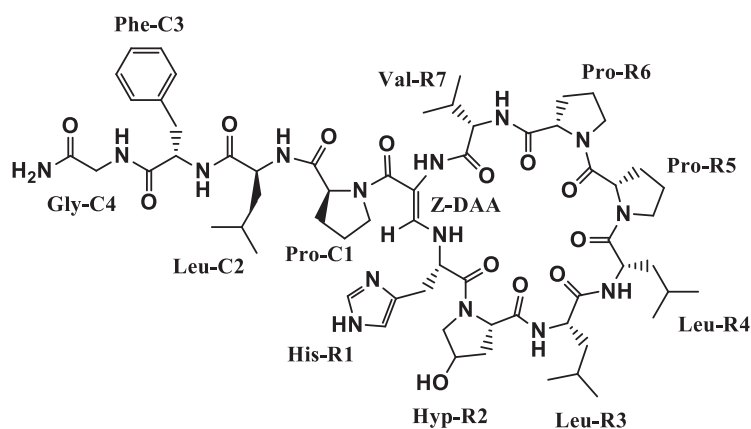| Callyaerin C	
Sample code	G4-8
Biological source	*Callyspongia aerizusa*
Sample amount	8.0 mg
Physical description	white amorphous powder
Molecular formula	$C_{63}H_{93}N_{15}O_{13}$
Molecular weight	1268.7 g/mol
Optical rotation $[\alpha]_D^{20}$	-52 (*c* 0.15, MeOH)

Compound **18** was obtained as a white amorphous solid. The MALDI-TOF-MS showed molecular ion peak at *m/z* 1290.7 [M+Na]$^+$ (base peak), respectively, which was consistent with the molecular weight of 1268.5 g/mol. The ^{1}H NMR spectrum showed six deshielded amine protons at δ_H 8.06 — 5.14 and a cluster of α-amino acid methines at δ_H 4.68 — 3.80, indicative of the peptidic nature of **18**. COSY and TOCSY spectra showed the spin systems of nine amino acid residues consisting revealed the spin systems for eleven amino acid residues consisting of Pro (3X), Leu (3X), Phe, Hyp, Val, Gly and His along with the DAA unit (Daletos *et al.*, 2015).

ROESY correlations between between Pro^{C1}-Hα/Leu^{C2}-NH, Leu^{C2}-Hα/Phe^{C3}-NH, and Phe^{C3}-Hα/terminal-NH$_2$, allowed us to establish the sequence of the linear side chain as Pro^{C1}-Leu^{C2}-Phe^{C3}-Gly-NH$_2$ (C1-C4). In the same manner the cyclic part of **18** was found to be composed of two peptide fragments Val^{R7}-DAA-His^{R1} and Leu^{R3}-Leu^{R4}. Key ROESY correlations between Leu^{R3}-NH/Hyp^{R2}-Hα, Val^{R4}-NH/Pro^{R5}-Hδ, and Val^{R7}-NH/Pro^{R6}-Hα connected these two fragments, and accordingly the cyclic part of **18** was established as *cyclo*(DAA-His^{R1}-Hyp^{R2}-Leu^{R3}-Leu^{R4}-Pro^{R5}-Pro^{R6}-Val^{R7}). The HMBC correlations of Leu^{R3}-NH/Hyp^{R2}-CO, Leu^{R4}-NH/Leu^{R3}-CO, and Val^{R7}-NH/Pro^{R6}-CO supported the interpretation of the ROESY spectrum. Finally, the HMBC correlation between Pro^{C1}-Hα/DAA-CO and the ROESY correlation between DAA-NH/Pro^{C1}-Hδ established the linkage between the linear side chain and the cyclic part of compound **18**. Further support for the linkage was provided by the fragment ion at *m/z* 942 for [M-(Pro+Leu+Phe+NH$_2$)]$^+$ that was observed in the ESI mass spectrum of **18**. Comparison of the NMR data and molecular weight of **18** with callyaerin C isolated from *C. aerizusa* indicated that both compounds were identical (Ibrahim *et. al.* 2010; Daletos *et al.*, 2015).

3.2.9. Callyaerin D (19, known natural product)

Callyaerin D	
Sample code	G4-9
Biological source	*Callyspongia aerizusa*
Sample amount	9.0 mg
Physical description	white amorphous powder
Molecular formula	$C_{69}H_{107}N_{15}O_{15}$
Molecular weight	1386.8 g/mol
Optical rotation $[\alpha]_D^{20}$	-49 (*c* 0.2, MeOH)
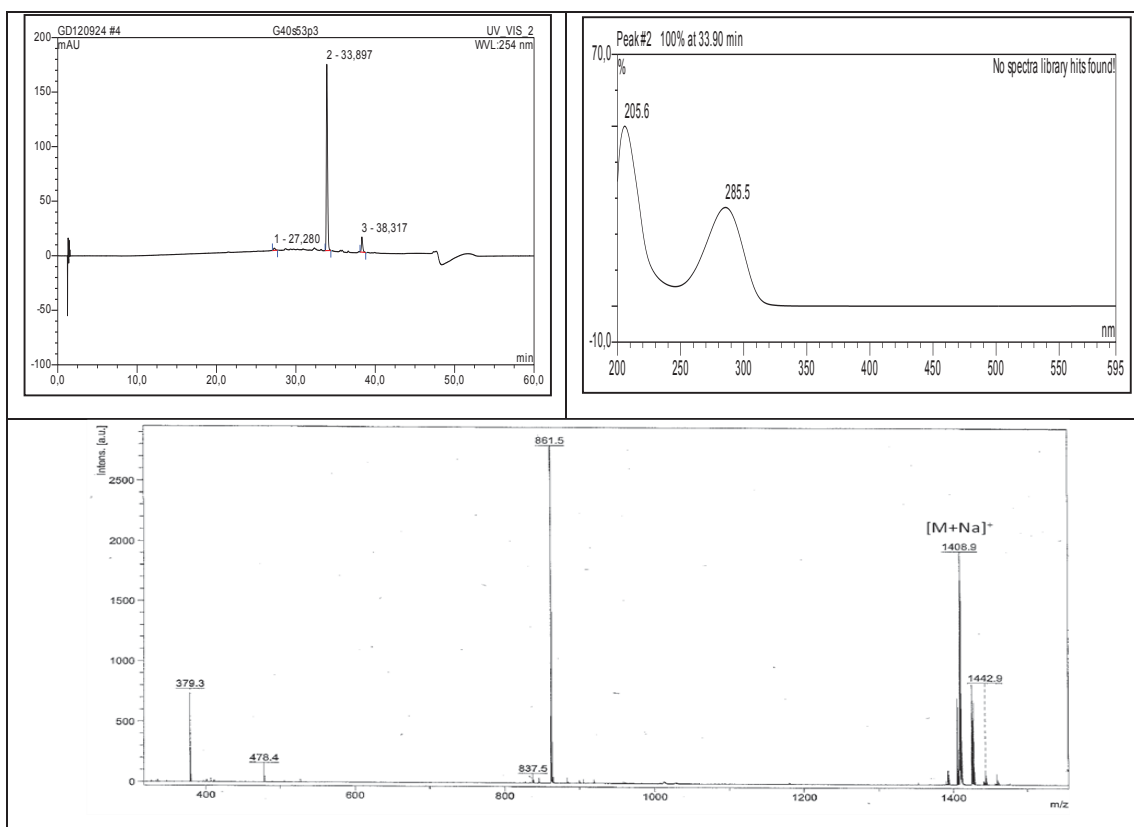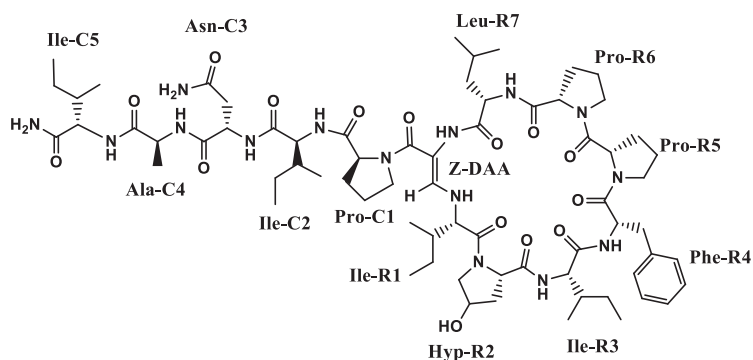
Compound **19** was isolated as a white amorphous powder. The MALDI-TOF-MS spectrum showed a prominent ion peak at *m/z* 1409.7 [M+Na]$^+$, suggesting a molecular weight of 1386 g/mol. The ^{1}H NMR and COSY spectra suggested that compound **19** was a peptide, due to the presence of a series of NH signals between δ_H 5.30 - 7.95 coupled to α-protons in the region from δ_H 3.95 - 4.64. ^{1}H-^{1}H-COSY and TOCSY spectra indicated the spin systems of eleven amino acid residues consisting of Ile(4X), Pro(3X), Phe, Leu, Asn, and Ala, together with the unusual amino acid γ-hydroxyproline (Hyp) and the DAA moiety. The presence of DAA was indicated by signals at δ 8.42 (1H, s, DAA-N*H*) and 7.38 (1H, d, *J* = 8.8 Hz, H-β). Two downfield singlet signals at δ 7.03 and 7.11 were assigned to the terminal NH$_2$ group. The obtained UV, NMR and mass spectral data were identical to those reported for callyaerin D, which was previously isolated from *C. aerizusa* (Ibrahim *et al.*, 2010). The sequence of amino acids, in the case of the callyaerins D had earlier been deduced only based on sequence correlations in the ROESY spectra, due to the insufficient material available to record heteronuclear NMR spectra (Ibrahim *et. al.* 2010). However, re-isolation of these compounds in the present study afforded sufficient amounts for further 2D NMR measurements (Daletos *et al.*, 2015).

Accordingly, ROESY correlations between Pro^{C1}-Hα/Ile^{C2}-NH, Ile^{C2}-Hα/Asn^{C3}-NH, Asn^{C3}-Hα/Ala^{C4}-NH, and Ala^{C4}-Hα/Ile^{C5}-NH, and Ile^{C5}- Hα/terminal-NH$_2$, as well as between Ile^{C2}-NH/Asn^{C3}-NH/Ala^{C4}-NH/ Ile^{C5}-NH/terminal NH$_2$, indicated the peptide fragment Pro^{C1}-Ile^{C2}-Asn^{C3}-Ala^{C4}-Ile^{C5}-NH$_2$. This was confirmed by HMBC cross-peaks between terminal NH$_2$/Ile^{C5}-CO, Ile^{C5}-NH/Ala^{C4}-CO, Ala^{C4}-NH/Asn^{C3}-CO, Asn^{C3}-NH/Ile^{C2}-CO, and Ile^{C2}-NH/Pro^{C1}-CO (δ_C 172.9). The MALDI-TOF mass spectrum gave a basic fragment ion peak at *m/z* 861 for [M-(Pro+2Ile+Asn+Ala+NH$_2$)]$^+$, further supporting the composition of the side chain as previously reported (Ibrahim *et al.*, 2010; Daletos *et al.*, 2015).

In the same manner, ROESY correlations between the amide protons of the cyclic moiety disclosed the presence of the partial peptide sequences Leu^{R7}-DAA-Ile^{R1} and Ile^{R3}-Phe^{R4}. The connectivity of these two fragments was justified based on ROESY cross-peaks between Ile^{R3}-NH/Hyp^{R2}-Hα, Phe^{R4}-NH/Pro^{R5}-Hδ, and Leu^{R7}-NH/Pro^{R6}-Hα, Pro^{R6}-Hβ, in association with the HMBC correlations between Leu^{R7}-NH/Pro^{R6}-CO, Pro^{R5}-Hα/Phe^{R4}-CO, and Phe^{R4}-Hα/Ile^{R3}-CO. Thus, the sequence of the cyclic part of **6** *cyclo*(DAA-IIe^{R1}-Ile^{R2}-Phe^{R3}-Pro^{R4}-Hyp^{R5}-Pro^{R6}-Leu^{R7}) should be

revised to *cyclo*(DAA-Ile[R1]-Hyp[R2]-Ile[R3]-Phe[R4]-Pro[R5]-Pro[R6]-Leu[R7]) as shown (Figure 3.19) (Daletos *et al.*, 2015).

Table 3.15: NMR data of **19** at 700 (^{1}H) and 176 (^{13}C) MHz (DMSO-d_6, δ in ppm)

unit	position	δc^a, type	δ_H (*J* in Hz)	HMBC	ROESY[b]
DAA	NH		8.42 (brs)	DAA-α, DAA-CO, R7-CO	C1-δ, R1-α, R1-NH, R7-α, R7-NH
	CO	167.2, C			
	α	98.7, C			
	β	143.6. CH	7.38 (d, 13.9)	R1-α, DAA-α, DAA-CO	R1-α, R1-γ, R1-δ, R1-NH
R1 Ile	NH		5.30 (dd, 13.9, 10.0)		R7- δ, DAA-β, DAA-NH
	CO	172.7, C			
	α	63.8, CH	4.41^c	R1-β, R1-γ, R3-γ', R1-CO	DAA-β
	β	35.9, CH	1.98 (m)	R1-α , R1-γ, R1-γ', R1-δ	
	γ	22.3, CH2	1.25 (m); 0.94 (m)	R1-α , R1-β, R1-γ', R1-δ	
	γ'	15.1, CH3	0.84^c	R1-α, R1-β, R1-γ	
	δ	11.3^d, CH3	0.83^c	R1-β, R1-γ	
R2 Hyp	CO	172.6, C			
	α	62.1, CH	4.13^c	R2-β, R2-CO	R3-NH
	β	37.5, CH2	2.06 (m); 1.97 (m)	R2-α, R2-γ, R2-δ	R3-NH
	γ	68.9, CH	4.40^c	R2-β	R3-NH
	δ	55.2, CH2	3.93 (m); 3.65 (brd 10.9)	R2-α, R2-β, R2-γ	
R3 Ile	NH		7.64 (d, 4.9)		R2-α, R2-β, R2-γ, R4-NH
	CO	170.5, C		R2-β, R2-γ, R2-δ	
	α	58.7, CH	4.00 (dd, 4.9, 3.5)	R3-β, R3-γ, R3-γ', R3-CO	
	β	35.7, CH	1.81 (m)	R3-α , R3-γ, R3-γ', R3-δ	
	γ	24.7, CH2	1.30 (m); 1.25 (m)	R3-α, R3-β, R3-γ', R3-δ	
	γ'	15.1, CH3	0.82^c	R3-α, R3-β, R3-γ	
	δ	11.1^d, CH3	0.82^c	R3-β, R3-γ	
R4 Phe	NH		7.50, (d, 6.0)	R4-α, R4-CO, R3-CO	R5-δ, R3-NH
	CO	169.0, C			
	α	53.4, CH	4.61 (ddd, 9.7, 6.0, 3.5)	R4-β, R4-1, R3-CO, R4-CO	R5-δ
	β	36.3, CH2	3.06 (dd, 13.1, 9.7); 2.77 (dd, 13.1, 3.5)	R4-α, R4-1, R4-2/6, R4-CO	
	aromatic	1: 138.0, C			
		2: 129.0, CH	7.24^c	R4-β, R4-3/5, R4-4	
		3: 128.2, CH	7.30^c	R4-2/6, R4-1	
		4: 126.5, CH	7.22^c		
		5: 128.2. CH	7.30^c	R4-2/6, R4-1	
		6: 129.0, CH	7.24^c	R4-β, R4-3/5, R4-4	
R5 Pro	CO	171.5, C			
	α	63.7, CH	4.32^c	R5-β, R5-γ, R5-CO, R4-CO	
	β	26.9, CH2	2.16 (m); 1.80 (m)	R5-α, R5-γ, R5-δ	
	γ	24.3, CH2	1.92 (m); 1.90 (m)	R5-α, R5-δ	
	δ	46.3, CH2	3.61 (t, 8.8); 3.38	R5-α, R5-β, R5-γ	R4-α, R7-NH

Residue	Position				
			(m)		
R6 Pro	CO	171.6, C			
	α	62.8, CH	4.17[c]	R6-β, R6-CO	R7-NH
	β	28.6, CH2	2.23 (m); 1.40 (m)	R6-α, R6-γ	R7-NH
	γ	25.5, CH2	1.69 (m); 1.47 (m)	R6-β, R6-δ	
	δ	46.5, CH2	3.27 (m); 2.23 (m)	R6-α, R6-β, R6-γ	R7-NH
R7 Leu	NH		7.54 (d, 9.5)	R7-α, R7-β, R6-CO	R6-α, R6-β, R6-δ, DAA-NH
	CO	172.5, C			
	α	50.6, CH	4.47 (td, 9.5, 5.5)	R7-β, R7-γ, R7-CO, R7-CO	
	β	41.2, CH2	1.85 (m); 1.71 (m)	R7-α, R7-γ, R7-δ, R7-δ'	
	γ	24.3, CH	1.76 (m)	R7-α, R7-β, R7-δ, R7-δ'	
	δ	22.3[d], CH3	0.85[c]	R7-β, R7-γ, R7-δ'	
	δ'	21.1[d], CH3	0.87[c]	R7-β, R7-γ, R7-δ	
C1 Pro	CO	173.6, C			C2-NH
	α	61.6, CH	4.30[c]	C1-β, C1-CO, DAA-CO	
	β	28.7, CH2	2.17 (m); 1.60 (m)	C1-α, C1-γ, C1-δ	
	γ	25.7, CH2	1.79 (m); 1.71 (m)	C1-α, C1-β, C1-δ	
	δ	48.5, CH2	3.53 (brt, 9.5); 3.30 (m)	C1-α, C1-β, C1-γ	
C2 Ile	NH		7.76 (d, 6.3)	C2-α, C2-β, C1-CO	C1-δ, C1-α, C3-NH
	CO	171.5, C			
	α	58.7, CH	3.93 (t, 6.3)	C2-β, C2-γ, C2-γ', C2-CO	C3-NH
	β	35.0, CH	1.90 (m)	C2-α, C2-γ, C2-γ', C2-δ	
	γ	24.6, CH2	1.40 (m); 1.28 (m)	C2-α, C2-β, C2-γ', C2-δ	
	γ'	15.1, CH3	0.87[c]	C2-α, C2-β, C2-γ	
	δ	11.0[d], CH3	0.82[c]	C2-β, C2-γ	
C3 Asn	NH		7.88 (d, 7.6)	C3-α, C2-CO	C2-α, C2-NH, C4-NH
	CO	171.1, C			
	α	50.0, CH	4.55 (q, 7.0)	C3-β, C3-CO, C3-CO(γ)	C4-NH
	β	37.2, CH2	2.69 (dd,15.1, 6.9); 2.35 (dd,15.1, 6.9)	C3-β, C3-CO, C3-CO(γ)	
	CO(γ)	171.3, C			
	NH2		6.93 (brs); 7.31 (brs)	C3-β, C3-CO	
C4 Ala	NH		7.57 (d, 6.9)	C4-α, C4-β, C3-CO	C3-α, C3-NH, C5-NH
	CO	171.9, C			
	α	48.8, CH	4.16[c]	C4-β, C4-CO	C5-NH
	β	17.1, CH3	1.25 (d, 6.9)	C4-α	
C5 Ile			7.34 (d, 6.7)	C5-α, C5-β, C4-CO	C4-NH, Terminal-NH2
	CO	172.9, C			
	α	57.1, CH	4.05 (dd, 8.9, 6.7)	C5-β, C5-γ, C5-γ', C5-CO	Terminal-NH2
	β	36.2, CH	1.77 (m)	C5-α, C5-γ, C5-γ', C5-δ	
	γ	24.1, CH2	1.12 (m); 1.45 (m)	C5-α, C5-β, C5-γ', C5-δ	
	γ'	15.1, CH3	0.83[c]	C5-α, C5-β, C5-γ	
	δ	11.1[d], CH3	0.83[c]	C5-β, C5-γ	
	NH2		7.11 (brs), 7.03 (brs)	C5-α, C5-CO	C5-α, C5-NH

[a] Data extracted from HSQC and HMBC spectra. [b] Sequential NOEs. [c] Signal overlap prevents determination of couplings. [d] Assignments may be interchanged within the same column.

Figure 3.19: Structure revision of callyaerin D (**19**)
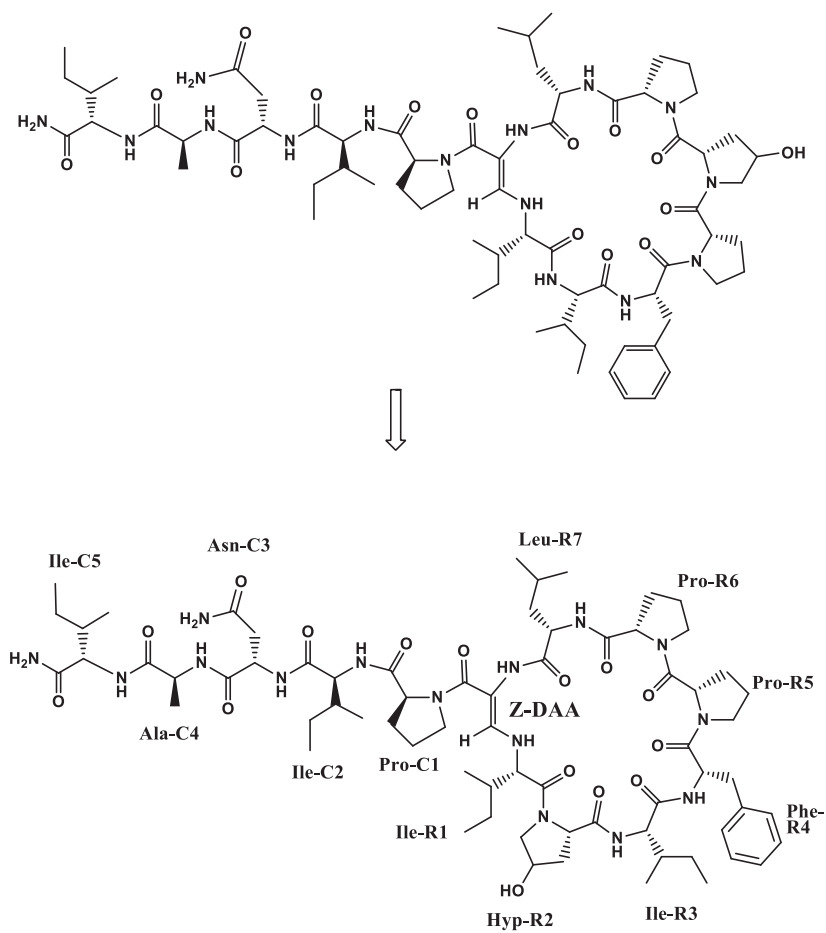
3.2.10. Callyaerin E (20, known natural product)

Callyaerin E	
Sample code	G4-10
Biological source	*Callyspongia aerizusa*
Sample amount	12.0 mg
Physical description	white amorphous powder
Molecular formula	$C_{66}H_{95}N_{13}O_{12}$
Molecular weight	1261.5 g/mol
Optical rotation $[\alpha]_D^{20}$	-68 (*c* 0.25, MeOH)
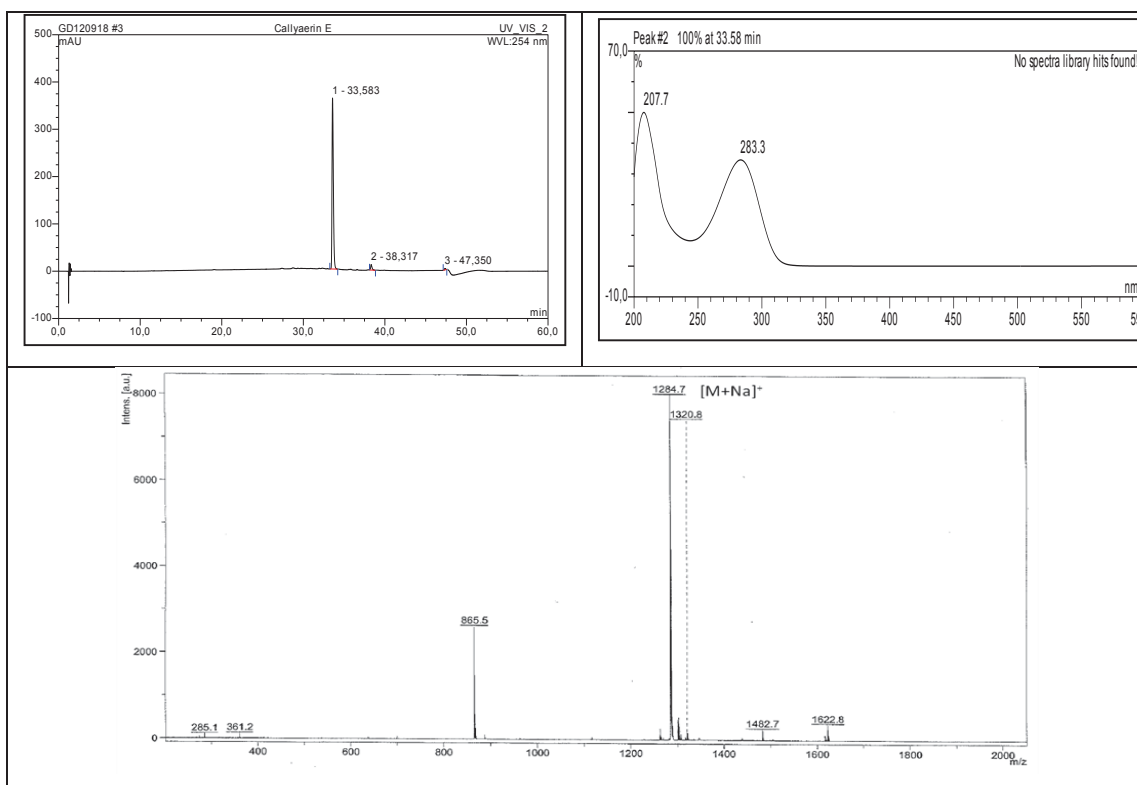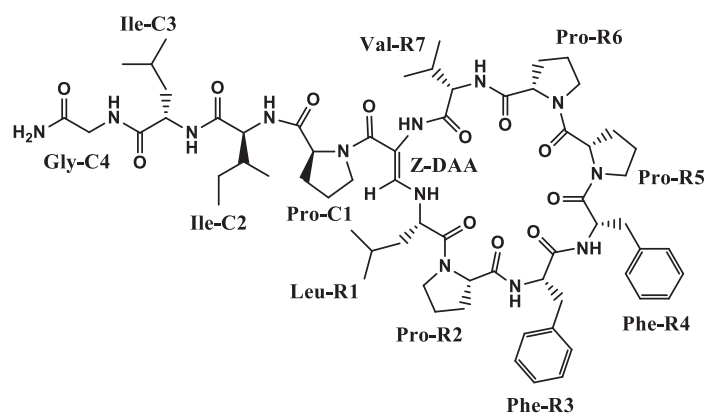
Compound **20** was isolated as a white amorphous powder. The MALDI-TOF-MS spectrum showed a prominent ion peak at *m/z* 1409.7 [M+Na]$^+$, suggesting a molecular weight of 1386 g/mol. The ^{1}H NMR and COSY spectra suggested that compound **20** was a peptide, due to the presence of a series of NH signals between δ_H 5.30 - 7.95 coupled to α-protons in the region from δ_H 3.95 - 4.64. ^{1}H-^{1}H-COSY and TOCSY spectra indicated the spin systems of eleven amino acid residues consisting of Ile(4X), Pro(3X), Phe, Leu, Asn, and Ala, together with the unusual amino acid γ-hydroxyproline (Hyp) and the DAA moiety. The presence of DAA was indicated by signals at δ 8.36 (1H, s, DAA-N*H*) and 7.28 (1H, d, *J* = 14.2 Hz, H-β). Two downfield singlet signals at δ 7.03 and 7.11 were assigned to the terminal NH$_2$ group. The sequence of amino acids, the position of the DAA, the terminal NH$_2$, and the cyclic structure of **20** were established by interpretation of HMBC and ROESY experiments (Daletos *et al.*, 2015).

The sequence of amino acids, the position of the DAA, the terminal NH$_2$ and the cyclic structure of callyaerin **20** were established by interpretation of HMBC and ROESY experiments. ROESY correlations between Pro^{C1}-Hα/Ile^{C2}-NH, Ile^{C2}-NH/Ile^{C3}-NH, and Ile^{C3}-NH/Gly^{C4}-NH, indicated the sequence of the linear side chain as Pro^{C1}-Ile^{C2}-Ile^{C3}-Gly^{C4}-NH$_2$. The HMBC correlations of Gly^{C4}-NH/Ile^{C3}-CO, Ile^{C3}-NH/Ile^{C2}-CO, and Ile^{C2}-NH/Pro^{C1}-CO further supported the assignments made from the ROESY spectrum (Daletos *et al.*, 2015).

Further ROESY correlations between Phe^{R3}-NH/Phe^{R4}-NH, and DAA-NH/Val^{R7}-Hα, Val^{R7}-NH, along with the HMBC correlations between Phe^{R4}-Hα/ Phe^{R3}-CO, and DAA-NH/ Val^{R7}-CO, established the partial structures Phe^{R3}-Phe^{R4} and DAA-Val^{R7}, respectively. The positions of the proline residues Pro^{R2} and Pro^{R5} were apparent from the ROESY correlations of their δ proton signals with the preceding residues Leu^{R1}-Hα and Phe^{R4}-Hα, respectively. In addition, HMBC correlations from the amide protons to adjacent carbonyls allowed the assignment of connections between Phe^{R3}-NH/Pro^{R2}-CO and between Val^{R7}-NH/Pro^{R6}-CO. This assignment was also evident from the ROESY cross-peaks between Phe^{R3}-NH/Pro^{R2}-Hα and Val^{R7}-NH/Pro^{R6}-Hβ, respectively, thus leading to the overall substructure Leu^{R1}-Pro^{R2}-Phe^{R3}-Phe^{R4}-Pro^{R5}-Pro^{R6}-Val^{R7}-DAA (Daletos *et al.*, 2015).

Moreover, the ROESY correlations observed for DAA-βH to Leu^{R1}-Hα and Leu^{R1}-NH, in addition to its COSY correlation to Leu^{R1}-NH, established the nature of the cyclization of compound **20** via the connection of the DAA unit with Leu^{R1},

fulfilling the degrees of unsaturation. Thus, the cyclic substructure was established as *cyclo*(Leu[R1]-Pro[R2]-Phe[R3]-Phe[R4]-Pro[R5]-Pro[R6]-Val[R7]-DAA). Finally, the connectivity of the cyclic part of **20** (R1-R7) and the linear chain (C1-C4) was established through the ROESY correlation of DAA-NH/Pro[C1]-Hδ, as well as by the HMBC correlation between Pro[C1]-Hα/DAA-CO. Further support was provided by ESI and MALDI-TOF MS spectra, which gave a fragment ion at m/z 865 for $[M-(Pro+Ile+Ile+Gly+NH_2)]^+$, arising from the cleavage of the linear side chain. The structure of compound **20** was confirmed by comparison of UV, ^{1}H, ^{13}C NMR and mass spectral data with those of callyaerin E previously isolated from the sponge *C. aerizusa*. (Ibrahim *et al.*, 2010; Daletos *et al.*, 2015).

3.2.11. Callyaerin F (21, known natural product)

Callyaerin F	
Sample code	G4-11
Biological source	*Callyspongia aerizusa*
Sample amount	15.0 mg
Physical description	white amorphous powder
Molecular formula	$C_{58}H_{84}N_{11}O_{10}$
Molecular weight	1094.0 g/mol
Optical rotation $[\alpha]_D^{20}$	-32 (*c* 0.15, MeOH)
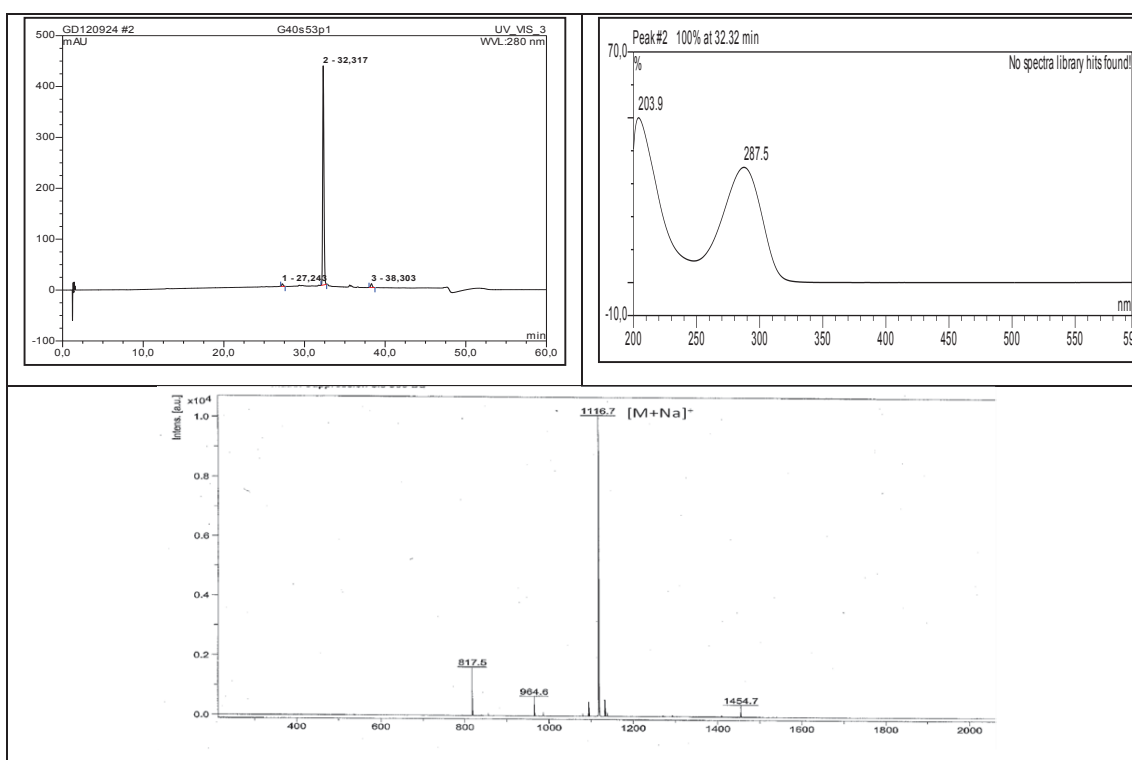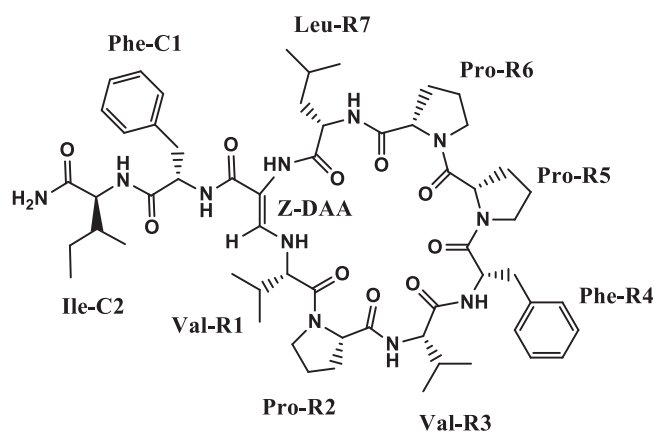
Compound **21** was obtained as a white amorphous solid. The MALDI-TOF-MS spectrum showed a prominent ion peak at *m/z* 1117.0 [M+Na]$^+$, suggesting a molecular weight of 1094 g/mol. The ^{1}H NMR spectrum indicated the peptidic nature of compound **21**. It showed six deshielded amine NH protons at δ_H 5.14-7.66 and a cluster of α amino acid metthines at δ_H 3.80-4.68, signals for methylenes, and aliphatic primary and secondary methyls, which suggested the presence of lipophilic amino acid residues (Table 3.15). Thorough inspection of 1D and 2D NMR data allowed the assignment of nine amino acid residues as Val (2X), Pro (3X), Phe (2X), Leu, and Ile The presence of DAA was indicated by signals at δ 8.36 (1H, s, DAA-N*H*) and 7.28 (1H, d, *J* = 14.2 Hz, H-β). Two downfield singlet signals at δ 7.03 and 7.11 were assigned to the terminal NH$_2$ group. Compound **21** was identified by comparing NMR and MS data with those of callyaerin F, previously isolated from the marine sponge *C. aerizusa* (Ibrahim *et. al.* 2010). The sequence of amino acids, in the case of callyaerin F had earlier been deduced only based on sequence correlations in the ROESY spectra, due to the insufficient material available to record heteronuclear NMR spectra (Ibrahim *et. al.* 2010). However, re-isolation of this compound in the present study afforded sufficient amounts for further 2D NMR measurements (Daletos *et al.*, 2015).

Accordingly, detailed interpretation of the ROESY relationships established the connectivities of the amino acids, similar to those previously reported for this compound (Ibrahim *et. al.* 2010). However, the HMBC correlations from Phe^{C1}-NH (Phe^{C3} in the original structure) to DAA-CO, as well as from DAA-NH to Leu^{R7}-CO (Leu^{C2} in the original structure), justified the assignment of the partial peptide sequences Phe^{C1}-DAA and DAA-Leu^{R7}, respectively. Thus, the sequence of the side chain of **21**, Pro^{C1}-Leu^{C2}-Phe^{C3}-Ile^{C4}-NH$_2$, should be revised to Phe^{C1}-Ile^{C2}-NH$_2$, while the sequence of the cyclic part, *cyclo*(DAA-Val^{R1}-Pro^{R2}-Val^{R3}-Phe^{R4}-Pro^{R5}), should be revised to *cyclo*(DAA-Val^{R1}-Pro^{R2}-Val^{R3}-Phe^{R4}-Pro^{R5}-Pro^{R6}-Leu^{R7}) (Figure 3.20). This was further corroborated by the base ion peak at *m/z* 817 for [M-(Phe+Ile+NH$_2$)]$^+$, that was observed in the ESI mass spectrum of **21** (Daletos *et al.*, 2015).

Table 3.15: NMR data of **21** at 700 (^{1}H) and 176 (^{13}C) MHz (DMSO-d_6, δ in ppm)

unit	position	$\delta_C{}^a$, type	δ_H (J in Hz)	HMBC	ROESY^b
DAA	NH		8.25 (brs)	DAA-α, DAA-CO, R7-CO	R7-α, R7-NH, C1-δ, R1-NH
	CO	165.8, C			
	α	97.9, C			
	β	142.7, CH	7.25 (d, 14.0)	R1-α, DAA-α, DAA-CO	R1-α, R1-NH, R7-γ
R1 Val	NH		5.14 (dd, 10.1, 13.7)	R1-α, DAA-α, DAA-β	DAA-NH, DAA-β
	CO	172.5, C			
	α	63.7, CH	4.38 (brd, 9.8)	R1-β, R1-γ, R1-γ', R1-CO	R2-δ, DAA-β
	β	29.6, CH	2.31 (m)	R1-α, R1-γ, R1-γ'	
	γ	18.4, CH$_3$	0.87 (d, 6.9),	R1-α, R1-β, R1-γ'	
	γ'	15.4, CH$_3$	0.66 (d, 6.9)	R1-α, R1-β, R1-γ	
R2 Pro	CO	172.5, C			
	α	63.8, CH	3.95 (dd, 10.3, 6.7)	R2-β, R2-γ, R2-CO	R3-NH
	β	29.2, CH$_2$	2.17 (m); 1.81 (m)	R2-α, R2-γ, R2-δ	
	γ	24.8, CH$_2$	2.03 (m); 1.84 (m)	R2-α, R2-β, R2-δ	
	δ	46.6, CH$_2$	3.86 (m); 3.74 (m)	R2-α, R2-β, R2-γ	R3-NH
R3 Val	NH		7.54 (d, 5.1)	R3-α, R2-CO	R2-α, R2-δ, R4-NH
	CO	170.7, C			
	α	59.8, CH	3.86 (m)	R7-β, R7-γ, R7-γ', R7-CO	R4-NH
	β	29.0, CH	2.11 (m)	R7-α, R7-γ, R7-γ'	
	γ	18.4, CH$_3$	0.93 (d, 6.7)	R7-α, R7-β, R7-γ'	
	γ'	18.3, CH$_3$	0.86 (d, 6.7)	R5-α, R5-β, R5-γ	
R4 Phe	NH		7.50 (d, 6.1)	R4-α, R4-CO, R3-CO	R3-α, R5-δ
	CO	168.7, C			
	α	53.8, CH	4.54 (ddd, 9.3, 6.1, 3.5)	R4-β, R4-1, R4-CO	R5-δ
	β	36.4, CH$_2$	3.01 (dd, 12.9, 9.3); 2.71 dd (12.9, 3.5)	R4-α, R4-1, R4-2/6, R4-CO	
	Aromatic	1: 138.1, C			
		2: 128.9, CH	7.21^c	R4-β	
		3: 128.1, CH	7.28^c	R4-2/6, R4-1	
		4: 126.5, CH	7.23^c	R4-2/6	
		5: 128.1, CH	7.28^c	R4-2/6, R4-1	
		6: 128.9, CH	7.21^c	R4-β, R4-3/5, R4-4	
R5 Pro	CO	170.9, C			
	α	63.4, CH	4.28 (m)	R5-β, R5-γ, R5-CO	
	β	27.0, CH$_2$	2.09 (m); 1.80 (m)	R5-α, R5-γ, R5-δ	
	γ	24.3, CH$_2$	1.91 (m); 1.83 (m)	R5-α, R5-β, R5-δ	
	δ	46.4, CH$_2$	3.58 (m); 3.35 (m)	R5-α, R5-β, R5-γ	R4-α, R4-NH
R6 Pro	CO	171.5, C		R6-β, R6-CO	
	α	63.1, CH	4.26 (m)	R6-α, R6-γ, R6-δ	R7-NH
	β	28.7, CH$_2$	2.29 (m); 1.42 (m)	R6-α, R6-β, R6-δ	
	γ	25.7, CH$_2$	1.73 (m); 1.45 (m)	R6-α, R6-β, R6-γ	
	δ	46.5, CH$_2$	3.23 (m); 2.17 (m)	R6-β	R7-NH
R7 Leu	NH		7.66 (d, 9.6)	R7-α, R7-β, R6-CO	R6-α, R6-δ, DAA-NH
	CO	171.8, C			
	α	50.2, CH	4.62 (dt, 10.1, 3.9)	R7-β, R7-γ, R7-CO	DAA-NH, C1-NH
	β	40.1, CH$_2$	1.93 (m); 1.67 (m)	R7-α, R7-γ, R7-δ, R7-δ', R7-CO	
	γ	24.4, CH	1.72 (m)	R7-α, R7-β, R7-δ, R7-δ'	
	δ	21.0, CH$_3$	0.94 (d, 6.7)	R7-β, R7-γ, R7-δ'	
	δ'	22.9, CH$_3$	0.84 (d, 6.2)	R7-β, R7-γ, R7-δ	
C1 Phe	NH		6.17 (d, 7.8)	C1-α, C1-β, DAA-CO	R7-α, C2-NH, DAA-NH
	CO	171.0, C			

	α	54.0, CH	4.42 (td, 7.6, 4.5)	C1-β, C1-1, C1-CO DAA-CO	C2-NH
	β	36.8, CH$_2$	2.93 (m); 2.90 (m)	C1-α, C1-1, C1-2/6, C1-CO	
	Aromatic	1: 136.9, C			
		2: 129.4, CH	7.18[c]	C1-β, C1-3/5, C1-4	
		3: 128.4, CH	7.28[c]	C1-2/6, C1-1	
		4: 126.1, CH	7.15[c]	C1-2/6	
		5: 128.1, CH	7.28[c]	C1-2/6, C1-1	
		6: 129.4, CH	7.18[c]	C1-β, C1-3/5, C1-4	
C2 Ile	NH		7.52 (d, 8.5)	C2-α , C2-β, C1-CO	C1-α, C1-NH, terminal-NH$_2$
	CO	173.1, C			
	α	57.6, CH	3.98 (dd, 8.3, 6.1)	C2-β, C2-γ, C2-γ', C2-CO, C1-CO	terminal-NH$_2$
	β	36.0, CH	1.73 (m)	C2-α, C2-γ, C2-γ', C2-δ	
	γ	23.8, CH$_2$	1.29 (m); 1.10 (m)	C2-α, C2- β, C2-γ', C2-δ	
	γ'	15.9, CH$_3$	0.77 (t, 7.3)	C2-α, C2-β, C2-γ	
	δ	11.0, CH$_3$	0.76 (d, 6.8)	C2-β, C2-γ	
	NH$_2$		7.04 (brs); 6.95 (br)s	C2-α, C2-CO	C2-α, C2-NH

[a] Data extracted from HSQC and HMBC spectra. [b] Sequential NOEs. [c] Signal overlap prevents determination of couplings

Figure 3.20: Structure revision of callyaerin F (**21**)
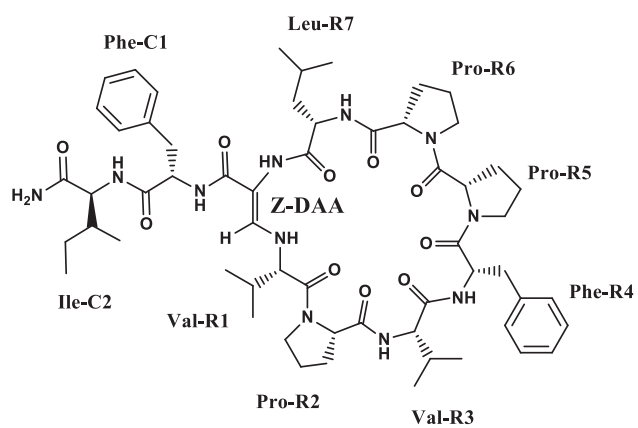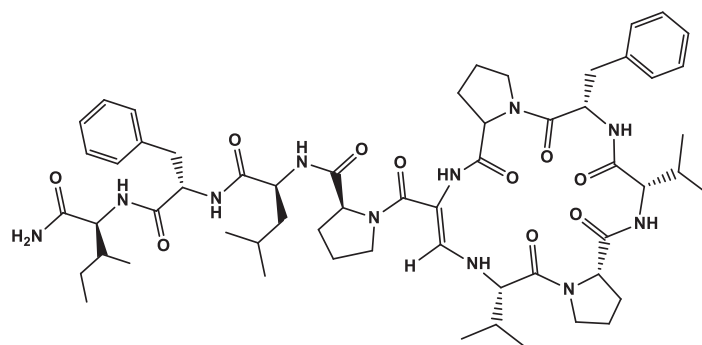
3.2.12. Callyaerin G (22, known natural product)

Callyaerin F	
Sample code	G4-12
Biological source	*Callyspongia aerizusa*
Sample amount	5.0 mg
Physical description	white amorphous powder
Molecular formula	$C_{58}H_{84}N_{11}O_{10}$
Molecular weight	1094.0 g/mol
Optical rotation $[\alpha]_D^{20}$	-32 (*c* 0.15, MeOH)

Compound **22** was obtained as a white amorphous solid. The MALDI-TOF-MS spectrum showed a prominent ion peak at *m/z* 1117.0 [M+Na]$^+$, suggesting a molecular weight of 1094 g/mol. The peptidic nature of **22** was evident from the abundance of signals in the amide NH region (δ_H 7.96-5.32), from the α-amino protons (δ_H 4.63-3.41) in the ^{1}H NMR spectrum and from the presence of carbonyl carbons (δ_C 174.1-168.3), as deduced from the HMBC spectrum. Interpretation of the COSY and TOCSY spectra allowed the assignment of eleven spin systems consisting of Leu (2X), Pro (5X), Phe (3X), and Gly. The presence of the DAA unit was evident from the ^{1}H NMR data at δ_H 8.23 (brs, NH) and δ_H 7.46 (d, *J* = 13.9 Hz, β-H). Two downfield singlet signals at δ 7.03 and 7.11 were assigned to the terminal NH$_2$ group (Daletos *et al.*, 2015).

The obtained UV, NMR and mass spectral data were identical to those reported for callyaerin G, which was previously isolated from *C. aerizusa* (Ibrahim *et al.*, 2008). Due to the insufficient material available to record heteronuclear NMR spectra, callyaerin G had earlier been deduced only based on sequence correlations in the ROESY spectra (Ibrahim et. al. 2008). However, re-isolation of this compound in the present study afforded sufficient amounts for further NMR measurements that prompted us to reconsider its structural assignments (Daletos *et al.*, 2015).

Key ROESY correlations between Pro^{C1}-Hα/Pro^{C2}-Hα, Pro^{C2}-Hα/Phe^{C3}-NH, and Phe^{C3}- Hα/Gly^{C4}-NH, as well as between Phe^{C3}-NH/Gly^{C4}-NH/terminal NH$_2$ disclosed the nature of the linear side chain as Pro^{C1}-Pro^{C2}-Phe^{C3}-Gly^{C4}-NH$_2$. This was supported by HMBC correlations between terminal NH$_2$/Gly^{C4}-CO (δc 171.1), Gly^{C4}-NH/Phe^{C3}-CO (δc 170.9), and Phe^{C3}-NH/Pro^{C2}-CO (δc 171.0) (Daletos *et al.*, 2015).

Additional ROESY correlations were observed between Leu^{R1}-NH/DAA-NH/Leu^{R7}-NH, and Phe^{R3}/Phe^{R4} corresponding to the peptide fragments Leu^{R1}-DAA-Leu^{R7} and Phe^{R3}-Phe^{R4}, respectively. Moreover, careful inspection of the ROESY correlations between Leu^{R1}-Hα, Phe^{R3}-NH/Pro^{R2}-Hα; Phe^{R4}-NH/Pro^{R5}-Hδ; and Leu^{R7}-NH/Pro^{R6}-Hα, Pro^{R6}-Hβ connected these two fragments, and accordingly the cyclic part of **4** was determined as *cyclo*(DAA-Leu^{R1}-Pro^{R2}-Phe^{R3}-Phe^{R4}-Pro^{R5}-Pro^{R6}-Leu^{R7}). The HMBC correlations of DAA-NH/Leu^{R7}-CO, Leu^{R7}-NH/Pro^{R6}-CO, Phe^{R4}-NH/Phe^{R3}-CO, and Phe^{R3}-NH/Pro^{R2}-CO corroborated the interpretation of the ROESY spectrum. Thus, the structure of **22** should be revised according to Figure

3.21, which is in agreement with the fragment ion at *m/z* 879 for [M-(2Pro+Phe+Gly)]$^+$ observed in the ESI mass spectrum (Daletos *et al.*, 2015).

**Table 3.16:** NMR data of **22** at 700 (^{1}H) and 126 (^{13}C) MHz (DMSO-*d$_6$*, δ in ppm)

unit	position	δc[a], type	δ$_H$ (*J* in Hz)	HBMC	ROESY[b]
DAA	NH		8.23 (brs)	DAA- α, R7-CO	C1-δ, R7-α, R7-β, R7-NH, R1-NH, DAA-β
	CO	168.0, C			
	α	98.0, C			
	β	145.3, CH	7.46 (d, 13.9)	R1-α, DAA-α, DAA-CO	R1-α, R1-NH
R1 Leu	NH		5.30 (dd, 13.9, 10.0)		DAA-β, DAA-NH
	CO	173.3, C			
	α	57.7, CH	4.27[c]	R1-β, R1-γ, DAA-β, R1-CO	R2-Hα, R2-Hδ
	β	42.0, CH$_2$	1.62 (m); 1.08 (m)		
	γ	23.3, CH	1.33 (m)		
	δ	23.3, CH$_3$	0.53 (d, 6.7)	R1-β, R1-γ, R1-δ'	
	δ'	20.2, CH$_3$	0.37 (d, 6.4)	R1-β, R1-γ, R1-δ	
R2 Pro	CO	172.2, C			
	α	63.0, CH	3.94[c]	R2-β, R2-γ, R2-CO	R1-Hα, R3-NH
	β	28.7, CH$_2$	2.10 (m); 1.59 (m)	R2-α, R2-CO,	R3-NH
	γ	24.9, CH$_2$	2.01 (m); 1.84 (m)		
	δ	46.0, CH$_2$	3.92 (m); 3.49 (m)	R2-α, R2-β	R1-Hα, R3-NH
R3 Phe	NH		7.71 (d, 6.8)	R3-β, R2-CO	R2-α, R2-β, R2-δ, R4-NH
	CO	170.7, C			
	α	53.8, CH	4.22[c]		R4-NH
	β	35.2, CH$_2$	2.86 (m)	R3-α, R3-1, R3-2/6, R3-CO	
	Aromatic	1: 138.3, C			
		2: 128.5, CH	7.12 (brd, 7.2)	R3-β, R3-4	
		3: 128.1, CH	7.25 (brt, 7.2)	R3-1	
		4: 126.5, CH	7.19 (brt, 7.2)	R3-2/6, R3-3/5	
		5: 128.1, CH	7.25 (brt, 7.2)	R3-1	
		6: 128.5, CH	7.12 (brd, 7.2)	R3-β, R3-4	
R4 Phe	NH		7.21[c]	R4-α, R4-β, R3-CO	R3-NH, R5-δ
	CO	169.6, C			
	α	52.3, CH	4.63 (q, 7.1)	R4-β, R4-CO	R5-δ
	β	36.4, CH$_2$	2.96 (m); 2.66 (dd, 13.4, 4.7)	R4-α, R4-CO, R4-1, R4-2/6	
	Aromatic	1: 137.7, C			
		2: 129.2, CH	7.18 (brd, 7.2)	R4-β, R4-3/5, R4-4	
		3: 128.1, CH	7.25 (brt, 7.2)	R4-1	
		4: 126.6, CH	7.22 (brt, 7.2)	R4-2/6	
		5: 128.1, CH	7.25 (brt, 7.2)	R4-1	
		6: 129.2, CH	7.18 (brd, 7.2)	R4-β, R4-3/5, R4-4	
R5 Pro	CO	171.7, C			
	α	63.5, CH	4.41 (dd, 9.8, 7.9)	R5-β, R5-CO	
	β	26.5, CH$_2$	2.15 (m); 1.83 (m)	R5-γ, R5-δ	
	γ	24.0, CH$_2$	1.92 (m); 1.90 (m)	R5-α, R5-β	
	δ	46.1, CH$_2$	3.45 (m); 3.38 (m)	R5-α, R5-β, R5-γ	R4-NH, R4-α

R6 Pro	CO	171.4, C			
	α	62.5, CH	4.24 (dd, 10.1, 7.4)	R6-β, R6-CO	R7-NH
	β	28.5, CH₂	2.28 (m); 1.48 (m)	R6-γ, R6-CO	R7-NH
	γ	25.4, CH₂	1.78 (m); 1.67 (m)	R6-δ	
	δ	46.5, CH₂	3.40 (m); 2.74 (td, 10.3, 6.2)	R6-α, R6-β, R6-γ	R7-NH
R7 Leu	NH		7.51 (d, 10.1)	R7-α, R6-CO	R6-α, R6-β, R6-δ, DAA-NH
	CO	171.9, C			
	α	50.0, CH	4.46 (dt, 10.1, 3.8)	R7-β, R7-γ, R7-CO	DAA-NH
	β	40.0, CH₂	1.92 (m); 1.75 (m)	R7-α, R7-γ, R7-CO	DAA-NH
	γ	24.2, CH	1.75 (m)	R7-α, R7-δ, R7-δ'	
	δ	20.6, CH₃	0.86 (d, 6.5)	R7-β, R7-γ, R7-δ'	
	δ'	22.7, CH₃	0.83 (d, 6.2)	R7-β, R7-γ, R7-δ	
C1 Pro	CO	171.9, C			
	α	64.0, CH	4.34 (dd, 9.8, 7.9)	C1-β, C1-CO, DAA-CO	C2-α, C2-δ
	β	26.1, CH₂	2.08 (m); 1.83 (m)	C1-α, C1-CO	
	γ	25.4, CH₂	1.95 (m); 1.78 (m)	C1-β	
	δ	45.9, CH₂	3.86 (m); 3.36 (m)	C1-β, C1-γ, C1-CO	DAA-NH
C2 Pro	CO	171.0, C			
	α	61.4, CH	4.11 (dd, 10.0, 7.5)	C2-γ, C2-CO	C1-α, C3-NH
	β	27.7, CH₂	1.89 (m); 1.06 (m)	C2-γ	
	γ	24.8, CH₂	1.69 (m)		
	δ	47.4, CH₂	3.84 (m); 3.37 (m)	C2-β, C2-γ	C1-α, C3-NH
C3 Phe	NH		7.67 (d, 7.0)	C3-α, C2-CO	C2-α, C2-δ, C4-NH
	CO	170.9, C			
	α	54.5, CH	4.23[c]	C3-β, C3-CO	C4-NH
	β	37.0, CH₂	3.23 (dd, 13.4, 2.7); 2.92 (m)	C3-α, C3-CO, C3-1, C4-2,6	
	Aromatic	1: 138.3, C			
		2: 130.0, CH	7.35 (brd, 7.2)	C3-β, C3-4	
		3: 128.1, CH	7.25 (brt, 7.2)	C3-1	
		4: 125.9, CH	7.17 (brt, 7.2)	C3-2/6, C3-3/5	
		5: 128.1, CH	7.25 (brt, 7.2)	C3-1	
		6: 130.0, CH	7.35 (brd, 7.2)	C3-β, C3-4	
C4 Gly	NH		7.96 (dd, 7.9, 5.0)	C3-CO	C3-NH, Terminal-NH₂
	CO	171.1, C			
	α	41.9, CH₂	3.91 (dd, 17.2, 7.9); 3.41 (dd, 17.2, 5.0)	C4-CO	Terminal-NH₂
	NH₂		7.12 (brs); 7.11 (brs)	C4-α, C4-CO	C4-α, C4-NH

[a] Data extracted from HSQC and HMBC spectra. [b] Sequential NOEs. [c] Signal overlap prevents determination of couplings

Figure 3.21: Structure revision of callyaerin G (**22**)
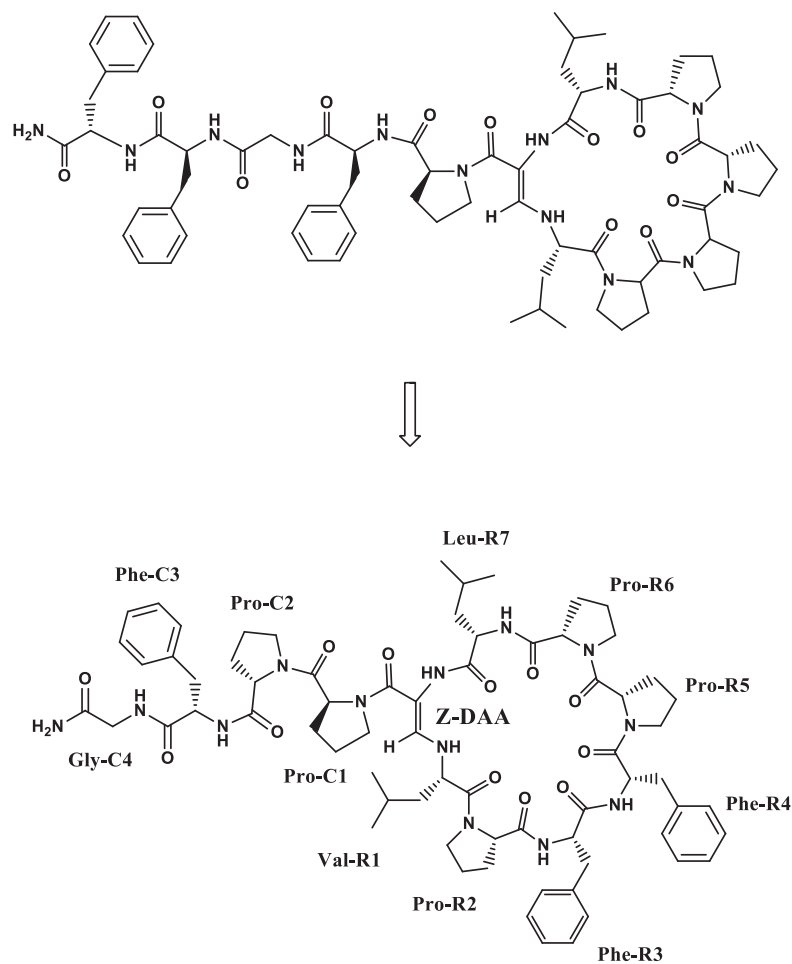
3.2.13. Bioactivity of compounds isolated from the marine sponge *C. aerizusa*

The new callyaerin derivatives **11 ─ 15**, together with the known derivatives callyaerin A (**16**), B (**17**), C (**18**), D (**19**), E (**20**), F (**21**), and G (**22**), were assayed *in vitro* against *M. tuberculosis* (Figure 3.22). Compounds **16** and **17** showed pronounced anti-TB activity with MIC_{90} values of 2 and 5 μM, respectively. Compound **18** was found to be less active with an MIC_{90} value of 40 μM (Table 3.17). The remaining congeners were inactive ($MIC_{90} > 100$ μM) in this assay (Daletos *et al.*, 2015).

All callyaerin derivatives were further assayed for their cytotoxicity toward THP-1 and MRC-5 cell lines (Figure 3.22). Compound **16**, which showed the strongest anti-TB activity, exhibited only low cytotoxicity against the two cell lines with IC_{50} values of 20 or 30 μM for THP-1 or MRC-5 cells, respectively that are at least 10-fold above the MIC_{90} (Table 3.17). Compound **17**, which was the second best inhibitor of *M. tuberculosis* growth, exhibited moderate activity towards the two cell lines studied. While **11** exhibited a low cytotoxicity profile similar to **16**, the remaining compounds showed weak cytotoxic activity only at concentrations >50 μM (Daletos *et al.*, 2015).

Mtb
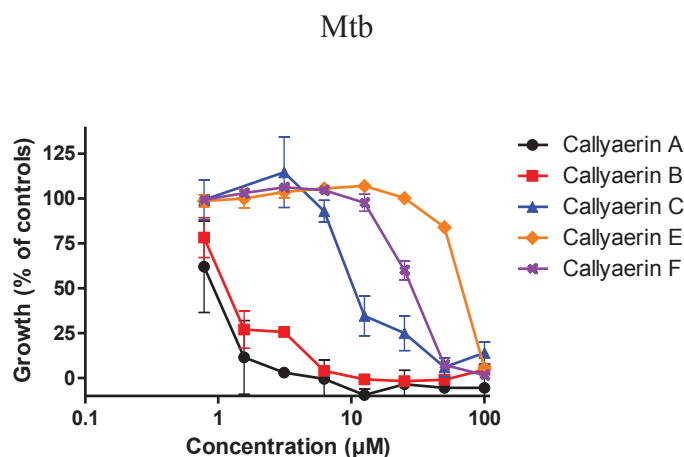
THP-1
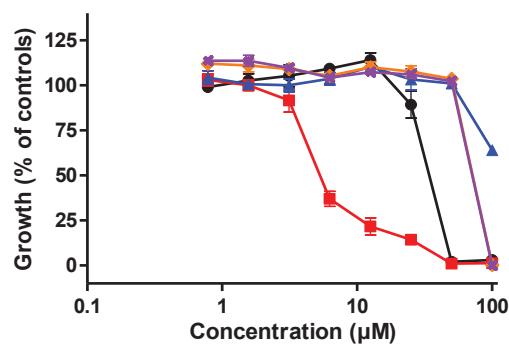
MRC5
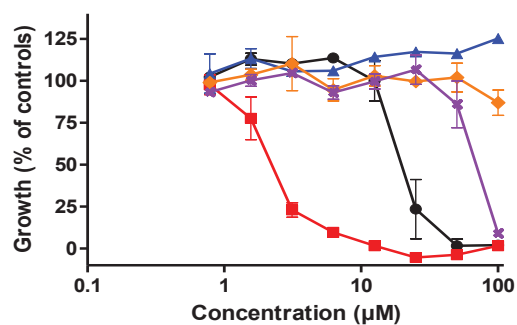
Figure 3.22: Anti-TB and cytotoxic profiles of callyaerins A-C (**16 ─ 18**), E (**20**) and F (**21**). Compounds I-M (**11 ─ 15**), D (**19**) and G (**22**) showed weak or no anti-TB activity at the range of the concentrations analyzed (MIC$_{90}$ >100 μM), and therefore they are not included in the corresponding graphs. Data are means of three independent experiments ± SD (Daletos *et al.*, 2015).

Table 3.17: Anti-TB assay and cytotoxic activities against THP-1 and MRC-5 cell lines of **16 － 18**

	M. tuberculosis		THP-1		MRC-5	
	MIC_{90} (μM)	MIC_{100} (μM)	IC_{50} (μM)	IC_{90} (μM)	IC_{50} (μM)	IC_{90} (μM)
Cal. A (**16**)	2	6	30	50	20	40
Cal. B (**17**)	5	10	5	30	2	6
Cal. C (**18**)	40	100	>100	>100	>100	>100

MIC_{90}: concentration for 90% bacterial growth inhibition

MIC_{100}: concentration for 100% bacterial growth inhibition

IC_{50}: concentration for 50% cell growth inhibition

IC_{90}: concentration for 90% cell growth inhibition

3.3. Isolated compounds from the sponge *Acanthostrongylophora ingens*

In this study, we investigated a specimen of *A. ingens* (class Demospongiae, order Haplosclerida, family Petrosiidae), collected at Ujung Pandang Island, Indonesia, in August 1996, and subsequently identified by Dr. Nicole de Voogd, National Museum of Natural History, Leiden, the Netherlands. The thawed sponge material was cut into small pieces and exhaustively extracted with MeOH (1L x 2) at room temperature. Total methanolic extract of the sponge was subjected to vacuum liquid chromatography (VLC) on silica gel using a stepwise gradient system from 100% n-Hexane to 100 % EtOAc, and from 100% DCM to 100% MeOH. Each fraction was purified by column chromatography using silica gel 60M and Sephadex LH-20 as stationary phases and MeOH as a mobile phase followed by semi-preparative reversed phase HPLC (C18 Eurosphere 100) for final purification using an eluting gradient of MeOH:H_2O. This led to the isolation of two known alkaloids, namely, annomontine (**23**) (Leboeuf *et al*., 1982) and 1- hydroxy-3,4-dihydronorharman (**24**) (Roa *et al*., 2003). In this part, the results of the chemical investigation of the secondary metabolites produced by *A. ingens* are presented (Daletos *et al.*, 2015).

3.3.1. Annomontine (23, known natural product)

Annomontine	
Sample code	G3-1
Biological source	*Acanthostrongylophora ingens*
Sample amount	7.0 mg
Physical description	Yellow crystalline solid
Molecular formula	$C_{15}H_{11}N_5$
Molecular weight	261 g/mol
Retention time (HPLC)	26.16 min (standard gradient)

No ionization in (-)-ESI-MS
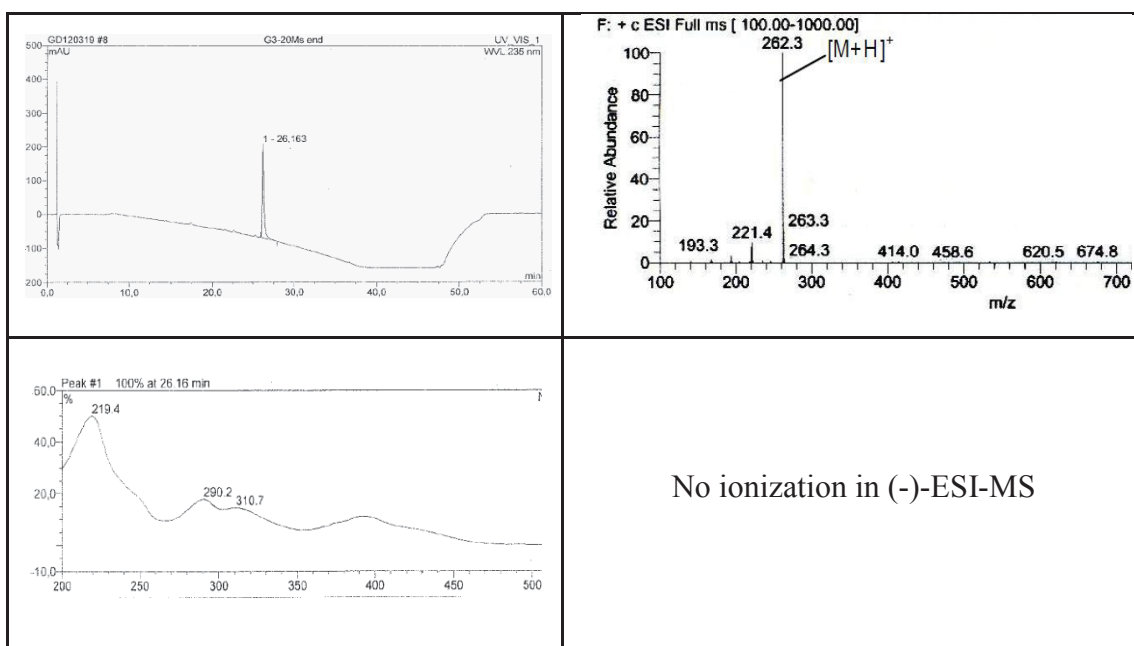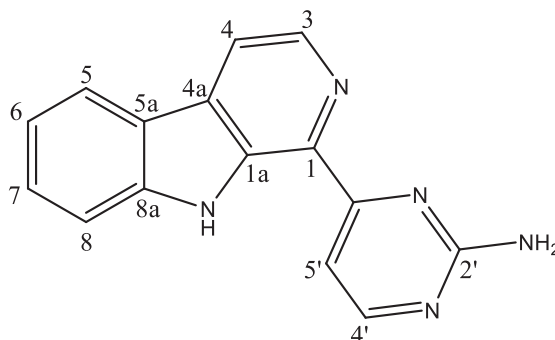
Compound **23** was isolated as a yellow crystalline solid. It has UV absorbances at λmax 229, 289 and 311 nm. It had a molecular weight of 261 g/mol, as derived from the ESIMS measurement that showed the ion peak at *m/z* 262 [M+H]+. The ^{1}H NMR spectrum revealed the presence of a disubstituted phenyl ring, containing four *ortho*-coupled protons at δ 8.31 (d, *J* = 7.9 Hz, H-5), 7.77 (d, *J* = 8.2 Hz, H-8), 7.64 (dt, *J* = 8.2, 0.9 Hz, H-7) and 7.29 (dt, *J* = 7.9, 0.9 Hz, H-6) (Figure 3.23). This ABCD system was corroborated by the COSY spectrum. The second spin system consisted of two downfield proton signals at δ 8.51 (d, *J* = 5.0 Hz, H-3) and 8.29 (*J* = 5.0 Hz, H-4) with a small coupling constant (Figure 3.23), indicating that these two protons are present in a nitrogen-bearing ring system, as found in pyridine. The downfield singlet at δ 11.54 was assigned to an indolic NH group, thus suggesting a β-carboline moiety. Comparison of the ^{1}H and ^{13}C NMR data with literature data (Coune *et al.*, 1980; Leboeuf *et al.*, 1982; Corbally, *et al.*, 2000) indicated the presence of a norharmane structure as found in compound **23**. Proton doublets at δ 8.44 and 7.68 with coupling constants of 5.3 Hz were positioned *ortho* to each other, as also indicated by their COSY correlations, which led to the elucidation of a 2-aminopyrimidine as the second substructure. Therefore, **23** was identified as a β-carboline alkaloid substituted at C-1 by a 2-aminopyrimidine unit, which is known as annomontine. Interestingly, annomontine was originally isolated from the bark of *Annona montana* (family *Annonaceae*) (Leboeuf *et al.*, 1982), which suggests a microbial origin of this class of compounds.
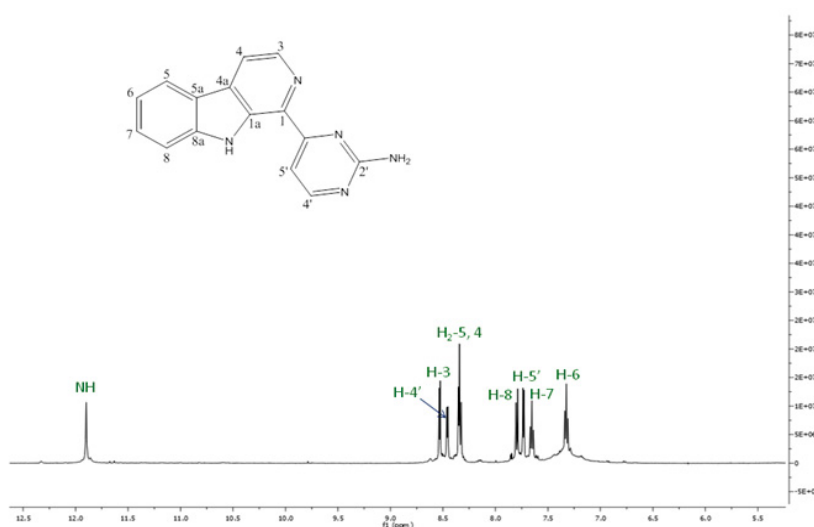
Figure 3.23: ^{1}H NMR spectrum of compound **23**

3.3.2. 1-Hydroxy-3, 4-dihydronorharman (24, known natural product)

1-Hydroxy-3, 4-dihydronorharman	
Sample code	G3-2
Biological source	*Acanthostrongylophora ingens*
Sample amount	2.5 mg
Physical description	Pale yellow amorphous powder
Molecular formula	$C_{11}H_{10}N_2O$
Molecular weight	186 g/mol
Retention time (HPLC)	22.55 min (standard gradient)

No ionization in (-)-ESI-MS
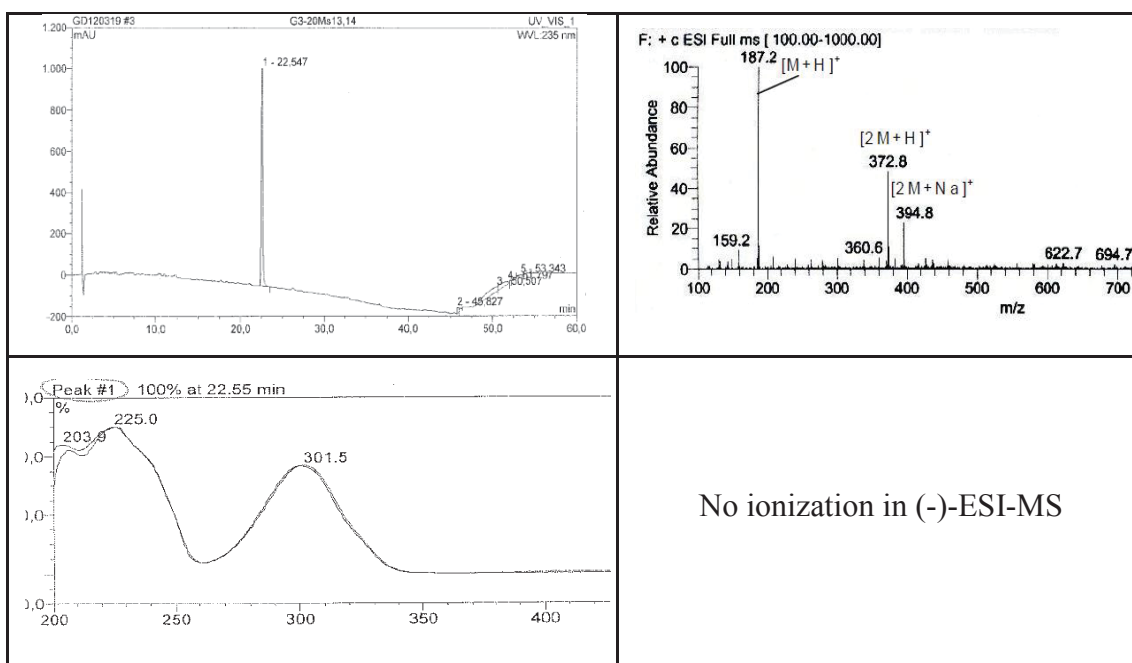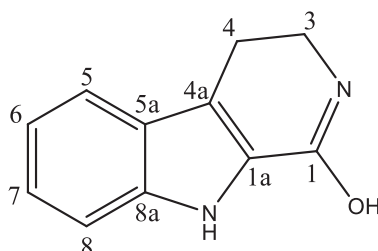
Compound **24** was obtained as a white amorphous powder. It showed UV absorbances at λ_{max} 206, 226, and 300 nm. The (+) ESIMS spectrum exhibited an ion peak at m/z 187 [M+H]$^+$, implying a molecular weight of 186 g/mol. ^{1}H NMR and COSY spectra revealed an exchangeable NH proton resonating at δ_H 7.55 ppm and an aromatic ABCD spin system comprising four protons in the aromatic region at δ_H 7.57 (d, J = 8.2 Hz, H-5), 7.37 (d, J = 8.2 Hz, H-8), 7.20 (dt, J = 8.2, 0.9 Hz, H-7) and 7.04 (dt, J = 8.2, 0.9 Hz, H-6) (Figure 3.24), representing signals for an indole moiety.

In addition, two methylene protons at δ 3.51 (t, J = 6.9 Hz, H2-3) and 2.91 (t, J = 6.9 Hz, H2-4) were positioned adjacent to each other as indicated by the respective COSY correlation, thus suggesting a dihydropyridine moiety attached to the indole ring. The remaining resonance in the ^{1}H NMR spectrum of **24** of an exchangeable proton at δ_H 11.51 was assigned to a hydroxy group (Figure 3.24). Based on these observations, as well as by comparison of the UV, ^{1}H NMR, and MS data with those reported in the literature, **24** was identified as 1-hydroxy-3,4-dihydronorharman (Roa *et al.*, 2003).
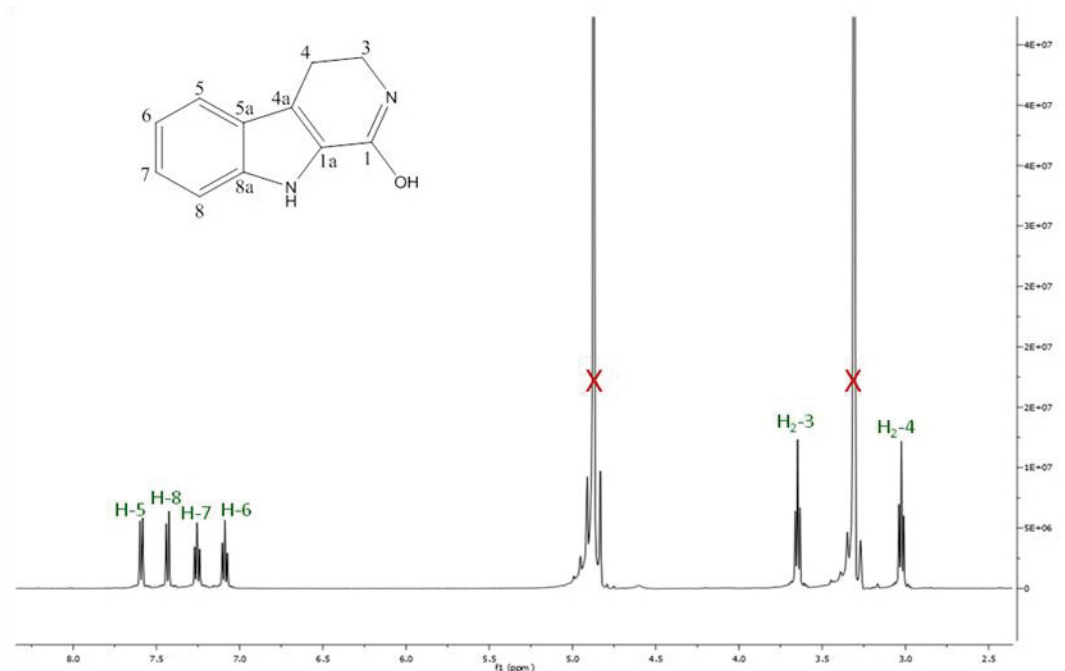
Fig 3.24: ^{1}H NMR spectrum of compound **24**

3.3.3. Bioactivity of compounds isolated from the marine sponge *A. ingens.*

The isolated compounds (**23** and **24**) were tested for their antibacterial activities against the bacterial strains *S. aureus*, *E. coli*, and *P. aeruginosa* (Table 3.18). In addition, the isolated compounds were subjected to bioassays aimed to determine their cytotoxic and protein kinase inhibitory profiles (Table 3.19).

Table 3.18: Antibacterial assay of compounds **23** and **24**:

Name	*E. Coli* MIC (µg/ml)	*S. aureus* MIC (µg/ml)	*P. aeruginosa* MIC (µg/ml)
Annomontine (**23**)	—	64	—
1-Hydroxy-3, 4-dihydronoharman (**24**)	—	—	—

Table 3.19: Residual activity (in %) of a panel of 7 different kinases for compounds **23** and **24** at concentrations of 10 µM.

Compound	Aurora B	AXL	FAK	MEk1-wt	PIM1	PRK1	VEGF-R2
Annomontine (**23**)	62	74	80	78	29	71	72
1-Hydroxy-3, 4-dihydronoharman (**24**)	72	90	90	86	96	97	85

3.4. Isolated compounds from the sponge *Sarcotragus spinosulus*

In this study, we investigated a specimen of *S. spinosulus* (class Demospongiae, order Haplosclerida, family Petrosiidae), collected in Fethiye, Turkey. Total methanolic extract of the sponge was subjected to liquid-liquid partition technique against n-Hexane, EtOAc, and BuOH. The bioactive EtOAc fraction was subjected to consecutive column chromatography on Sephadex LH-20, using MeOH as a mobile phase. Further purification was achieved by semi-preparative reversed phase HPLC (C18 Eurosphere 100) using an eluting gradient of MeOH:H_2O to yield a 3:1 mixture of two known linear sesterterpenes ircinin-1 and ircinin-2. The structures of the isolated compounds were unambiguously elucidated based on 1D- and 2D-NMR spectroscopy and mass spectrometry, as well as by comparison with the literature (Daletos *et al.*, 2014, 2015). In this part, we report the results of the chemical investigation of the secondary metabolites produced by *S. spinosulus*, as well as bioassay results employing the L5178Y mouse lymphoma cell line and a panel of protein kinases.

3.4.1. Ircinin-1 (25, known natural product)

Ircinin-1	
Sample code	B6-sp2
Biological source	*Sarcotragus spinosulus*
Sample amount	2.5 mg
Physical description	Light yellow oil
Molecular formula	$C_{25}H_{29}O_5$
Molecular weight	410 g/mol
Optical rotation $[\alpha]_D^{20}$	+32.3 (*c* 0.05, MeOH)

3.4.2. Ircinin-2 (26, known natural product)

Ircinin-2	
Sample code	B6-sp2
Biological source	*Sarcotragus spinosulus*
Sample amount	2.5 mg
Physical description	Light yellow oil
Molecular formula	$C_{25}H_{29}O_5$
Molecular weight	410 g/mol
Optical rotation $[\alpha]_D^{20}$	+32.3 (*c* 0.05, MeOH)

Compounds (**25**) and (**26**) were isolated as an inseparable mixture (3:1). The EI-MS of **25** and **26** showed an ion peak at *m/z* 410 [M]$^+$. The carbon skeletons of **25** and **26** were established as bisfuranoditerpenes by analysis of the UV, ^{1}H and COSY spectra. Accordingly, the ^{1}H NMR spectrum revealed signals attributable to three α protons (δ_H 7.29, 7.22, and 6.99) and two β protons (δ_H 6.25, 5.78) of the furan ring, suggesting the existence of both a β-substituted and an α-disubstituted furan rings. A vinylic proton (δ_H 5.14, t, *J* = 6.6 Hz) and a vinylic methyl (δ_H 1.52) suggested the presence of a trisubstituted double bond. In addition, the ^{1}H NMR spectrum showed six distinct methylenes; a singlet at δ_H 3.70 (s, H-5), a triplet at δ_H 2.37 (H-10, t, *J* = 7.5 Hz), and four multiplets at δ_H 2.20, 1.99, 1.36, and 1.29 (H-11, 15, 16, and 17, respectively). The COSY spectrum showed long range correlations between the singlet at δ_H 3.70, the two β protons (δ_H 6.25 and 5.78) and the α-proton (δ_H 7.29) of the furan rings, thus indicating that the rings are linked to each other by a methylene group (CH$_2$-5). Moreover, the ^{1}H-NMR signals of a vinylic proton at δ_H 5.28 (H-20, d, *J* = 10.2 Hz) and a singlet vinylic methyl at δ_H 1.74, indicated the presence of a conjugated tetronic acid moiety.

On comparison of the different intensities in the ^{1}H-NMR spectrum as well as by analysis of the COSY spectral data, two sets of individual data corresponding to each isomer could be delineated. In the first set of correlations, the COSY spectrum showed a spin system composed of a vinyl methine (CH-12), and two methylene groups (CH$_2$-10 and CH$_2$-11). However, in the second set of data, the COSY spectrum allowed us to establish a long spin system within the molecule starting from a vinyl methine (CH-15) and sequentially extending until CH-20. These data suggested that the two isomers differ at the position of the central double bond (C12/13 and C13/15), which were in accordance with the values reported for the known linear sesterterpenes ircinin-1 and ircinin-2, respectively (Cimino *et al.* 1971). The absolute configuration of C-18 was determined to be *R* on the basis of the positive [α]$_D$ value of compounds **25** and **26** (3:1) (+32.3 *c* 0.05, MeOH).

3.4.3. Bioactivity of compounds isolated from the marine sponge *S. spinosulus*

The 3:1 mixture of ircinin-1 (**25**) and ircinin-2 (**26**) was subjected to bioassays aimed to determine the cytotoxicity and the protein kinase inhibitory profiles of these compounds. Interestingly, ircinin-1,2 (3:1) proved to be highly active against ALK, AXL, FAK, IGF1-R, SRC, and VEGF-R2 kinases (Table 3.20), whereas it showed only weak cytotoxicity toward the mouse lymphoma cell line L5178Y (16.6% inhibition at a dose of 10 μg/ml) as well as toward the human ovarian cancer A2780 sens (cisplatin-sensitive) and A2780 CisR (cisplatin-resistant) cell lines (Figure 3.25). The bioactivity test results are shown below:

Ircinin-1,2 (3:1):
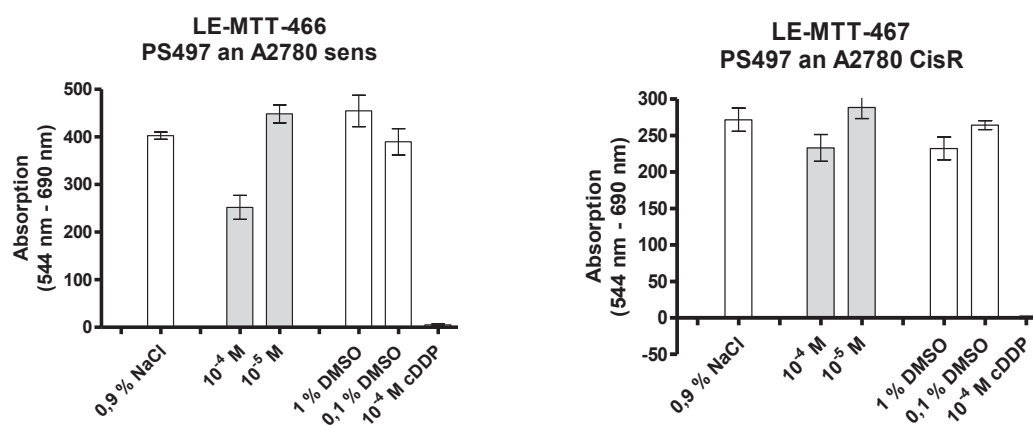
Figure 3.25: Cytotoxicity of ircinin-1,2 (3:1) against A2780 (sens and CisR) cell lines

Table 3.20: Residual activity (in %) of a panel of 16 kinases for **ircinin 1,2 (3:1)** at 10 μM

							IC$_{50}$ [μM]								
AKT1	ALK	ARK5	Aurora-B	AXL	FAK	IGF1-R	MEK1 wt	MET wt	NEK2	NEK6	PIM1	PLK1	PRK1	SRC	VEGF-R2
100	0	70	45	1	2	0	100	75	63	77	95	82	97	0	0

3.5. Isolated compounds from the sponge *Dysidea avara*

In this study, we investigated a specimen of *D. avara* (class Demospongiae, order Dictyoceratida, family Dysideidae), collected in Ayvalic, Turkey. Total methanolic extract of the sponge was subjected to liquid-liquid partition technique against n-Hexane, EtOAc, and BuOH. The bioactive EtOAc fraction was further subjected to consecutive column chromatography using Sephadex LH-20 as stationary phase and MeOH as a mobile phase. Further purification was achieved by semi-preparative reversed phase HPLC (C18 Eurosphere 100) using an eluting gradient of MeOH:H_2O. This led to the isolation of two known sesquiterpene quinols/quinones, namely, avarol (**23**) and avarone (**24**) (Minale *et al.*, 1974). In this part, the isolation and structure elucidation of the secondary metabolites produced by *D. avara* is presented, as well as results from different bioassays, including cytotoxicity (MTT), antibacterial and *in vitro* protein kinase assays (Daletos *et al.*, 2014).

3.5.1. Avarol (27, known natural product)

Avarol	
Sample code	B23-1
Biological source	*Dysideas avara*
Sample amount	2.0 mg
Physical description	White amorphous solid
Molecular formula	$C_{21}H_{30}O_2$
Molecular weight	314 g/mol
Optical rotation $[\alpha]_D^{20}$	+10.8 (*c* 0.1, $CHCl_3$)
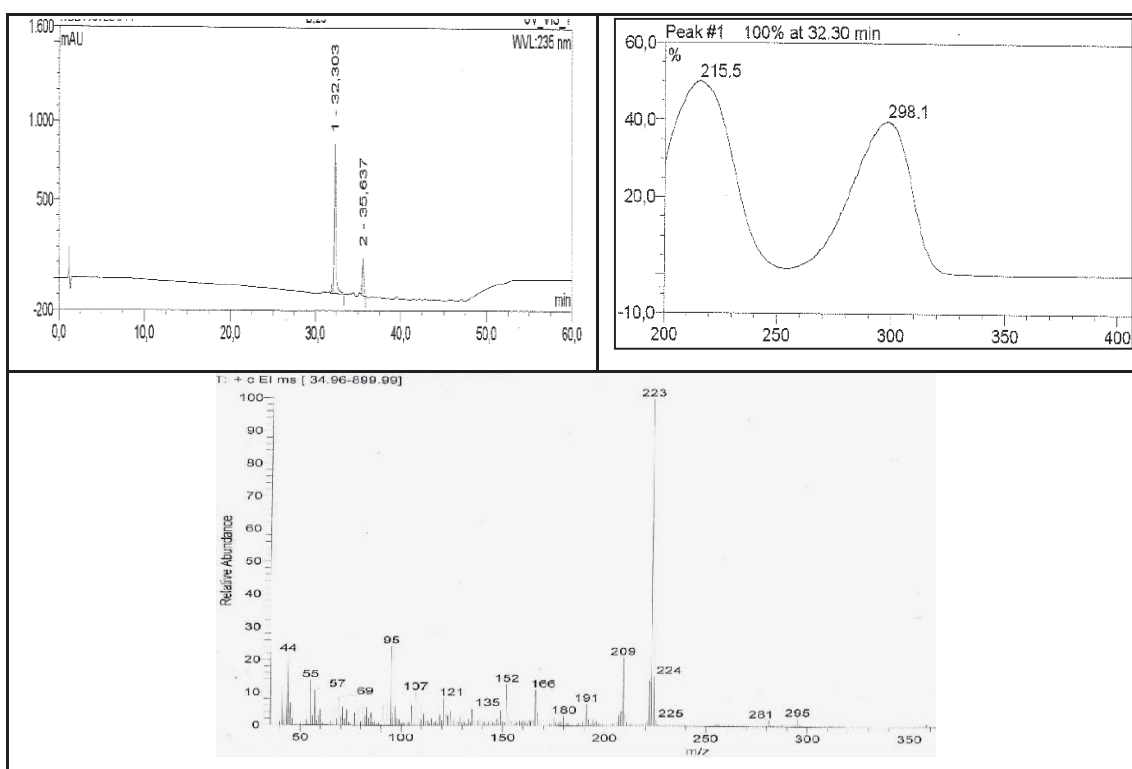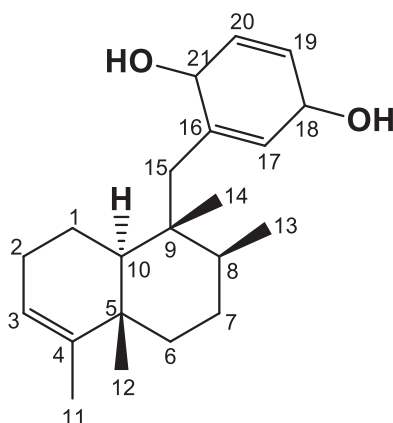
Compound **27** was obtained as a white amorphous solid. It displayed UV absorbances at λ_{max} 215 and 298 nm. The EIMS showed molecular ion peak at m/z 314 $[M]^+$ indicating a molecular weight of 314 g/mol. The NMR spectral data revealed two substructures consisting of a sesquiterpene and a trisubstituted benzene moiety. The ^{1}H NMR chemical shifts corresponding to the sesquiterpene substructure indicated among others the presence of an olefinic methyl group at δ_H 1.51 ppm (H$_3$-11), a secondary methyl group split to a doublet at δ_H 1.00 (3H, d, J = 6.6 Hz, H$_3$-13), and two tertiary methyl signals at δ_H 1.02 and 0.86 ppm (H$_3$-12 and H$_3$-14, respectively). In addiditon, the COSY spectrum of **8** comprised two continuous spin systems, CH(10)CH$_2$(1)CH$_2$(2)CH(3) and CH$_2$(6)CH$_2$(7)CH(8)CH$_3$(13), indicative of a *trans*-4,9-friedodrim-3-ene subunit. The remaining signals in the ^{1}H NMR spectrum of **27** (Table 3.21) showed an ABX spin system, including a doublet of doublets at δ_H 6.55 (1H, dd, J = 1.5, 8.2 Hz), and two doublets at δ_H 6.60 (1H, d, J = 8.2 Hz) and δ_H 6.57 (1H, d, J = 1.5 Hz), thus suggesting the presence of a 1,2,5- trisubstituted benzene ring. The structure of **27** was further confirmed by comparison of its spectroscopic data (UV, MS, and ^{1}H NMR) with those reported for avarol (Minale *et al.*, 1974).

3.5.2. Avarone (28, known natural product)
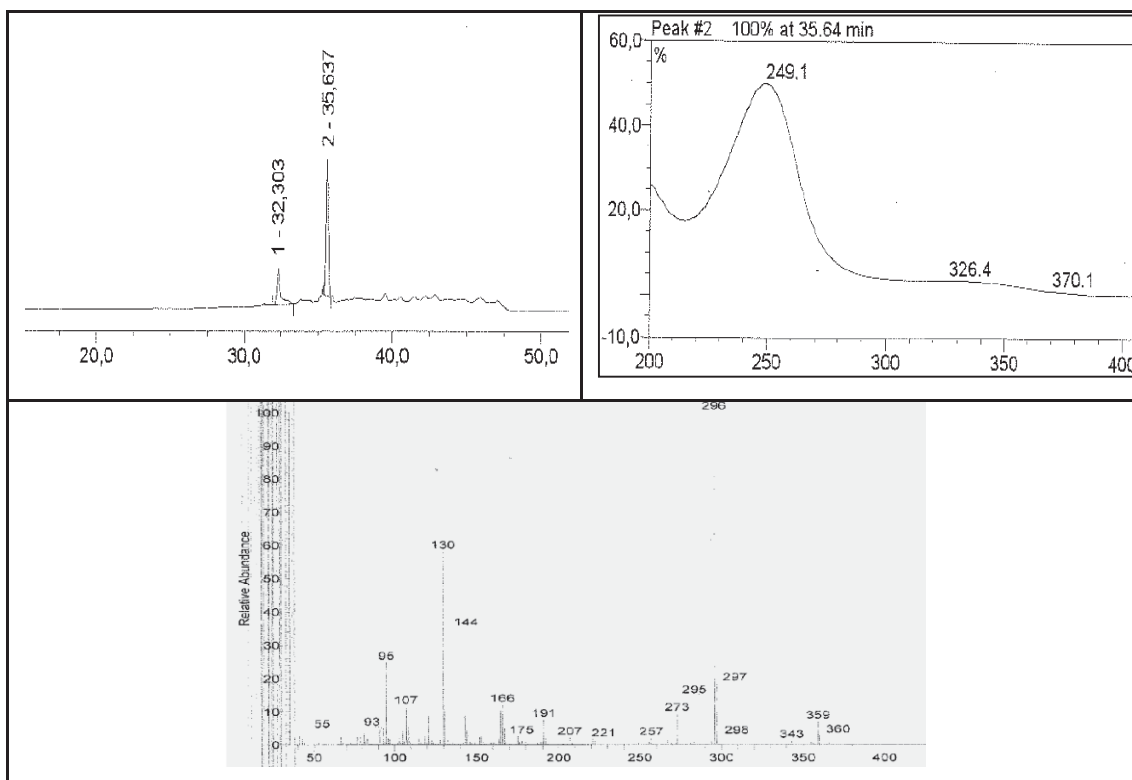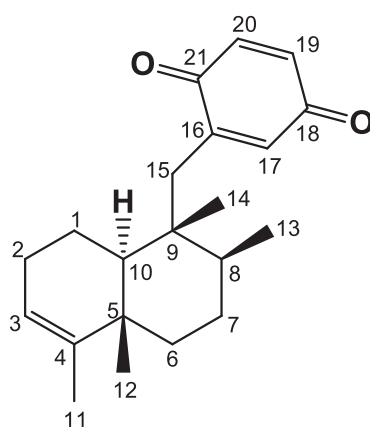
Avarone	
Sample code	B23-2
Biological source	*Dysideas avara*
Sample amount	0.5 mg
Physical description	Purple amorphous solid
Molecular formula	$C_{21}H_{28}O_2$
Molecular weight	312 g/mol

Compound **28** was obtained as a white amorphous solid. The UV spectrum, revealing absorbances at λ_{max} 326 and 490 nm, suggested the presence of a quinone chromophore in the molecule. The EIMS showed molecular ion peak at m/z 313 [M +H]$^+$ indicating a molecular weight of 312 g/mol. The[1]H NMR spectrum of **2** (Table 3.21) was similar to that of **1**, except for the marked downfield shifts observed for H-19 and H-20 resonating at δ_H 6.75 and 6.70, respectively. The above spectral differences suggested that **28** is the quinone analogue of avarol (**27**), which accounts for the 2 amu molecular weight difference between both compounds. From the above data and by comparison with the literature, compound **28** was identified as avarone (Minale *et al.*, 1974).

Table 3.21: ^{1}H NMR data of **27** and **28** at 600 MHz (CDCl$_3$)

Nr.	27	28
	δ_H (*J* in Hz)	δ_H (*J* in Hz)
3	5.14 (1H, br s)	5.13 (1H, br s)
11	1.51 (3H, br s)	1.53 (3H, br s)
12	1.02 (3H, s)	1.00 (3H, s)
13	1.00 (3H, d, *J* = 6.6 Hz)	0.93 (3H, d, *J* = 6.6 Hz)
14	0.86 (3H, s)	0.85 (3H, s)
15a	2.56 (1H, d, *J* = 14.2 Hz)	2.43 (1H, d, *J* = 13.4 Hz)
15b	2.67 (1H, d, *J* = 14.2 Hz)	2.64 (1H, d, *J* = 13.4 Hz)
17	6.57 (1H, d, *J* = 1.5 Hz)	6.51 (1H, d, *J* = 2.5 Hz)
19	6.55 (1H, dd, *J* = 1.5, 8.2 Hz)	6.70 (1H, dd, *J* = 2.5, 10.1 Hz)
20	6.60 (1H, d, *J* = 8.2 Hz)	6.75 (1H, d, *J* = 10.1 Hz)

3.5.3. Bioactivity of compounds isolated from the marine sponge *D. avara.*

The isolated compounds (**27** and **28**) were tested for their antibacterial activities against several bacterial strains (Table 3.22). In addition, the isolated compounds were subjected to bioassays aimed to determine their cytotoxic (Table 3.23) and protein kinase inhibitory profiles (Table 3.24).

Table 3.22: Antibacterial assay of compounds **27** and **28**

Name	MRSA MIC (µg/ml)	*S. pneumonia* MIC (µg/ml)	*E. faecalis* MIC (µg/ml)	*E. Coli* MIC (µg/ml)
Avarol (**27**)	3.91	3.91	3.91	-
Avarone (**28**)	7.81	7.81	3.91	-

Table 3.23: Cytotoxic activity of **27**

Name	% Growth of L5178Y (10µg/ml)
Avarol (**27**)	6.2

Table 3.24: Residual activity (in %) of a panel of 16 kinases for **27** at 10 µM

							IC_{50} [*µM*]								
AKT1	ALK	ARK5	Aurora-B	AXL	FAK	IGF1-R	MEK1 wt	MET wt	NEK2	NEK6	PIM1	PLK1	PRK1	SRC	VEGF-R2
100	92	100	19	70	100	54	100	45	70	100	100	100	100	100	100

3.6. Isolated compounds from the sponge *Agelas oroides*

In this study, we investigated a specimen of *A. oroides* (class Demospongiae, order Agelasida, family Agelasidae), collected in Ayvalic, Turkey. The bioactive EtOAc fraction was subjected to consecutive column chromatography on Sephadex LH-20, using MeOH as a mobile phase. Further purification was achieved by semi-preparative reversed phase HPLC (C18 Eurosphere 100) using an eluting gradient of MeOH:H_2O to yield a known bromopyrrole compound. The structure of the isolated compound was unequivocally determined on the basis of NMR spectroscopy and mass spectrometry (ESIMS), as well as by comparison with the literature. In this part, we report the structure elucidation of the bromopyrrole secondary metabolite produced by *A. oroides*, as well as results from different bioassays, including cytotoxicity (MTT) and antibacterial assays (Daletos *et al.*, 2014).

3.6.1. 4,5-Dibromo-1*H*-pyrrole-2-carboxylic acid (29, known natural product)

4,5-Dibromo-1*H*-pyrrole-2-carboxylic acid	
Sample code	B10-1
Biological source	*Agelas oroides*
Sample amount	4.0 mg
Physical description	White amorphous solid
Molecular formula	$C_5H_3{}^{79}Br_2NO_2$
Molecular weight	267 g/mol
Optical rotation $[\alpha]_D^{20}$	-

No ionization in (+)-ESI-MS
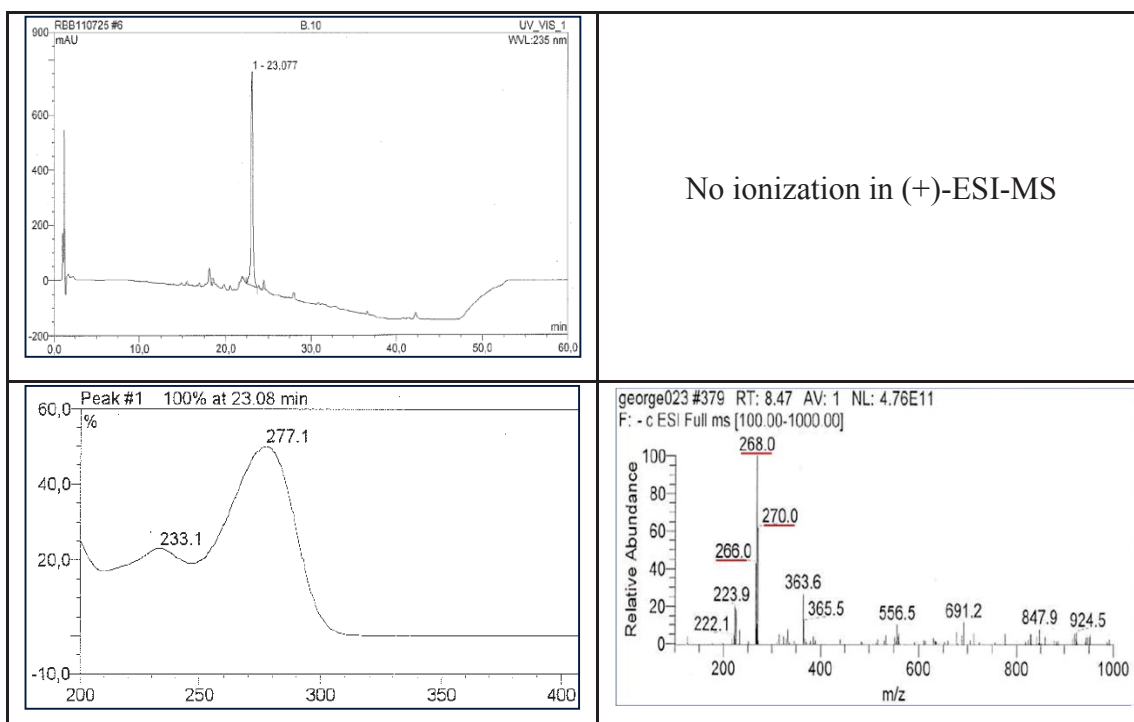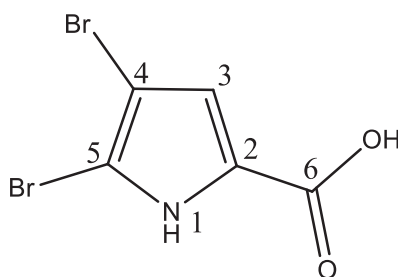
Compound **29** was isolated as white amorphous solid. The UV spectrum, revealing absorbances at λ_{max} 233 and 277 nm, suggested the presence of a pyrrole chromophore in the molecule. The ESIMS spectrum indicated two bromines in the molecule as shown by a cluster of molecular ion peaks at *m/z* 266/268/270 [M-H]⁻ having an intensity ratio of 1:2:1. In addition, the ¹H NMR spectrum of **29** measured in MeOH-*d4* disclosed the presence of a downfield signal resonating at δ_H 6.82 (1H, s, H-3). Based on these observations, as well as by comparison of the UV, ¹H NMR and mass spectral data with published data, **29** was identified as 4,5-dibromo-1*H*-pyrrole-2-carboxamide (Forenza *et al*., 1971).

3.6.2. Bioactivity of compound isolated from the marine sponge *A. oroides.*

The isolated compound (**29**) was examined for its effect on the growth of the L5178Y mouse lymphoma cell line using the MTT assay (Table 3.25). Moreover, compound **29** was evaluated for its antimicrobial activity against a panel of different bacterial strains (Table 3.26); however, it exhibited no significant activity to any of the cell lines tested.

Table 3.25: Cytotoxic activity of **29**

Name	% Growth of L5178Y (10µg/ml)
4,5-Dibromopyrrole-2-carboxylic acid (**29**)	98.9

Table 3.26: Antibacterial assay of compound **29**

Name	MRSA MIC (µg/ml)	*S. pneumonia* MIC (µg/ml)	*E. faecalis* MIC (µg/ml)	*E. Coli* MIC (µg/ml)
4,5-Dibromopyrrole-2-carboxylic acid (**29**)	>125	>125	—	>125

4. Discussion

4.1. Metabolites isolated from marine sponges

4.1.1. Metabolites isolated from the marine sponge *Dactylospongia metachromia.*

Sponges of the genus *Dactylospongia* are a rich source of bioactive secondary metabolites, the majority of which are sesquiterpene quinones/quinols (Rodriguez *et al.,* 1992). This class of compounds includes constituents of mixed biogenetic origin, which frequently consist of sesquiterpene moieties linked to quinones, quinols or structural analogues (Daletos *et al.,* 2014). The sesquiterpene unit is of biosynthetic interest as it usually features a drimane or a 4,9-friedodrimane type skeleton comprising a *trans* or a less common *cis* fused ring junction (Daletos *et al.,* 2014). These compounds have attracted considerable interest due to their pronounced biological activities including antitumor (Müller *et al.,* 1985) anti-inflammatory (Lucas *et al.* 2003) and antiviral activities (Loya *et al.,* 1990). *D. metachromia* has not been intensively investigated so far. It is important to mention, however, that this species was originally described as *Hippospongia metachromia* by De Laubenfels in 1954. (De Laubenfels *et al.,* 1954) The reassignment by Bergquist in 1965 led to the currently accepted name *D. metachromia.* (Bergquist *et al.,* 1990) Reports on *D. metachromia* describe the isolation of a sesterterpene lactone (Nakagawa *et al.,* 1986) sesterterpene sulfates (Musman *et al.* 2001) and sesquiterpene quinones/quinols (Luibrand *et al.,* 1979; Ishibashi *et al.,* 1988; Daletos *et al.,* 2014).

In this study we investigated a specimen of *D. metachromia* collected at Ambon, Indonesia. The extract exhibited considerable *in vitro* cytotoxicity against mouse lymphoma L5178Y cells. Subsequent bioactivity guided isolation yielded five new sesquiterpene aminoquinones (**1-5**), two new sesquiterpene benzoxazoles (**6** and **7**), along with the known analog 18-hydroxy-5-epi-hyrtiophenol (**8**) and a known glycerolipid (**9**) (Daletos *et al.,* 2014).

Literature surveys revealed that sesquiterpene quinones/quinols structurally related to **1-8**, are reported from sponges of the order Dictyoceratida. Compounds incorporating a nakijiquinone core structure, as in **1-5**, have hitherto been isolated only from *Spongia* sp. (Shigemori *et al.,* 1994), *Dactylospongia elegans* (Rodriguez *et al.,* 1992), *Smenospongia* sp. (Kondracki *et al.,* 1989) and *Hippospongia* sp. (Oda *et al.,* 2007). These compounds have attracted considerable interest as they display a wide range of biological activities, including cytotoxic, antimicrobial, inhibitory

activity against the tyrosine kinase EGFR and protein kinase C, as well as differentiation-inducing activity of K562 cells into erythroblasts (Kobayashi *et al.,* 2007; Oda *et al.,* 2007) The nakijiquinones belong to a relatively rare group of natural products that selectively inhibit the Her-2/Neu receptor tyrosine kinase (Kondracki *et al.,* 1989) known to be overexpressed in approximately 30% of primary breast and gastric carcinomas (Stahl *et al.*, 2001; Geng *et al.*, 2013; Ross and Fletcher, 1999). Structurally related sesquiterpene benzoxazoles (**6** and **7**) are rarely encountered in nature. Interestingly, nakijinols A and B, isolated from *Spongia* sp. (Kobayashi *et al.,* 2007) and *Dactylospongia elegans* (Rodriguez *et al.,* 1992), respectively, are so far the only representatives of this class of compounds (Daletos *et al.,* 2014).

4.1.1.1. Biosynthesis of sesquiterpene quinones/quinols.

The proposed biosynthesis of nakijiquinones includes farnesyl pyrophosphate, derived from the mevalonate pathway, and p-hydroxy benzoic acid, derived from the shikimate pathway, as starting units. C-alkylation of the aromatic unit with farnesyl pyrophosphate ortho to the phenol group, which could be catalyzed by p-hydroxy benzoic acid polyprenyl transferase (Coq2), leads to intermediate A (Figure 4.1). Subsequently, the cyclic terpene (4,9-friedodrimane) unit is formed through a series of carbocation-mediated reactions. Then, the aromatic ring could undergo different modifications, such as decarboxylation and oxidation reactions to afford a quinone ring, and subsequent nucleophilic attack of the amino group of an amino acid followed by decarboxylation, could give rise to the core structure of nakijiquinones (Minale *et al.*, 1979; Rudney *et al.*, 1995; Sladic *et al.,* 2006).
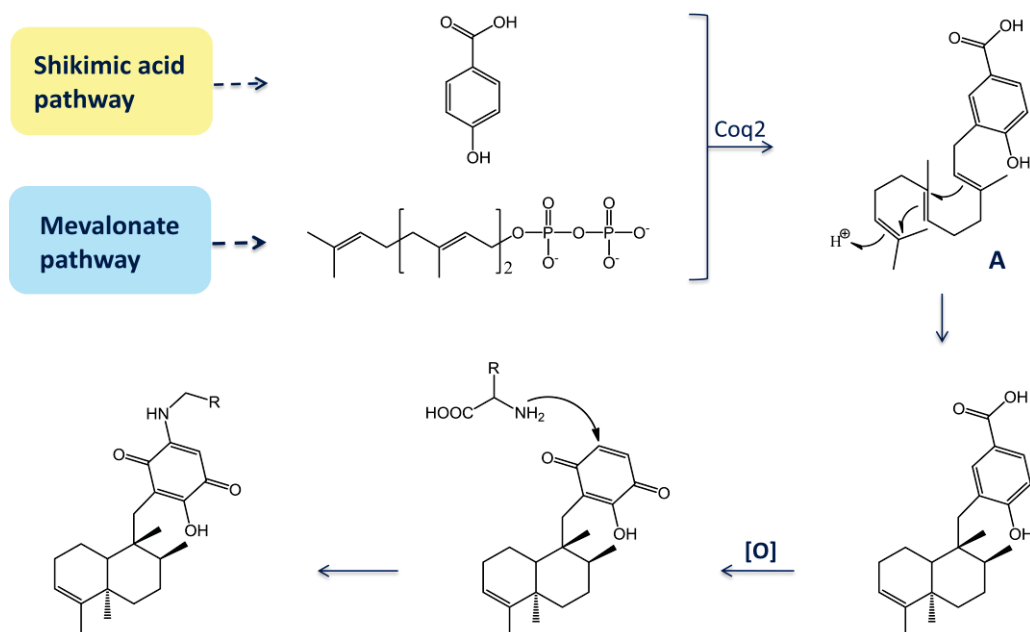
Figure 4.1: Proposed biosynthesis of nakijiquinones.

4.1.1.2 Bioactivity of isolated compounds from *Dactylospongia metachromia*.

Compounds **1-8** were subjected to a cellular cytotoxicity (MTT) assay against L5178Y mouse lymphoma cells. The sesquiterpene quinones (**1-5**) showed pronounced cytotoxicity against L5178Y cells with IC_{50} values ranging between 1.1-3.7 μM (Table 3.8) compared to kahalalide F as a positive control (IC_{50} 4.30 μM). Interestingly, the loss of the aminoquinone core structure, as in **6-8**, resulted in a significant decrease of cytotoxic activity, indicating that the aminoquinone moiety plays an important role in mediating cytotoxicity (Daletos *et al.,* 2014).

The compounds (**1-8**) were further tested against 16 protein kinases, which have been shown to be involved in the regulation of tumor growth and metastasis at a dose of 10 μM each. The protein kinase activity assay results revealed comparable activity for **1-5**, particularly inhibiting ALK, FAK, IGF1-R, SRC and VEGF-R2. The nakijinols (**6** and **7**) showed a slightly narrower spectrum of protein kinase inhibition. Both compounds inhibited ALK, FAK and IGF1-R, and only **6** inhibited VEGF-R2 as well. 18-Hydroxy-5-*epi*-hyrtiophenol (**8**) exhibited a broader spectrum of activity inhibiting ALK, Aurora-B, FAK, MET wt, NEK6, SRC and VEGF-R2. IC_{50} values were determined for compounds **5**, **6** and **8**, which inhibited the activity of at least one

of the 16 kinases by more than 75% (Table 3.9). The lack of cytotoxic activity for **6-8** in spite of their protein kinase inhibitory activity indicated that the pronounced cytotoxic activity of **1-5** is most likely due to another cellular mechanism which needs to be further investigated (Daletos *et al.,* 2014).

4.1.2. Metabolites isolated from the marine sponge *Callyspongia aerizusa*.

Sponges belonging to the genus C*allyspongia* are extensively investigated for bioactive natural products. Many new bioactive natural products have been isolated from different *Callyspongia sp.*, including polyacetylene derivatives (Youssef *et al.,* 2003), uncommon fatty acids (Carballeira and Pagan 2001), triterpenes (Fukami *et al* 1997), macrolides (Dat *et al.,* 2013) and cyclic peptides, such as phoriospongins A and B from *C. bilamellata* (Capon *et al.,* 2002), callynormine A from *C. abnormis* (Berer *et al* 2004) and callyaerins from *C. aerizusa* (Ibrahim, *et al.*, 2010; Daletos, *et al.*, 2015).

In this study we examined four separate collections of *C. aerizusa* obtained from three different regions in Indonesia. The respective crude EtOAc extracts exhibited strong *in vitro* activity against *M. tuberculosis*. Subsequent fractionation of the EtOAc extracts yielded five new callyaerin derivatives I – M (**11 ─ 15**), along with seven known callyaerins A – G (**16 ─ 22**) (Daletos, *et al.*, 2015).

Callyaerins constitute a unique class of sponge-derived peptides. The basic structural unit of these peptides comprises a cyclic part and a linear side chain, both of variable size, joined through the non-proteinogenic (*Z*)-2,3-diaminoacrylic acid (DAA) (Ibrahim *et al.*, 2010). It was speculated that DAA biogenetically arises from oxidation of a serine or cysteine unit to give a formyl glycine which will undergo Schiff base formation with the amino group of the next amino acid in the ring, followed by double bond migration (Berer *et al*., 2004). This endiamino group is of special interest, as it is expected to introduce rigidity into cyclic peptide structures.[7] In addition, callyaerins contain an unusually high number of proline residues (or γ-hydroxyprolines), which provide additional rigidity to the peptide backbone due to their restricted dihedral angles and may lead to higher affinity and selectivity for protein binding.[8,12] The remaining residues are predominantly hydrophobic amino acids such as IIe, Leu, Val, and Phe, with all amino acids present in the L-configuration. Apart from our previous reports on this class of peptides (Ibrahim *et al.*, 2010), there is only one further example, callynormine A, which had been isolated from the Kenyan sponge *Callyspongia abnormis* (Berer *et al*., 2004). Thus, this intriguing class of peptides is currently restricted to the sponge genus *Callyspongia*. In this context, our report highlights the potential of these derivatives as promising anti-TB agents (Daletos, *et al.*, 2015).

4.1.2.1. Biosynthesis of nonribosomal peptides

Nonribosomal peptides (NRPs) are secondary metabolites that are mainly produced by microorganisms, such as bacteria and fungi (Dewick, 2008). In contrast to ribosomal peptide synthesis, nonribosomal peptides biogenetically arise from specific enzymes, called nonribosomal peptide synthetases. Each nonribosomal peptide synthetase is responsible for the production of only one type of peptide. NRPs commonly undergo structural modifications that lead to additional structural diversity and make them resistant against enzymatic hydrolysis or even increase their biological activities. NRPs feature linear, cyclic or branched moieties and they often contain non-proteinogenic amino acid residues in their structures, such as D-amino acids. Examples of NRPs are the antibiotic vancomycine, the antitumor bleomycin or the siderophore pyoverdin (Marahiel *et al.,* 1997; Caboche *et al.*, 2008).

Nonribosomal peptide synthetases contain repeating units, called modules that are specific for each amino acid. Each module typically contains three domains, including an adenylation (A) domain, a peptidyl carrier protein (PCP) domain, and a condensation (C) domain. The A domain is responsible for the activation of a specific amino acid through reaction with ATP. The activated amino acid is then transferred to the PCP domain forming a thioester. Finally the C domain is responsible for the amide bond formation between two amino acids, and thus elongation of the growing peptide chain (Walsch *et al.*, 2003; Dewick, 2008).

Callyaerins are suggested to biogenetically arise from nonribosomal peptide synthetases, which are specific for each of these peptides (Dewick, 2008). The proposed biosynthesis of callyaerin F is shown in Figure 4.2. The peptide chain grows by an amino acid each time, through the repeating modules of the responsible enzyme, until the final sequence is completed. Then, chain termination is achieved through a thioesterase (TE) domain, which cleaves the thioester bond and releases the linear peptide chain. However, callyaerin F contains a cyclic domain, which is formed through a non-proteinogenic diaminoacrylic acid unit. The postulated mechanism of this unusual unit is through the condensation of the terminal amino group of valine with the aldehyde group of a formyl glycine unit, which is derived by oxidation of serine or cysteine (Figure 4.2). Thus, formation of the cyclic part and subsequent cleavage of the peptide would yield callyaerin F (Daletos, *et al.*, 2015).

Figure 4.2: Proposed biosynthesis of callyaerin F.

4.1.2.2 Bioactivity of isolated compounds from *Callyspongia aerizusa*

All compounds were tested *in vitro* against *Mycobacterium tuberculosis*, as well as against THP-1 (human acute monocytic leukemia), and MRC-5 (human fetal lung fibroblast) cell lines in order to assess their general cytotoxicity (Figure 3.22).

Based on these bioassay data, a number of preliminary structure-activity relationships may be concluded. The most active compounds, callyaerin A (**16**) and B (**17**), share similar amino acid sequences in their ring moieties that may contribute to their potent antitubercular activity. Both compounds nevertheless differ with regard to the number and sequence of amino acids in the linear part of their molecules which finds a reflection in the weaker anti TB activity and stronger cytotoxicity of callyaerin B (**17**) compared to callyaerin A (**16**). Callyaerin C (**18**) and M (**15**) exhibit moderate or no antitubercular activity, respectively, and both compounds differ only with regard to the first amino acid residue in their ring systems. Furthermore, it is suggested that the presence of hydrophobic amino acids (IIe, Leu and Val), and the absence of amino acids with bulky substituents (Phe) in the ring, as in **16 − 18**, may contribute to the increased biological activity of these peptides perhaps by allowing them to pass through membranes and/or by allowing a better fit to (their unknown) target molecules (Daletos, *et al.*, 2015).

4.1.3. Metabolites isolated from the marine sponge *Acanthostrongylophora ingens*

Chemical investigation of the EtOAc extract of the sponge *Acanthostrongylophora ingens* yielded two known compounds, namely, annomontine (**23**) and 1-hydroxy-3,4-dihydronorharman (**24**). Notably, these alkaloids have likewise been obtained from the bark of *Annona montana* (family Annonaceae) (Leboeuf, *et al.*, 1982), which suggests their possible microbial origin. This class of compounds is of great interest as it comprises a wide array of structurally unique metabolites possessing potent bioactivities. For example, carboline and harman alkaloids inhibit monoamine oxidases (Kim *et al.*, 1996), interact with benzodiazepine receptors (Robinson *et al.*, 2003), and they are known to intercalate into DNA (Sobhani *et al.*, 2002).

4.1.3.1. Biosynthesis of β-carbolines

Marine sponges are prolific sources of numerous indole alkaloid derivatives, such as alkaloids comprising an intact β-carboline skeleton. The latter, also called β-carbolines feature a tricyclic pyrido (3,4-b) indole ring system with different substitution patterns. Alkaloids containing a β-carboline skeleton are suggested to be derived from tryptophan, which forms the indole moiety of the β-carboline unit (Gröger, 1969, Cordell, 1974). Interestingly, chemical investigation of the Indonesian marine sponge *A. ingens* yielded the known alkaloids annomontine (**23**) (Leboeuf *et al.*, 1982) and 1- hydroxy-3,4-dihydronorharman (**24**) (Roa *et al.*, 2003). In this part, the results of the chemical investigation of the secondary metabolites produced by *A. ingens* are presented. The putative biosynthesis of **24** is suggested to start with tryptamine (originating from tryptophan) and a formaldehyde unit to generate a six-membered heterocyclic ring via a Mannich-type reaction, which could then undergo further oxidation reactions to yield the hydroxylated product (Figure 4.3). In a similar manner, the biosynthesis of **23** is suggested to start with the imine formation of tryptamine and the aldehyde derivative A followed by complete aromatization of the tryptamine heterocyclic ring (Slaytor, *et al.*, 1968; Trossell *et al.*, 1997, Dewick, 2008).
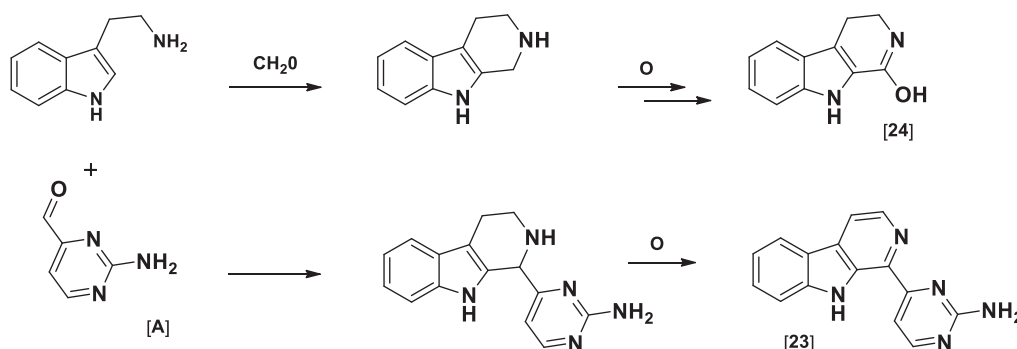

Figure 4.4: Proposed biosynthesis of **23** and **24** (Trossell *et al.*, 1997; Dewick, 2008).

4.1.3.2 Bioactivity of isolated compounds from *Acanthostrongylophora ingens*

The isolated compounds (**23** and **24**) were tested for their antibacterial activities against the bacterial strains *S. aureus*, *E. coli*, and *P. aeruginosa*, but only **21** showed weak inhibition of *S. aureus*, with a MIC of 64 µg/mL (Table 3.18). The isolated compounds were further examined for their effects on the growth of the L5178Y mouse lymphoma cell line employing the MTT assay; however both of them were inactive ($IC_{50} > 10\mu M$) in this assay.

In addition, the isolated compounds were subjected to bioassays aimed to determine their protein kinase inhibitory profiles (Table 3.19). Compound **23** showed moderate inhibitory activity with 71% inhibition against PIM1 kinase at a dose of 10 μg/ml, whereas **24** exhibited no activity. According to the above results, it is suggested that the presence of the 2-aminopyrimidine moiety is an essential structural feature for the activity of these compounds.

4.1.4. Metabolites isolated from the marine sponge *Sarcotragus spinosulus*

Sponges belonging to the genus *Sarcotragus* are commonly found in swallow Mediterranean marine ecosystems. Chemical investigation of these sponges has afforded several interesting metabolites, including unusual linear sesterterpenes, bearing furan and tetronic acid functional groups (Cimino *et al.*, 1972). These pentaprenyl terpenoid metabolites are considered to be derived from geranylfarnesyl diphosphate. Apart from the marine habitat, this group of terpenes has been described from various sources, including higher plants, terrestrial fungi, lichens, and insects (Liu *et al.*, 2007). These intriguing metabolites exhibit a wide array of biological activities. For example, sesterterpene analogues derived from *Sarcotragus sp.* displayed potent brine shrimp toxicity (De Rosa *et al.*, 1994), fish lethality (Fusetani *et al.*, 1984), as well as analgesic and anti-inflammatory effects through regulation of phospholipase A2 (De Pasquale *et al.*, 1991; Gil *et al.*, 1993).

In this study we investigated a specimen of *Sarcotragus spinosulus* collected in Fethiye, Turkey. Chemical investigation of the ethyl acetate extract of this sponge afforded a 3:1 mixture of two known linear sesterterpenes ircinin-1 (**25**) and ircinin-2 (**26**).

Ircinin 1,2 (3:1) (**25** and **26**) showed weak cytotoxicity against the mouse lymphoma cell line L5178Y (16.6% inhibition at a dose of 10 μg/ml) as well as against human ovarian cancer A2780 sens (cisplatin-sensitive) and A2780 CisR (cisplatin-resistant) cell lines (Figure 3.25). However, in a study by Liu *et al.*, ircinin-1 was shown to selectively inhibit the activity against a small panel of solid human tumor cell lines (Liu *et al.*, 2001). Interestingly, ircinin-1 was found to inhibit proliferation of human malignant melanoma cells through its effect on cell cycle-related proteins (CDKs). Moreover, mechanistic studies further suggested that ircinin-1 induced apoptosis through the activation of the mitochondrial and the Fas/Fas ligand pathway (Choi *et al.*, 2005).

Therefore, this prompted us to test the *in vitro* inhibitory potential of ircinin 1,2 (3:1) (**25** and **26**) employing 16 different protein kinases (Table 3.20). Interestingly, ircinin 1,2 (3:1) (**25** and **26**) exhibited potent inhibitory activity against ALK, AXL, FAK, IGF1-R, SRC, and VEGF-R2 kinases (Table 3.20), which are implicated in human lung, skin, prostate and colon cancers. These results were in agreement with those in the literature, thus indicating that the mechanism of its

selective cytotoxicity is most probably due to interaction with specific cell cycle-regulatory proteins and their associated kinase activity (Choi *et al.*, 2005).
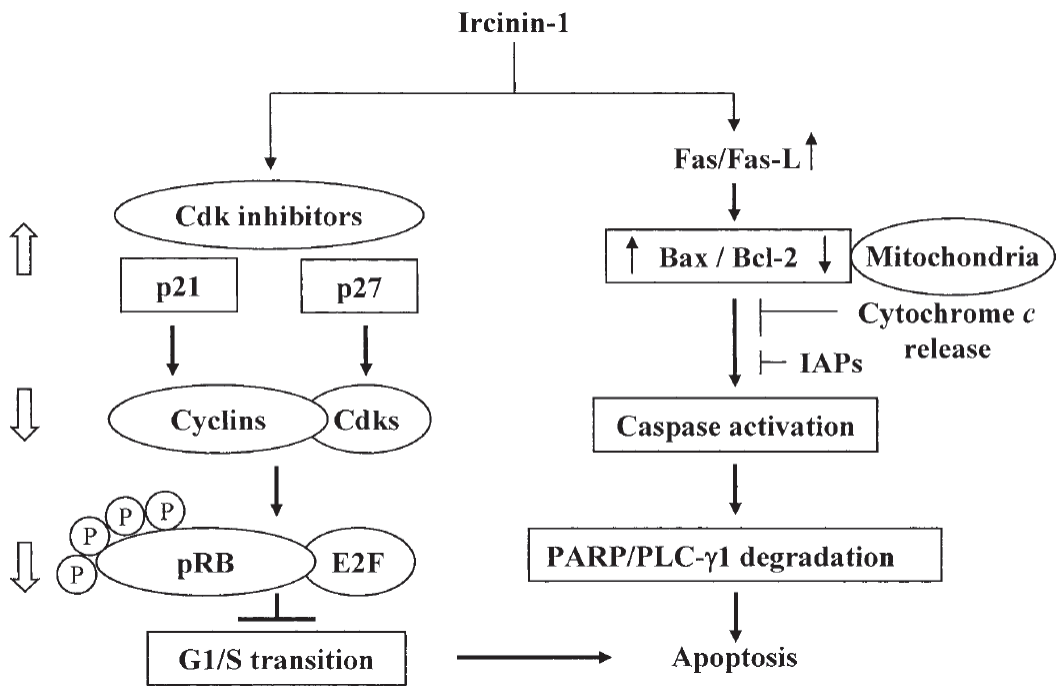

Figure 4.4: Mode of action of ircinin-1 (Choi *et al.*, 2005)

5. Summary

Marine sponges are undoubtedly among the richest sources of secondary metabolites with a great variety of unique and fascinating structures. Most of the isolated metabolites have shown potent activities in a wide array of bioassays, and therefore they could be considered as potential lead structures for the development of novel therapeutic agents.

This study involved the isolation, structural elucidation and biological screening of the active constituents of six marine sponge samples originated from different collection sites in Indonesia and Turkey.

Structure elucidation of secondary metabolites was performed using state-of-the-art analytical techniques, including 1D (^{1}H, ^{13}C) and 2D (COSY, TOCSY, ROESY, HSQC, HMBC) NMR spectroscopy and mass (EI, ESI, MALDI-TOF) spectrometry. Moreover, in the case of selected optically active natural products, chiral derivatization methods (i.e. Marfey's method) were applied for the determination of their absolute configuration. Finally, the isolated compounds were subjected to various bioassays to examine their cytotoxic and antimycobacterial activities, as well as their inhibitory profiles toward selected protein kinases.

1. *Dactylospongia metachromia*

Chemical investigation of the sponge *Dactylospongia metachromia* (Indonesia) afforded five new sesquiterpene aminoquinones and two new sesquiterpene benzoxazoles. Moreover, three known compounds were isolated, including a sesquiterpene quinol, an indole derivative and a glycerolipid. The sesquiterpene quinone/quinol derivatives showed high cytotoxicity when tested against L5178Y mouse lymphoma cell line as well as pronounced protein kinase inhibitory activity.

2. *Callyspongia aerizusa*

A detailed chemical investigation of four separate collections of *Callyspongia aerizusa* (Indonesia) yielded 12 structurally related cyclic peptides (callyaerins), including five new congeners. All compounds were investigated *in vitro* against *M. tuberculosis*, as well as against THP-1 (human acute monocytic leukemia) and MRC-5 (human fetal lung fibroblast) cell lines in order to assess their general cytotoxicity. Callyaerin A followed by callyaerin B were found to inhibit *M. tuberculosis* at low

micromolar concentrations making these compounds interesting candidates for further studies.

3. *Acanthostrongylophora ingens*

Chemical investigation of the sponge *Acanthostrongylophora ingens* (Indonesia) afforded two known β-carboline alkaloids, namely, annomontine and 1-hydroxy-3,4-dihydronorharman. The isolated compounds were tested for their antibacterial activities against the bacterial strains *S. aureus*, *E. coli,* and *P. aeruginosa*. In addition, the isolated compounds were subjected to bioassays aimed to determine their cytotoxic and protein kinase inhibitory profiles. Annomontine exhibited weak inhibition towards *S. aureus*. In addition, it showed moderate inhibitory activity against PIM1 kinase, whereas 1-hydroxy-3,4-dihydronorharman exhibited no activity.

4. *Sarcotragus spinosulus*

Bioactivity-guided fractionation strategy of *Sarcotragus spinosulus* (Turkey) extract was performed leading to the isolation of a 3:1 mixture of two known linear sesterterpenes ircinin 1 and ircinin 2. Ircinin-1,2 (3:1) were subjected to bioassays aimed to determine the cytotoxicity and the protein kinase inhibitory profiles of these compounds. Interestingly, ircinin-1,2 (3:1) proved to be highly active against a panel of protein kinases, whereas it showed only weak cytotoxicity against the mouse lymphoma cell line L5178Y

5. *Agelas oroides*

Chemical investigation of the sponge *Agelas oroides* (Turkey) extract afforded one known bromopyrrole alkaloid. 4,5-Dibromopyrrole-2-carboxylic acid was tested for its cytotoxic and antibacterial activities, however, it exhibited no activity.

5. *Dysidea avara*

Two known sesquiterpene quinones/quinols have been purified and identified from the methanolic extract of the marine sponge *Dysidea avara* (Turkey) namely, avarol and avarone. Avarol revealed interesting bioactivity results in different bioassays, including cytotoxicity (MTT), antibacterial and *in vitro* protein kinase assays.

6. References

Aly A.H., Edrada-Ebel R., Indriani I.D., Wray V., Muller W.E.G., Totzke F., Zirrgiebel U., Schachtele C., Kubbutat M.H.G., Lin W. H., Proksch P., Ebel R. (**2008**). Cytotoxic metabolites from the fungal endophyte *Alternaria* sp. and their subsequent detection in its host plant *Polygonum senegalense*. *J. Nat. Prod.*, *71*, 972-980.

Akinleye A., Furqan M., Mukhi N., Ravella P., Liu D. J. (**2013**). MEK and the inhibitors: from bench to bedside. *Hematol. Oncol.*, *6*, 27.

Andjelic C., Planelles V. Barrows L. (**2008**). Characterizing the anti-HIV activity of papuamide A. *Mar. Drugs*, *6*, 528-549.

Ancheeva E., Daletos G., Muharini R., Lin W.H., Teslov L., Proksch P. (**2015**) Flavonoids from *Stellaria nemorum* and *Stellaria holostea*. *Nat. Prod. Commun. 3,* 437-40.

Ang K.K.H., Holmes M.J., Higa T., Hamann M.T., Kara U.A.K. (**2000**). In vivo antimalarial activity of the betacarboline alkaloid manzamine A. *Antimicrob. Agents Chemother.*, *44*, 1645-1649.

Aoki S., Kong D., Matsui K., Rachmat R., Kobayashi, M. (**2004**). Sesquiterpene aminoquinones, from a marine sponge, induce erythroid differentiation in human chronic myelogenous leukemia, K562 cells. *Chem. Pharm. Bull.*, *52*, 935-937.

Arai M., Sobou M, Vilchéze C., Baughn A., Hashizume H., Pruksakorn P., Ishida S., Matsumoto M., Jacobs W.R. Jr., Kobayashi M. (**2008**). Halicyclamine A, a marine spongean alkaloid as a lead for anti-tuberculosis agent. *Bioorg Med Chem.*, *16*, 6732-6736.

Arai T. and Sano H. (**1994**). Novel UV-absorbing compounds FK17-P2a, FK-17-P2b1, FK17-P2b2, and FK17-P3 and manufacture of the compounds with *Aspergillus* sp. *Jpn. Kokai Tokkyo Koho*, *93*, 121677.

Baer E., Fischer H.O.L. (**1941**). Studies on acetone-glyceraldehyde, and optically active glycerides: IX. Configuration of the natural batyl, chimyl, and selachyl alcohols. *J. Biol. Chem.*, *140*, 397-410.

Bartik K., Braekman J.-C., Daloze D., Stoller C., Huysecom J., Vandevyver G., Ottinger R. (**1987**). Topsentins, new toxic bis-indole alkaloids from the marine sponge *Topsentia genitrix*. *Can. J. Chem.*, *65*, 2118-2121.

Barreca A., Lasorsa E., Riera L., Machiorlatti R., Piva R., Ponzoni M., Kwee I., Bertoni F., Piccaluga P.P., Pileri S.A., Inghirami G J. (**2011**). Anaplastic lymphoma   kinase in human cancer. *Mol. Endocrinol.*, *47*, R11-23.

Batke E., Ogura R., Vaupel P., Hummel K., Kallinowski F., Gasić M.J., Schröder H., Müllerm W. (**1988**). Action of the antileukemic and anti-HTLV-III (anti-HIV) agent avarol on the levels of superoxide dismutases and glutathione peroxidase activities in L5178y mouse lymphoma cells. *Cell Biochem. Funct.*, *6*, 123-129.

Bergquist P.R. (**1965**). The Sponges of Micronesia, Part I. The Palau Archipelago. *Pac. Sci.*, *19*, 123-204.

Bharate, S. B., S. D. Sawant, P. P. Singh and R. A. Vishwakarma (**2013**). Kinase Inhibitors of Marine Origin. *Chemical Reviews* **113**: 6761-6815.

Brault L., Gasser C., Bracher F., Huber K., Knapp S., Schwaller J. (**2010**). PIM serine/threonine kinases in the pathogenesis and therapy of hematologic malignancies and solid cancers. *Haematologica*, *95*, 1004-1015.

Becerro M.A., Goetz G., Paul V.J. & Scheuer P.J. (**2001**). Chemical defenses of the sacoglossan mollusk *Elysia rufescens* and its host alga *Bryopsis* sp. *J. Chem. Ecol.*, *27*, 2287-2299.

Blunt J.W., Copp B.R., Keyzers R.A., Munro M.H.G., Prinsep, M.R. (**2013**). Marine natural products. *Nat. Prod. Rep.*, *30*, 237-323.

Bergmann W., Feeney R.J. (**1951**) Contributions to the study of marine products. XXXII. The nucleosides of sponges. I. *J. Org. Chem.*, *16*, 981-987.

Brown A.P., Morrissey R.L., Faircloth G.T., Levine B.S. (**2002**). Preclinical toxicity studies of kahalalide F, a new anticancer agent: single and multiple dosing regimens in the rat. *Cancer Chemother. Pharmacol.*, *50*, 333-340.

Burgoyne D. L., Andersen, R. J., Allen T. M. (**1992**). Contignasterol, a higly oxygenated steroid with the "unnatural" 14β configuration from the marine sponge *Petrosia contignata* Thiele, 1899. *J. Org. Chem.*, *57*, 525-528.

Cafieri F., Fattorusso E., Taglialatela-Scafati O., Ianaro A. (**1999**). Metabolites from the sponge *Plakortis simplex*. Determination of absolute stereochemistry of plakortin. Isolation and stereostructure of three plakortin related compounds. *Tetrahedron*, *55*, 7045-7056.

Campagnuolo C., Fattorusso E., Romano A., Taglialatela-Scafati O., Basilico N., Parapini S., Taramelli D. (**2005**). Antimalarial polyketide cycloperoxides from the marine sponge *Plakortis simplex*. *Eur. J. Org. Chem.*, *2005*, 5077-5083.

Choi, H. J., Choi, Y. H., Yee, S.-B., Im, E., Jung, J. H., Kim, N. D. (**2005**) Ircinin-1 induces cell cycle arrest and apoptosis in SK-MEL-2 human melanoma cells. *Molecular Carcinogenesis, 44*, 162-173.

Cimino G., de Rosa S., de Stefano S., Mazzarella L., Puliti R., Sodano G. (**1982**). Isolation and X-ray crystal structure of a novel bromo-compound from two marine sponges. *Tetrahedron Lett.*, *23*, 767-768.

Cimino G., de Stefano S., Minale, L. (**1974**). Scalaradial, a third sesterterpene with the tetracarbocyclic skeleton of scalarin, from the sponge *Caccospongia mollior*. Experientia, **30**, 846

Coleman J.E., de Silva E.D., Kong F., Andersen R.J., Allen, T.M. (**1995**) Cytotoxic peptides from the marine sponge *Cymbastela* sp. *Tetrahedron*, *51*, 10653-10662.

Coulson F. R., O'Donnell S.R. (**2000**). The effects of contignasterol (IZP-94,005) on allergen-induced plasma protein exudation in the tracheobronchial airways of sensitized guinea-pigs *in vivo*. *Inflamm. Res.*, *49*, 123-127

Coutinho A.F., Chanas B., de Souza T.M.L., Frugrulhetti I.C.P.P., de A Epifanio R. (**2002**) Anti HSV-1 alkaloids from a feeding deterrent marine sponge of the genus *Aaptos*. *Heterocycles*, *57*, 1265-1272.

Cuadrado, A., Garcia-Fernandez L.F., Gonzalez L., Suarez Y., Losada A., Alcaide V., Martinez T., Fernandez-Sousa J.M., Sanchez Puelles J.M., Munoz A. (**2003**). Aplidin™ induces apoptosis in human cancer cells via glutathione depletion and sustained activation of the epidermal growth factor receptor, Src, JNK, and p38 MAPK. *J. Biol. Chem.*, *278*, 241-250.

Cui J., Yu Y., Lu G.F., Liu C., Liu X., Xu Y.X., Zheng P.Y. (**2013**). Overexpression of ARK5 is associated with poor prognosis in hepatocellular carcinoma. *Tumour Biol.*, *34*, 1913-1908.

De Carvalho M. S., Jacobs R. S., (**1991**), Two-step inactivation of bee venom phospholipase A2 by scalaradial, *Biochem. Pharmacol.*, **42**, 1261-1266.

Degenhardt Y., Lampkin T. (**2010**).Targeting Polo-like kinase in cancer therapy. *Clin. Cancer Res.*, *16*, 384-389.

De Laubenfels M.W. (**1954**). The sponges of the West-Central Pacific. Oregon State Monographs. Studies in zoology. *Oregon State College: Corvallis*, *7*, 11-12.

De Silva E. D., Scheuer P. J. (**1980**). Manoalide, an antibiotic sesquiterpenoid from the marine sponge *Luffariella variabilis*. *Tetrahedron Lett.*, *21*, 1611-1614.

De Souza M.V. (**2004**). (+)-discodermolide: a marine natural product against cancer. *Scientific World Journal*, **4**, 415-436.

De Souza M.V. (**2009**) Promising candidates in clinical trials against multidrug-resistant tuberculosis (MDR-TB) based on natural products. *Fitoterapia*, **80**, 453-460.

Dewick, P.M. *Medicinal natural products: a biosynthetic approach.* 3rd ed. (**2008**) Wiley, United Kingdom.

Ebel, R., M. Brenzinger, A. Kunze, H. J. Gross and P. Proksch (1997). "Wound Activation of Protoxins in Marine Sponge Aplysina aerophoba." *J. Chem. Ecol., 23*, 1451-1462.

Ellis L.M., Hicklin D.J. (**2008**). VEGF-targeted therapy: mechanisms of anti-tumour activity. *Nat. Rev. Cancer*, **8**, 579-591.

Esté J., Telenti A. (**2007**). HIV entry inhibitors. *Lancet*, **370**, 81-88.

Fabbro, D., Ruetz, S., Buchdunger, E., Cowan-Jacob, S. W., Fendrich, G., Liebetanz, J., Mestan, J., O'Reilly, T., Traxler, P., Chaudhuri, B., Fretz, H., Zimmermann, J., Meyer, T., Caravatti, G., Furet, P., Manley, P. W. (**2002**) Protein kinases as targets for anticancer agents: from inhibitors to useful drugs. *Pharmacology & Therapeutics*, *93*, 79-98.

Fattorusso E., Taglialatela-Scafati O. (**2009**). Marine antimalarials. *Mar Drugs*, *7*, 130-152.

Fattorusso C., Campiani G., Catalanotti B., Persico M., Basilico N., Parapini S., Taramelli D., Campagnuolo C., Fattorusso E., Romano A., Taglialatela-Scafati O. (**2006**). Endoperoxide derivatives from marine organisms: 1,2-dioxanes of the Plakortin family as novel antimalarial agents. *J. Med. Chem.*, *49*, 7088-7094.

Fidock, D. A., P. J. Rosenthal, S. L. Croft, R. Brun and S. Nwaka (2004). Antimalarial drug discovery: efficacy models for compound screening. *Nat Rev Drug Discov* **3**: 509-520.

Ford P., Gustafson K., McKee T., Shigematsu N., Maurizi L., Pannell L., Williams D. de Silva E., Lassota P., Allen T. (**1999**). Papuamides A–D, HIV-Inhibitory and cytotoxic depsipeptides from the sponges *Theonella mirabilis* and *Theonella swinhoei* collected in Papua New Guinea. *J. Am. Chem. Soc., 121*, 5899-5909.

Gabay C. (2006). Interleukin-6 and chronic inflammation. Arthritis Res Ther., **8**, S3 doi: 10.1186/ar1917.

García A., Bocanegra-García V., Palma-Nicolás J.P., Rivera G. (**2012**). Recent advances in antitubercular natural products. *Eur J Med Chem.*, *49*, 1-23.

Garcia-Fernandez, L.F., Losada A., Alcaide V., Alvarez A.M., Cuadrado A., González L., Nakayama K., Nakayama K.I., Fernández-Sousa J.M., Muñoz A., Sánchez-Puelles J.M. (**2002**). Aplidin induces the mitochondrial apoptotic pathway via oxidative stress-mediated JNK and p38 activation and protein kinase C delta. *Oncogene*, *21*, 7533-7544.

Garcia-Rocha M., Bonay P., Avila J. (**1996**). The antitumoral compound Kahalalide F acts on cell lysosomes. *Cancer Lett.*, *99*, 43-50.

Gazave, Eve; Lavrov, Dennis V.; Cabrol, Jory; Renard, Emmanuelle; Rocher, Caroline; Vacelet, Jean; Adamska, Maja; Borchiellini, Carole; Ereskovsky, Alexander V. (**2013**) Systematics and Molecular Phylogeny of the Family Oscarellidae (Homoscleromorpha) with Description of Two New Oscarella Species. *PLoS One*, *8*, e63976

Geng Y., Chen X., Qiu J., Zhou Y., Wang J., Liu L., Shao Y., Yin Y. (**2013**). Human epidermal growth factor receptor-2 expression in primary and metastatic gastric cancer. *Int. J. Clin. Oncol.*, *19*, 303-311.

Gherardi E., Birchmeier W., Birchmeier C., Vande Woude G. (**2012**) Targeting MET in cancer: rationale and progress. *Nat. Rev. Cancer*, *12*, 89-103.

Glaser K.B., de Carvalho M.S., Jacobs R.S., Kernan M.R., Faulkner D.J. (**1989**). Manoalide: structure-activity studies and definition of the pharmacophore for phospholipase A2 inactivation. *Mol Pharmacol.*, *36*, 782-788.

Global tuberculosis report 2013; World Health Organization: Geneva, Switzerland, 2013.

Gunasekera S.P., Gunasekera M., Longley R.E., Schulte G.K. (**1990**). Discodermolide: a new bioactive polyhydroxylated lactone from the marine sponge *Discodermia dissoluta*. *J. Org. Chem.*, *55*, 4912-4915.

Haefner B. (**2003**). Drugs from the deep: marine natural products as drug candidates. *Drug Discov Today*, *8*, 536-544.

Hamann M.T., Scheuer P.J. (**1993**). Kahalalide F: a bioactive depsipeptide from the Sacoglossan mollusk *Elysia rufescens* and the green alga *Bryopsis* sp. *J. Am. Chem. Soc.*, *115*, 5825-5826.

Harada, N., T. Sugioka, Y. Ando, H. Uda and T. Kuriki (**1988**). Total synthesis of (+)-halenaquinol and (+)-halenaquinone. Experimental proof of their absolute stereostructures theoretically determined. *J. Am. Chem. Soc. 110*, 8483-8487.

Hennings H., Blumberg P.M., Pettit G.R., Herald C.L., Shores R., Yuspa S.H. (**1987**). Bryostatin 1, an activator of protein kinase C, inhibits tumor promotion by phorbol esters in SENCAR mouse skin. *Carcinogenesis*, *8*, 1343-1346.

Higgs M.D., Faulkner D.J. (**1978**). Plakortin, an antibiotic from *Plakortis halichondrioides*. *J. Org. Chem.*, *43*, 3454-3457.

Hinterding K., Knebel A., Herrlich P., Waldmann H. (**1998**). Synthesis and biological evaluation of aeroplysinin analogues: a new class of receptor tyrosine kinase inhibitors. *Bioorg. Med. Chem.*, *6*, 1153-1162.

Hung D.T., Chen J., Schreiber, S.L. (**1996**). (+)-Discodermolide binds to microtubules in stoichiometric ratio to tubulin dimers, blocks taxol binding and results in mitotic arrest. *Chem. Biol.*, *3*, 287-293.

Hooper D., Buchmann N., Degrange V., Dı́az S.M., Gessner M., Grime, P. (**2002**). Species diversity, functional diversity and ecosystem functioning. Biodiversity and Ecosystem Functioning. *Oxford University Press*, 195-208.

Ishibashi M., Ohizumi Y., Cheng J.F., Nakamura H., Hirata Y., Sasaki T., Kobayashi J. (**1988**). Metachromine A and B, novel antineoplastic sesquiterpenoids from the Okinawan sponge *Hippospongia* cf. *metachromia*. *J. Org. Chem.*, *53*, 2855-2858.

Jaspars M., Pasupathy V., Crews P. (**1994**). A tetracyclic diamine alkaloid, halicyclamine-A, from the marine sponge Haliclona sp. *J. Org. Chem.*, *59*, 3253-3255.

Keen N., Taylor S. (**2004**). Aurora-kinase inhibitors as anticancer agents. *Nat. Rev. Cancer*, *4*, 927-936.

Kitagawa I., Kobayashi M., Kitanaka K., Kido M., Kyogoku Y. (**1983**). Marine natural products. XII. On the chemical constituents of the Okinawan marine sponge *Hymeniacidon aldis*. *Chem. Pharm. Bull.*, *31*, 2321-2328.

Kobayashi J., Madono T., Shigemori H. (**1995**). Nakijiquinones C and D, new sesquiterpenoid quinones with a hydroxy amino acid residue from a marine sponge inhibiting c-erbB-2 kinase. *Tetrahedron*, *51*, 10867-10874.

Kobayashi J., Madono T., Shigemori H. (**1995**). Nakijinol, a novel sesquiterpenoid containing a benzoxazole ring from an Okinawan sponge. *Tetrahedron Lett.*, *36*, 5589-5590.

Kobayashi J., Naitoh K., Sasaki T., Shigemori H. (**1992**). Metachromins DH, new cytotoxic sesquiterpenoids from the Okinawan sponge *Hippospongia metachromia*. *J. Org. Chem.*, *57*, 5773-5776.

Kobayashi, J.; Murayama, T.; Ohizumi, Y. (**1989**). Metachromin C, new cytotoxic sesquiterpenoid from the Okinawan sponge *Hippospongia metachromia. J. Nat. Prod.*, *52*, 1173-1176.

Kondracki M.-L., Guyot M. (**1989**). Biologically active quinone and hydroquinone sesquiterpenoids from the sponge smenospongia sp. *Tetrahedron*, *45*, 1995-2004.

Koopmans M., Martens D. and Wijffels R.H. (**2009**). Towards commercial production of sponge medicines. *Mar. Drugs*, *7*, 787-802.

Kreuter M.H., Robitzki A., Chang S., Steffen R., Michaelis M., Kljajić Z., Bachmann M., Schröder H.C., Müller W.E.G. (**1992**). Production of the cytostatic agent aeroplysinin by the sponge *Verongia aerophoba* in *in vitro* culture. *Comp. Biochem. Physiol. C*, *101*, 183-187.

Laport, M. S., O. C. S. Santos and G. Muricy (2009). Marine Sponges: Potential Sources of New Antimicrobial Drugs. *Current Pharmaceutical Biotechnology* 10: 86-105.

Laport, M. S., O. C. S. Santos and G. Muricy (2009). Marine Sponges: Potential Sources of New Antimicrobial Drugs. *Current Pharmaceutical Biotechnology* 10: 86-105.

Laroche M., Imperatore C., Grozdanov L., Costantino V., Mangoni A., Hentschel U., Fattorusso E. (**2006**). Cellular localization of secondary metabolites isolated from the Caribbean sponge *Plakortis simplex*. *Marine Biol.*, *151*, 1365-1373.

Lee, R. H., Slate, D. L., Moretti, R., Alvi, K. A., Crews, P. (**1992**) Marine sponge polyketide inhibitors of protein tyrosine kinase. *Biochemical and Biophysical Research Communications* 1992, 184, 765-772.

Li Y., Ye X., Tan C., Hongo J.A., Zha J., Liu J., Kallop D., Ludlam M.J., Pei L. (**2009**). Axl as a potential therapeutic target in cancer: role of Axl in tumor growth, metastasis and angiogenesis. *Oncogene*, *28*, 3442-3455.

Liu Y., Jung J.H., Ji H., Zhang S. (**2006**). Glycerolipids from a *Sarcotragus* species sponge. *Molecules*, **11**, 714-719.

Liu Y. (**2012**). Renaissance of marine natural product drug discovery and development. *J. Marine. Sci. Res. Development*, **2**, 1-2.

Leal M.C., Puga J., Serôdio J., Gomes N.C.M., Calado R. (**2012**). Trends in the discovery of new marine natural products from invertebrates over the last two decades – where and what are we bioprospecting? *PLoS One*, **7**, e30580.

Loganzo F., Discafani C.M., Annable T., Beyer C., Musto S., Hari M., Tan X., Hardy C., Hernandez R., Baxter M., Singanallore T., Khafizova G., Poruchynsky M.S., Fojo T., Nieman J.A., Ayral-Kaloustian S., Zask A., Andersen R.J., Greenberger L.M., (**2003**). HTI-286, a synthetic analogue of the tripeptide hemiasterlin, is a potent antimicrotubule agent that circumvents P-glycoprotein-mediated resistance in vitro and in vivo. *Cancer Res.*, **63**, 1838-1845.

Longley R.E., Caddigan D., Harmody D., Gunasekera M., Gunasekera S.P. (**1991**). Discodermolide − a new, marine-derived immunosuppressive compound. I. In vitro studies. *Transplantation*, **52**, 650-656.

Loya S., Hizi A. (**1990**). The inhibition of human immunodeficiency virus type 1 reverse transcriptase by avarol and avarone derivatives. *FEBS Lett.*, **269**, 131-134.

Lucas R., Giannini C., D' Auria, M.V., Payá M. (**2003**). Modulatory effect of bolinaquinone, a marine sesquiterpenoid, on acute and chronic inflammatory processes. *J. Pharmacol. Exp. Ther.*, **304**, 1172-1180.

Luibrand R.T., Erdman T.R., Vollmer J.J., Scheuer P.J., Finer J., Clardy J. (**1979**). *Tetrahedron*, **35**, 609-612.

Manning G., Whyte D. B., Martinez R., Hunter T. (**2002**). The protein kinase complement of the human genome. *Science*, **298**, 1912-1934.

Martello L.A., McDaid H.M., Regl D.L., Yang C.P., Meng D., Pettus T.R., Kaufman M.D., Arimoto H., Danishefsky S.J., Smith A.B., Horwitz S.B. (**2000**). Taxol and discodermolide represent a synergistic drug combination in human carcinoma cell lines. *Clin. Cancer Res.*, **6**, 1978-1987.

Martins A., Vieira H., Gaspar H., Santos S. (**2014**). Marketed marine natural products in the pharmaceutical and cosmeceutical industries: tips for success. *Mar. Drugs*, **12**, 1066-1101.

Mattia C.A., Mazzarella L., Puliti R. (**1982**). 4-(2-Amino-4-oxo-2-imidazolin-5-ylidene)-2-bromo-4,5,6,7-tetrahydropyrrolo-[2,3-C]azepine-8-one methanol solvate: a new bromo compound from the sponge *Acanthella aurantiaca*. *Acta Crystallogr.*, *38*, 2513-2515.

Mayer A.M., Glaser K.B., Cuevas C., Jacobs R.S., Kem W., Little R.D., Mclntosh J.M., Newman D.J., Potts B.C., Shuster D.E. (**2010**). The odyssey of marine pharmaceuticals: a current pipeline perspective. *Trends Pharmacol. Sci*, *31*, 255-265.

Mayer A.M.S., Rodríguez A.D., Scafati O.T., Fusetani N. (**2013**). Marine pharmacology in 2009-2011: marine compounds with antibacterial, antidiabetic, antifungal, anti-Inflammatory, antiprotozoal, antituberculosis, and antiviral activities; affecting the immune and nervous systems, and other miscellaneous mechanisms of action. *Mar. Drugs*, *11*, 2510-2573.

McLean G.W., Carragher N.O., Avizienyte E., Evans J., Brunton V.G., Frame M.C. (**2005**). The role of focal-adhesion kinase in cancer − a new therapeutic opportunity. Nat. Rev. Cancer, 5, 505-515.

Meijer L., Thunnissen A.M., White A.W., Garnier M., Nikolic M., Tsai L.H., Walter J., Cleverley K.E., Salinas P.C., Wu Y.Z., Biernat J., Mandelkow E.M., Kim S.H., Pettit G.R. (**2000**). Inhibition of cyclin-dependent kinases, GSK-3β and CK1 by hymenialdisine, a marine sponge constitutent. *Chem. Biol.*, *7*, 51-63

Minale L., Riccio R., Sodano G. (**1974**) Avarol a novel sesquiterpenoid hydroquinone with a rearranged drimane skeleton from the sponge. *Tetrahedron Lett.*, *15*, 3401-3404.

Mishra S.K., Satpathy S.K., Mohanty S. (**1999**). Survey of malaria treatment and deaths. *Bull. World Health Organ.*, *77*, 1020.

Mitra A., Sept D. (**2004**). Localization of the antimitotic peptide and depsipeptide binding site on β-tubulin. *Biochemistry*, *43*, 13955-13962.

Molinski T. F., Dalisay D. S., Lievens, S. L., Saludes J. P. (**2009**). Drug development from marine natural products. *Nature*, *8*, 69-85.

Müller W.E.G., Maidhof A., Zahn R.K., Schröder H.C., Gasić M.J., Heidemann D., Bernd A., Kurelec B., Eich, E., Seibert G. (**1985**). Potent antileukemic activity of the novel cytostatic agent avarone and its analogues in vitro and in vivo. *Cancer Res.*, *45*, 4822-4826.

Müller W.E., Schroder H.C., Reuter P., Sarin P.S., Hess G. Meyer, Buschenfelde K.H., Kuchino Y., Nishimura, S. (**1988**). Inhibition of expression of natural UAG suppressor glutamine tRNA in HIV-infected human H9 cells in vitro by Avarol. *AIDS Res. Hum. Retroviruses*, *4*, 279-286.

Musman M., Ohtani I.I., Nagaoka D., Tanaka J., Higa T. (**2001**). Hipposulfates A and B, new sesterterpene sulfates from an Okinawan sponge, *Hippospongia* cf. *metachromia*. *J. Nat. Prod.*, *64*, 350-352.

Mutter R., Wills M. (**2000**). Chemistry and clinical biology of the bryostatins. *Bioorg. Med. Chem.*, *8*, 1841-1860.

Nakagawa M., Ishihama M., Hamamoto Y., Endo M. (**1986**). *Tennen Yuki Kagobutsu Toronkai Koen Yoshishu*, *28*, 200-207.

Nassirpour R., Shao L., Flanagan P., Abrams T., Jallal B., Smeal T., Yin M.J. (**2010**) Nek6 mediates human cancer cell transformation and is a potential cancer therapeutic target. *Mol. Cancer Res.*, *8*, 717-728.

Nerenberg, J.B., Hung, D.T., Somers, P.K., Schreiber, S.L. (**1993**). Total synthesis of the immunosuppressive agent (–)-discodermolide. *J. Am. Chem. Soc.*, *115*, 12621-12622.

Newman, D. J. and G. M. Cragg (2004). Marine Natural Products and Related Compounds in Clinical and Advanced Preclinical Trials. *J. Nat. Prod. 67,* 1216-1238.

Newman D.J., Cragg G.M., Battershill C.N. (**2009**). Therapeutic agents from the sea: biodiversity, chemo-evolutionary insight and advances to the end of Darwin's 200th year. *Diving Hyperb. Med.*, *39*, 216-225.

Oda T., Wang W., Fujita A., Mochizuki M., Ukai K., Namikoshi M. (**2007**). Promotion of IL-8 production in PMA-stimulated HL-60 cells by sesquiterpene quinines from a marine sponge, *Hippospongia* sp. *J. Nat. Med.*, *61*, 434-437.

Ovenden S.P.B., Nielson J.L., Liptrot C.H., Willis R.H., Tapiolas D.M., Wright A.D., Motti C.A. (**2011**). Metachromins U-W: cytotoxic merosesquiterpenoids from an Australian specimen of the sponge *Thorecta reticulata*. *J. Nat. Prod.*, *74*, 65-68.

Pawlik J.R. (**2011**). The chemical ecology of sponges of Caribbean Reefs: natural products shape natural systems. *BioScience, 61*, 888-898

Pettit, G. R., C. L. Herald, D. L. Doubek, D. L. Herald, E. Arnold and J. Clardy (**1982**). "Isolation and structure of bryostatin 1." *J. Amer. Chem. Soc., 104*, 6846-6848.

Pham C.-D., Hartmann R., Müller W.E.G., de Voogd N., Lai D., Proksch P. (**2013**). Aaptamine derivatives from the Indonesian sponge *Aaptos suberitoides*. *J. Nat. Prod.*, *76*, 103-106.

Pham C.-D., Weber H., Hartmann R., Wray V., Lin W., Lai D. Proksch P. (**2013**). New cytotoxic 1,2,4-thiadiazole alkaloids from the ascidian *Polycarpa aurata*. *Org. Lett.*, *15*, 2230-2233.

Pollak M. (**2012**). The insulin and insulin-like growth factor receptor family in neoplasia: an update. *Nat. Rev. Cancer*, *12*, 159-169.

Pope R.M., Lovis R., Mungre S., Perlman H., Koch A.E., Haines G.K. (**1999**). C/EBPβ in rheumatoid arthritis: correlation with inflammation, not disease specifity. *Clin. Immunol.*, *91*, 271-282

Priestap H.A., de los Santos C., Quirke J.M.E. (**2010**). Identification of a reduction product of aristolochic acid: implications for the metabolic activation of carcinogenic aristolochic acid. *J. Nat. Prod.*, *73*, 1979-1986.

Proksch P., (**1994**). Defensive roles of secondary metabolites from marine sponges and sponge-feeding nudibranchs. *Toxicon*, *32*, 639-655.

Proksch, P., Ebel, R., Edrada R.A., Schupp, P., Lin, W.H., Sudarsono, S., Wray, V., Steube, K. (**2003**). Detection of pharmacologically active natural products using ecology: selected examples from indopacific marine invertebrates and sponge-derived fungi. *Pure Appl. Chem.*, *75*, 343-352.

Proksch P., Edrada R.A., Ebel, R. (**2002**). Drugs from the seas − current status and microbiological implications. *Appl. Microbiol. Biotechnol.*, *59*, 125-134.

Proksch P., Putz A., Ortlepp S., Kjer J., Bayer M. (**2010**). Bioactive natural products from marine sponges and fungal endophytes. *Phytochem. Rev.*, *9*, 475-489.

Rao K.V., Santarsiero B.D., Mesecar A.D., Schinazi R.F., Tekwani B.L., Hamann M.T. (**2003**). New manzamine alkaloids with activity against infectious and tropical parasitic diseases from an Indonesian sponge. *J. Nat. Prod.*, *66*, 823-828.

Roll DM, Scheuer PJ, Matsumoto GK, Clardy J. (**1983**) Halenaquinone, A pentacyclic polyketide from a marine sponge. *J. Am. Chem. Soc.*, 105, 6177-78.

Rinehart K.L. (**2000**) Amtitumor compounds from tunicates. *Med. Res. Rev.*, *20*, 1-27.

Higgs M.D., Faulkner D.J. (**1978**) Plakortin, an antibiotic from *Plakortis halichondrioides*. *J. Org. Chem.*, *43*, 3454-3457.

Hubbard S.R., Till J.H. (**2000**) Protein Tyrosine Kinase Structure and Function. *Annual Review of Biochemistry*, *69*, 373-398

Ring M.W., Schwär G., Thiel V., Dickschat, J.S. Kroppenstedt R.M. Schulz S., Bode H.B. (**2006**). Novel iso-branched ether lipids as specific markers of developmental sporulation in the myxobacterium *Myxococcus xanthus*. *J. Biol. Chem.*, *281*, 36691-36700.

Rodriguez J., Quiñoá E., Riguera R., Peters B.M., Abrell L.M., Crews P. (**1992**). The structures and stereochemistry of cytotoxic sesquiterpene quinones from *Dactylospongia elegans*. *Tetrahedron*, *48*, 6667-6680.

Ross J.S., Fletcher J.A. (**1999**). The HER-2/neu oncogene: prognostic factor, predictive factor and target for therapy. *Semin. Cancer Biol.*, *9*, 125-138.

Sagar S., Kaur M., Minneman K.P. (**2010**). Antiviral lead compounds from marine sponges. *Mar. Drugs*, *7*, 787-802

Sakai R., Higa T., Jefford C.W., Bernardinelli G. (**1986**). Manzamine A, a novel antitumor alkaloid from a sponge. *J. Am. Chem. Soc.*, *108*, 6404-6405.

Salmoun M., Devijver C., Daloze D., Braekman J.C. Gomez R., de Kluijver M., Van Soest R.W.M. (**2000**). New sesquiterpene/quinones from two sponges of the genus *Hyrtios*. *J. Nat. Prod.*, *63*, 452-456.

Sarin P., Sun, D., Thornton A., Muller W. (**1987**). Inhibition of replication of the etiologic agent of acquired immune deficiency syndrome (human T-lymphotropic retrovirus/lymphadenopathy-associated virus) by avarol and avarone. *J. Natl. Cancer Inst.*, *78*, 663-666.

Schmitz, F. J. and S. J. Bloor (**1988**). Xesto- and halenaquinone derivatives from a sponge, Adocia sp., from Truk lagoon. *J. Org. Chem. 53*, 3922-3925.

Schumacher M., Cerella C., Eifes S., Chateauvieux S., Morceau F., Jaspars M., Dicato M., Diederich M. (**2010**). Heteronemin, a spongean sesterterpene, inhibits TNF alpha-induced NF-kappa B activation through proteasome inhibition and induces apoptotic cell death. *Biochem. Pharmacol.*, *79*, 610-622.

Sewell J.M., Mayer I., Langdon S.P., Smyth J.F., Jodrell D.I., Guichard S.M. (**2005**). The mechanism of action of Kahalalide F: variable cell permeability in human hepatoma cell lines. *Eur. J. Cancer*, *41*, 1637-1644.

Sharma V., Lansdell T.A., Jin G., Tepe J.J. (**2004**). Inhibition of cytokine production by hymenialdisine derivatives. *J. Med. Chem.*, *47*, 3700-3703.

Sipkema D., Franssen M.C.R., Osinga R., Tramper J., Wijffels R.H. (**2005**). Marine Sponges as Pharmacy, *Mar. Biotechnol.*, *7*, 142-162.

Shen Y.-C., Chen C.-Y., Kuo Y.-H. (**2001**). New sesquiterpene hydroquinones from a Taiwanese marine sponge, *Hippospongia metachromia*. *J. Nat. Prod.*, *64*, 801-803.

Shigemori H., Madono T., Sasaki T., Mikami Y., Kobayashi J. (**1994**). Nakijiquinones A and B, new antifungal sesquiterpenoid quinones with an amino acid residue from an Okinawan marine sponge. *Tetrahedron*, *50*, 8347-8354.

Sipkema D., Franssen M.C.R., Osinga R., Tamper J., Wijffels R.H. (**2005**). Marine sponges as pharmacy. *Mar. Biotechnol.*, *7*, 142-162.

Skropeta D., Pastro N., Zivanovic A. (**2011**). Kinase inhibitors from marine sponges. *Mar. Drugs*, **9**, 2131-2154.

Smith, I. (2003). "Mycobacterium tuberculosis Pathogenesis and Molecular Determinants of Virulence." *Clinical Microbiology Reviews* **16**: 463-496.

Snow R.W., Guerra C.A., Noor A.M., Myint H.Y., Hay S.I. (**2005**). The global distribution of clinical episodes of *Plasmodium falciparum* malaria. *Nature*, *434*, 214-217.

Souza T., Abrantes J., de A Epifanio R., Fontes C., Frugulhetti I. (**2007**). The alkaloid 4-methylaaptamine isolated from the sponge *Aaptos aaptos* impairs Herpes simplex virus type 1 penetration and immediate-early protein synthesis. *Planta Med.*, *73*, 200-205.

Stahl P., Kissau L., Mazitschek R., Huwe A., Furet P., Giannis A., Waldmann H. (**2001**). Total synthesis and biological evaluation of the nakijiquinones. *J. Am. Chem. Soc.*, *123*, 11586-11593.

Stewart, B., Wild, C. P., (2014), World cancer report 2014. World Health Organization: Geneva, Switzerland, 2014.

Suárez Y., González L., Cuadrado A., Berciano M., Lafarga M., Muñoz A. (**2003**). Kahalalide F, a new marine-derived compound, induces oncosis in human prostate and breast cancer cells. *Mol. Cancer Ther.*, *2*, 863-872.

Takahashi Y., Ushio M., Kubota T., Yamamoto S., Fromont J., Kobayashi J. (**2010**). Nakijiquinones J-R, sesquiterpenoid quinones with an amine residue from okinawan marine sponges. *J. Nat. Prod.*, *73*, 467-471.

Talpir R., Benayahu Y., Kashman Y., Pannell L., Schleyer, M. (**1994**). Hemiasterlin and geodiamolide TA: two new cytotoxic peptides from the marine sponge *Hemiasterella minor* (Kirkpatrick). *Tetrahedron Lett.*, *35*, 4453-4456.

Takahashi Y., Kubota T., Ito, J., Mikami Y., Fromont J., Kobayashi J. (**2008**). Nakijiquinones G-I, new sesquiterpenoid quinones from marine sponge. *Bioorg. Med. Chem.*, *16*, 7561-7564.

Takei M., Burgoyne, D. L., Andersen, R. J. (**1994**), Effect of contignasterol on histamine release induced by anti-immunoglobulin E from rat peritoneal mast cells. *J. Pharm. Sci.*, *83*, 1234-1235.

Tan P., Luscinskas F.W., Homer-Vanniasinkam S. **(1999)** Cellular and molecular mechanisms of inflammation and thrombosis. *Eur. J. Endovasc. Surg.*, *17*, 373-389.

Tokunaga E., Oki E., Egashira A., Sadanaga N., Morita M., Kakeji Y., Maehara Y. (**2008**). Deregulation of the Akt pathway in human cancer. *Curr. Cancer Drug Targets*, *8*, 27-36.

Toyooka N, Nagaoka M, Sasaki E, Qin H, Kakuda H, Nemoto H. (2002) Model studies toward the total synthesis of halenaquinol and halenaquinone. *Tetrahedron, 58,* 6097–6101.

Turner E.C., Kavanagh D.J., Mulvaney E.P., McLean C., Wikström K., Reid H.M., Kinsella B.T. (**2011**). Identification of an interaction between the TPalpha and TPbeta isoforms of the human thromboxane A2 receptor with protein kinase C-related kinase (PRK) 1: implications for prostate cancer. *J. Biol. Chem.*, *286*, 15440-15457.

Uriz M.J., Turon X., Becerro M.A., Agell G. (**2003**) Siliceous spicules and skeleton frameworks in sponges: origin, diversity, ultrastructural patterns, and biological functions. *Microsc. Res. Tech., 62*, 279-299.

Van Soest, R.W.M; Boury-Esnault, N.; Hooper, J.N.A.; Rützler, K.; de Voogd, N.J.; Alvarez de Glasby, B.; Hajdu, E.; Pisera, A.B.; Manconi, R.; Schoenberg, C.; Janussen, D.; Tabachnick, K.R., Klautau, M.; Picton, B.; Kelly, M.; Vacelet, J.; Dohrmann, M.; Díaz, M.-C.; Cárdenas, P.; Carballo, J. L. (2015). World

Porifera database. Accessed at http://www.marinespecies.org/porifera on 2015-05-18

Wang, S.; Li, W.; Liu, N.; Zhang, F.; Liu, H.; Liu, F.; Liu, J.; Zhang T., Niu Y. (**2012**). Nek2A contributes to tumorigenic growth and possibly functions as potential therapeutic target for human breast cancer. *J. Cell. Biochem.*, *113*, 1904-1914.

Weiss B., Ebel R., Elbrächter M., Kirchner M., Proksch P. (**1996**). Defense metabolites from the marine sponge *Verongia aerophoba*. *Biochem Syst Ecol*, 1-7, 9-12.

Global tuberculosis report 2015; World Health Organization: Geneva, Switzerland, 2014

Wonganuchitmeta S.N., Yuenyongsawad S., Keawpradub N., Plubrukarn A. (**2004**). Antitubercular sesterterpenes from the Thai sponge *Brachiaster* sp. *J. Nat. Prod.*, *67*, 1767-1770.

Wylie L., Grace K., Jacobs R.S. (**1995**). Bis-indole alkaloid marine natural products as novel antiinflammatory agents. *FASEB J.*, *9*, A955.

Xie W., Ding D., Zi W., Li G., Ma D. (**2008**). Total synthesis and structure assignment of papuamide B, a potent marine cyclodepsipeptide with anti-HIV properties. *Angew. Chem. Int. Ed. Engl.*, *47*, 2844-2848.

Yasuhara-Bell, J., Lu, Y. (**2010**) Marine compounds and their antiviral activities. *Antiviral Research*, *86*, 231-240.

Yeatman, T. J. (**2004**). A renaissance for SRC. Nat. Rev. Cancer, *4*, 470-480.

Yousaf M., Hammond N.L., Peng J., Wayhuono S., McIntosh K.A., Charman W.N., Mayer A.M.S., Hamann M.T. (**2004**). New manzamine alkaloids from an Indo-Pacific sponge. Pharmacokinetics, oral availability, and the significant activity of several manzamines against HIV-I, AIDS opportunistic infections, and inflammatory diseases. *J. Med. Chem.*, *47*, 3512- 3517.

7. List of abbreviations

$[\alpha]_D^{20}$	Specific rotation at the sodium D-line
br	Broad singnal
$CDCl_3$	Deuterated chloroform
$CHCl_3$	Chloroform
CI	Chemical ionization
COSY	Correlation spectroscopy
d	Doublet signal
DCM	Dichloromethane
dd	Doublet of doublet signal
DEPT	Distortionless enhancement by polarization transfer
DMSO	Dimethyl sulfoxide
DPPH	2,2-Diphenyl-1-picryl-hydrazyl
ED	Effecive dose
EI	Electron impact ionization
ESI	Electron spray ionization
et al.	et altera (and others)
EtOAc	Ethyl acetate
eV	Electron Volt
FAB	Fast atom bombardment
g	Gram
HMBC	Heteronuclear multiple bond connectivity
HMQC	Heteronuclear multiple quantum coherence
H_2O	Water
HPLC	High performance liquid chromatography
hr	Hour
HR-MS	High resolution-mass spectrometry
Hz	Hertz
L	Liter
LC	Liquid chromatography
LC-MS	Liquid chromatography-mass spectrometry
m	Multiplet signal
MeOD	Deuterated methanol
MeOH	Methanol

mg	Milligram
MHz	Mega Hertz
min	Minute
mL	Milliliter
MS	Mass spectrometry
MTT	Microculture tetrazolium assay
m/z	Mass per charge
μg	Microgram
μL	Microliter
μM	Micromolar
ng	Nanogram
NMR	Nuclear magnetic resonance
NOE	Nuclear Overhauser effect
NOESY	Nuclear Overhauser and exchange spectroscopy
q	Quartet signal
ROESY	Rotating frame Overhauser enhancement spectroscopy
RP 18	Reversed phase C 18
s	Singlet signal
t	Triplet signal
TFA	Trifluoroacetic acid
TLC	Thin layer chromatography
UV	Ultra-violet
VLC	Vaccum liquid chromatography
n-BuOH	*n*-Butanol

8. Attachments

Attachment 1: The ^{1}H NMR spectrum of 5-*epi*-nakijiquinone S (**1**)
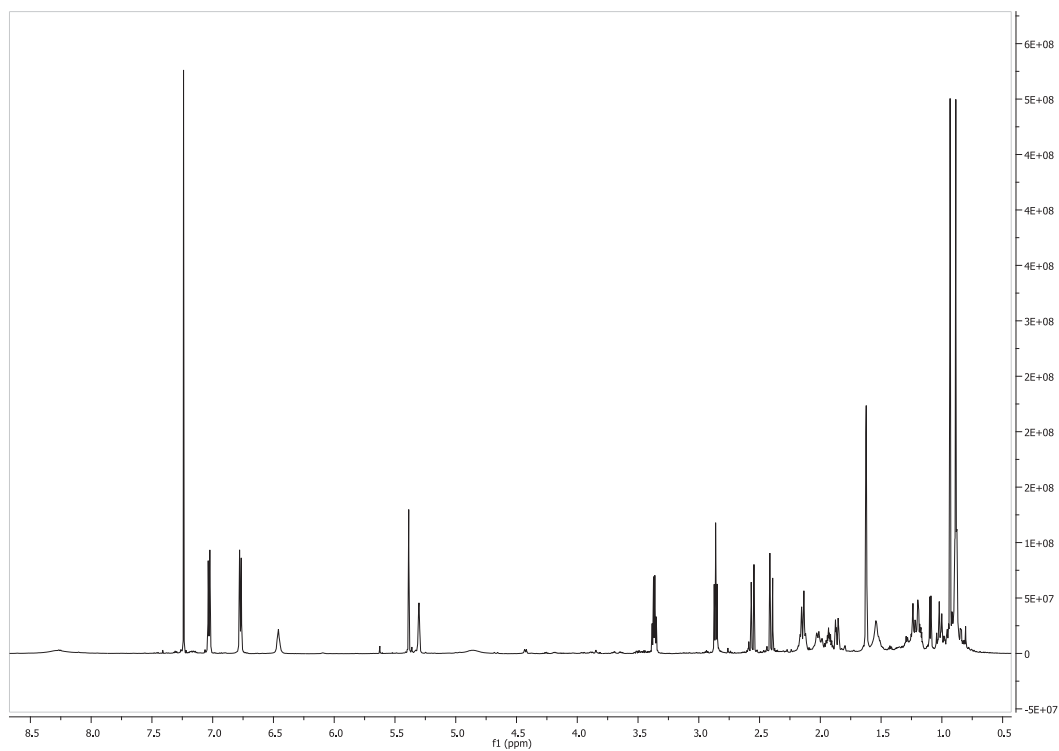
Attachment 2: The ^{1}H NMR spectrum of 5-*epi*-nakijiquinone Q (**2**)
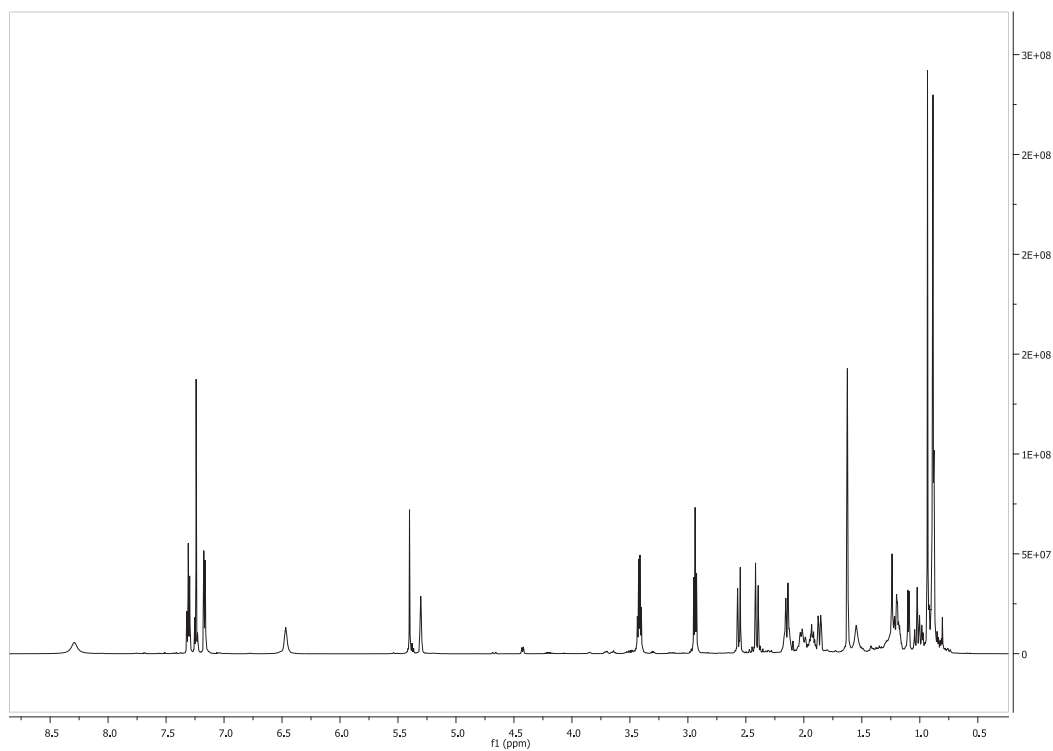
Attachment 3: The ¹H NMR spectrum of 5-*epi*-nakijiquinone T (**3**)
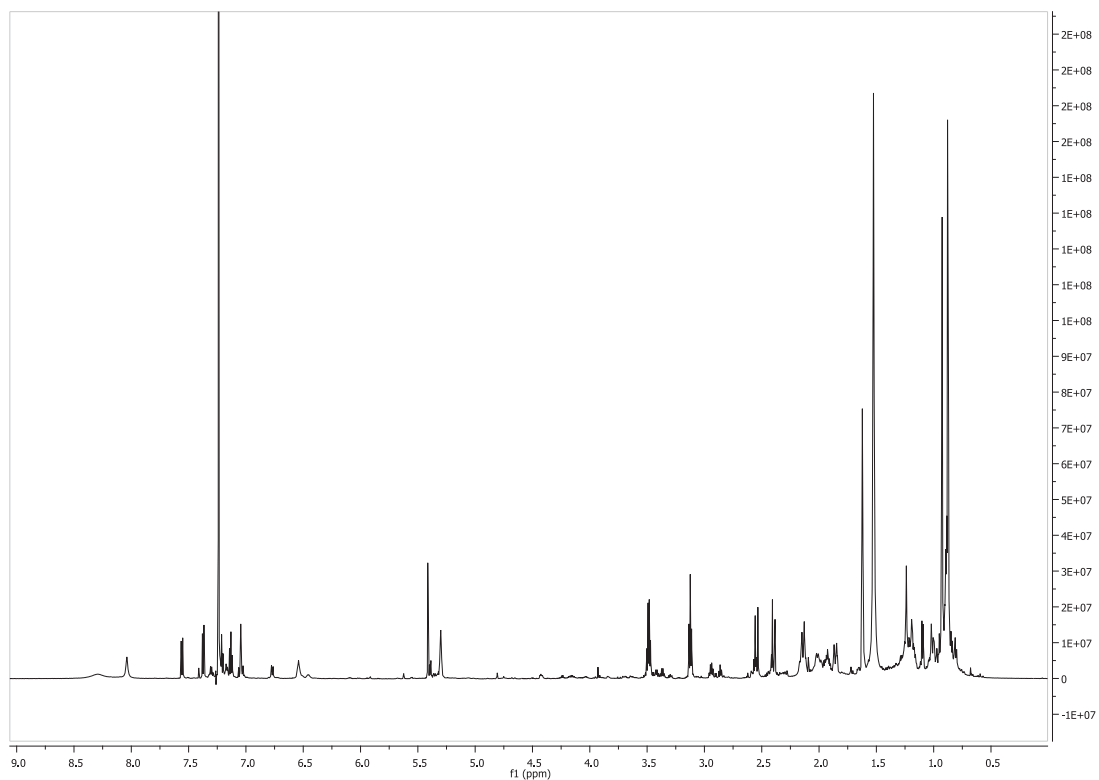
Attachment 4: The ¹H NMR spectrum of 5-*epi*-nakijiquinone U (**4**)
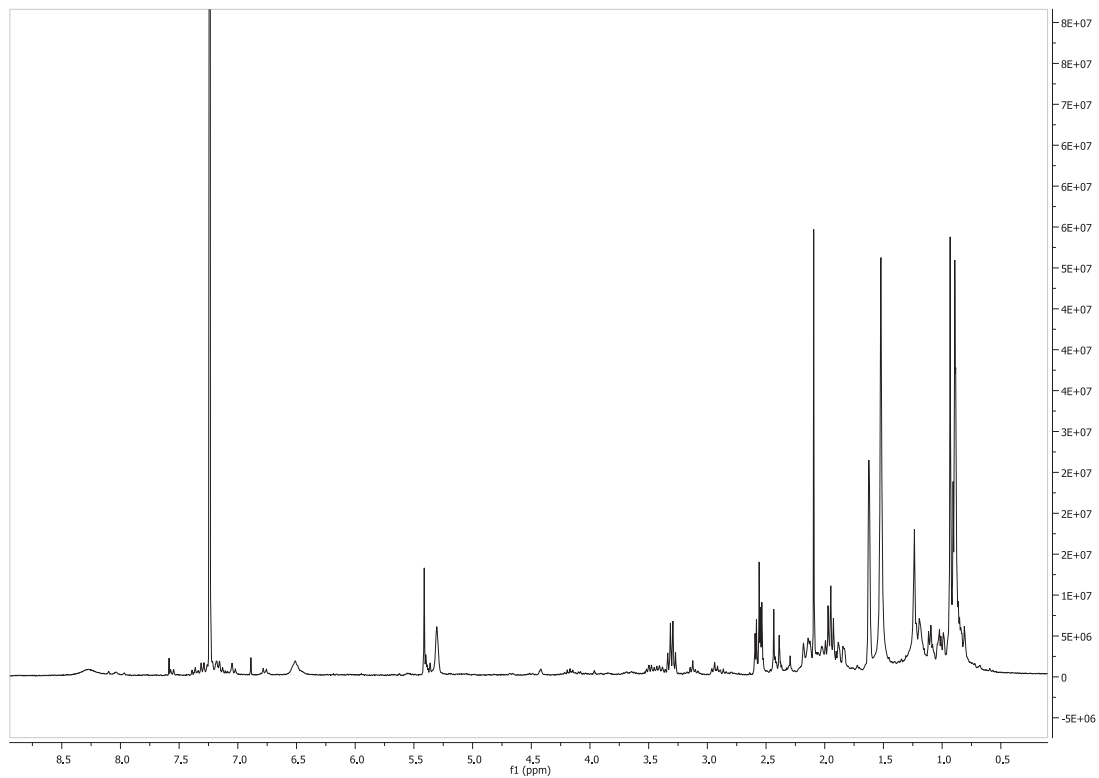
Attachment 5: The ^{1}H NMR spectrum of 5-*epi*-nakijiquinone N (**5**)
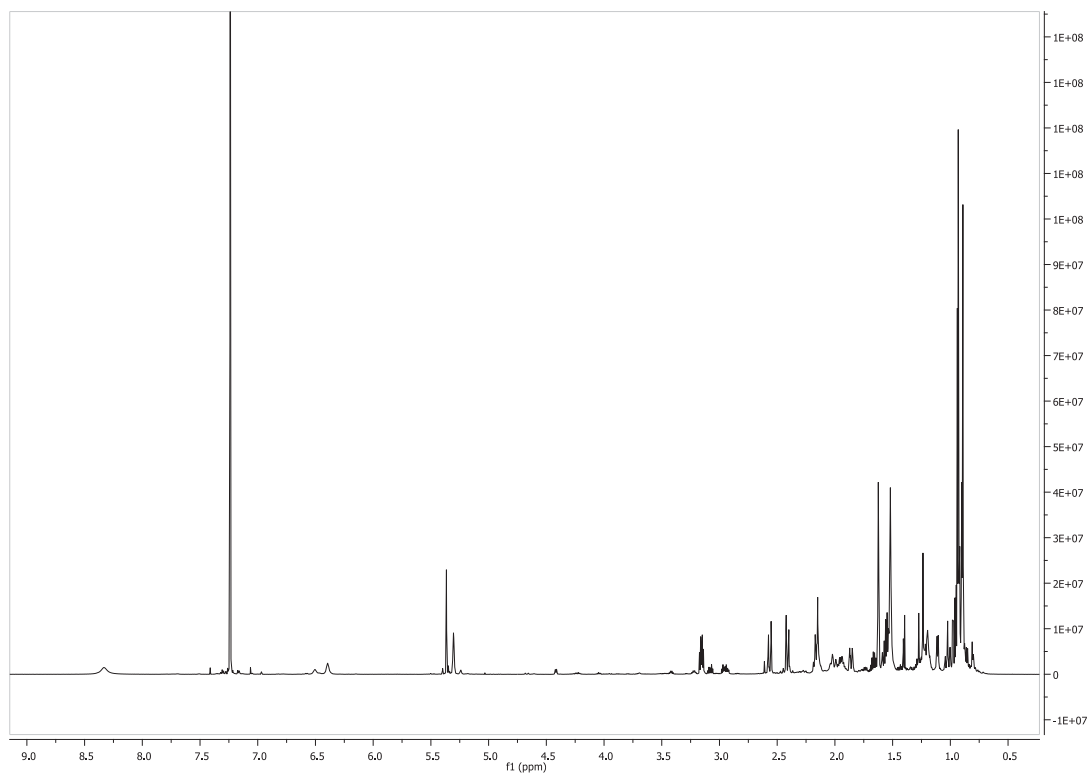
Attachment 6: The ^{1}H NMR spectrum of 5-*epi*-nakijinol C (**6**)
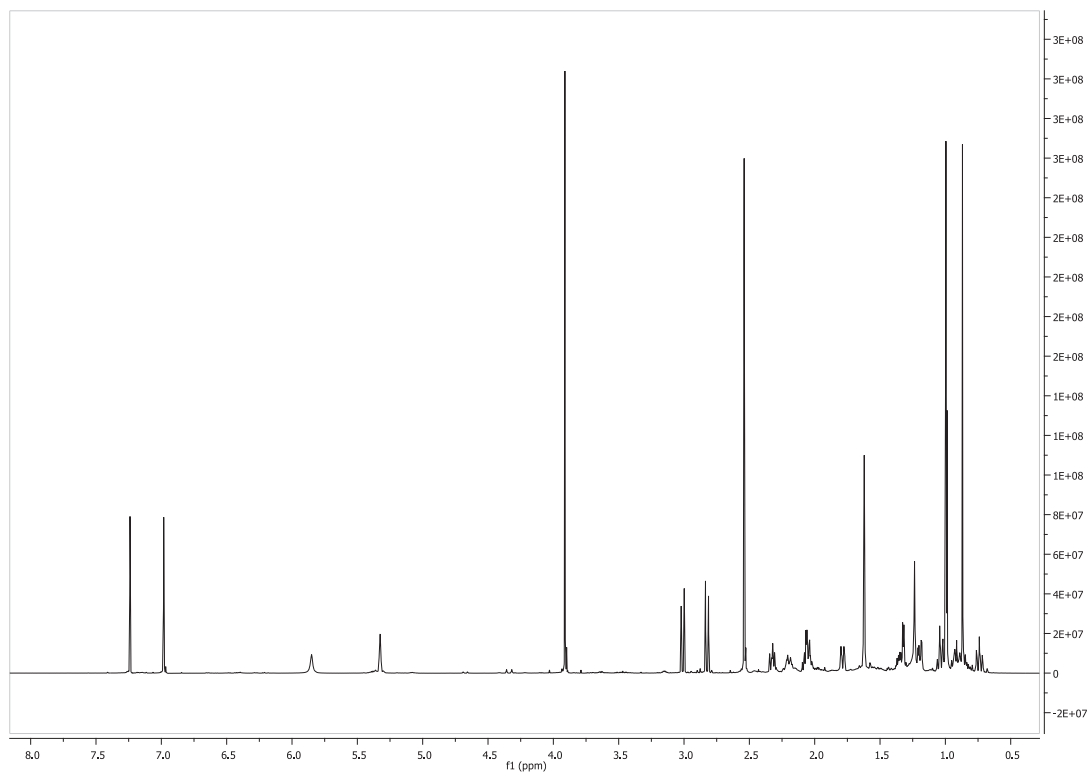
Attachment 7: The ¹H NMR spectrum of 5-*epi*-nakijinol D (**7**)
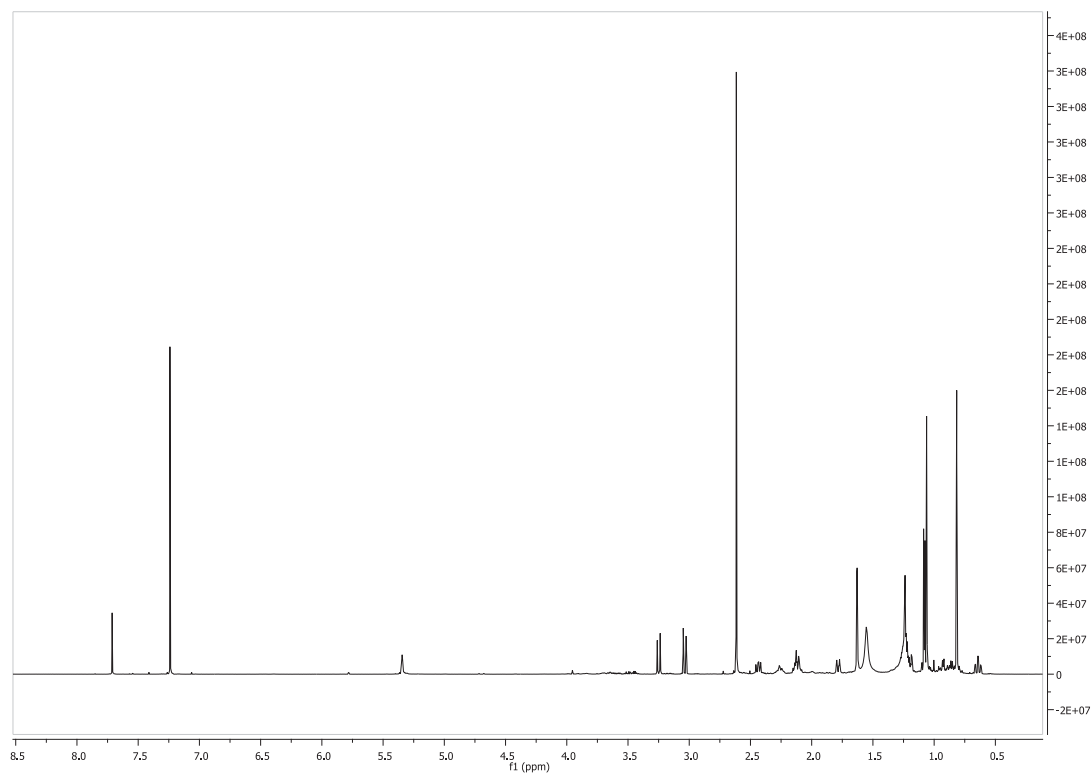
Attachment 8: The ¹H NMR spectrum of 18-hydroxy-5-*epi*-hyrtiophenol (**8**)
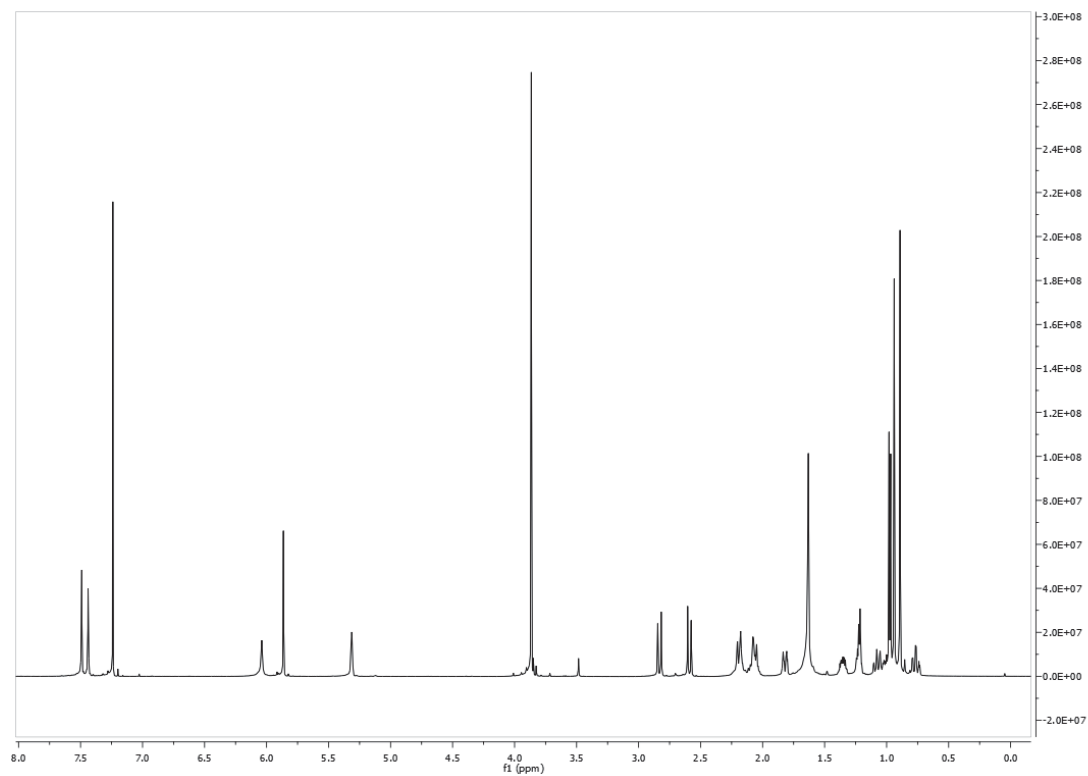
Attachment 9: The ¹H NMR spectrum of 1,2-propanediol, 3-[(13-methyltetradecyl)oxy]-, (2*S*)- (**9**)
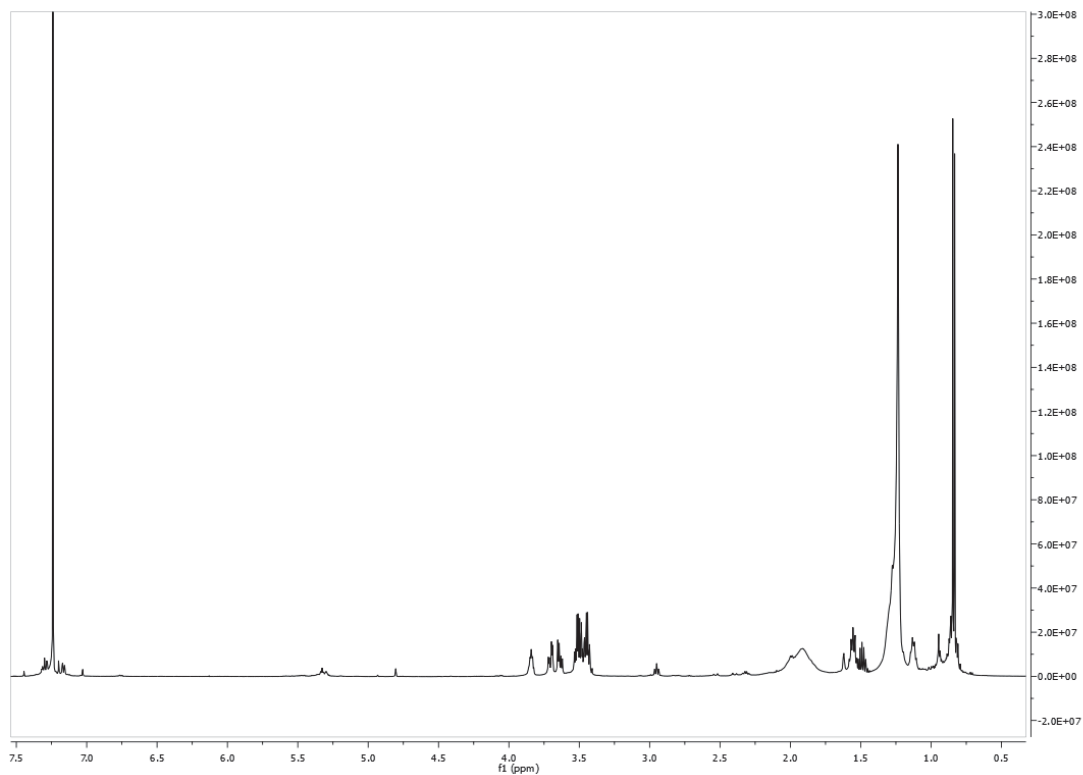
Attachment 10: The ¹H NMR spectrum of indole-3-carboxyaldehyde (**10**)
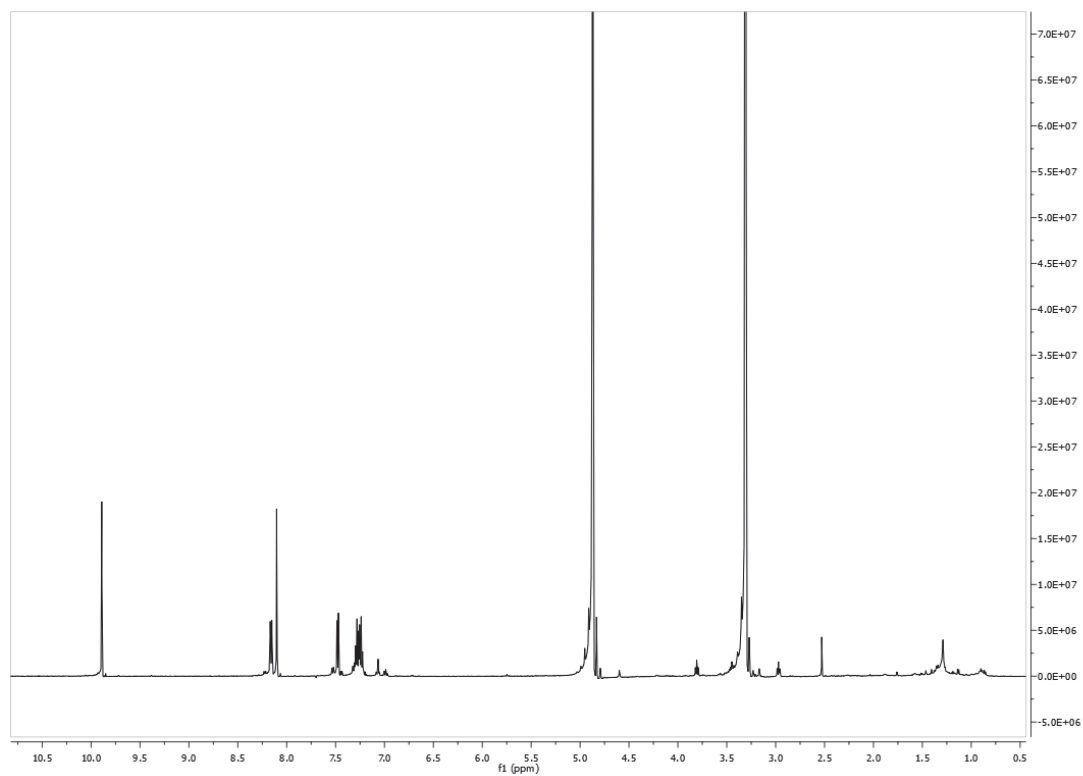
Attachment 11: The ^{1}H NMR spectrum of callyaerin I (**11**)
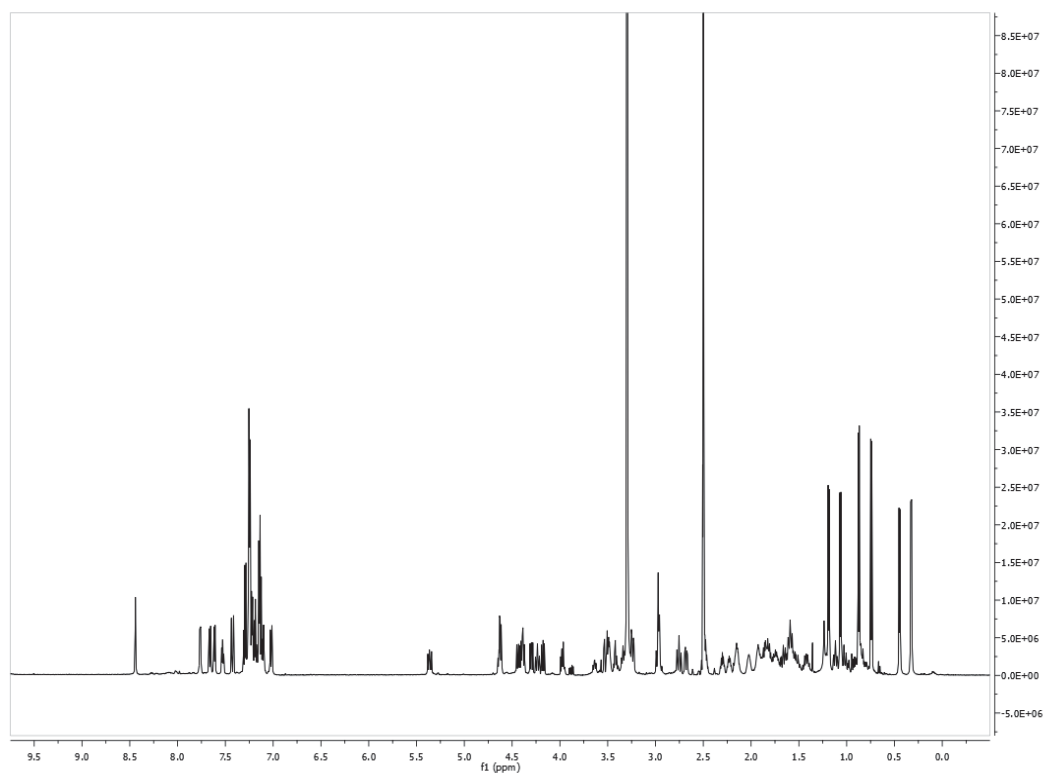
**Attachment 12:** The ^{1}H NMR spectrum of callyaerin J (**12**)
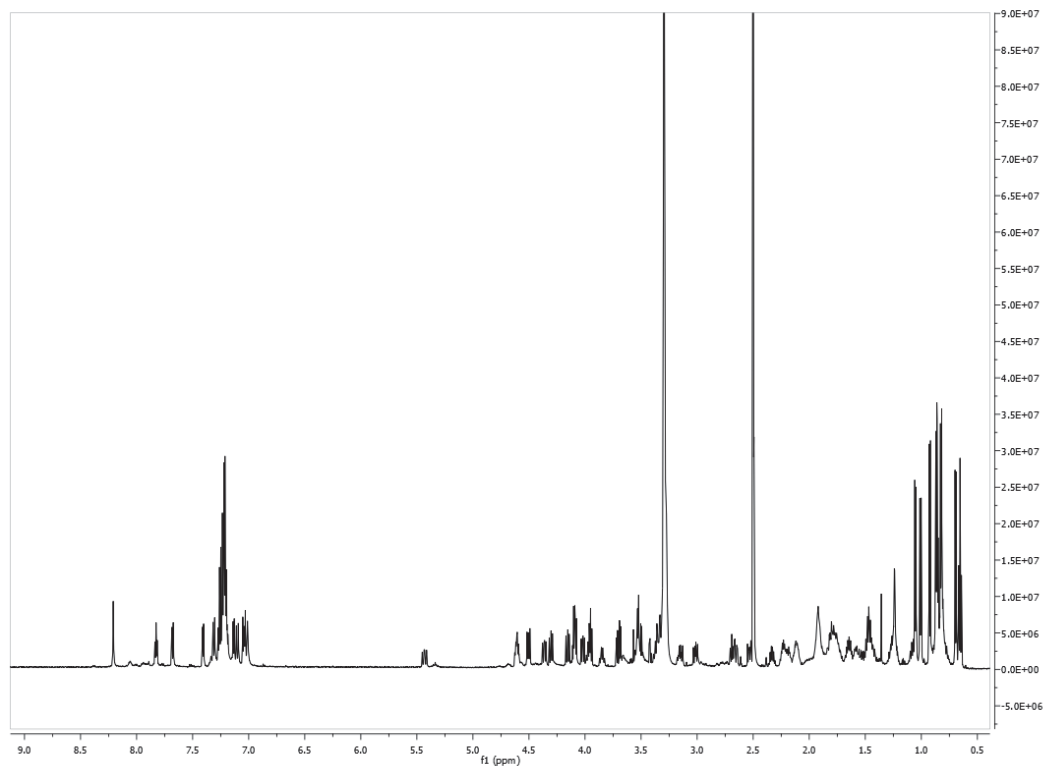
Attachment 13: The ^{1}H NMR spectrum of callyaerin K (**13**)
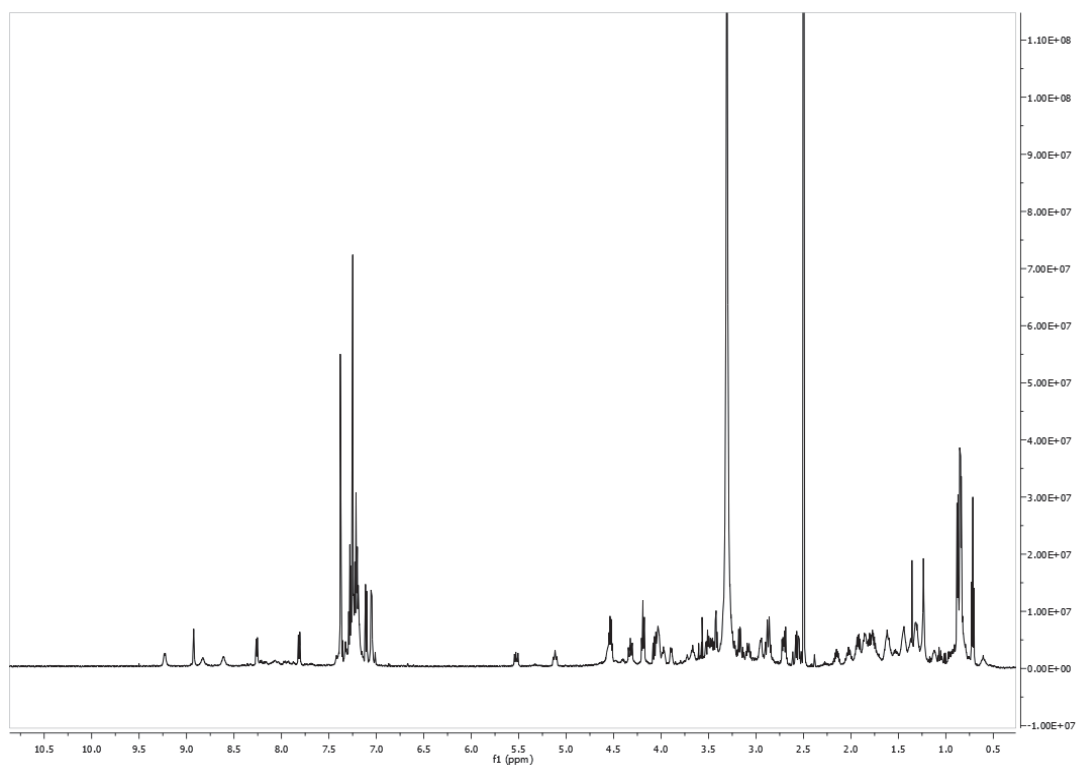
Attachment 14: The ^{1}H NMR spectrum of callyaerin L (**14**)
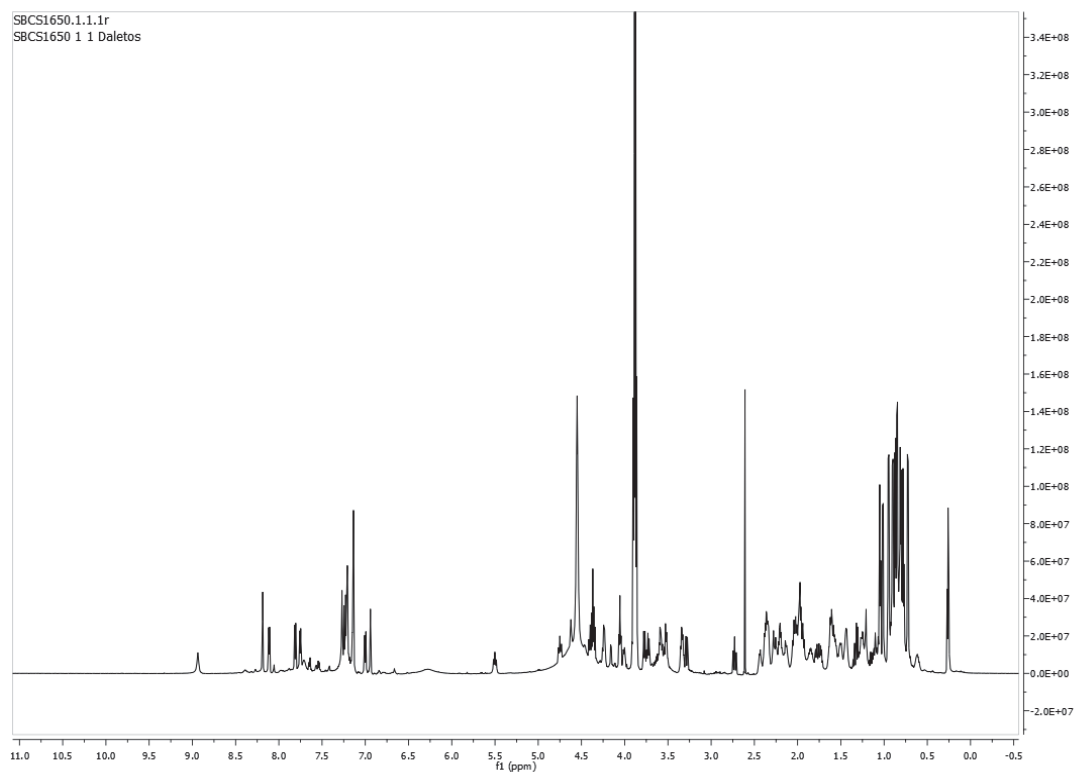
Attachment 15: The ^{1}H NMR spectrum of callyaerin M (**15**)
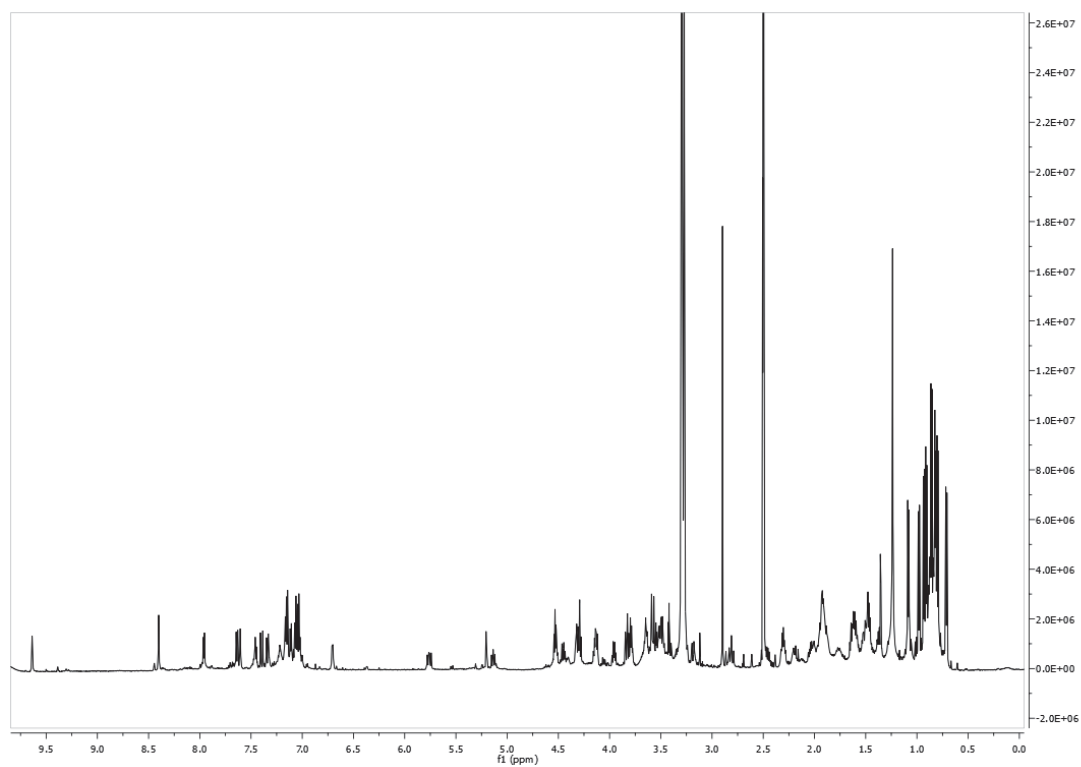
Attachment 16: The ^{1}H NMR spectrum of callyaerin A (**16**)
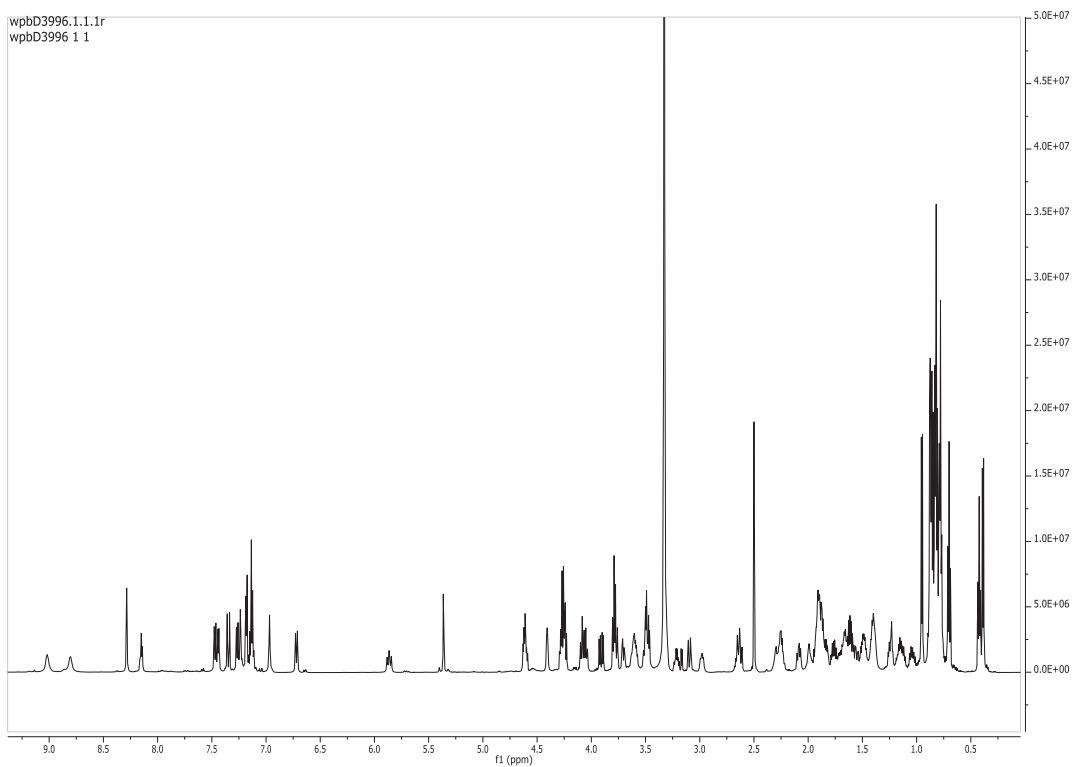
Attachment 17: The ^{1}H NMR spectrum of callyaerin B (**17**)
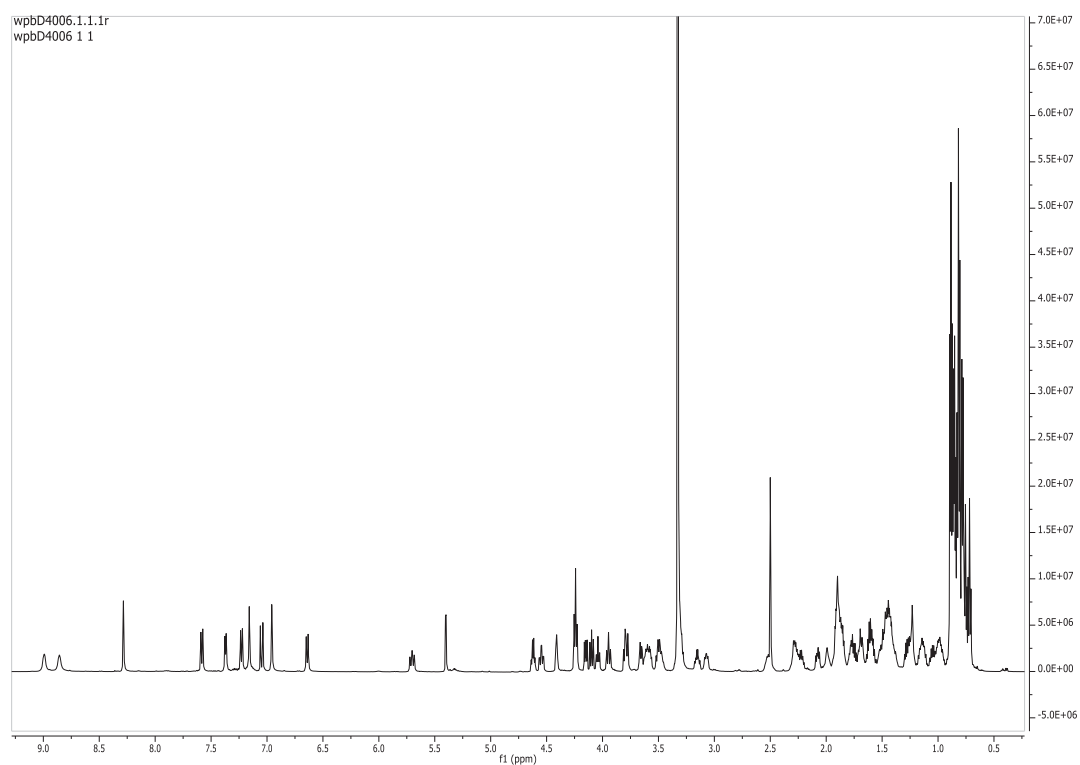
Attachment 18: The ^{1}H NMR spectrum of callyaerin C (**18**)
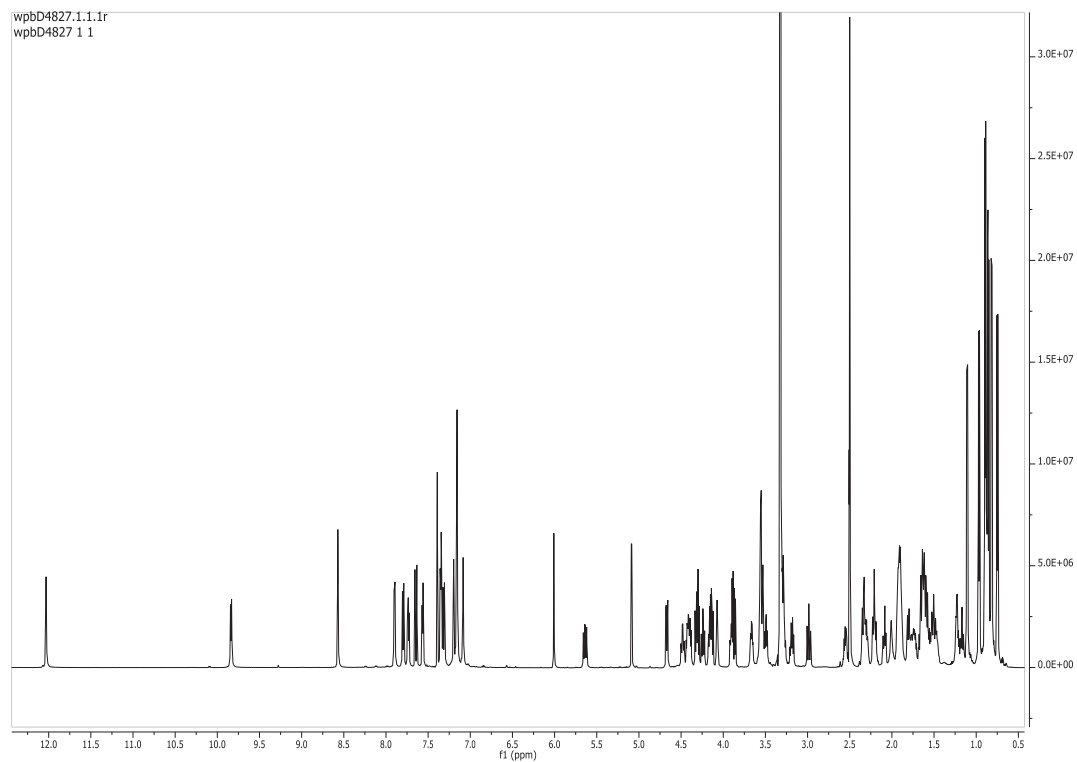
Attachment 19: The ^{1}H NMR spectrum of callyaerin D (**19**)
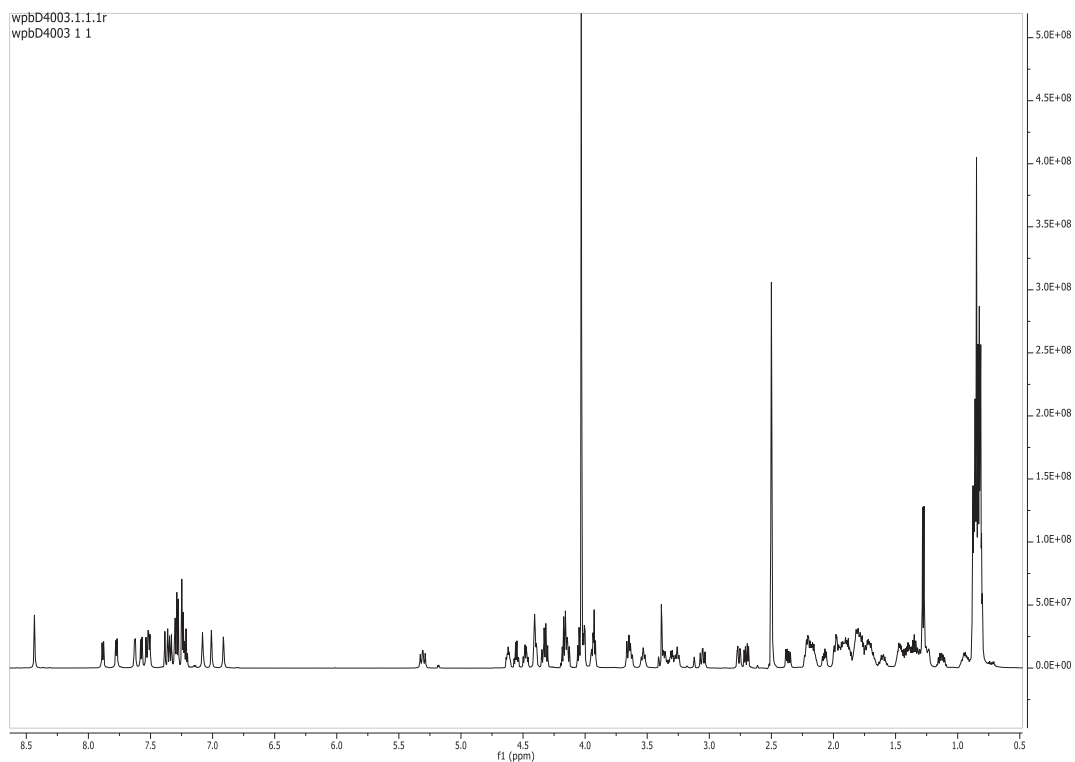
Attachment 20: The ^{1}H NMR spectrum of callyaerin E (**20**)
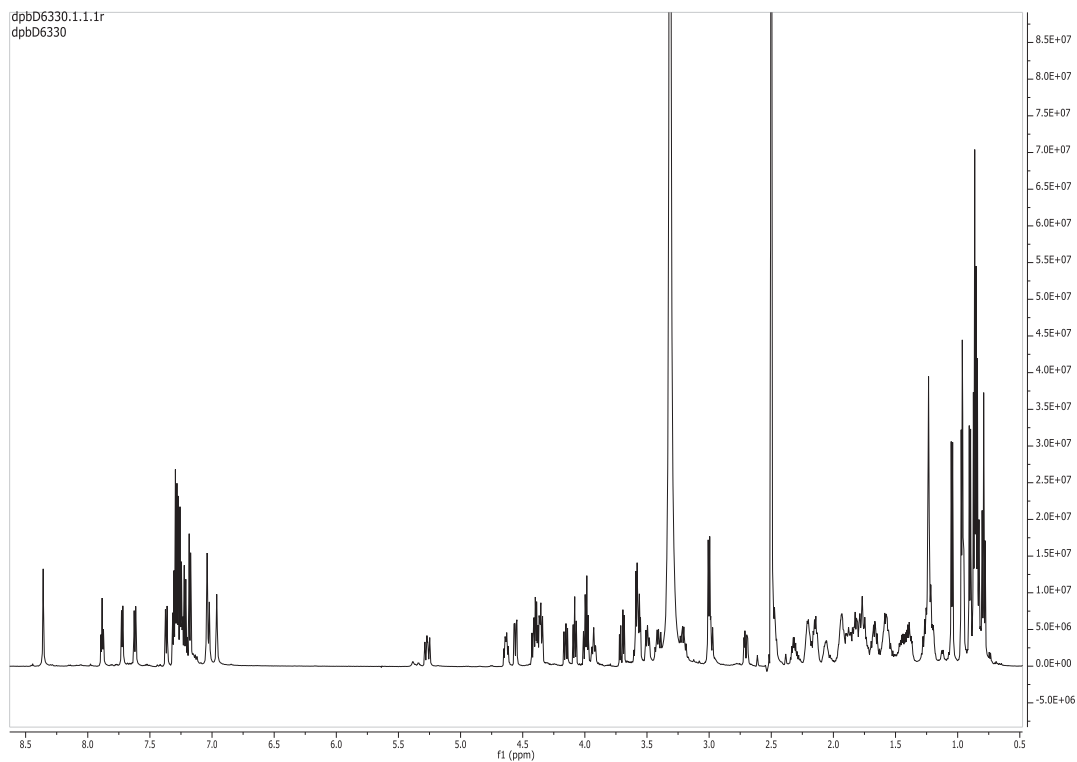
Attachment 21: The ^{1}H NMR spectrum of callyaerin F (**21**)
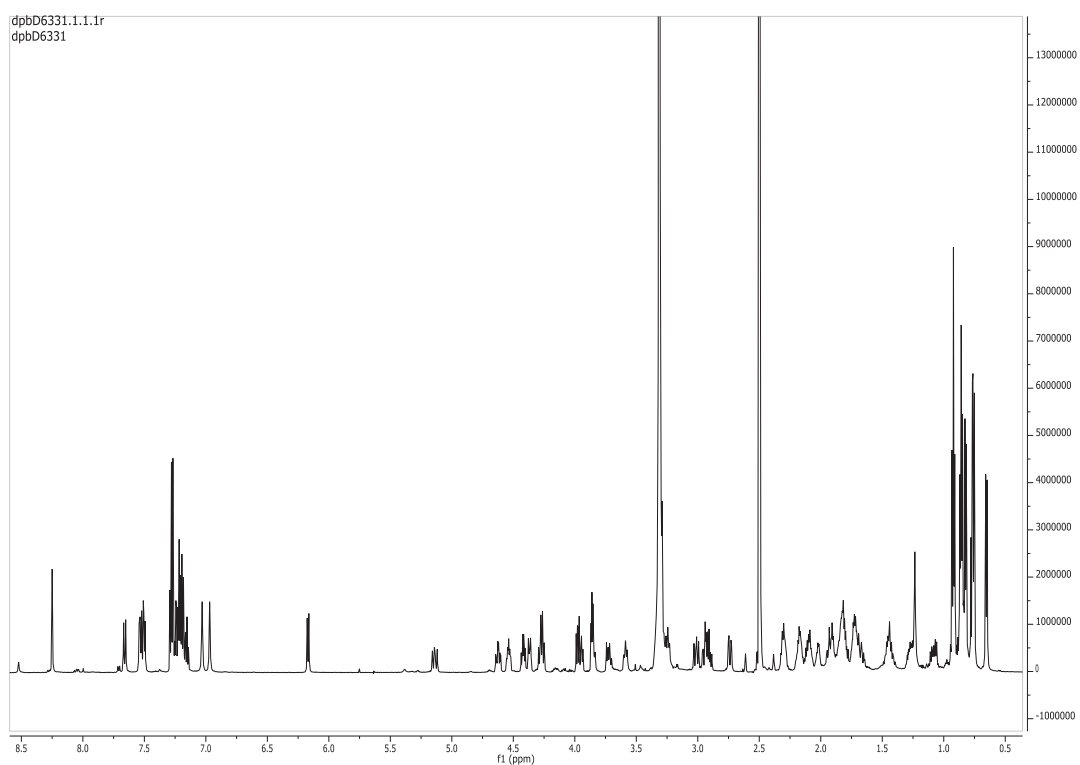
Attachment 22: The ^{1}H NMR spectrum of callyaerin G (**22**)
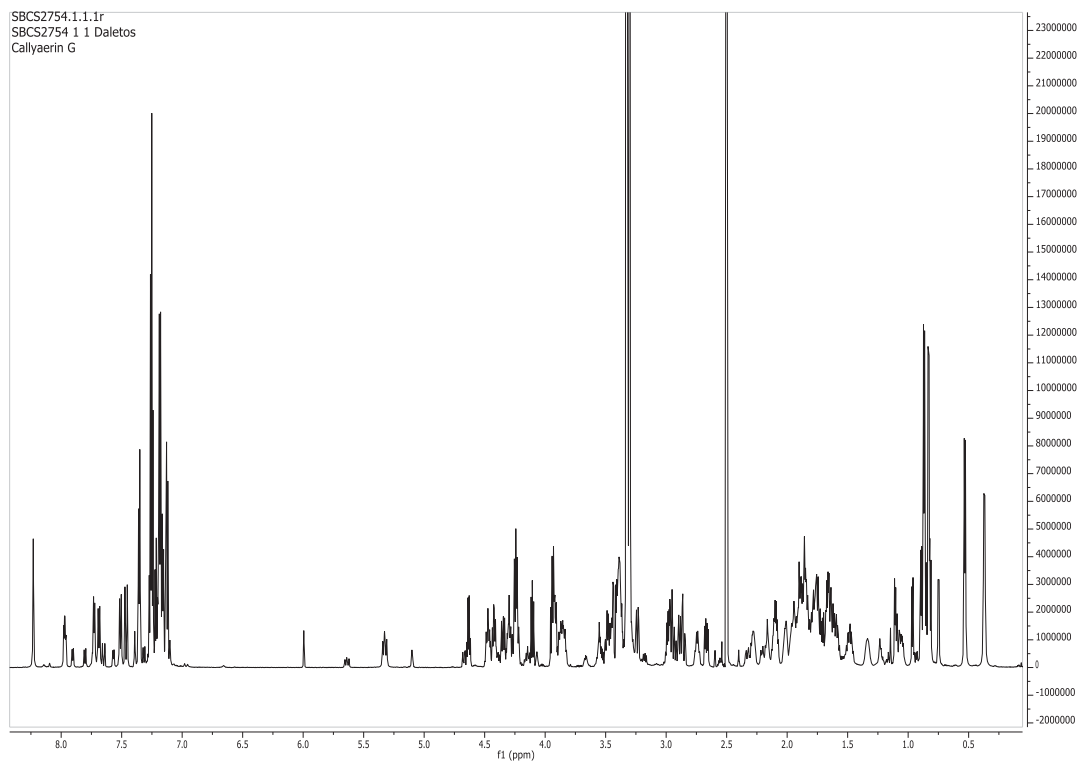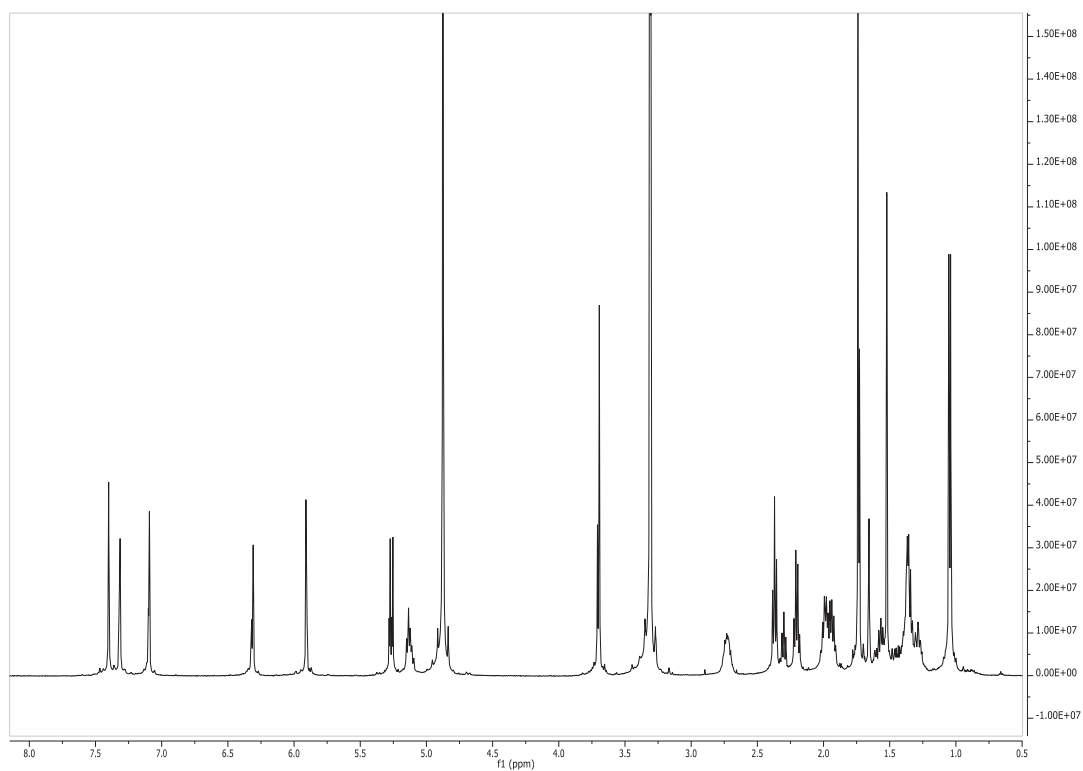
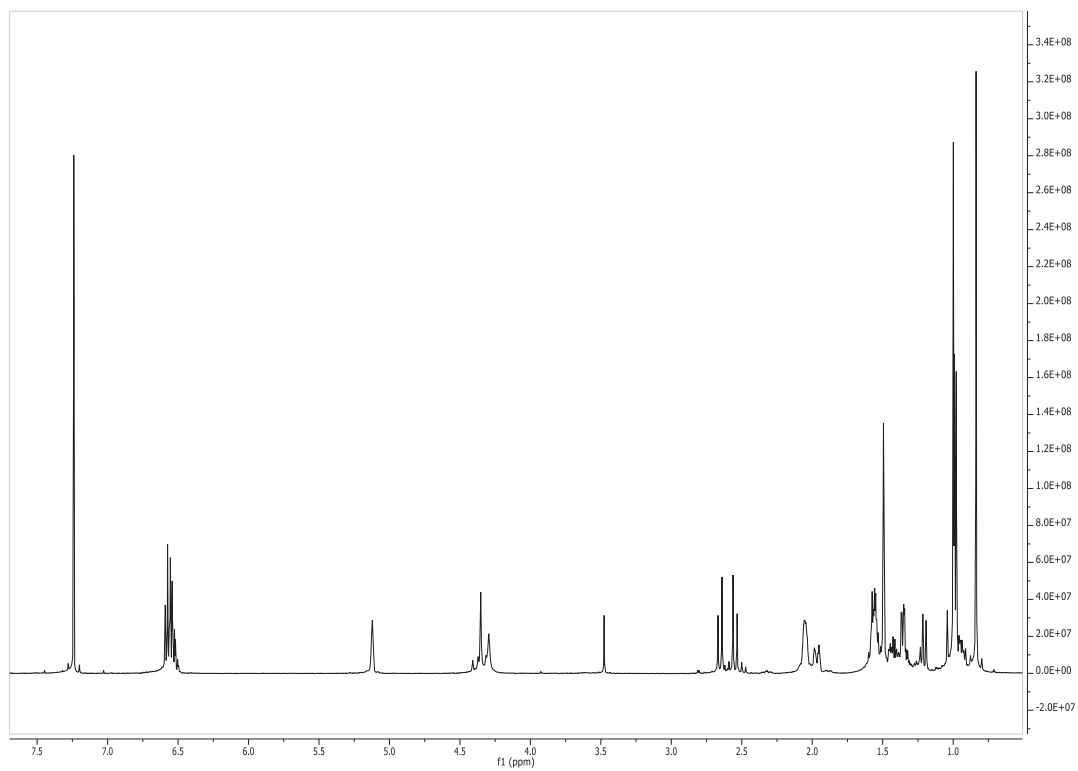**Attachment 23:** The ^{1}H NMR spectrum of annomontine (**23**)
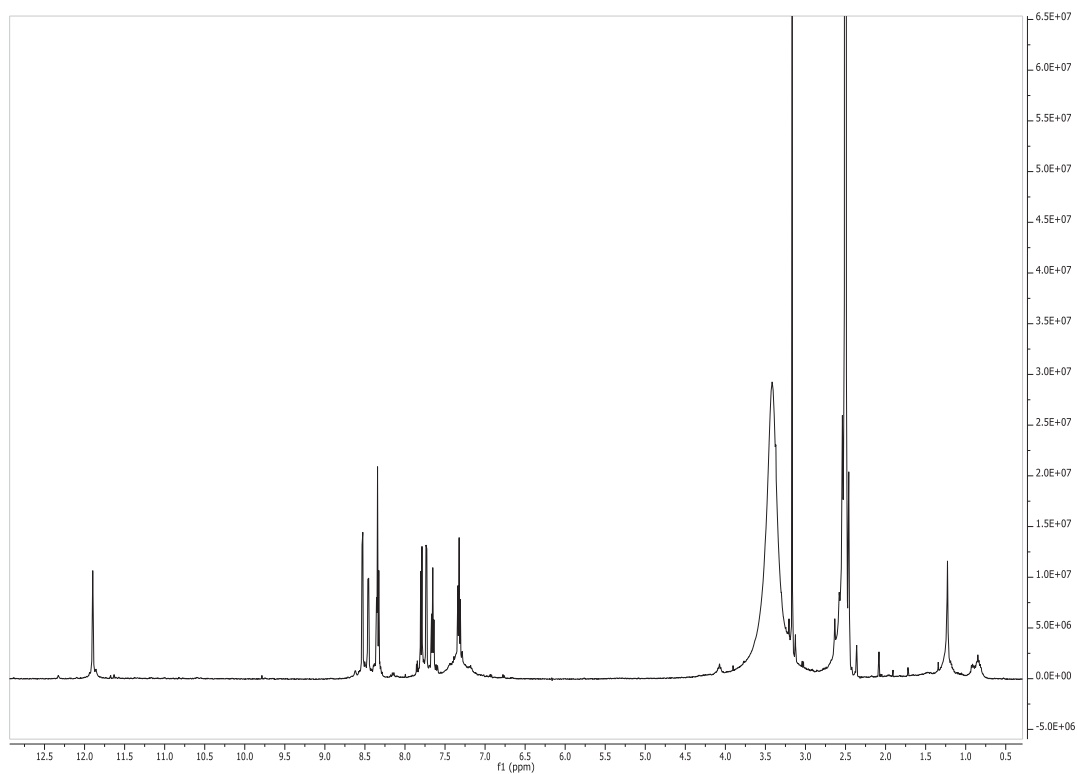
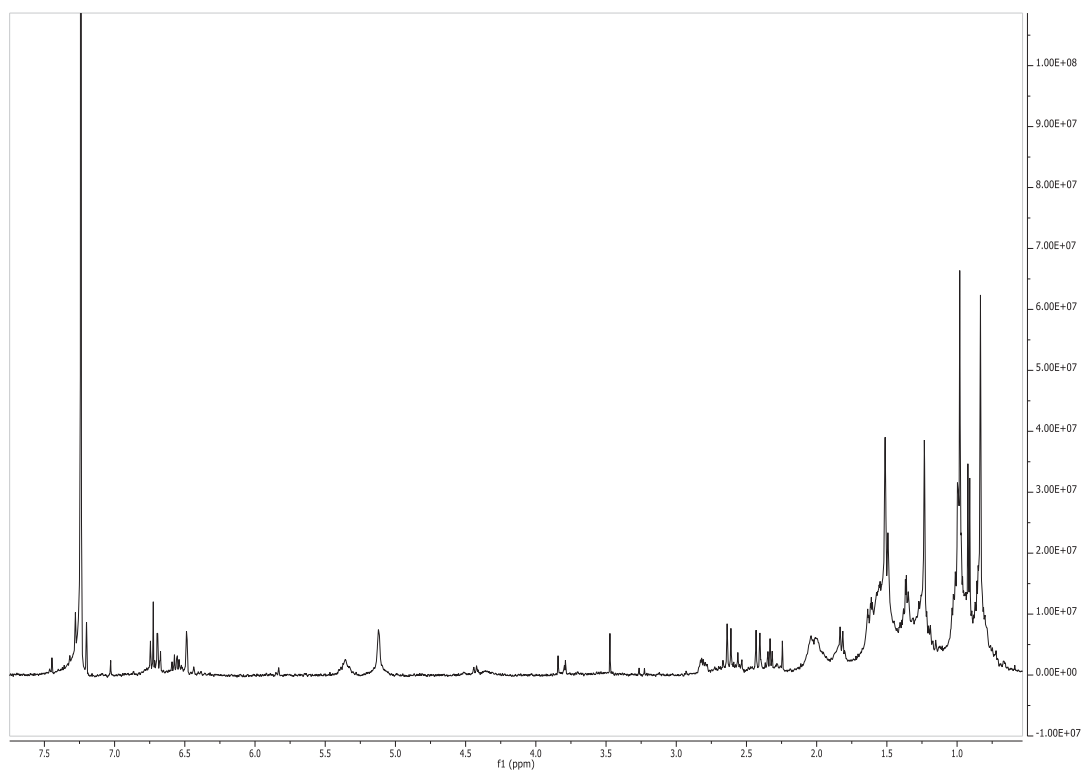**Attachment 24:** The ^{1}H NMR spectrum of 1-Hydroxy-3,4-dihydronorharman (**24**)
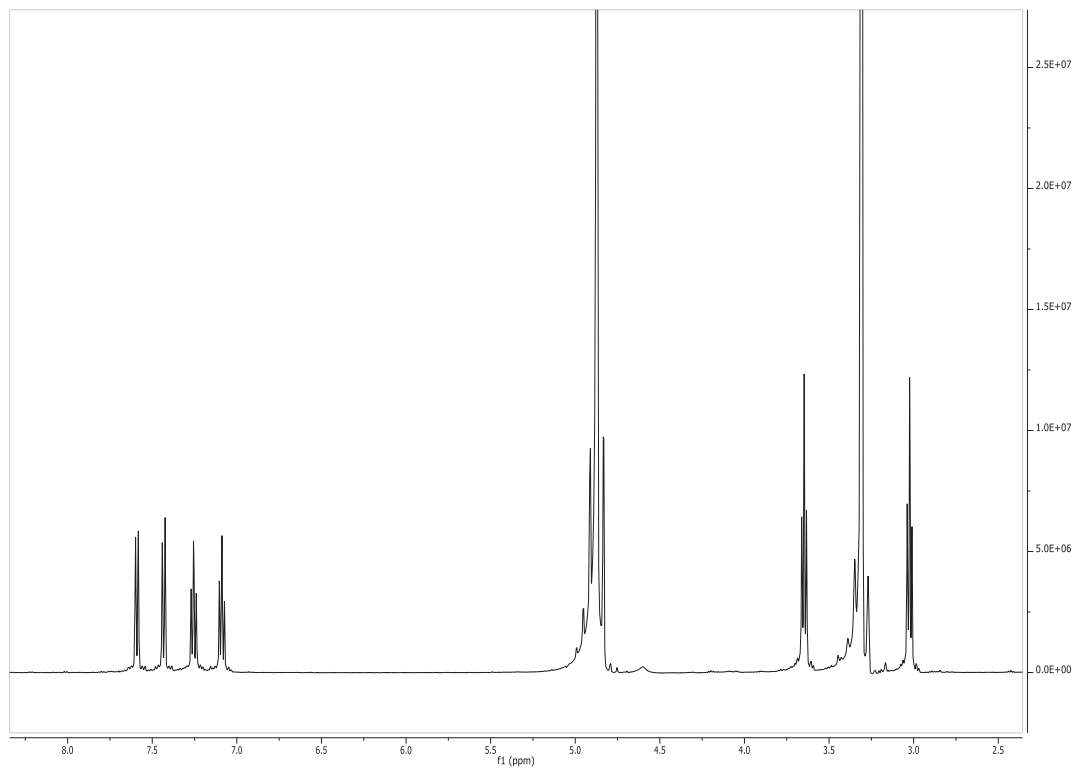
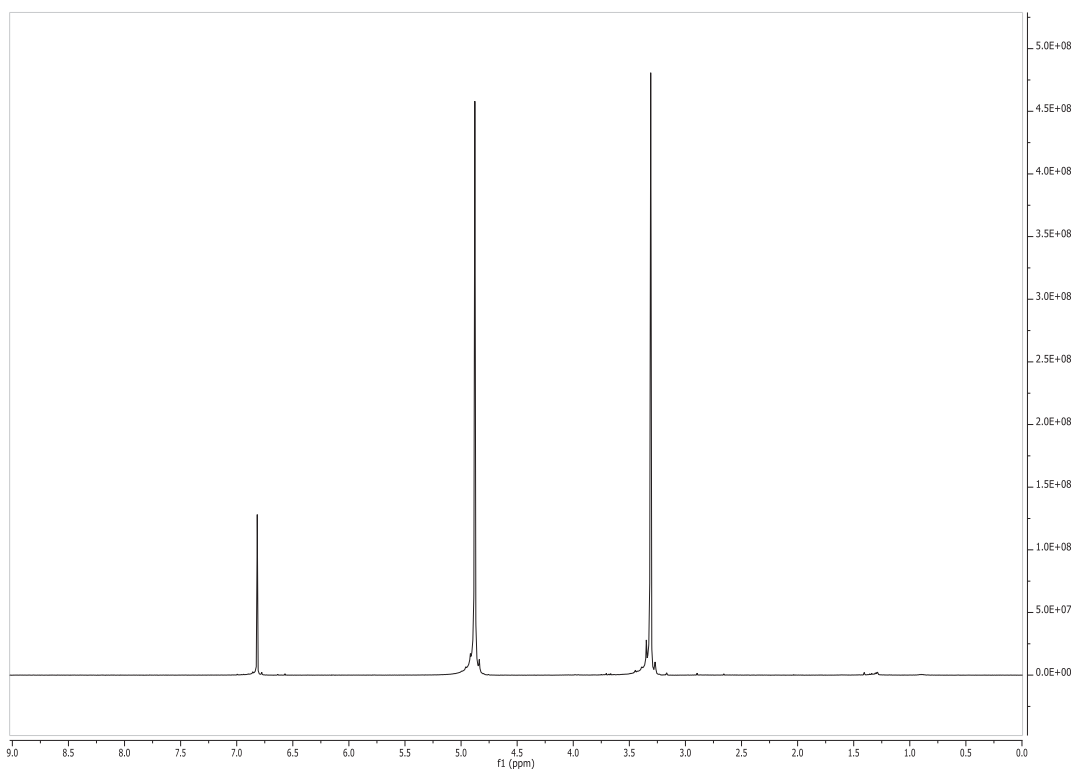**Attachment 25:** The ^{1}H NMR spectrum of ircinin-1,2 (3:1) (**25** and **26**)

Attachment 26: The ^{1}H NMR spectrum of avarol (**27**)

Attachment 27: The ^{1}H NMR spectrum of avarone (**28**)

Attachment 28: The ^{1}H NMR spectrum of 4,5-Dibromo-1*H*-pyrrole-2-carboxylic acid (**29**)

RESUME

Name: Georgios Daletos

Nationality: Greek

Profession: Pharmacist

E-mail: Georgios.Daletos@uni-duesseldorf.de

EDUCATION

- 07/2002, Graduation of the 1st high school of Nafpaktos, Greece

- 11/2007, Diploma in Pharmacy, University of Patras, Greece

- 09/2010, Graduate Diploma of Specialization (GDS) student in the Department of Pharmacognosy and Chemistry of Natural Products, University of Patras, Greece
  Development of New Synthetic Cysteine-based Oligopeptides and Study of their Action against α4β1 Integrin
  Supervisor: Assist. Prof. Vassiliki Magafa

- 11/2010, Ph.D. candidate at the Institute of Pharmaceutical Biology and Biotechnology, Heinrich Heine University of Düsseldorf, Germany
  Isolation and Structure Elucidation of Bioactive Secondary Metabolites from Marine Sponges
  Supervisor: Prof. Dr. Peter Proksch

PRACTICAL TRAINING

- 02/2006 – 04/2006. Department of Pharmacy, University of Lisbon, Portugal
  Complexes of Thymol and Carvacrol with Beta-Cyclodextrins and Study of their Organoleptic Properties
  Supervisor: Prof. Helena Maria Cabral Marques

- 02/2010 – 04/2010. Institute of Pharmaceutical Biology and Biotechnology, Heinrich Heine University of Düsseldorf, Germany.
  Isolation and Identification of Natural Products from Plant Endophytic Fungi
  Supervisor: Prof. Dr. Peter Proksch